THICKNESS VARIABILITY EFFECTS ON THE PROPERTIES OF UNSTABILIZED FULL DEPTH RECLAIMED AGGREGATES

by

Rizwana Haque

Submitted in partial fulfilment of the requirements
for the degree of Master of Applied Science

at

Dalhousie University
Halifax, Nova Scotia
March 2014

DEDICATION

I dedicate my thesis ……..

To my respected and beloved parents for the endless love, support and blessings;

To my husband for his love, patience and constant support;

To my mother-in-law for her good wishes and;

Last but not the least my father-in-law who we have lost recently, for his faith in my capability.

"Baba, you know you will always be in our hearts"

TABLE OF CONTENTS

LIST OF TABLES

LIST OF FIGURES

ABSTRACT

Inadequate financial allocation for road maintenance is a threat to the impaired rural highways in Atlantic Canada. The conventional means of pavement rehabilitation has been to place a hot mix asphalt concrete overlay on the existing worn out pavement which is only a short term adjustment. The purpose is to provide a smooth wearing surface at a low cost. This traditional way of pavement repair does not fix the damage embedded within the pavement structure. After a certain extent of time the cracks in the original pavement start to reflect to the smooth new wearing surface, causing deterioration on the overlay. The advanced approach which is becoming more popular is the application of Full Depth Reclamation (FDR). This technique helps to repair the extensively defective roads by pulverizing the flexible pavement along with a fraction of the underlying damaged base layer. Thus a damage free base layer can be obtained by stabilizing and recompacting the pulverized materials. FDR is a sustainable and an environmentally beneficial repair method as it re-uses the in-situ materials.

FDR process has been used around the world for over 25 years yet confronts some difficulties regarding the fluctuation in the strength of materials in various projects. It is inferred that some of these difficulties are due to the variability and poor quality in the restored materials. The variability in the recycled base layer is a result of currently utilizing a retroactive depth control method to attain a specific blend of asphalt concrete to granular base for the pulverized materials. Two FDR projects applying two different pulverization control methods (conventional retroactive and GPR depth control methods) were analyzed to investigate the improvements in consistency of the restored materials by using Ground Penetrating Radar (GPR). A wide range of asphalt concrete/base layer blend ratio was detected in retroactive control section, while consistent blend ratio was maintained in GPR survey by mapping the variability in the depth of pavement and sub-dividing the test sections accordingly.

A GPR controlled constant blend ratio during pulverization displayed improvements in consistency of materials, physical and mechanical properties and performance as anticipated. The materials obtained by using the conventional retroactive depth control method exhibited higher variability in grain size distribution, optimum moisture content, optimum density, California Bearing Ratio, resilient modulus and shear strength. All materials from both projects exhibited excessive air voids and inadequate fines content as the as-obtained particles acted as conglomerated particles and enough fines were not generated after the pulverization. It is recommended that efficient quality control, precise specifications and appropriate pulverization methods will provide more reliable and impressive FDR pavements.

LIST OF ABBREVIATIONS AND SYMBOLS USED

A	Mass of dry specimen in air, g
A_{r1}	Amplitude of reflection from surface material
A_{r2}	Amplitude of reflection from base material
A_m	Amplitude of a metal plate
B	Mass of sample at saturated surface dry condition, g
BR	Blend Ratio (asphalt concrete thickness/base layer thickness)
AASHTO	American Association of State Highway and Transportation Officials
AC	Asphalt Cement
ACPA	American Concrete Pavement Association
ASCE	American Society for Civil Engineers
ASTM	American Society for Testing Materials
C	Cohesion of soil, kPa
ºC	Degree Celsius
c	Speed of light at vacuum, 0.3 m/ns
cm	Centimeter, 10^{-2} m
CBR	California Bearing Ratio
d	Selected sieve size
D	Maximum particle size
D_l	Mass of lid and vessel filled with water at 25 ºC, g

D_s	Diameter of the specimen for ITS test, mm
E	Elastic modulus
E_l	Mass of lid, vessel, sample and water at 25 ºC, g
E_r	Average resilient axial deformation
ER	Expansion Ratio
ESAL	80 kN equivalent single-axle load
e_r	Relative dielectric permittivity
e_{r1}	Dielectric permittivity of surface materials
e_{r2}	Dielectric permittivity of base materials
ε_r	Resilient axial strain
FDR	Full Depth Reclamation
FHWA	Federal Highway Administration
ϕ	Angle of internal friction
g	Gram, 10^{-3} kg
γ	Unit weight of materials, N/mm^3
γ_{max}	The unit weight of aggregate materials at zero air void
γ_w	The unit weight of water, 1000 kg/m^3
GPR	Ground Penetrating Radar
G_{mb}	Bulk specific gravity of aggregate materials
G_{mm}	Maximum specific gravity of aggregate materials
G_s	Specific gravity of aggregate materials

h	Pavement layer thickness
HMA	Hot Mix Asphalt
in	Inch
ITS	Indirect Tensile Strength
ITS_{soaked}	Soaked Indirect Tensile Strength
ITS_{dry}	Dry Indirect Tensile Strength
InDOT	Indiana Department of Transportation
JMF	Job Mix Formula
K	Conversion constant depending on units of density and volume
K_0	Coefficient of earth pressure at rest
k_1, k_2	Regression constants
kPa	kiloPascal, kN/m^2
L	Original length of the specimen in resilient modulus test, mm
LB	Lower bound
LVDT	Linear Variable Differential Transducer
m	Moisture content in percentage
MPa	megaPascal, N/mm^2
mm	Millimeter, 10^{-3} m
M_R	Resilient modulus
M_t	Mass of mold and moist soil in the mold, g
M_{md}	Mass of compaction mold, g

μ_r	Magnetic permeability
N	Newton
n	Gradation coefficient, usually taken as 0.45
ns:	Nanosecond, 10^{-9} second
NBDOT	New Brunswick Department of Transportation
NSTIR	Nova Scotia Transport and Infrastructure Renewal
OMC	Optimum Moisture Content of untreated materials
P	Percent by mass of materials passing sieve size "d"
P_{max}	Maximum applied load at ITS test, N
PCA	Portland Cement Association
PG	Penetration Grade
psi	Pounds per square inch
R	Reflection coefficient
RAP	Recycled Asphalt Pavement
ρ_d	Dry density of specimen at compaction point, g/cm^3 or optimum density
ρ_m	Moist density of compacted specimen at compaction point, g/cm^3
S	Shearing resistance of the aggregate particles, kPa
$S_{contact}$	Contact stress, MPa
S_{cyclic}	Cyclic axial stress, MPa
S_{max}	Maximum applied stress, MPa
S_t	Indirect tensile strength, kPa

σ:	Applied vertical stress, kPa
σ_1	Major principal or axial stress, MPa
σ_3	Minor principal or confining stress, MPa
σ_Z	Vertical stress, MPa
σ_r	Radial stress, MPa
σ_t	Tangential stress, MPa
t	Two way travel time, ns
t_h	Specimen height immediately before ITS test, mm
θ	Stress invariant, MPa
TMD	Theoretical Maximum Density
TRRL	Transport and Road Research Laboratory
TSR	Tensile Strength Ratio
TxDOT	Texas Department of Transportation
τ_{max}	Peak shear stress, kPa
$\tau_{1/2}$	Half-life
UB	Upper Bound
V	Wave velocity of GPR
V_c	Volume of compaction mold, cm^3
VMA	Voids in Mineral Aggregate
z	Depth below the ground surface, mm

ACKNOWLEDGEMENTS

I would like to express my appreciation to my supervisor Dr. Nouman Ali. I would also like to convey my sincere gratitude to my previous supervisor and one of the committee members Dr. Christopher L. Barnes for his proper guidance, patience, encouragement, valuable suggestions, countless hours in planning, discussing and cooperating in all possible ways throughout my research work. My appreciation extends to Dr. Don Jones for graciously taking time to review my thesis and serve on my committee.

I would like to cordially thank Dalhousie Civil Technicians: Blair Nickerson, Brian Kennedy and Jesse Keane for being available and helping in every possible way during the whole Laboratory works. Special Thanks to my fellow students Peter Salah, who helped me with Route 790 materials testing data needed for my thesis and Ahmed Hammad.

This research project also required assistance, cooperation and expertise from a number of companies. I would like to thank them all for their contributions. They all made the research project possible:

- ***NSERC-IPS:*** For funding me throughout the research period. Without the financial support it would be impossible to carry on my research.

- ***AMEC:*** For giving me access to their laboratory equipment, as well as their technicians' time and expertise teaching me how to use the equipment properly. Special thanks to Phil Sullivan, Julie Hughes, Gordon Shupe and Alex Gale for their endless help, valuable expertise and priceless advice.

- ***Industrial Cold Milling:*** For providing the opportunity to run a Ground Penetrating Radar survey on their construction project and supplying the materials used in this research project. Special thanks to Cathy Alward for providing all necessary data from their previous projects.

CHAPTER 1: INTRODUCTION

1.1 Background

A deteriorating old pavement network faces a restriction of maintenance budget that results in too infrequent overlay treatment in Atlantic Canada. Sometimes the repairs are done with so much delay that the deterioration progress too far. The effective service life of the pavement is lessened subsequently and the pavement resumes quickly to its deteriorated position until the next infrequent treatment is budgeted. According to Barnes (2008), the problems with the roads and highways are not entirely budget related. The empirical design methods which have been used for many years may not properly indicate the actual behavior of the materials. Excessive traffic and increased tire pressure accelerate the premature failure of pavement.

North America is facing challenges of deteriorating transportation infrastructure due to limited public funds for maintaining this infrastructure. Total federal, state, and local capital investment in the United States of America increased to $91 billion annually to improve the conditions and performances of roads though this is well below $170 billion estimated by the Federal Highway Administration (ASCE, 2013).

This insufficient investment is creating a decline in performance and conditions of pavement in the long run (ASCE, 2013). In Canada, emphasis has been given on the restoration of transportation infrastructure within a constrained budget. In light of the limited budgets, appropriate management systems should be used to assess the condition of the infrastructure for the optimization of repair arrangement; select the means of restoration to make fiscal estimates to extend the service life (Barnes, 2008). The Nova Scotia Department of Transportation and Infrastructure Renewal has paved more than 1,900 kilometers in the last three years with another 500 kilometers planned in 2012-13. The total highway capital budget is $281 million and a further $82 million will be spent in 2012-13 using operational funding for highway maintenance improvements. That

means $363 million will be invested in Nova Scotia roads this construction season (NSTIR, 2013).

A newer approach has been to repair these heavily damaged roads using a full depth pulverization (FDR) technique which provides for grinding and stabilization of the upper portion of the existing road to provide a new base layer that is free of defects (PCA, 2005). The FDR process removes crack damage from the bound hot mix asphalt (HMA) layers, thus removing the areas of localized flexibility. As a result, the service life of FDR pavement is increased compared to conventional method of putting overlays on the top of the pavement. FDR can be used to stiffen the total pavement structure over the subgrade to reduce rutting effects. FDR also presents a very attractive method for fixing rural Canadian roads to a suitable serviceability level and a low decay rate.

1.2 Scope of the Study

A pavement can be damaged in many ways. Excessive load repetition, poor construction materials and several environmental factors such as freeze, thaw and heat contribute to the deterioration of pavement. Distress in pavement can occur through various mechanisms such as cracking, rutting, shoving and raveling. Any of these factors will lead the pavement to a structural failure. Further damage occurs when water infiltrates the cracks in the pavement. Water weakens the asphalt-aggregate bond, and as a result, the stiffness of the pavement is reduced. Cyclic loads, moisture condition, fluctuation in temperature and environmental effects such as freezing and thawing throughout the year can accelerate the deterioration of the asphalt layer which eventually affects the smoothness and ride quality of the road. Vehicle safety is predominantly dependent on the smoothness of the road, which is impacted by the cracks in the layer. Surveys can be carried out to investigate the cause of cracking.

Plastic deformation in the pavement occurs due to excessive, repetitive load in the wheel path. This type of pavement distortion includes rutting and shoving. The depression in the wheel path is caused by shear failure, excessive stress in subgrade soil and further compaction in Hot Mix Asphalt (HMA). Slippage between the layers of the pavement

and unstable mix cause shear flow in layers which results in shoving. Rutting or shoving not only affects the rideability but also causes safety issues. Ponding can occur in the pavement when rainwater fills the ruts and pot holes that ultimately promote the failure in pavement structure.

Inferior materials, poor gradation, low density and other inadequate material properties cause disintegration in pavement layers. Stripping in the pavement causes dispersion of particles called raveling. Several factors cause raveling in the pavement such as (a) deficient asphalt content, (b) insufficient amount of fine aggregate matrix to hold the coarse aggregate together, (c) high air void content due to lack of compaction, and (d) excessively aged (oxidized or brittle) asphalt cement binder (Roberts et al., 1996). Raveling causes the loss of skid resistance, roughness, and loose debris on the pavement. Vehicle hydroplaning occurs in raveled locations. Identification of disintegration problems in asphalt pavement is important.

The condition of the existing asphalt pavement should be investigated prior to the reconstruction of the pavement. A thorough survey can identify the basic cause of deteriorated asphalt pavement which can provide a solution for the structural or material problems. Halsted (2010) found that FDR is the most applicable pavement repair method under the following circumstances:

- If base or subgrade failure causes existing distress in pavement;
- If more than 15-20% of the existing pavement surface area requires full depth patching;
- If seriously damaged pavement cannot be corrected by placement of an overlay; and,
- If the pavement requires increased structural capacity

Many rural distressed roads in Atlantic Canada exhibit all of the above features. Because of inadequate maintenance funding and limited opportunity of alternate construction materials and methods, many roads in Atlantic Canada are generally subject to a cycle of pothole patching and overlay treatments to manage pavement condition.

FDR pavements have shown results superior to conventional method of maintenance in several roads and highways. Some of the FDR pavements stabilized with expanded asphalt have shown extremely low degrees of roughness and minimal cracking even after ten years of construction (Salah, 2013). For last 10 years the Trans-Canada Highway near Wawa, Ontario had been monitored annually by the Ministry of Transportation Ontario by using Automated Road Analyzer (ARAN), which measures International Roughness Index (IRI) and rutting. The Trans-Canada highway is a perfect example of properly constructed FDR pavement (Lane et al., 2012), which is an economically better option than the conventional reconstruction method.

Considering all the benefits of using a FDR reconstruction method, further analysis was carried out in two separate projects in New Brunswick. The properties of the materials in those projects were extensively examined as an example of consistent pavement materials for FDR construction.

1.3 Hypothesis of the Study

The hypothesis of the study is that, pulverizing the variable thickness pavement to a constant depth to achieve a specific blend of asphalt concrete to granular base for the pulverized materials, may contribute to the observed variability in the recycled varying base layer. The use of typical pavement structure investigation tools such as the relatively scattered test pits and cores along the road regardless of variable thickness may have caused the strength differences between the as-built FDR base materials and the job mix formula. Ground Penetrating Radar (GPR) may be an option to enhance the site investigation technique by contributing a much stronger statistical measure of the varying layer thickness of the pavement. Many pavements chosen for restoration with FDR may have undergone several periods of patchwork, overlays or other measures which were meant to elongate the service life. Thus, significant variation in asphalt thickness is expected throughout the length of a given road and may have a significant impact on the nature and quality of FDR aggregates and the resulting stabilized base.

1.4 Objective of the Study

The objective of this study is based on the hypothesis mentioned above. The purpose is to observe the effect of variable pavement thickness on the properties of unstabilized full depth reclaimed aggregates. This study analyzes the effect of blend ratio of recycled asphalt concrete materials to the total pulverized materials, on the quality of the FDR aggregates.

The purpose of the study was also to investigate the feasibility of using GPR for improvement of the full depth pulverized aggregate properties. The variability in pavement thickness may be reduced with a controlled uniform blend ratio throughout the pavement section by using GPR.

In order to examine the advantage of GPR, materials from two FDR projects applying two different pulverization control methods (conventional retroactive method in which the pulverizing depth is changed instantly in the field and GPR depth control methods) were analyzed and the material properties were compared. It is anticipated that the more the improvement in consistency of the FDR materials, the easier it will be to produce a well-engineered and uniform base material.

Another objective of this study is to evaluate the service life of the two pavement sections by distress analysis and the life cycle cost of each pavement section. It is expected that the usefulness of controlling the material properties would be better understood from measured service life of the pavement and cost related to it.

A better understanding about the control and quality of FDR pavements may be developed upon the accomplishments of these research objectives.

1.5 Experimental Tasks

Two projects, from New Brunswick, Canada, Route 335 near Caraquet and Route 790 near Lepreau, were taken to analyze the material properties. For the full depth reclamation in Route 335, the samples were collected in retroactive method. In this method some cores were drilled along a test section to determine the average thickness of the pavement. During the pulverization process, the depth of the pulverizing machine was changed instantly to meet the average thickness of asphalt in the pavement. In Route 790, prior to the pulverization process, a Ground Penetrating Radar survey was conducted to measure the average thickness of asphalt. During the pulverization process, the whole pavement section was divided into subsections where the blend ratios (ratio of thickness of asphalt concrete to the thickness of granular materials) were same. Prior to the FDR process the untreated materials are initially rested. Materials are collected from cores and test pits along the road to be repaired by field sampling. Those materials are then crushed and a Job Mix formula is prepared for the FDR project by the contractors.

Section 1.1 of this study suggests that the strength difference between the job mix formula and as-built FDR base could result from the thickness variability that was not accounted for by the retroactive control method of pulverization. Laboratory tests were conducted on all samples from the six locations in each of Route 335 and Route 790 projects. The lab tests were conducted to compare the consistency of the outcomes as a function of the blend ratio of HMA/granular materials.

The experimental research was carried out in six segments:

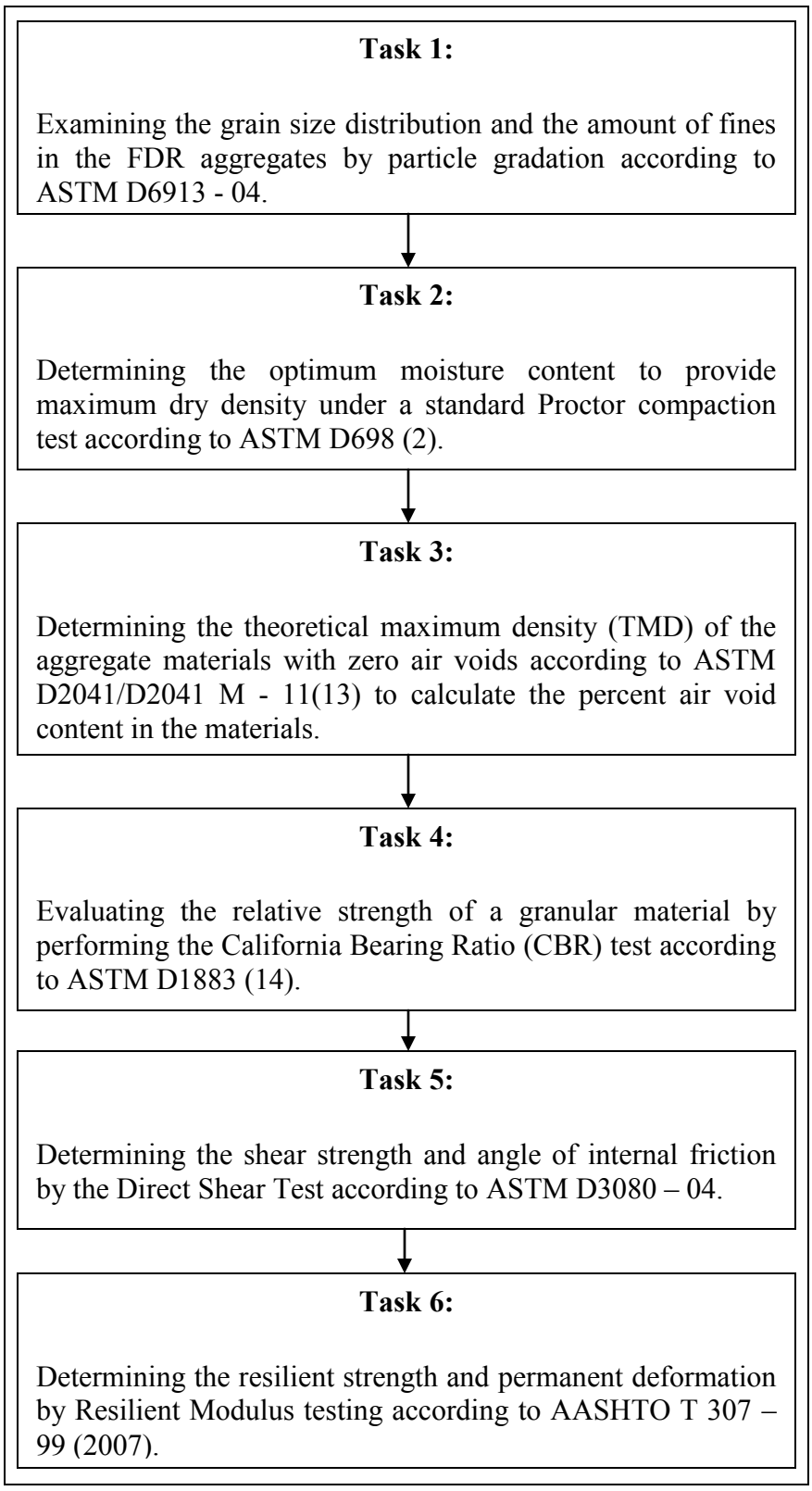

All of the above tests were done to monitor the consistency and performance of the materials and decide whether the materials could be used as an unstabilized granular base or should be stabilized to provide a suitable pavement base layer.

1.6 Organization of the Thesis

This thesis is arranged in five chapters. Chapter 1 is an introductory chapter highlighting the background of FDR. Chapter 2 is the literature review describing the FDR method and its application in Atlantic Canada. A study focusing on previous studies on the properties of the unstabilized full depth reclaimed aggregates is also provided in this chapter. Chapter 3 reports the experimental methodologies, which include the GPR technique and preparation of all the samples for Gradation, Proctor, CBR, TMD, Direct Shear test, Resilient Modulus test of all the Route 335 FDR materials. Chapter 4 of this thesis presents all the test results and provides discussion on the results. This thesis draws the conclusion in Chapter 5, which presents summary, conclusion and recommendations.

CHAPTER 2: LITERATURE REVIEW

2.1 Introduction

This purpose of this chapter is to describe the FDR process, benefits of FDR, current construction and design methods in Atlantic Canada. The fluctuation in asphalt concrete thickness on a pavement section can be one of the factors that affects the quality of FDR aggregates and resulting stabilized base materials. Expanded asphalt FDR was used in rejuvenating two individual pavement sections in New Brunswick, situated on Route 790 near Lepreau and on Route 335 near Caraquet, to analyze the result of two distinct approaches of FDR aggregate production control. In both projects the physical and mechanical properties of the materials were determined by several laboratory tests. A brief summary of the material properties are also provided in the current chapter.

2.2 What is FDR?

Full Depth Reclamation (FDR) process has been used for pavement repair around the world for more than 25 years (Sayed, 2007). The FDR process includes pulverization, stabilization and re-compaction of an entire depth of flexible pavement with a portion of underlying layer of unbound granular materials to prepare a strong and sound base layer (Wirtgen, 2010). This rejuvenated base layer is then laminated with a chip seal, thin HMA or other appropriate layer to act as a wearing surface (PCA, 2012). Research has been done on how the FDR process could be used to provide an environmentally friendly and economical means of structurally rehabilitating damaged pavements. FDR has become an immensely popular technology to reconstitute the service life of pavement structures requiring substantial structural repair and to extend attainable funding for pavement rehabilitation (Diefenderfer et al., 2011).

2.2.1 Unbound Granular Materials

Unbound granular materials are generally non-cohesive, heterogeneous materials consisting of aggregate particles, air voids and water (Chen et al., 1990). The characterization of unbound granular materials should be established on the behavior of the individual constituent elements and their interaction. Properties such as density, stress history, temperature, pore-water pressure, time and void ratio influence the mechanical behavior of unbound granular materials. It is important to understand the behavior of pavement materials and their accurate characterization for the successful implementation of any mechanistic-empirical design procedure (Adu-Osei, 2000). Additives such as emulsified or foamed asphalt, lime, cement and fly ash can be used to stabilize the unbound reclaimed materials.

2.3 FDR Construction and Design Procedure

The Wirtgen Cold Recycling Technology manual (Wirtgen, 2002) provides a FDR design method which is one of the most frequently exercised. Prior to the FDR process, the condition of the asphalt pavement must be examined and the materials of the existing pavement must be sampled and tested to determine the number, type and thickness of the pavement structure and the most appropriate sustenance treatment (Kearney et al., 1999). If the FDR concept is accepted for the project, asphalt concrete samples collected from the pavement are crushed and blended with underlying granular materials to obtain an optimal blend ratio to suit a certain gradation requirement.

According to Morian et al. (2012) the FDR construction process mainly consists of four steps following the process of placing the final surface course on the top of the pavement. The construction steps are as follows:

- Pulverization
- Stabilization
- Shaping
- Compaction

2.3.1 FDR Pulverization Procedure

In pulverization process, the asphalt layer along with the pre determined portion of base layer is ground to the desired depth. Several factors such as, thickness of the asphalt pavement, subgrade soil conditions, and expected future traffic are taken into consideration for determining the depth of the full depth reclamation (Kearney et al., 1999). The pulverizing machine, resembling to a large rototiller, has carbide teeth mounted on a cutting head with a typical width of 244 to 427 cm (8-14 ft) which is able to cut to a depth of about 457 mm (18 in). Typical depth of pulverization is generally 150 to 254 mm (6 to 10 in). The rotation of the cutting head is always in the 'up' direction (Morian et al., 2012). Figure 2-1 shows a picture of cutting head.

Figure 2-1 Cutting head of a pulverizing machine (Morian et al., 2012)

2.3.2 FDR Stabilization Procedure

The next stage after the pulverization process is stabilization. There are generally three methods of stabilization, such as mechanical, chemical and bituminous. The selection of a stabilizer to be used is dependent on the changes to various physical properties required for each project (Barnes et al., 2012). For improving gradation and increasing the strength of the pulverized materials, granular materials are added to the in-place materials. The stabilization of pulverized materials by adding granular materials is called mechanical stabilization (Kearney et al., 1999). Portland cement, calcium chloride, hydrated lime and coal fly ash are used in chemical stabilization process. The addition of chemical stabilizers changes the particle structures and leads to improved material properties. If the pavement is stabilized by using the chemical stabilizers, it should be cured to gain strength (Salah, 2013). Emulsified asphalt and expanded asphalt are used in bitumen stabilization process. Bituminous stabilization reduces fatigue and moisture susceptibility and increases stiffness and shear strength (Muthen, 1998).

2.3.2.1 Bituminous Stabilization with Expanded Asphalt

The FDR aggregate formed from the pulverization if stabilized with the expanded asphalt yields a higher inter-particulate frictional resistance to deformation. The expanded asphalt stabilized FDR aggregate will also add cohesion and stiffness within the material. Rutting failure instead of fatigue tends to happen in the expanded asphalt stabilized FDR bases, as the aggregates are discontinuously bound. On the other hand, Portland cement binder produces a more continuous bond throughout the layer, resulting in a comparatively weak, rigid base that tends to ultimately fail under fatigue loading. As reported by Halsted (2010), mechanical properties of unbound granular materials that are capable of improvment with additives include:

- Plasticity index
- Dust generation at the time of construction;
- Durability and strength;

- Moisture susceptibility; and,
- Moisture content

Expanded asphalt is produced by injecting cold water into hot asphalt cement, which results in spontaneous foaming and expansion when the liquid is turned into vapor and trapped by thousands of asphalt bubble (Asphalt Academy, 2009). The foam dissipates in less than a minute. In mixing machine there is an expansion chamber in which this process is occurred. Asphalt Academy (2009), describes the expansion chambers as "relatively small thick-walled steel tubes, approximately 50 mm in depth and diameter, into which asphalt and water (plus air on some systems) are injected at high pressure". Figure 2-2 is used to illustrate the procedure.

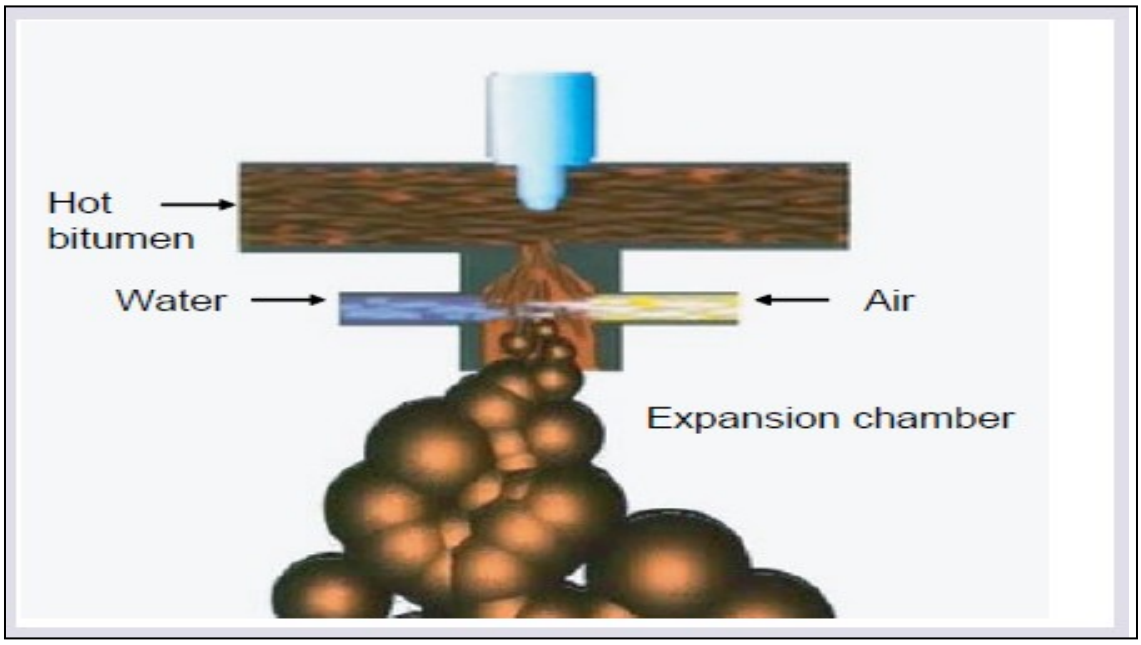

Figure 2-2 Foamed asphalt (expanded asphalt) production in expansion chamber (Asphalt Academy, 2009)

The higher volume of the foam results in better distribution of the asphalt in the aggregate. After this process the expanded asphalt is combined with the aggregates and within a minute the water is vaporized leaving the aggregates coated with asphalt cement.

Asphalt Academy (2009), explained the procedure which is given below.

"The asphalt bubbles erupt during the mixing process that produces tiny asphalt particles and disseminate throughout the aggregate by adhering to fines and form mastic. The moisture, added in the mix before the inclusion of the foamed bitumen, influences the dispersion of the asphalt during mixing. During compaction, the asphalt particles in the mastic are substantially compressed against the larger aggregate particles that result in localized non-continuous bond called 'spot welding'."

These asphalt coated aggregates regain original adhesive properties (Muthen, 1998). Asphalt Academy (2009), says that the expanded asphalt does not coat the aggregates completely and the cement dispersion primarily takes place among the finer particles of the materials. If there are insufficient fines in the materials, a poor mix will result with many bitumen rich lumps or "stringers". This is the reason why, the minimum requirement normally specified is 5% (by mass) passing the 0.075 mm sieve which will result in low Voids in Mineral Aggregates in the particle packing.

Expansion Ratio (ER) and Half-life ($\tau_{1/2}$) are the two important factors for the basis of asphalt's suitability for use. According to Wirtgen (2010), the definitions of the both terms are given below:

"Expansion Ratio: It is the measure of the viscosity of the foam and determines how well the bitumen will disperse in the mix. It is calculated as the ratio of the maximum volume of foam relative to the original volume of bitumen." and

"Half-life: It is a measure of the stability of the foam and provides an indication of the rate of collapse of the foam. It is calculated as the time taken in seconds for the foam to collapse to half of its maximum volume."

As stated in Asphalt Academy (2009), the optimum water content required for obtaining the foaming properties of the expanded asphalt FDR can be determined by the average value of the following water contents:

- Those yielding the minimum acceptable expansion ratio (≥ 8 times), which is the ratio of the maximum expanded volume to original binder volume; and,
- The minimum acceptable half life (≥ 6 seconds), which is the time required for the expanded asphalt to collapse to half of its maximum volume.

The method of determining the optimum water content required for the foaming properties of the expanded asphalt is shown in Figure 2-3.

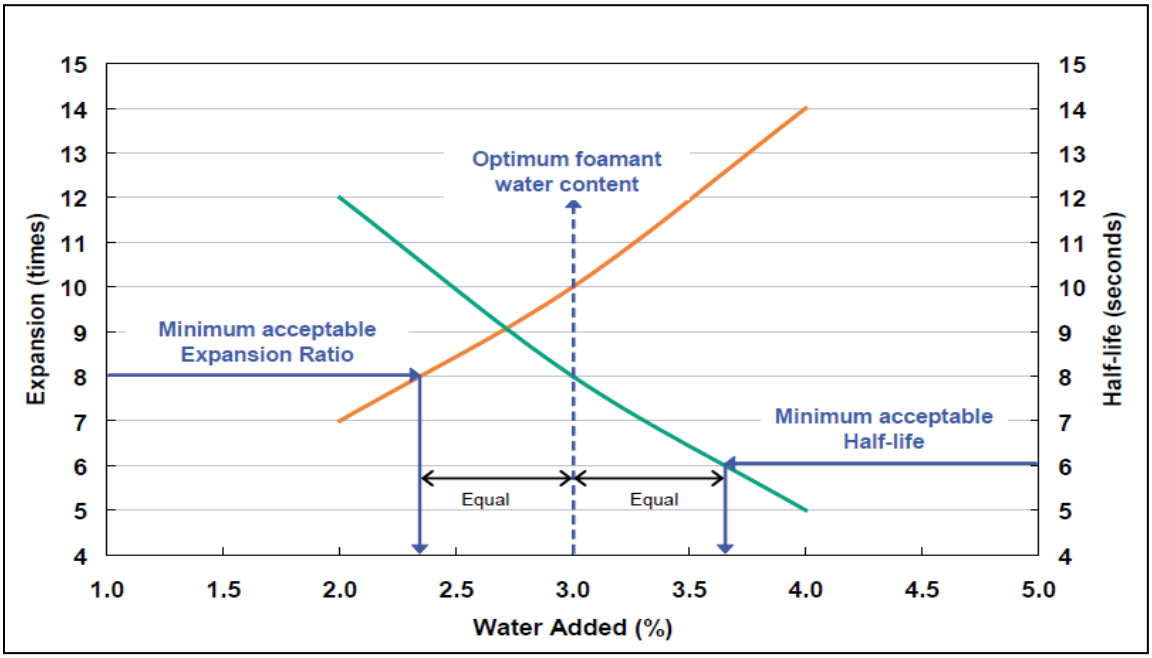

Figure 2-3 Determination of optimum foamant water content (Asphalt Academy, 2009)

2.3.3 FDR Shaping and Compaction Procedure

After the stabilization the pavement is shaped and compacted. A grader is used to shape the pavement. After shaping the pavement, a sheep's foot roller is used for compaction.

Compaction techniques should be selected according to the depth of the reclamation (Morian et al., 2012). The base layer should attain the maximum density during compaction. Figure 2-4 and Figure 2-5 are provided to illustrate the shaping and compaction procedure.

Figure 2-4 Shaping the pavement with a grader (Morian et al., 2012)

Figure 2-5 Compacting the pavement with a sheep's foot roller (Morian et al., 2012)

2.4 Typical Construction and Design of FDR in Atlantic Canada

Atlantic Canada uses the jaw crusher to decrease the asphalt concrete specimens to a manufactured Recycled Asphalt Pavement (RAP) since the Wirtgen manual does not give precise instruction on the materials preparation and blending method. The in-situ asphalt content can be determined by extracting the asphalt binder from a sample of the prepared RAP, permitting post-stabilization quality assurance testing which assures the addition of the correct dosage of expanded asphalt to the stabilized base materials. A Job Mix Formula (JMF) is designed for a blend of FDR aggregates, which contains a blend of Manufactured RAP, some mineral filler to simulate dust production at the time of secondary stabilization phase of construction, possibly a small percentage of Portland cement and in situ granular materials. To obtain the gradation within the specified limits, the proportion of RAP and granular materials can be adjusted and corrective aggregate may be used if needed. For plasticity index of recycled materials exceeding 10, 0.5-1.0% Portland cement may be substituted by 2% hydrated lime (Wirtgen, 2010). The New Brunswick Department of Transportation (NBDOT) specified that the gradation limits for expanded asphalt stabilized FDR would be within the range of 45-70% passing the 4.75 mm sieve opening and 5-20% passing the 0.075 mm sieve opening which fall within the limit set by Wirtgen manual (2010) (NBDOT, 2011).

The gradation limit suggested by the Wirtgen manual is listed in Table 2-1. These limits are given to ensure the adequacy of the mechanical and strength properties of the stabilized base. The total pulverization depth is dependent on the bulk densities of crushed RAP and granular base and also the mean HMA thickness within the design section, which means that the proportion by mass of the two materials should meet the gradation requirement (Barnes et al., 2012).

Table 2-1 Recommended expanded asphalt FDR aggregate gradation limits (Wirtgen, 2010).

Sieve Opening (mm)	Percent Passing (%)	
	Ideal Range	Less Suitable Range
50	100	
37.5	87 - 100	
26.5	77 - 100	100
19.0	66 - 99	99 - 100
13.2	67 - 87	87 - 100
9.6	49 - 74	74 - 100
6.7	40 - 62	62 - 100
4.75	35 - 56	56 - 95
2.36	25 - 42	42 - 78
1.18	18 - 33	33 - 65
0.600	14 - 28	28 - 54
0.425	12 - 26	26 - 50
0.300	10 - 24	24 - 43
0.150	7 - 17	17 - 30
0.075	4 - 10	10 - 20

Trial batches are prepared by mixing JMF design FDR aggregate blend with the different amounts of binder at the expected optimum value. Sufficient water is added to obtain the optimum moisture content and density to prepare 100 mm diameter briquettes for both indirect and direct tensile strength testing. Generally, the Marshall method is used for compacting mixtures with 75 blows on each face of the specimens. The mean dry and soaked Indirect Tensile Strength (ITS) are obtained from various trial batches to calculate the optimum binder content to meet the specified soaked and dry ITS values and Indirect Tensile Strength Ratio. Dry ITS was used to be done on the materials at 60^0C before and at that temperature the shape of the materials were deformed as asphalt tend to soften and the materials were more stiff. The MTO changed the temperature to 40^0C, so that the shape of the materials does not change and at 40^0C the materials are not as stiff as used to be at 60^0C. That is why the MTO specifications reduced the dry and soaked ITS values in 2012 which listed in Table 2-2.

Table 2-2 Strength Specifications for Expanded Asphalt Stabilized FDR Base

Year	Minimum Dry ITS (kPa)	Minimum Soaked ITS (kPa)	Tensile Strength Ratio	Standard Specification
2011	300	150	0.5	NBDOT
2012	225	100	0.5	MTO

Recent history of many projects in New Brunswick showed significant variation of as-built material properties in spite of a well established design process. The mean soaked and dry ITS of expanded asphalt FDR and corresponding indirect TSR, those obtained from various projects of New Brunswick since 2006, are listed in Table 2-3.

Table 2-3 Sample of strength parameters from various FDR project in New Brunswick. (Alward, 2011).

Location	Soaked ITS (kPa)	Dry ITS (kPa)	TSR
Churchland	392 - 422	427 - 463	0.47-0.80
Rte. #313	182 - 302	324 - 398	0.52-0.79
Rte. 114, 0.8 km	205 - 237	77 - 99	0.70-0.73
Rte. 335, Sect. 2	151 - 260	378 - 514	0.31-0.55
Rte. 335, Sect. 1	151 - 170	304 - 354	0.46-0.56
Rte. 335	127 - 270	320 - 626	0.29-0.43
Rte. 335	147 - 257	283 - 412	0.37-0.62
Rte. 790	113 - 194	168 - 274	0.55-0.89
St. Marys St.	103	300	0.34
Rte. 3	299 - 592	316 - 634	0.50-0.90

From Table 2-3, it is clear that neither the dry nor soaked ITS followed the minimum specification requirements in most of the cases. It may be possible that some of the actual pavement structure features do not match the conditions assumed during the preparation of the design. The stiffness of the materials may vary significantly with variable depth of pavement. From the above table it can be seen that some of the samples fail to reach the specification for dry ITS, some of them fail to reach the specified soaked ITS. All the samples must meet the minimum specification of dry ITS, soaked ITS and TSR. It is not accepted if the samples just meet the minimum specification for TSR but not meeting the specification for soaked or dry ITS. For Route 114, 0.8 km as mentioned in Table 2-3, the soaked ITS and TSR meet the minimum specification but the samples failed to reach the minimum dry ITS.

2.4.1 Typical method of Pulverization in Atlantic Canada

Atlantic Canada accounts for a two stage in-situ FDR process. The first stage suggests utilizing data obtained from core or test pits to measure the average thickness of the asphalt concrete layer. In this process, the initial pulverization and compaction takes place on the degraded pavement so that it can carry the local traffic until the next stabilization work starts. Typically one pass is used in first stage. The second pass is needed to ensure adequate pulverization and stabilization when it is foamed. The same equipment is used during the second stage of pulverization for mixing the pulverized FDR aggregates with the binder. In this way large HMA chunks which may not have been fully pulverized during the first stage of pulverization are further degraded. Some anecdotal evidence also indicated that approximately two percent of dust is generated in gradation after the second stage of pulverization (Geiger et al., 2007).

Sufficient pulverization depth should be provided to cool the cutting tools with ambient moisture residing in the granular materials seems to reduce wear on the equipment. Approximately 50:50 blend of HMA to granular materials is the best to ensure adequate grinding of HMA and minimize pulverization tool wear. When the tools contact the asphalt, the pulverization depth should be shallow enough so that it can avoid a vertical or slightly forward and upward cutting motion. In cases where relative thickness of HMA layer is small compared to the total pulverization depth, large chunks of asphalt start to break, rather than form into FDR aggregate particles. If the HMA layer is too thick compared to the total pulverization depth, the cutting tool gets hot and the teeth start to wear. The pulverization process is showed in Figure 2-6.

Figure 2-6 Typical pulverization process (Scott, 2010)

Barnes et al. (2012) mentioned about the two general methods which are used for controlling the pulverization depth:

- A constant pulverization depth is established based on average thicknesses of the pavement at these sample locations. Sometimes specific pulverization depths at various locations are cited according to the pavement thickness detected at the nearest core locations.
- The second method is via the use of a retroactive depth control approach where the HMA thickness is observed to vary significantly in the field. The thickness of the asphalt concrete is measured by this method at the time of construction at the edge of the pulverized material behind the pulverization process. This measurement is then used to assume the thickness of the asphalt concrete ahead of the pulverizing equipment. An adjustment in the pulverization depth is made for maintaining the specific blend ratio.

Optimum moisture content maximizes the compaction density; hence sufficient additional moisture is often added. Water is typically added only during the stabilization process. An amount of water should be set and added carefully so that the additional water does not soak the pavement materials. The pulverization process enables aeration

of the wet pavement and dries the materials below the optimum moisture content (at optimum moisture content the highest density can be attained) for the second stage of the process. Two adjacent passes are generally needed to fully cover a typical 3.5 meters wide lane. For a desired approximate final depth, grade and cross slope, the stabilized FDR aggregate materials are laid and shaped on the pavement. To establish a strong and sound pavement, proper compaction of reclaimed materials helps to develop adequate strength and modulus (Kearney et al., 1999).

2.5 Benefits of FDR

There are some environmental benefits of using FDR which include eliminating waste materials by reusing the existing pavement materials on-site, reducing the requirement for virgin aggregates, and reducing emissions associated with transportation of materials (TxDOT, 2005).

In pavement engineering several recycling alternatives such as cold in-place (CIR), hot in-place (HIR) and full-depth reclamation (FDR) can be applied depending upon the pavement categories and type of deterioration (Holt et al., 2009). According to Kearney et al., (1999), in partial depth reclamation such as CIR or HIR only the materials obtained from the asphalt layer are reused therefore, partial depth recycling procedure is applicable when the distress is just at the pavement surface and not resulting from base or subgrade failure. The pulverization depth in HIR process is typically 19 to 37.5 mm (0.75 to 1.5 in) whereas in CIR the depth of pulverization is 75 to 100 mm (3 to 4 in). In CIR or HIR, the asphalt pavement is required to be sealed with a thin HMA surface course. The partial depth reclamation is good for the distresses like cracking, raveling or minor rutting (Kearney et al., 2009). When the failure occurs in the base layer FDR is the best option to mitigate the problem as in this process, the total asphalt layer along with a portion of underlying base layer is uniformly crushed, pulverized and stabilized for getting a damage free base. The typical pulverization depth in FDR process is 150 to 300 mm (6 to 12 in) (Kearney et al., 1999).

Structural benefits could be gained by using FDR as well. One maintenance approach that has been used in Canada is to put a hot mix asphalt concrete overlay on the top of the existing damaged asphalt concrete pavement. Areas with severely deteriorated pavement are generally recommended to be repaired by removal and replacement with new hot mix asphalt concrete prior to overlay placement, but this is rarely practiced on rural highways. Stress concentrations in the overlay are a result of the localized reduction in stiffness caused by the pre-existing cracking damage in supporting materials which eventually causes reflective cracking that reaches to the surface (Barnes et al., 2012). FDR process can remove the damage caused by stress concentration and cracks from the pavement by crushing the bound materials to aggregate structure and stabilizing it or by using the aggregate structure as a granular base. The cohesiveness, strength and modulus of the base can be improved by stabilizing the FDR aggregates. It thus reduces the stresses on subgrade and needs thinner wearing surface to withstand the traffic load.

Cost benefits include the reduction in processing and trucking aggregates to the site as well as a fast production rate compared to most alternative rehabilitation methods, thus reducing both construction and user delay costs (Barnes, 2010). By utilizing FDR, construction costs have been found to be reduced by as much as 25 to 50 percent, compared to conventional rehabilitation methods (Marquis, 2007). PCA (2005) has shown some real life projects where the cost was reduced by using the cement stabilized FDR which is illustrated in Table 2-4.

Table 2-4 Cost comparison of stabilized FDR and conventional method (PCA, 2005)

Year	Project	FDR stabilized	Removal / replacement w/aggregate and asphalt overlay	Cost savings
1999	Westminster, California	6% cement with asphalt overlay cost $10.98 / sy	Cost $21.78 / sy	50%
1999	Spokane County, Washington	5% cement with a chip seal overlay cost $91,000 / mi	Cost $135,000 / mi	33%
2004	Long County, Georgia	7% cement with asphalt overlay cost $127,000 / mi	$218,000 / mi	42%
2004	Hudson, Ohio	10% cement cost $12.94 / sy	$22.66 / sy	43%

Figure 2-7 FDR process in existing pavement

2.6 Studies for the Tests on Unstabilized Granular Materials

A pavement is a structure containing different layers of chosen materials arranged on top of a natural or filled subgrade (Araya, 2011). The most practical composition of the pavement layer incorporates the material types and thickness for the pavement, the properties of the sub-soil, the climatic condition, cost and the traffic to be carried throughout the service life (Araya, 2011). The pavement layers constitute the top asphalt layer, base and/or sub-base with/without an underlying capping layer (Araya, 2011). Many factors such as void ratio, density, stress history, time, pore-water pressure, and temperature affect the mechanical properties such as strength, stiffness or modulus, and resistance to permanent deformation of unstabilized full depth reclaimed aggregate materials (Adu-Osei, 2000). For this reason it is essential to control the material related

factors such as gradation, soil moisture and optimum density that affect those mechanical properties of reclaimed aggregate materials (Geiger et al., 2007). The aggregate properties include the structure, density, void ratio, permeability and strength, all of which change with different conditions such as construction, loads, environment etc. (Araya, 2011). The gradation of aggregates is one of the fundamental tests of the pavement components to attain the compaction with minimum effort to develop a tight interlock. After measuring the amount of constituent part of the reclaimed aggregates that is coarse and fine materials, the next stage comes with the establishment of an optimum moisture and optimum density relationship for the aggregates. The ultimate stage is to measure the strength and stiffness of the materials (Geiger et al., 2007). For achieving all these qualities a reasonably constant gradation of aggregates is required.

2.6.1 Gradation for Unstabilized Full Depth Reclaimed Materials

For determining the specification for the aggregate gradation, the particle size distribution of the existing pavement should be considered (Wisconsin Department of Transportation, 1997). Studies have shown that even though a vast range of particle size distributions function well as unstabilized sub-base, it is essential to make a reasonably consistent gradation for the sub-base materials so that the compaction equipment can produce uniform support necessary for good pavement performance (ACPA, 2008). The performance of recycled base is precisely related to the proper gradation of FDR aggregate materials. All the other physical properties such as density, moisture, strength, modulus and stiffness are affected by the gradation of the material. The effect of gradation on the recycled pavement is so great that it is essential to optimize and control the particle size distribution of the pulverized material accordingly (Geiger et al., 2008).

At the time of pulverization, precautions should be taken so that the resultant materials should neither be too coarse nor too fine and thereby can affect the gradation (Holt et al., 2009). In 1907, Fuller and Thompson established an equation for a grading curve given in Equation (2-1) in which the maximum density can be acquired for an aggregate when n = 0.5 (Fuller et al., 1907). United States Federal Highway Administration altered the

equation in the 1960s by using the "n" value 0.45 to delineate the optimum size distribution to attenuate the Voids in Mineral Aggregate (VMA) of hot mix asphalt concrete (Roberts et al., 1996). A gradation curve developing maximum density would associate a particle organization in which small grains are locked within the larger particles contracting the void space in particles (Pavement Interactive, 2009).

The equation for Fuller's maximum density curve (Fuller et al., 1907) is as follows:

$$P = 100 \left(\frac{d}{D}\right)^n \qquad (2-1)$$

where,

P = total percent by mass of material passing sieve size, 'd' ;

d = selected sieve size;

D = maximum size of the aggregate; and,

n = gradation coefficient, according to Fuller and Thompson the value is 0.5, but later FHWA adapted the value to 0.45.

size of the particles and sieve openings are given in mm for this study

Denser particle packing with the least void space among the aggregate particles followed by maximum compaction and density can be obtained if the gradation curve matches nearly to this theoretical curve formed from Equation (2-1) (Roberts et al., 1996). A higher density renders a higher modulus of stiffness by increasing the inter-particulate contact and load transfer through the base. Thom et al. (1988) showed that an excessive amount of fines lowers the stiffness and minimizes the resistance to permanent deformation. An elevated density and stiffness in the base layer reduces tensile stress in the wearing surface as well as enhances reduction in the vertical stress applied on the subgrade. To assure durability in HMA, a certain amount of air voids is needed that allows asphalt cement to be inserted (Roberts et al., 1996). An inadequate amount of fines will result in improper dispersion of foamed asphalt particles following poor adhesion in recycled particles as the dispersion of asphalt cement takes place among the finer particles in the material (Diefenderfer et al., 2011).

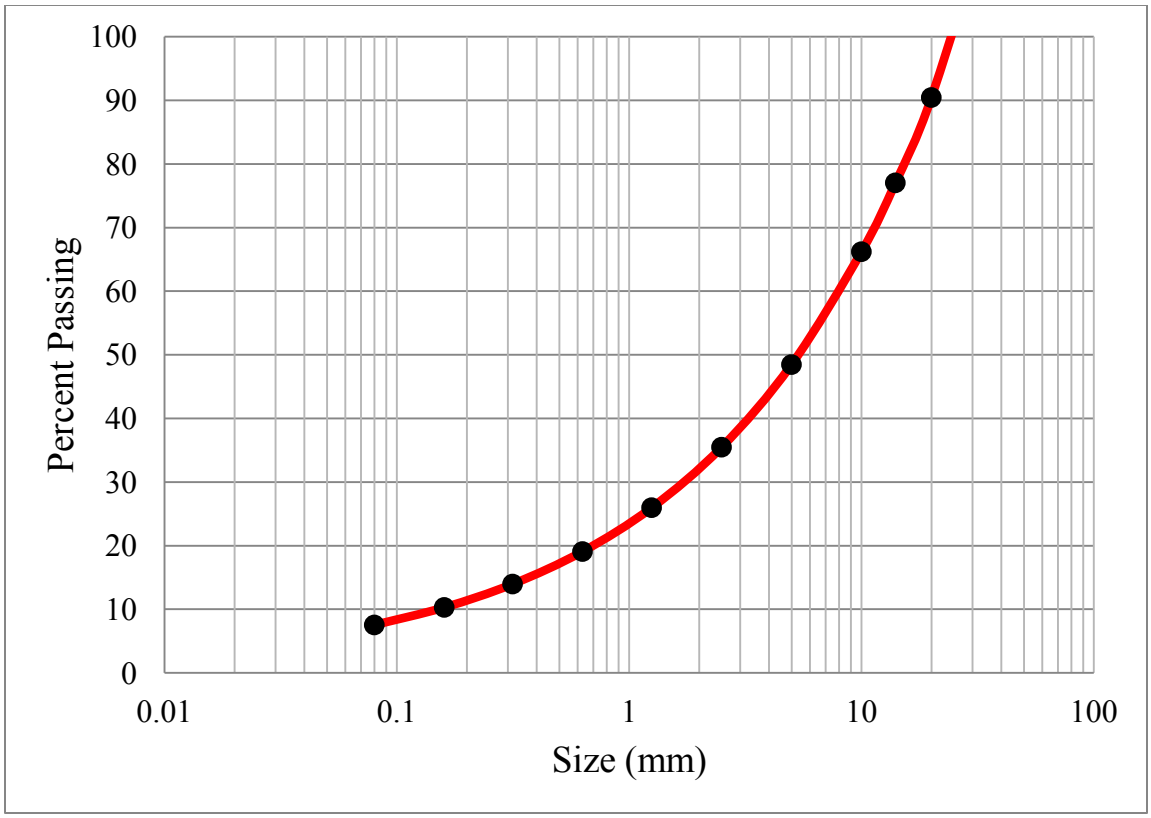

Figure 2-8 Optimum gradation of a material with maximum aggregate size 25 mm

By using Equation (2-1) the optimum gradation can be obtained by which the maximum particle packing could be achieved. An example is shown in Figure 2-8 with maximum particle size 25 mm for a typical FDR project. The size distribution acquired from the Equation (2-1) attenuates the Voids in Mineral Aggregate (VMA); as a result, the density, strength, modulus and stability are improved. The load transfer of the FDR granular materials depend on the inter-particle contact. The purpose of mixing the pulverized materials at the time of FDR should be obtaining the aggregates which are near to the particle size of maximum density. According to Asphalt Academy (2009), various factors can create difficulties in the blending of pulverized materials for maximum density which are as follows:

- Original asphalt mix;
- Geometry and amount of cracking of pavement;

- Thickness of the existing pavement;
- Conditions and bonding between any overlays;
- Degree of oxidation of the reclaimed aggregates;
- Temperature of asphalt during recycling process; and,
- Equipment.

The main limitation of gradation is that it only considers the size distribution without providing the description of shape, texture and surface roughness of particles. Several studies, by Barksdale et al., (1989), Kuo et al., (1996) and Molenaar et al., (2006), described that the aggregates' morphological properties such as shape, surface texture, angularity and roughness significantly impact the performance of unbound granular materials. Araya (2011) mentioned, "*It is generally recognized that aggregates with equi-dimensional, angular shapes and rough surfaces increase the strength and durability of unbound granular layers in pavements*". To reproduce the exact gradation in the field is challenging. As a result, the gradation limits have been established to keep the particles within a limited range of values. Most of the pavement construction agencies often specify the maximum particle size, percent passing a 5 mm sieve for the coarse aggregate and percent passing a 0.08 mm sieve for fine aggregates (Salah, 2013).

According to the Portland Cement Association (2005) the typical specifications for proper gradation after pulverization is 100 percent passing the 75 mm sieve, a minimum of 95 percent passing the 50 mm sieve, and a minimum of 55 percent passing the 5 mm sieve. The specification followed by Nova Scotia and New Brunswick are listed in Table 2-5.

Table 2-5 Standard specifications for expanded asphalt for FDR mixes of NBDOT (2011) and NSTIR (2012)

Sieve Size (mm)	Cumulative Percent Passing	
	NBDOT Specification	NSTIR Specification
50.0	100	100
5.00	45-70	35-65
0.08	5-20	7-15

A better unstabilized sub-base can be produced by providing maximum particle size of no more than one third of the sub-base thickness and by limiting the amount of fines by less than 15% passing the 0.08 mm sieve (ACPA, 2008). Too many fines in an unstabilized sub-base may hold water for longer period of time which will lead to erosion, pumping and frost action. For preventing damage caused by frost action, ACPA (2008) recommended materials to be provided are: ±10% for materials 1 in. (25 mm) and larger, ±8% for materials between 1 in. and No. 4 (25 mm and 4.75 mm) and ±5% for materials No. 4 (4.75 mm) and smaller.

As there is immense tolerance for variability in the specified gradation requirements by various agencies responsible for FDR, The Wirtgen Group (2010) provided an instruction on the specific gradation limit to minimize the variability in expanded asphalt stabilized materials. Particle gradation satisfying the limits are considered as the most suited for expanded asphalt stabilization. The Wirtgen specification is shown in Figure 2-9.

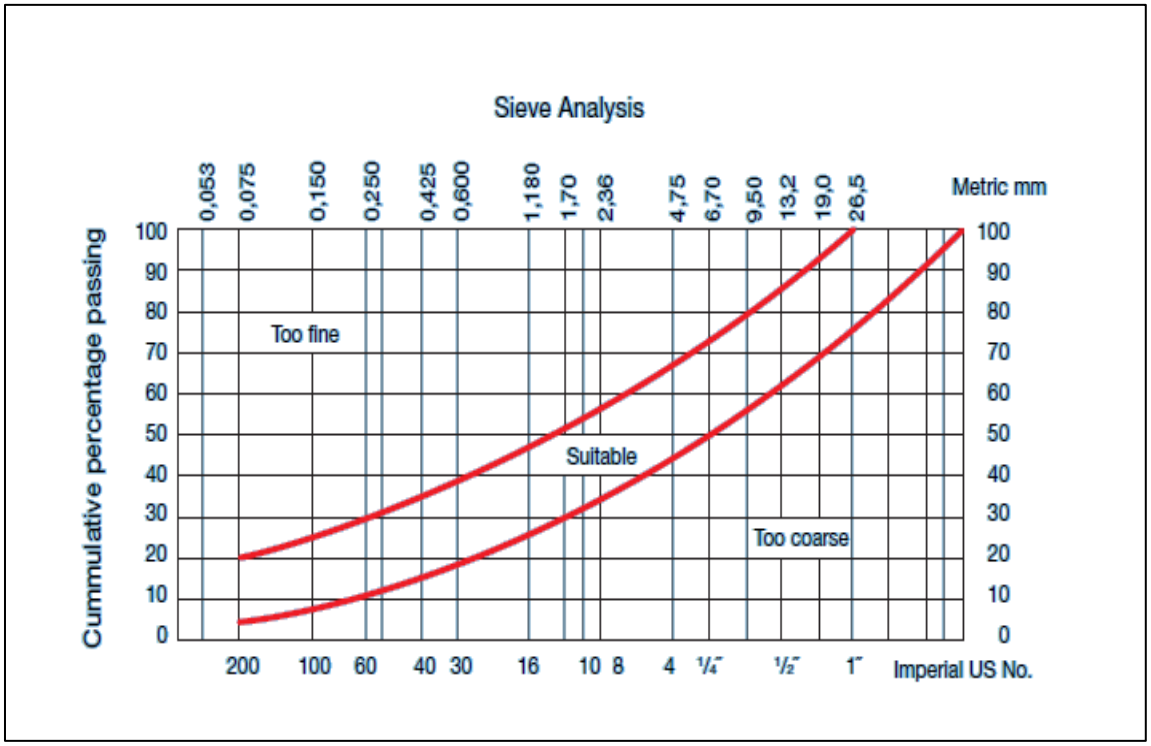

Figure 2-9 Wirtgen recommendation of FDR gradation limit for expanded asphalt stabilization (Wirtgen Group, 2010)

The Wirtgen manual does not specify the state of the materials that is whether the gradations were done on the unbound FDR materials after the extraction of the asphalt cement or the gradations were done on the conglomerated particles prevailing in the FDR materials bound with finer particles together.

2.6.2 Laboratory Compaction Test for the Unstabilized Full Depth Reclaimed Material

Compaction is the mechanical densification of soil by eliminating air voids and rearranging soil particles with little or no reduction in moisture content (Das, 2010). Compaction has some undeniable benefits (Handy, 2007). As dry unit weight of materials is used to measure the degree of compaction, it helps to improve the strength of loose soil materials (Das, 2010). Compacted soils exhibit some benefits over un-compacted soils by hardening and diffusing more water (Handy, 2007). Compaction of materials helps to increase the bearing capacity, slope stability and decrease the unsuitable settlement and hydraulic conductivity (Das, 2010).

Figure 2-10 Test setup and equipments for standard and modified Proctor Compaction test (adopted from TEST-LLC, 2013)

Compaction is dependent on the water content of the material. Water acts as a softening agent on the materials to be compacted. With insufficient water the compaction is not satisfactory, at optimum moisture content the most suitable compaction can be attained and if the water added is more than the optimum moisture content, the soil starts to flow as very little air is left in the soil and this produces a poor compaction (Das, 2010). In a compaction test, the dry unit weight of material increases with an increase in added water. After a certain point, dry unit weight tends to decrease with an increase in moisture content. That particular water content after which the unit weight decreases is the optimum moisture content. At the optimum water content, dry unit weight reaches its maximum value.

The purpose of using the standard Proctor test is to maintain a constant level of compaction effort. It also helps to find the optimum moisture content as well as optimum density for the field (Das, 2010).

According to Asphalt Academy (2009), the optimum moisture content and moisture to density relationship is dependent on the compaction method applied. The optimum moisture content of the untreated materials is used in road construction. The moisture content of the mixed material is one of the most influential variables that has a precise impact on the end-product (Asphalt Academy, 2009). A blend of Reclaimed Asphalt from patches and pavement layers with a granular base material will yield a mix of a lower optimum moisture content value than the initial base material.

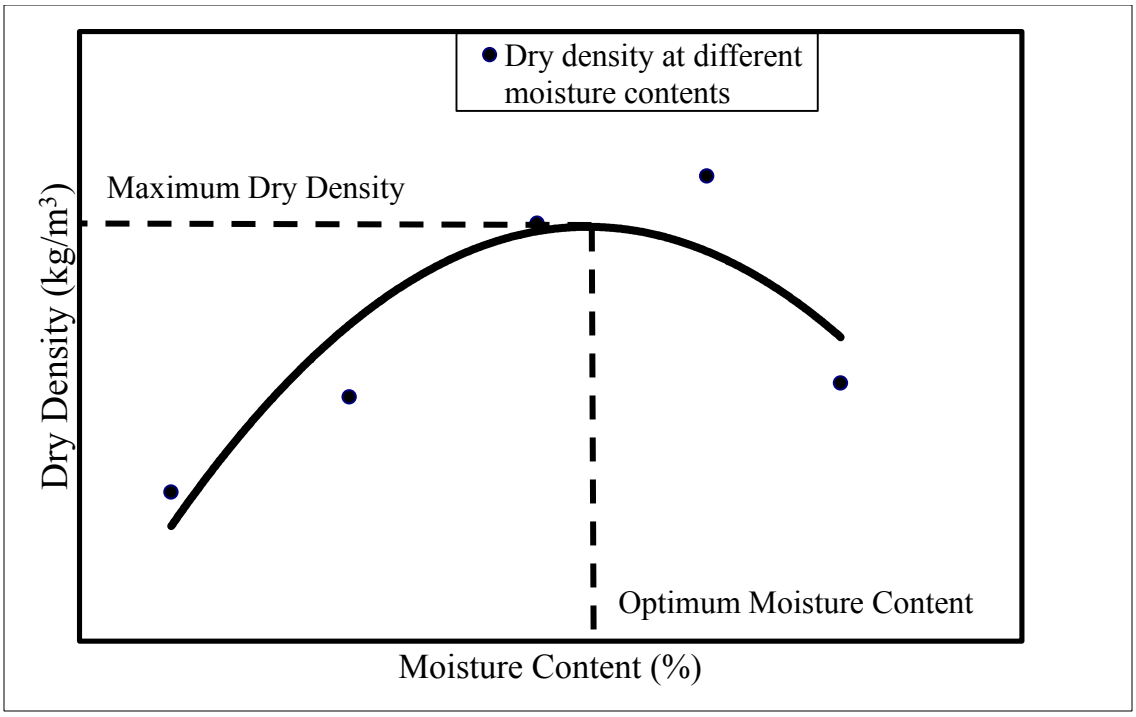

Figure 2-11 Typical Moisture – Density relationship curve

2.6.2.1 Optimum Moisture Content

Moisture content is an extremely sensitive issue in determining the resilient behavior of the unstabilized granular materials (Araya, 2011). According to Semmelink (1991), the ultimate strength of the pavement is influenced by several factors such as moisture content, effort of compaction applied and support of material beneath at the time of compaction. After extensive research on granular materials, Sweere (1990) found that moisture plays an important role in stiffness characteristics in the granular materials.

In the past it had been predicted that the optimum moisture content provides the ideal amount of water for lubricating granular materials to decrease sliding friction, whereas the effect of water on non-clay aggregate materials is to increase the sliding friction rather than decrease it (Handy, 2007). Water is a polar element with molecules of positive and negative direction that attenuates ionic bonding in a mineral surface which results in

the intrusion of water more easily and consequently it develops sliding friction (Araya, 2011).

Proctor (1933) acknowledged that the compaction is primarily influenced by moisture content which led him to design a test which defines the role of moisture content by keeping the other variables constant. He came to the conclusion that the optimum moisture content yields the highest density for a given compactive effort. He also found that more energy will be required to accomplish a certain density for extremely dry soil, and that for obtaining the same density for extremely wet soil, no energy will be adequate. The optimum moisture content of coarse aggregate is considerably modified by its absorption (Jackson, 2012). According to Raad et al., (1992), the resilient properties of well graded materials with excessive amounts of fines are more susceptible to the amount of water added.

The aim of performing laboratory tests is to check the optimum amount of mixing water needed for field compaction to attain highest density in the field. For a certain compactive effort and given dry density the soil is likely to be less coagulated for compaction on the wet side and more on the dry side. For particular water content in the mold, an increase in the compactive effort makes the soil more scattered on the dry side and additional water content makes the soil less permeable on the dry side of the optimum moisture content as well. Raising the compactive effort decreases permeability by increasing the dry density and orientation of particles. A sample compacted at high stress is less compressible at wet side whereas at low stress it is less compressible at the dry side (Das, 2010).

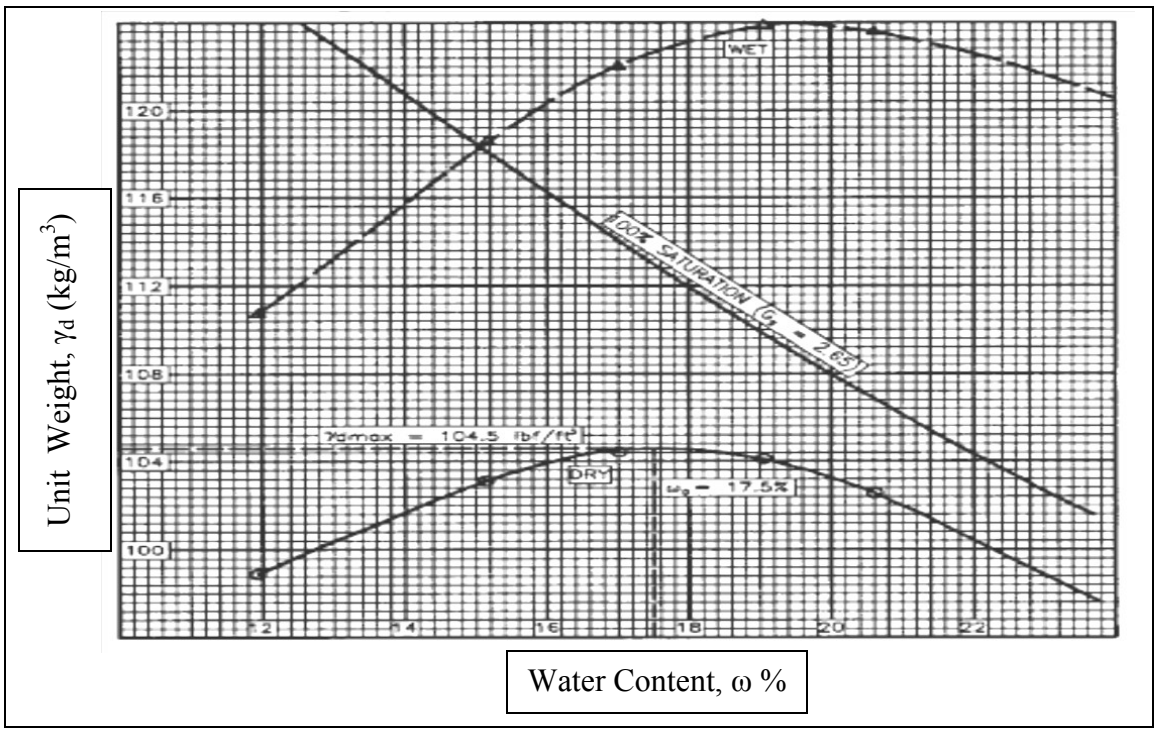

Figure 2-12 Compaction curve with 100% saturation (zero air void) line (ASTM, 2007)

2.6.2.2 Optimum Density

According to Asphalt Academy (2009), the optimum density of a material is the highest density obtained at a specific compaction carried out at different moisture level. The moisture level corresponding to the optimum density is called the optimum moisture content. Various levels of compaction effort are demanded for a pavement section with varied material quality for maximizing the density. As a result, the maximum dry density may differ along that pavement section. A pavement section may notice various levels of modulus, strength and performance which would be responsible for the distinctive as-built strength result. In the construction of a pavement, the density of total aggregate framework is one of the most essential factors controlling stiffness and protecting the pavement from permanent deformation (Araya, 2011). Barksdale (1972) noticed that an increase in the degree of compaction (expressed as percent of maximum Proctor dry density) raises the stiffness and resistance to rutting of materials. During the construction

of a granular layer, the field compaction level is generally stated as a percentage of maximum dry density obtained in a laboratory Proctor compaction test (Araya, 2011). Though the standard Proctor Test is the most commonly used test, some literature (Semmelink, 1991) suggests that vibratory compaction method is the more suitable for unbound granular materials.

Thom et al. (1988) and Barksdale (1991) found that additional fines content in aggregate materials decrease the effect of density. Shear strength of materials increases with increasing dry density. According to Araya (2011), "*A material having high shear strength may be more difficult to compact, as they also resist the shear stresses induced by the compaction.*" Semmelink (1991) noticed that at lowest optimum moisture content, well graded coarse materials show highest maximum dry density. Optimum moisture content increases with increasing fine materials which eventually decreases the maximum dry density. The physical surface area of the material increases with reduced particle size, and as a result more moisture is needed to make the surface wet (Semmelink, 1991). Thus the particle size distribution influences the optimum moisture content and maximum dry density of the material. During stabilization, additional fines increase the optimum moisture content and decrease the dry density (Paige-Green et al., 1989).

The shape and texture of aggregate materials also influence dry density and optimum moisture content. The impact of shape and texture on maximum density and optimum moisture content is lessened with modification of gradation of materials from well graded to uniformly graded or well graded to poorly graded (Semmelink 1991). In some literature it is also mentioned that negative pore water pressure creates the concave portion on the dry side of the moisture density curve (Olson, 1963).

Materials with uniform particle sizes produce a less dense mixture than materials with a wide range of particles. As a result, different sizes of particles are blended together to obtain improved density with higher stability. Proper compaction of materials ensures higher modulus and prevents the pavement layer from unnecessary deformation (Semmelink, 1991).

2.6.2.3 Zero Air Voids Line

For a particular density the saturation moisture content, often called the zero air void line or 100 percent saturation curve is presented in the moisture density curve. The zero air void line also defines the boundary of the restricted zone (Handy, 2007). Voids totally filled with water leave no air to be released. The saturated unit weight can be calculated by using the following Equation (2-2).

$$\gamma_{max} = \frac{G_s \gamma_w}{\left[1 + G_s \left(\frac{m}{100}\right)\right]} \qquad (2-2)$$

where,

γ_{max} = the unit weight of aggregate materials at zero air void,
γ_w = the unit weight of water
m = the moisture content in percentage
G_s = the specific gravity of aggregate materials (Handy, 2007).

2.6.3 Theoretical Maximum Density

In order to produce durable pavements the volumetric properties of HMA are needed to be constrained during the design and production (INDOT, 2009). The main difference between the optimum dry density of the moisture density curve and the Theoretical Maximum Density (TMD) is in the air voids content. In Theoretical Maximum Density there is zero air voids between the aggregate particles (Roberts et al., 1996). Practically it is impossible to attain zero air voids and obtain the maximum density at field compaction. The value of the theoretical maximum density contributes the basis for resolving the volume of air voids incorporated within the compacted mix. One of the most substantial things in determining the density in the laboratory is that the laboratory density should be as close as possible to the maximum density of pavement, which would be obtained after several years of traffic (Roberts et al., 1996).

Many states in the United States of America express field density requirement as a percent of the Theoretical Maximum Density. As a result, density can be achieved by increased compaction, asphalt content or filler content or some other methods that help to reduce the air voids. As density is normally articulated as a percentage of the Theoretical Maximum Density, anything reducing the number of in-place air voids will increase the percent density (Roberts et al., 1996). In the field, compaction is measured as a number of in-place air voids (Pavement Interactive, 2011). In compacted HMA, the distinctive concern should be reducing the volume of air (Pavement Interactive, 2011). The volume of air is assessed as a percentage of air voids by volume and asserted as percent air voids. At various compaction levels the number of air voids can be determined from the Theoretical Maximum Density, and bulk density (Roberts et al., 1996). The Theoretical Maximum Density (TMD) should be normally estimated from the pavement materials which are to be fixed for obtaining the correct TMD to compare with the in-place density. For satisfying the density requirements for reduction of in-place air voids, additional asphalt cement should not be added (Roberts et al., 1996).

Figure 2-13 Test set up for Theoretical Maximum Density

2.6.4 California Bearing Ratio

The California Bearing Ratio (CBR) is a ratio of strength of materials (to be determined) to that of a standard material consisting of well graded crushed stone (ASTM, 2007). It is a quick penetration test to estimate the relative strength of the base or subgrade materials of a pavement. Initially the CBR test was established to evaluate the in-situ subgrade strength in the laboratory (Araya, 2011). CBR value is one of the index properties of soil materials. In engineering design practice, the correlations between CBR values and performance of the materials are generally used although the results acquired from the CBR test are empirical. CBR value is a constituent part of the pavement design method. Almost all the design for the pavement foundations are based on the value of the CBR as it estimates the supporting value of subgrade (Toll, 1997).

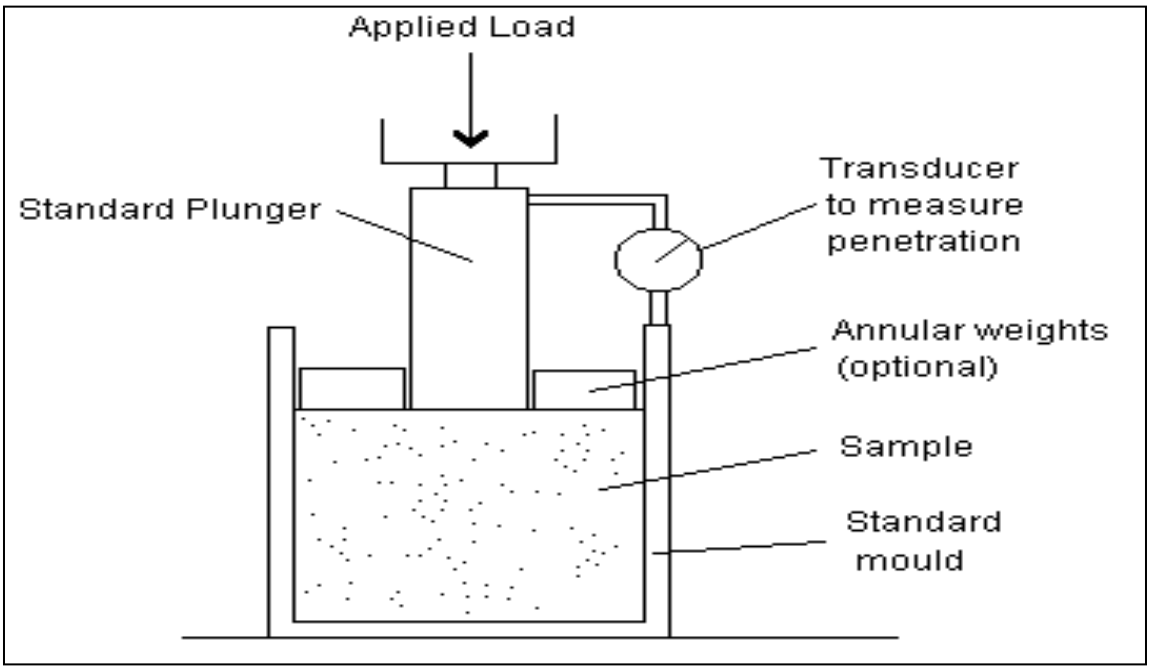

Figure 2-14 Schematic diagram for CBR test procedure (Toll, 1997)

The CBR values may be acknowledged as an indication of the quality of the stabilized base and also of the inter-particulate contact and ability of load transfer (Araya, 2011). In CBR a standard piston of 1935 mm^2 cross sectional area is penetrated in the materials at a standard rate of 1.3 mm per minute. The CBR value is expressed as the ratio of pressure at each 2.5 mm up to 12.7 mm penetration of aggregate materials to the bearing value of standard crushed rock (Huang, 1993). Most of the time an increase in penetration decreases the CBR. The ratio at a penetration of 2.5 mm (0.1 inches) is normally used as the CBR. If the ratio at 5 mm (0.2 inches) is greater than the ratio at 2.5 mm then the CBR value at 5 mm should be used. For the preparation of the materials for the CBR test, the optimum moisture content determined from the standard proctor test should be used (Huang, 1993). The standard values of high quality crushed rock are listed in Table 2-6.

Table 2-6 Penetration pressure values of Standard Crushed Rock (Huang, 1993)

Penetration for CBR test	Pressure
0.1 in (2.5 mm)	1000 psi (6.9 MPa)
0.2 in (5.0 mm)	1500 psi (10.4 MPa)
0.3 in (7.6 mm)	1900 psi (13.1 MPa)
0.4 in (10.2 mm)	2300 psi (15.9 MPa)
0.5 in (12.7 mm)	2600 psi (17.9 MPa)

In some of the literature it is shown that there is a correlation between the resilient modulus and CBR. According to Heukelom et al. (1962) for fine grained soils the correlation is shown following in Equation (2-3),

$$M_R = 1500\ (CBR) \qquad (2-3)$$

In this correlation, the resilient modulus, M_R is expressed in psi. The coefficient of 1500 varies from 750 to 3000 with a factor 2 depending on the type of materials. The CBR test was initially designed to evaluate the strength of materials with maximum particle sizes

less than 19 mm (ASTM, 2007). In many pavement design methods, including the Transport and Road Research Laboratory (TRRL) and American Association of State Highway and Transportation Officials (AASHTO) methods, CBR is used as an input value (Araya, 2011).

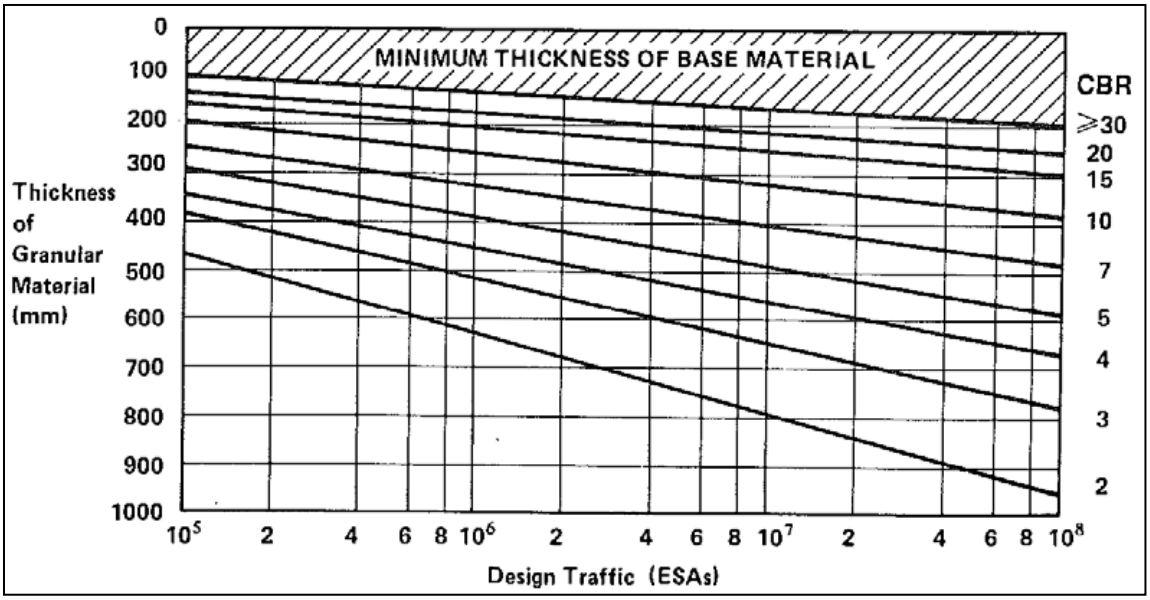

Figure 2-15 AUSTROADS design chart for granular pavements with thin bituminous surfacing (Austroads, 2004)

According to ASTM D 1883-07, "*CBR value is obtained at the optimum water content or range of water content found from the specified Proctor Compaction Test and specified dry unit weight. The dry unit weight is usually given as a percentage of maximum dry unit weight determined by Test Methods.*" Two types of CBR test value are generally used: soaked CBR and unsoaked CBR. For Soaked CBR the compacted sample has to be immersed in water for 96 hours with a scale to measure the swell after the sample has been taken out of the water.

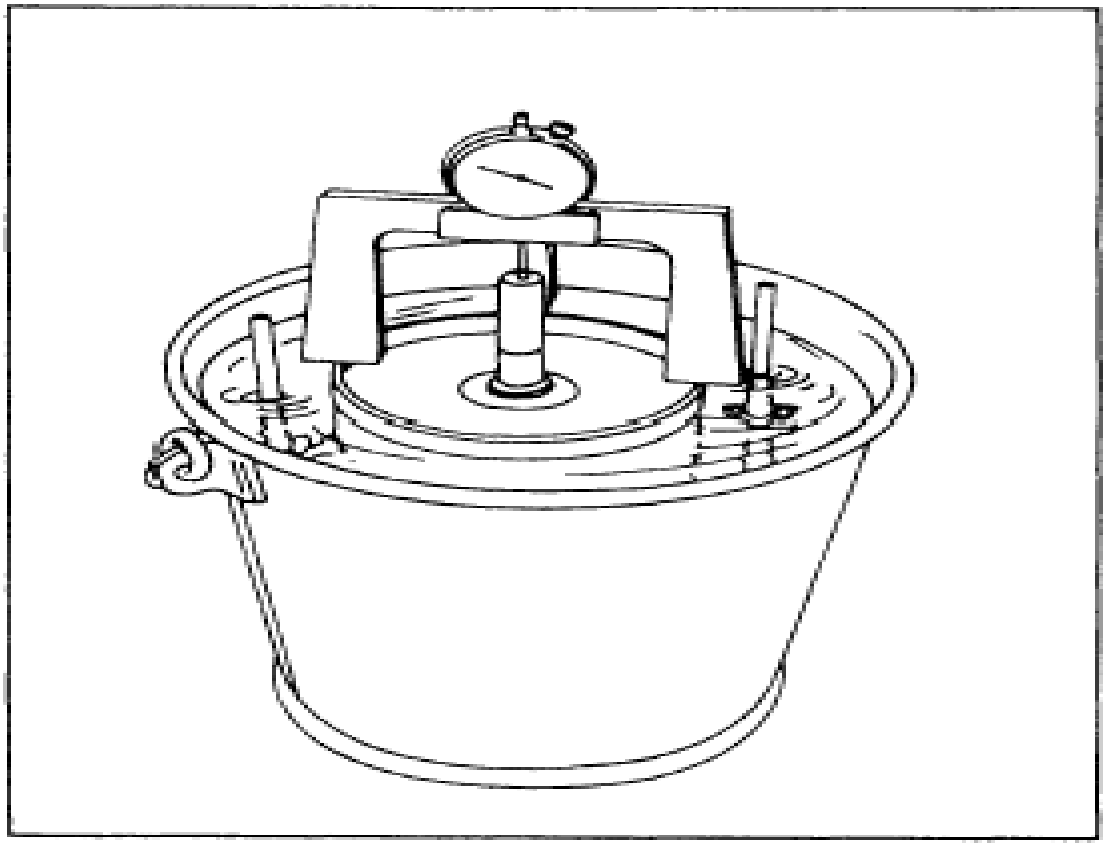

Figure 2-16 Schematic diagram for specimen submerged in water for soaked CBR (adapted from TPUB, 1994)

According to the Austroads pavement design guide (Austroads, 2004), for a known traffic volume and subgrade CBR value the thickness of the unbound thin surface granular pavement can be determined by using the pavement thickness design chart. Sometimes the CBR test is carried on with the Proctor compaction test to acquire a dry density – moisture content – CBR relation (Araya, 2011). Currently as a qualitative means of characterizing of the bearing capacity of unbound base and sub-base materials the laboratory CBR test is provided as a rapid method all over the world. In analytical design procedure the CBR test is used in determining the stiffness parameter for input (Araya, 2011). As a result, some empirical correlations between CBR and Elastic Modulus, E had been developed (Araya, 2011).

2.6.5 Indirect Tensile Strength

The tensile strength of the compacted bituminous mixtures is deduced by a test method called the Indirect Tensile Strength (ITS) test (TxDOT, 2010). The cracking properties of the pavement also can be determined from the ITS (Tayfur et al., 2005). The test is performed to determine the ultimate tensile strength of the cured bituminous specimen (Grubba et al., 2008). The test is performed by applying a compressive load that acts parallel to and along the vertical diametrical plane through two opposite loading strip at a specified rate of deformation (ASTM, 2012). The compressive load is applied at a rate of 50.8 mm per minute at 25ºC for a 100 mm diameter specimen. The specimens are loaded along the specimen height through 12.7 mm wide loading strips (Barnes, 2008). This method of loading creates tensile stress with relative uniformity acting perpendicular to the applied load plane causing the failure of the specimen by splitting it along the loaded plane (Anagnos et al., 1972).

Figure 2-17 Loading strip and bituminous specimen for Indirect Tensile Strength (Pavement Interactive, 2011)

The ITS value can be determined using the following Equation (1-4) (ASTM, 2012).

$$S_t = \frac{2000 * P_{max}}{\pi * t_h * D_s} \qquad (2-4)$$

where,

S_t = indirect tensile strength, (kPa)

P_{max} = maximum applied load, (N)

t_h = specimen height immediately before the test, (mm)

D_s = diameter of the specimen, (mm)

This test can be done by using the Marshall specimens and the result of the test is not affected by the surface irregularities (Tayfur et al., 2005). The tensile strength is basically a function of the binder property and decreasing air voids increases the tensile strength (Khosla et al., 2007). To assess the potential rutting or cracking of the pavement the values of the ITS test could be used for laboratory mix design testing and evaluating the relative quality of the bituminous mixture (ASTM, 2012). Moisture damage would decrease the Indirect Tensile Strength of materials over time (Diefenderfer et al., 2011). A decrease in the tensile strength exponentially decreases the fatigue life of the pavement. The aggregate structure is affected due to the moisture damage which eventually causes the loss of tensile strength as a result, rut depth of the bituminous pavement mixture increases with decrease in tensile strength (Khosla et al., 2007). According to ASTM D6931-12, "*The ITS results can also be used to determine the potential for field pavement moisture damage when results are obtained on both moisture conditioned and unconditioned specimens*."

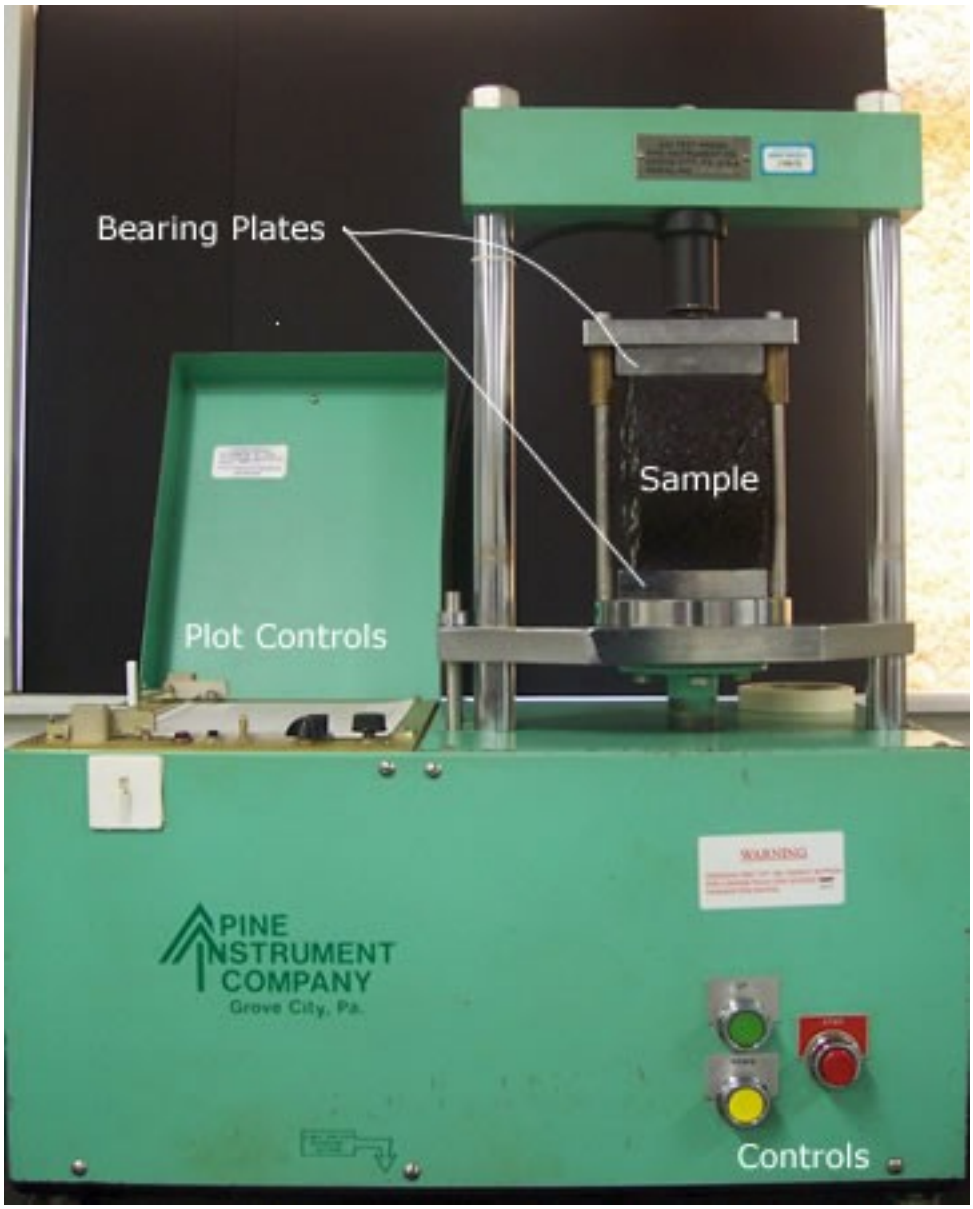

Figure 2-18 Test set up with bituminous specimen for Indirect Tensile Strength testing (Pavement Interactive, 2011)

The Indirect Tensile test supports two useful mixture properties for characterizing the HMA. The first property is the tensile strength used for the evaluation of water susceptibility of the mixture and the second property is the tensile strain failure used for the prediction of cracking potential (Roberts et al., 1996). For determining the Tensile

Strength Ratio (TSR), the tensile strength of the conditioned specimen is compared to that of the control specimen, as a result, Indirect Tensile Strength of pavement materials is determined both in dry and soaked conditions (Liang, 2008). Studies have shown that, the ITS value of a bituminous specimen depends on the type of aggregate used, absorption of the aggregate, aggregate interlock in the specimen and the cohesion of the binding agent (Khosla et al., 2007). For the assessment of the effect of moisture damage on the performance of the pavement the individual values of tensile strength of unconditioned and conditioned specimens in addition to the TSR values are used (Khosla et al., 2007). The relationship between the TSR and ITS have been shown in Equation (2-5).

$$TSR = \frac{ITS_{Conditioned}}{ITS_{Control}} = \frac{ITS_{Soaked}}{ITS_{dry}} \qquad (2-5)$$

It has been found from some research that bitumen mixtures containing additives have higher values of tensile strength at failure under static loading (Tayfur et al., 2005).

2.6.6 Direct Shear Test

The pavement performance and long-term maintenance is significantly influenced by the strength, stiffness and compressibility of materials underlying an asphalt surface (Mokwa et al., 2006). The direct Shear test is used to determine the stress dependent shear strength of aggregates (Fernandes et al., 2000). The shear box used for the direct shear testing has the capability of applying both the vertical and shear loads on the test specimen simultaneously (El-Desouky et al., 2008). The Mohr-Coulomb failure parameters such as cohesion, c and angle of internal friction, ϕ are used to define the failure behavior of granular materials (Van Neikerk et al., 2000). The rut performance of the asphalt mixes can be determined by one of the most important factors of asphalt concrete mixes, including shear properties (El-Desouky et al., 2008). Adequate shear strength in the asphalt mixture prevents rutting for a long time. Some studies have found that the mixture gradations and their design method affect the angle of internal friction and that

the continuously dense graded mixtures have smaller friction angle than the well-interlocked gap-graded mixtures (Wang et al., 2008). The internal friction is a substantial parameter that designates the degree of interaction among the particles (Srinivasan, 2004).

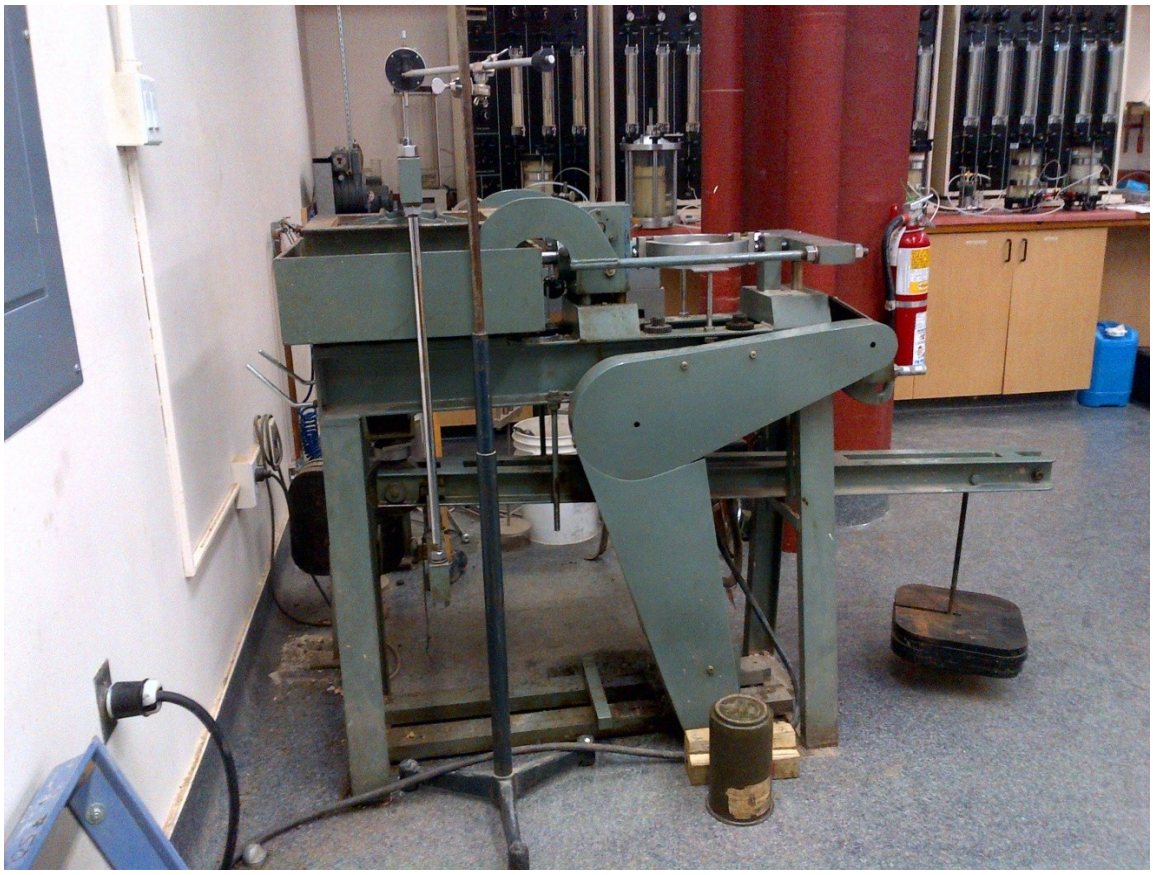

Figure 2-19 Apparatus for Direct Shear testing

In various studies, some testing parameters, such as asphalt content, loading rate and testing temperature, showed exceptional influences on the cohesion, c and slight influences on the angle of internal friction, ϕ (Wang et al., 2008). The relationship between the shear stress and normal stress, angle of internal friction and cohesion is shown in Equation (2-6),

$$S = C + \sigma \tan\phi \qquad (2-6)$$

where,

S = shearing resistance of the aggregate particles, (kPa)
C = cohesion, (kPa)
σ = applied vertical stress, (kPa)
ϕ = angle of internal friction due to the interlocking resistance of the particles. (Roberts et al., 1996).

Studies have suggested that the increase in the degree of compaction increases considerably both the cohesion and angle of internal friction with respect to the failure behavior of granular base materials (Van Neikerk et al., 2000). The shear strength is highly particle dependent as a result, greater angularity of particles in the aggregate mass increases the angle of internal friction, which means that the aggregate mix with rounded particles has less internal friction than the mix with crushed aggregate (Roberts et al., 1996). The addition of asphalt cement to an aggregate mass to be compacted initially reduces the internal friction between the aggregate particles as the lubricating effect of the asphalt allows the particles to slide against each other. The filler bitumen factor affects the mass viscosity of the matrix surrounding the coarse aggregate particles (Roberts et al., 1996). According to ASTM D3080 (2011), shear failure of the unstabilized full depth reclaimed material occurs when the maximum shear stress is achieved. Sometimes the shear failure occurs when shear stress reaches 10% of the relative displacement depending on the soil behavior and field application. In the aggregate materials there is no specific rupture point like in concrete or steel materials (Coduto, 1999). In the shear box, the test is ended when the machine extents to its highest capacity of displacement, which results in some remaining shear resistance in the materials without considering the amount of displacement (Salah, 2013).

2.6.7 Resilient Modulus Testing

The term "resilient" means the portion of energy applied into a material while it is being loaded and totally restored when it is unloaded (Adu-Osei et al., 2001). Some non-recoverable deformation in granular materials is seen after each load application, though the granular materials are not elastic (Huang, 1993). Hicks et al. (1971) suggested that the following factors may have a significant influence on the stress-deformation characteristics under short duration repeated loads: (a) stress level (confining pressure), (b) degree of saturation, (c) dry density (or void ratio), (d) fines content (percent passing No. 200 sieve), and (e) load frequency and duration. Load in the granular materials causes deformation like consolidation, distortion and attrition (Lekarp et al., 2000). According to Adu-Osei (2000), the degree of saturation, current stress level and stress history play important roles in the elastic response of aggregate materials and the increment of the non recoverable deformation is lower than the increment of resilient/recoverable deformation after the first few load applications while the transient load is applied. Resilient Modulus (M_R) is an engineering parameter which is used to analyze the elastic theory in response to traffic load.

Repeated load triaxial testing is used to attain the resilient modulus and the calculation is based on the axial recoverable strain under repeated axial loads (Adu-Osei, 2000). The strain obtained from the repeated load triaxial testing has two parts; one is the elastic or resilient part for the resilient modulus and the other is the plastic part for the permanent deformation (Lekarp et al., 2000). The granular resilient modulus is similar to Young's modulus for the elastic materials and the deformation of the granular materials is almost entirely restorable under each load repetition; if the load applied is smaller compared to the strength of the materials and iterated for a large number of times, then the materials can be considered as elastic (Huang, 1993). Pavement structural response to the wheel load can be calculated from the resilient modulus values incorporated with the structural response analysis and with pavement design procedure to design pavement structure (AASHTO, 2007).

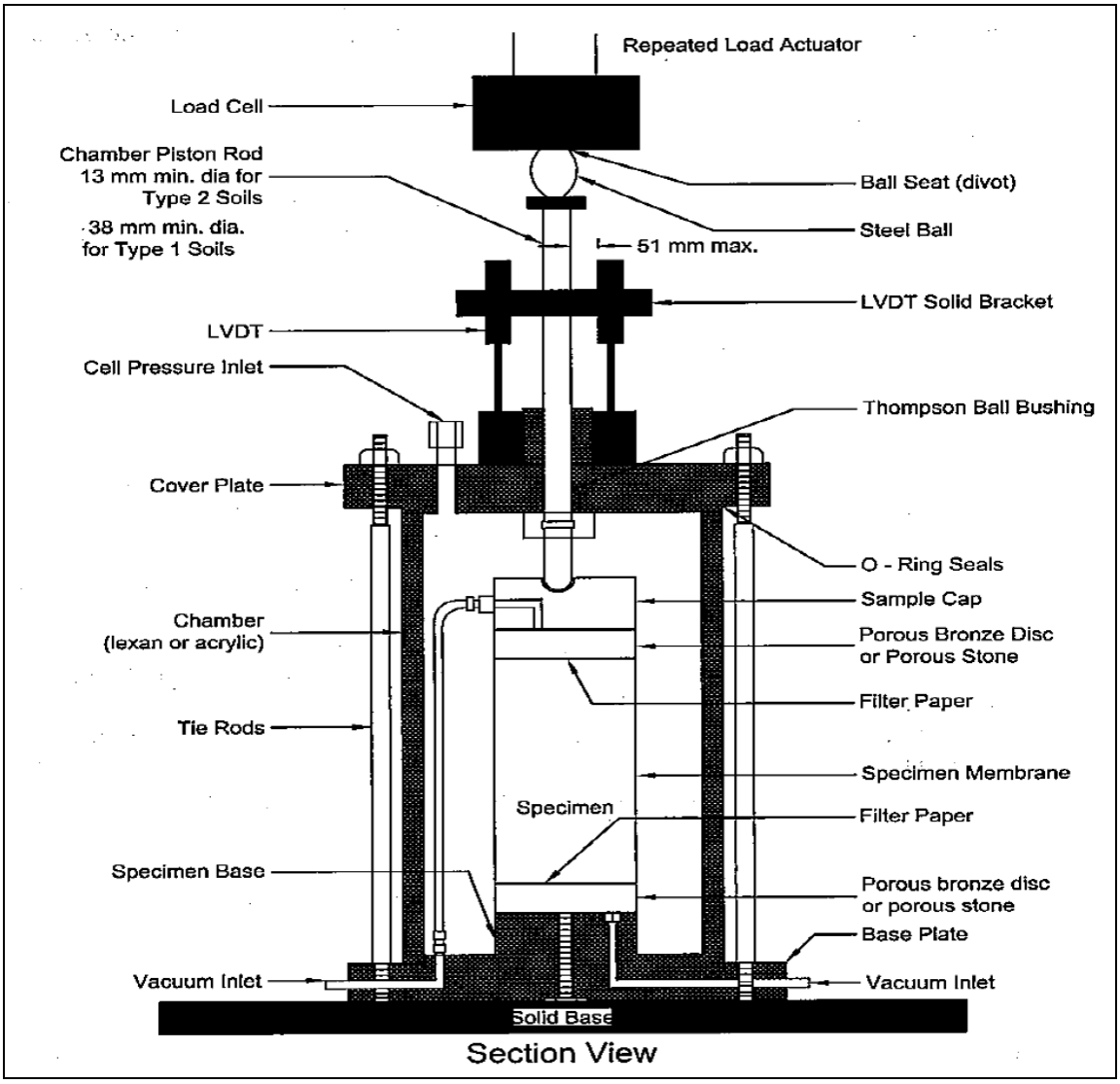

Figure 2-20 Resilient Modulus test configuration with triaxial chamber and load cell (AASHTO, 2007)

In the repeated loading triaxial test the type and duration of loading is anticipated to be the same as in field. In the pavement the stress at a particular point is zero if the wheel load is significantly far from that point and maximum stress is experienced if the wheel is directly on that point (Huang, 1993). According to Barksdale (1971), the stress pulse can be estimated by a triangular or haversine load function. The main differences between the indirect tensile strength test and resilient modulus test is that the test equipment for the

resilient modulus should be capable of applying repeated loads (Roberts et al., 1996). The specimen for resilient modulus testing is loaded to a stress level between 5-20% of indirect tensile strength and the specimen is loaded to failure while measuring the resilient modulus (Roberts et al., 1996). At a given stress level, the modulus increased with increasing density, particle angularity or surface roughness with decreasing fines content and decreasing degree of saturation (Hicks et al., 1971).

The load is applied in a haversine manner with 0.1 sec loading period and 0.9 sec rest period with no applied load. The load duration has an insignificant effect on the resilient modulus for granular materials and a significant effect on bituminous materials (Huang, 1993). The axial deformation is measured by two Linear Variable Differential Transducers (LVDTs). The specimen is placed in a triaxial cell where the confining pressure on the sample within the membrane is created by compressed air. The resilient modulus is calculated after all test sequences have been completed.

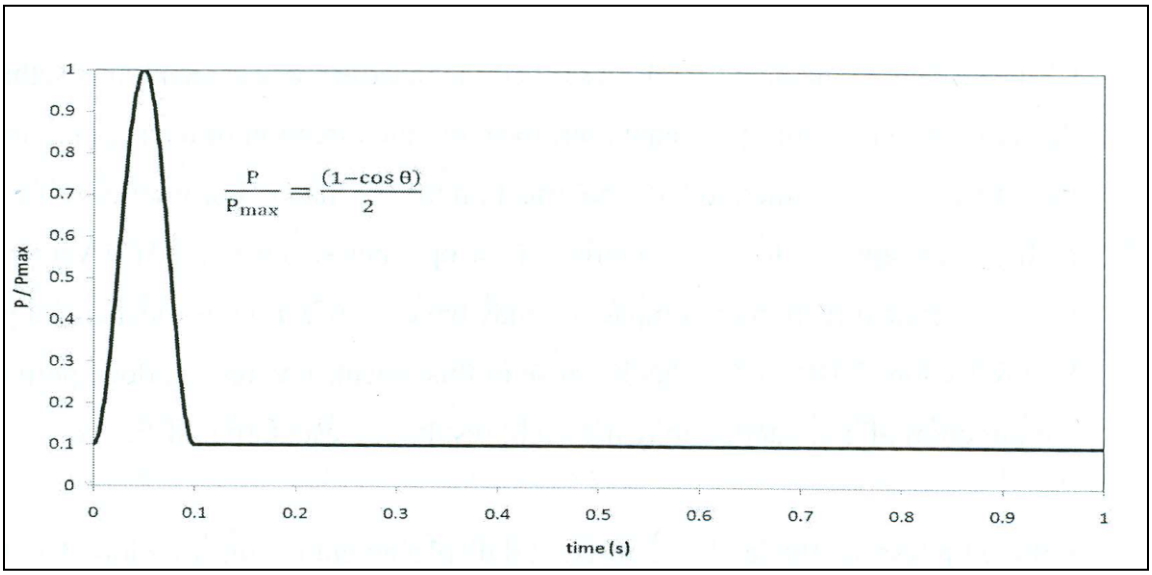

Figure 2-21 Haversine load pulse (Salah, 2013)

Equation (2-7) below is given for measuring the resilient modulus for each value of stress invariant which is a combination of confining pressure and applied load.

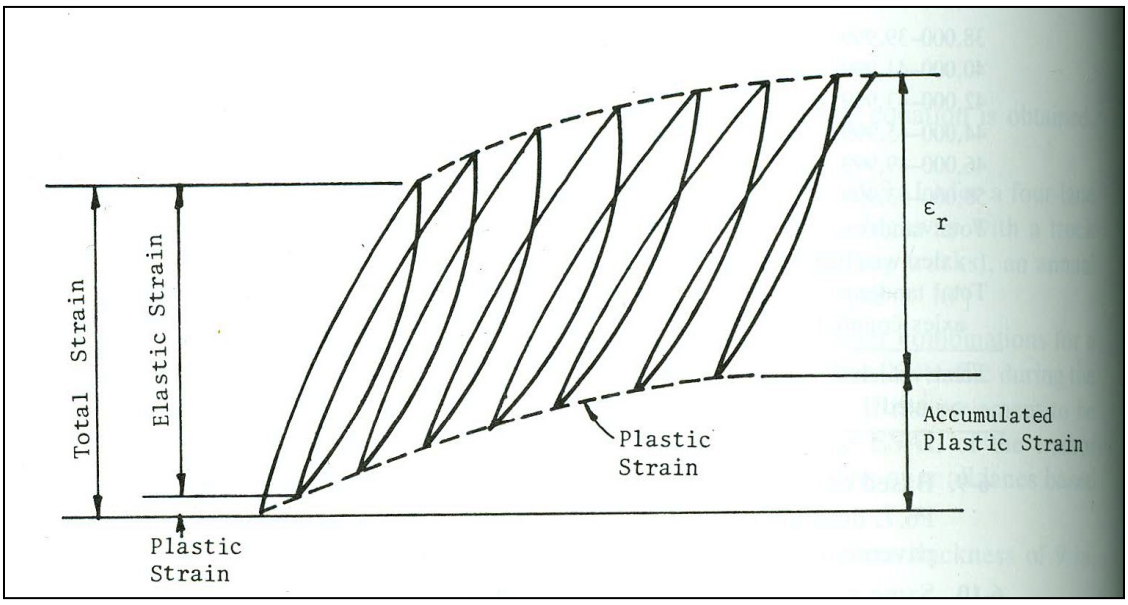

Figure 2-22 Strains under repeated loads (Huang, 1993)

$$M_R = \frac{Repeated\ Axial\ Stress}{Recoverable\ Axial\ Strain} = \frac{S_{cyclic}}{\varepsilon_r}$$

From AASHTO T 307, the resilient modulus has been derived as following:

$$M_R = \frac{S_{max} - S_{contact}}{\frac{E_r}{L}} = \frac{(S_{max} - S_{contact}) * L}{E_r}$$

$$M_R = \frac{(S_{max} - S_{contact}) * L}{E_r} \qquad (2-7)$$

where,

M_R = resilient modulus, (MPa)

S_{cyclic} = cyclic axial stress, (MPa)

ε_r = resilient (recovered) axial strain due to S_{cyclic}

S_{max} = maximum applied axial stress, (MPa)

$S_{contact}$ = contact stress, (MPa)

E_r = average resilient (recovered) axial deformation due to S_{cyclic}

L = original length of the specimen, (mm)

Stress invariant or bulk stress is a combined effect of normal stress applied to the material at a chosen point in the pavement system (Salah, 2013). Huang (2004) suggested the calculation method for stress invariant which is shown in Equation (2-8).

$$\theta = \sigma_z + \sigma_r + \sigma_t + \gamma z\,(1 + 2K_0) \qquad (2-8)$$

where,

θ = stress invariant, (MPa)

σ_z = vertical stress, (MPa)

σ_r = radial stress, (MPa)

σ_t = tangential stress, (MPa)

γ = unit weight of materials, (N/mm^3)

z = depth below ground surface, (mm)

K_0 = coefficient of earth pressure at rest

The simplified form of Equation (2-8) was used in this thesis where the stress invariant was taken as the sum of major and minor principal stress as described in Equation (2-9).

$$\theta = \sigma_1 + 2\sigma_3 \qquad (2-9)$$

where,

θ = sum of principal stresses or first stress invariant, (MPa)

σ_1 = major principal or axial stress, (MPa)

σ_3 = minor principal or confining stress, (MPa)

The combination of confining pressure and applied load should be chosen in such a way that the service loading conditions are best represented. The most appropriate resilient

modulus value for design can be selected by evaluating the stress state of the material in service (Salah, 2013). According to the AASHTO T 307 test standard there are 15 testing sequences provided for each type of material with 100 load cycles in each sequence.

2.6.7.1 K – θ Model

The K-θ model is used in the AASHTO guide for designing the pavement structure, which was proposed by Hicks et al. (1971) for nonlinear description of the resilient modulus for unbound granular materials. The stress level affects the resilient properties of untreated granular materials greatly. The modulus increased significantly with the confining pressure and slightly with the repeated axial stress (Hicks et al., 1971). Various studies also showed that granular materials possess distinctly nonlinear stress vs. strain behavior with the resilient modulus increasing with an increase in sum of principal stresses (Hicks et al., 1971). As shear failure does not occur, the modulus can be approximately related to the sum of the principle stresses provided in Equation (2-10).

$$M_R = k_1\theta^{k_2} \qquad (2-10)$$

where,

M_R = resilient modulus, (MPa)
θ = sum of principal stresses or first stress invariant, (MPa)
k_1, k_2 = regression constants

The resilient modulus value calculated with Equation (1-7) and the stress invariant values for all the test sequences are plotted in logarithmic scale for the correlation between the parameters as shown in the following figure.

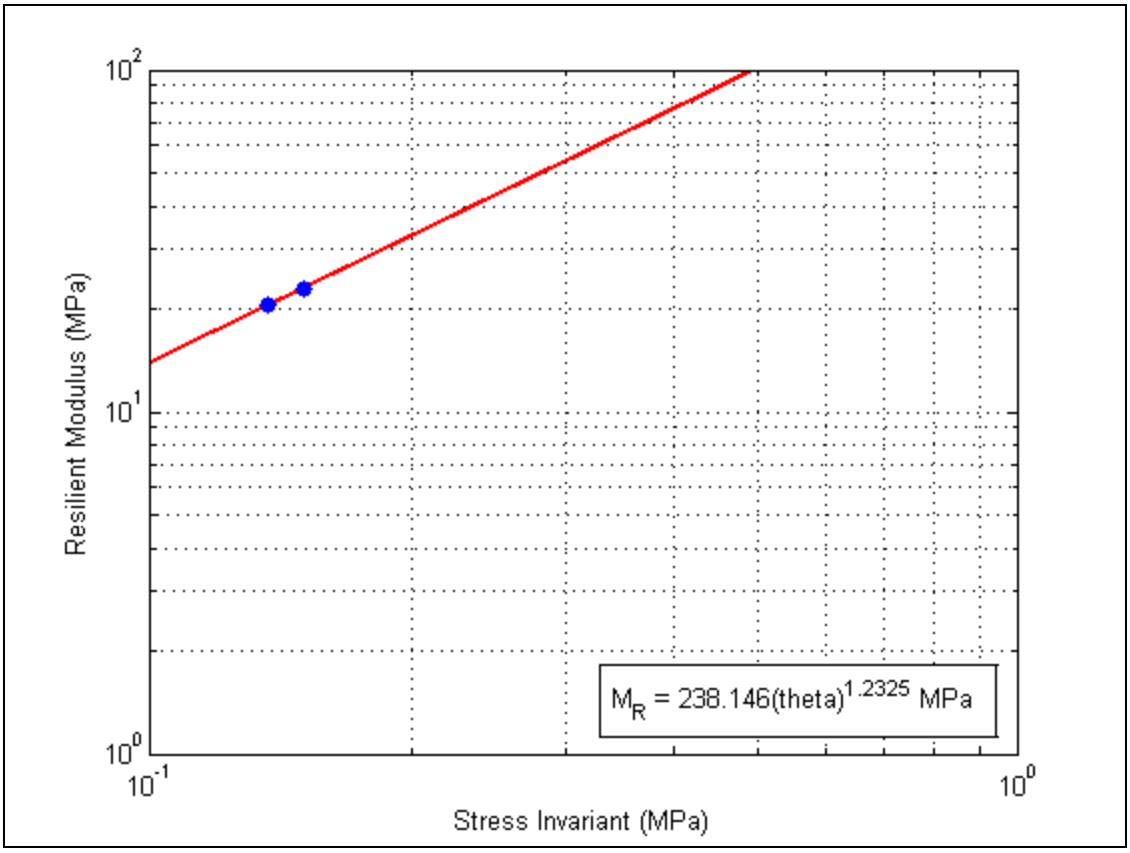

Figure 2-23 Graphical representation of Resilient Modulus and Stress Invariant

2.6.7.2 Effect of Moisture - Density Variability on the Resilient Modulus

The resilient modulus tends to decrease with increasing moisture content. Studies have shown that the resilient modulus was reduced significantly when the specimens were compacted at the wet portion of optimum moisture content. An increase in dry density increases the resilient modulus as less volume is occupied by the voids, which consequently results in the increase in the strength of soil (Kim et al., 2006). For non-cohesive aggregate materials the dry density plays a significant role in the resilient modulus. Studies have also shown that non-cohesive specimens of dune sand exhibited higher values of resilient modulus as the dry density increased (Lee et al., 1995). Hicks et al. (1971) suggested from tests performed on a granular subgrade that an increase in the relative dry density for both coarse-graded and fine grading subgrade increased the

resilient modulus. The resilient modulus is highly dependent on the initial moisture content at which the specimen is compacted. In a study of the effect of moisture content variation on resilient modulus, Khoury et al. (2009) explained that the relationship between the resilient modulus and moisture content is governed by three factors:

- Soil suction within the void space,
- Repulsive forces due to moisture content and Born[1] repulsion, and
- Short and long ranged attractive forces[2].

These forces mentioned above control the soil mass resistance to compression and stress as well as the flocculated and deflocculated behavior of soil which in turn affects the resilient modulus of soil at different moisture content. An increase in moisture content decreases the resilient modulus as water has a lubricating effect at contacts between particles (Thom et al., 1987). Fine particles fill the voids in the granular materials without dispersing and create a dense assembly with good mechanical characteristics, which gradually increases water sensitivity and decreases drainage capacity (Brown et al., 1996). Higher fine contents cause the mechanical properties of the unbound granular materials to be more sensitive to water as water is more readily held in the pores due to capillary attraction (Raad et al., 1992).

1. Born forces are one type of force that acts upon atoms in an ionic lattice. In simplest terms, because ions have some finite size, electron-electron and nucleus-nucleus interactions occur and give rise to repulsion forces and electrostatic potential, both called Born forces (ChemWiki, 2013).

2. Short range and long range forces are Intermolecular forces which can be attractive or repulsive forces between molecules. Short range forces are created when the centers of the molecules are separated by three angstroms (10^{-8} cm) or less. Short range forces tend to be repulsive, where the long range forces that act outside the three angstroms range are attractive. Long range forces are also known as Van der Waals forces (ChemWiki, 2013).

CHAPTER 3: EXPERIMENTAL MATERIALS AND METHODS

3.1 Introduction

This research involved a laboratory experiment to determine the material properties of unstabilized FDR base materials that were believed to vary with thickness. The objective of this analysis is to compare the consistency of the materials from an FDR project that used the retroactive method of pulverization with another FDR project that used a GPR survey as a proactive pulverization depth control method to see if pavement thickness effects on the blend ratio translate into differences in physical characteristics and performance.

3.2 Route 335 and Route 790 Projects of New Brunswick

Two projects from New Brunswick were chosen for this research in which the sample collection methods were different to compare the consistencies of materials. The retroactive depth control approach was used in Route 335. In this approach the asphalt concrete thickness was measured during construction at the edge of the pulverized material behind the pulverization process. This measurement was used as an estimate of the asphalt concrete thickness in front of the pulverization machine. The pulverization depth was adjusted in an attempt to retain the specific blend ratio. The HMA thickness was observed to vary significantly in the field.

Field testing was done in Route 790 section with the help of GPR survey, described in Section 3.2.2.1, in the first stage of this research program. The layer thickness was determined by a GPR survey before the construction. The asphalt concrete thickness was determined throughout the section beforehand. The pulverization depths were specified within appropriate subsections to reflect the true variation in thickness.

The exact locations and the JMF are described for the both projects in the next section.

3.2.1 Route 335 near Caraquet

Figure 3-1 The pavement section in Route 335, Caraquet, New Brunswick

The retroactive control procedure was applied in Route 335 project. Core sampling and test pits were used to determine the average pavement thickness. In the retroactive depth control method, at the beginning, the recycling machine was adjusted to the intended depth of pulverization but needed to change settings shortly after noticing the dissimilarity between the actual asphalt concrete thicknesses and the average thickness measured from the test pits. The pulverization depth was adjusted approximately every 10 m of pavement section in response to changes in the asphalt thickness which varied between 40 and 180 mm at over a 200 m section of pavement. The changes of the thick asphalt concrete beyond the recycling machine to the thin asphalt concrete ahead resulted in the variation in the as-built blend ratio and vise versa. Samples of the granular materials were collected for lab tests from six distinct locations that rendered a variation in mass blend ratios ranging from 0.32 to 0.90.

Table 3-1 JMF gradation of materials used in Route 335 pavement section

Size (mm)	Granular Material	RAP	Portland Cement	Blended Job Mix Formula	NBDOT minimum	NBDOT Maximum
			% Passing			
50.0	100.0	100.0		100.0	100	100
25.0	96.5	100.0		98.9		
19.0	92.5	100.0		97.5		
16.0	88.7	100.0		96.3		
13.2	85.2	97.8		93.7		
9.50	76.5	91.1		86.4		
4.75	65.8	68.6		68.0	45	70
2.36	57.5	49.8		52.8		
1.18	50.9	35.8		41.4		
0.630	43.0	24.3		31.2		
0.300	19.0	16.8		18.3		
0.150	10.1	11.2		11.7		
0.0750	7.60	8.2		8.9	5	20
% AC		5.43		6.14		

The dry ITS, soaked ITS and TSR values of the JMF mixture for the Route 335 were 590.8 kPa, 512.7 kPa, and 0.868 respectively. All the values mentioned above surpassed the corresponding minimum values of 300 kPa, 150 kPa and 0.5 according to NBDOT specification. The JMF tabulated in Table 3-1 for Route 335 was prepared with the proportion by mass of 65.33% RAP, 32.18% granular materials and 2.5% of expanded PG 58-28 (penetration grade) Asphalt Cement (AC). 47 deflection locations in North Bound and South Bound lane of Route 335, computed from GPR at deflection stations are shown in Figure 3-2.

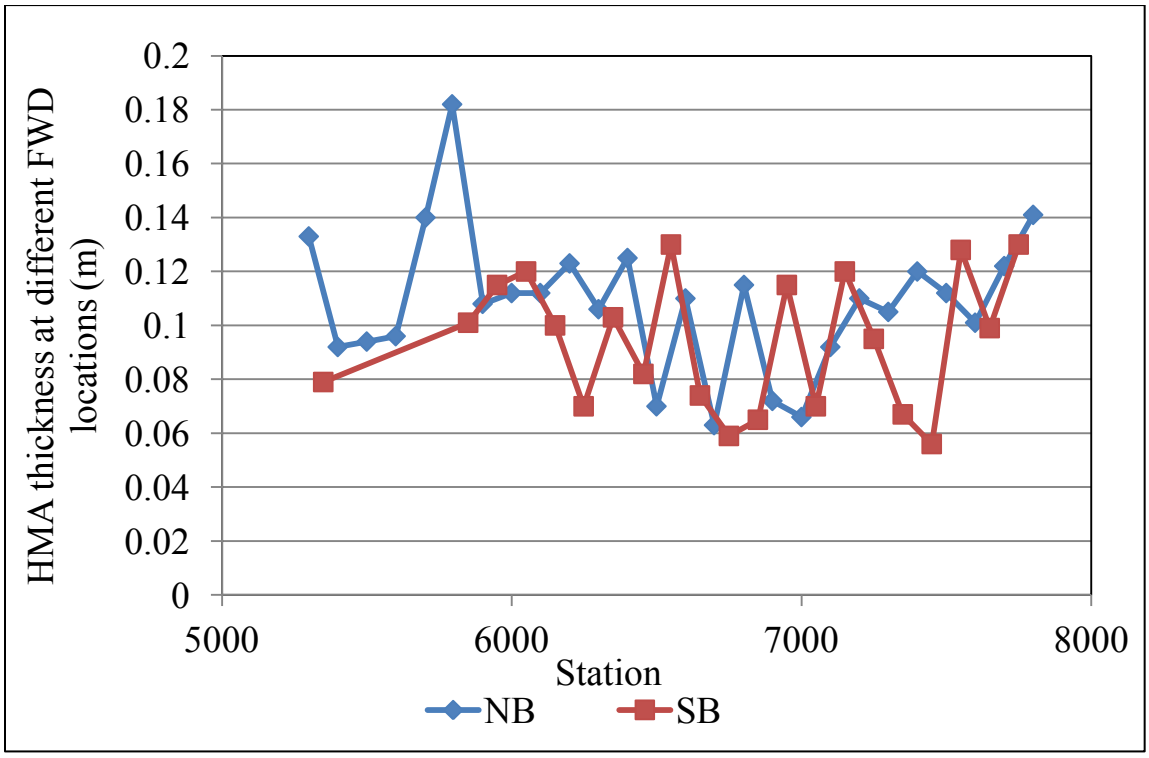

Figure 3-2 Change in pulverization depth with distance by conventional method for the northbound and southbound lane of Route 335, Caraquet, New Brunswick

3.2.2 Route 790 near Lepreau

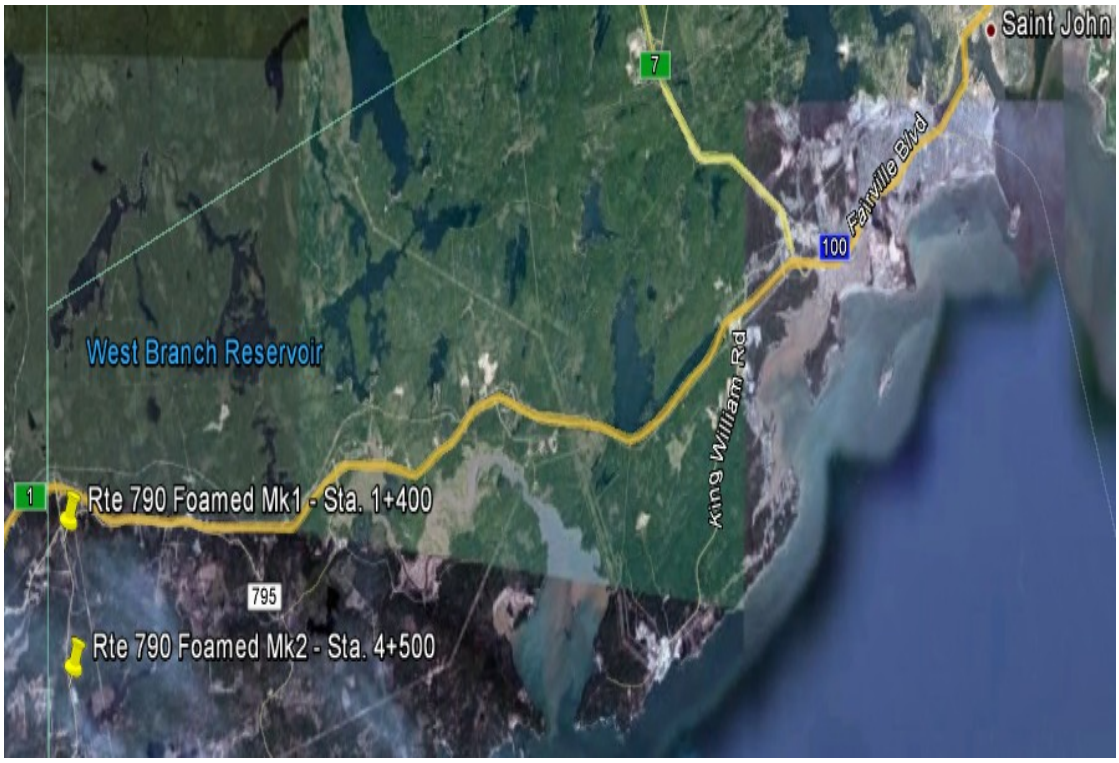

Figure 3-3 The pavement section in Route 790, Lepreau, New Brunswick

A GPR, coupled with 2 GHz horn antenna, was used to survey the Route 790 section before performing the test pit sampling for estimating the pavement layer thickness. The thickness of the asphalt layer determined from various test pits was used to calibrate the average GPR signal velocity in the asphalt layer. This average signal velocity was applied at every 10 cm interval to assess the HMA thickness of the entire pavement section. Figure 3-4 illustrates the estimated total fluctuation in the thickness of the asphalt concrete on the northbound lane of the Route 790 test section and also shows the suggested pulverization depth for different subsections. Figure 3-5 presents an identical outcome for the southbound lane.

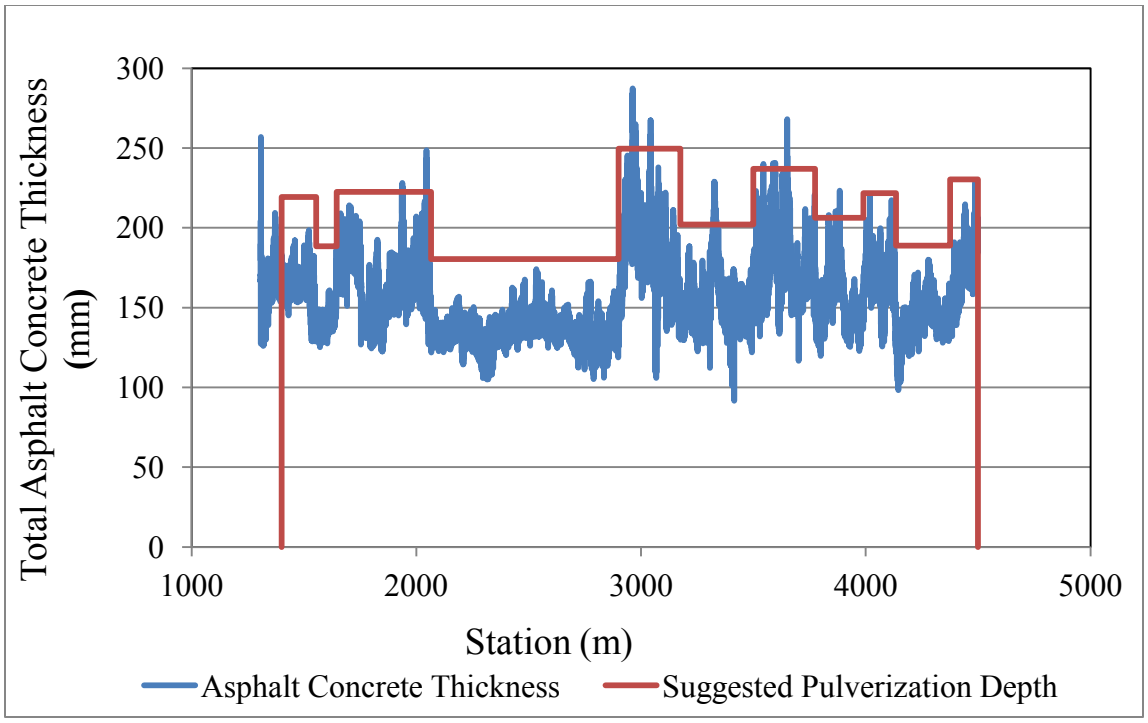

Figure 3-4 GPR based total asphalt concrete thickness and suggested pulverization depth for the northbound lane of Route 790, Lepreau, New Brunswick

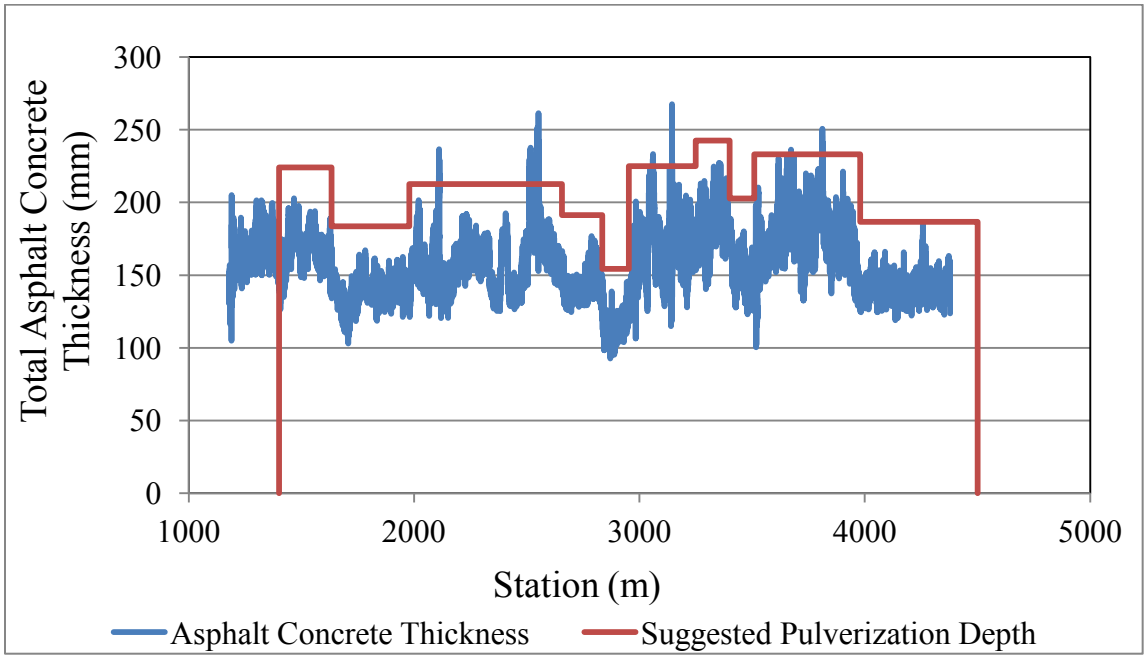

Figure 3-5 GPR based total asphalt concrete thickness and suggested pulverization depth for the southbound lane of Route 790, Lepreau, New Brunswick

A number of subsections of relatively consistent thickness and a corresponding pulverization depth were depicted from this extensive GPR survey data. The survey data helped to attain the blend ratio of RAP and granular materials as specified in the JMF. Table 3-2 displays the contents of the designed JMF gradation with the proportions by mass of 72.96% RAP, 24.35% granular materials, 0.49% of Portland cement and 2.2% of expanded PG 58-28 asphalt.

Table 3-2 JMF gradation of materials used in Route 790 pavement section

Size (mm)	Granular Material	RAP	Portland Cement	Blended Job Mix Formula	NBDOT Minimum	NBDOT Maximum
			% Passing			
50.0	100.0	100.0	100.0	100.0	100	100
25.0	90.4	100.0	100.0	97.6		
19.0	85.0	100.0	100.0	96.3		
16.0	79.9	100.0	100.0	95.0		
13.2	74.7	92.3	100.0	88.0		
9.50	66.0	83.2	100.0	79.2		
4.75	51.6	57.1	100.0	56.4	45	70
2.36	41.0	41.1	100.0	42.0		
1.18	30.5	27.4	100.0	29.3		
0.630	20.8	20.3	100.0	21.6		
0.300	12.5	14.1	100.0	15.0		
0.150	8.1	9.2	100.0	10.2		
0.0750	6.4	6.0	100.0	7.5	5	20
% AC		5.68		6.44		

The dry ITS, soaked ITS and TSR values of the JMF mixture for the Route 790 materials were 332.4 kPa, 290.6 kPa, and 0.874 respectively. All the values mentioned above surpassed the corresponding minimum values of 300 kPa, 150 kPa and 0.5 according to the NBDOT specification.

3.2.2.1 Ground Penetrating Radar (GPR)

Ground Penetrating Radar (GPR) is an electromagnetic non-destructive instrument to assess different layers of pavements and estimates their thickness and permittivity (dielectric constant) (Li, 2011). Information about the layer structure and thickness are some of the key elements of a pavement performance study. According to Maser et al. (1992) the principles of Ground Penetrating Radar are:

- A transmitter relays short pulses of microwave energy through the pavement by providing an air-coupled antenna attached to a survey vehicle for the pavement investigation.
- The pulses reflect back to the receiver in antenna.
- The arrival time and amplitude of the microwaves are dependent on the location and nature of dielectric differences in the materials (air-base, air-asphalt etc.).
- Formation of "Radar Waveforms" is made by the series of pulses which are displayed on an oscilloscope by capturing the reflected energy over a range of time in nanoseconds.
- The pavement layer thickness and properties are recorded in the waveform.
- Thickness of each layer of a pavement with particular materials is a function of the travel time of electromagnetic pulse and the electrical properties of the material

The radar wave transmits through a medium at a velocity, V which depends on the relative magnetic permeability, μ_r and relative dielectric permittivity e_r. Relative dielectric permittivity is an estimation of the capacity of a material to for allowing the passage of electromagnetic energy (Loizos et al., 2006). According to Equation (3-1), the

velocity, V is primarily a function of the relative dielectric permittivity, e_r; and, since most construction materials are non-magnetic, the relative magnetic permeability value is assumed to be 1. The GPR velocity in air is assumed to be the same as the speed of light in a vacuum, (c = 300 mm/ns) (Barnes et al., 2012). The total transmitted pulse is divided into two parts; the interface of electrically unlike materials reflects a part of the energy, whereas the remaining part of energy amplitude is sent through the boundary to advance into underlying materials. The velocity of the pulse in the underlying materials relies on the relative dielectric permittivity of the layer (Barnes et al., 2012). Surface layer dielectric constant can be computed from the reflection coefficient, R which is the ratio of the reflection of radar energy from the asphalt to the amplitude of radar energy that is incident on the pavement as illustrated in Equation (3-2), where the subscripts 1 and 2 represent the successive layers (Maser et al., 1992). Equation (3-2) also measures the layer velocity since the relative dielectric permittivity of air is 1.

Relative dielectric permittivity is different for each material. The change in relative dielectric permittivity happens when an electromagnetic pulse passes through different layers that cause reflection by which different layers are identified (Salah, 2013). Both electric and magnetic fields cause attenuation of electromagnetic waves while traveling through different media (Daniels, 2004). The pavement materials have very low magnetic response for which the magnetic response can be ignored. Table 3-3 is presented below with the relative dielectric permittivity of different materials.

Table 3-3 Typical relative dielectric permittivity of different materials (Daniels, 2004)

Material	Relative dielectric permittivity
Air	1
Asphalt, wet	6-12
Asphalt, dry	2-4
Concrete, wet	10-20
Concrete, dry	4-10
Dry sand	2-6
Freshwater	81

The dielectric permittivity can be calculated from the amplitude of the incident energy by calibrating the radar data reflected off a flat metal plate placed on the pavement surface, as the reflection from the metal plate is 100 percent (Maser et al., 1992). The purpose of calibration is to figure out the amplitude of incidental wave, or proportion of signal reflected of the metal plate. The dielectric permittivity of the surface layer can be calculated by using Equation (3-3) (Saarenketo et al., 2000). The relative dielectric permittivity is calculated by using metal plate reflection amplitude and the amplitude of reflection of electromagnetic waves travelling from air into the surface layer of the pavement.

$$V = \frac{c}{\sqrt{e_r}} \qquad (3-1)$$

$$R = \frac{\sqrt{e_{r2}} - \sqrt{e_{r1}}}{\sqrt{e_{r2}} + \sqrt{e_{r1}}} = \frac{V_2 - V_1}{V_2 + V_1} \qquad (3-2)$$

$$e_{r1} = [\frac{(1 + A_{r1}/A_m)}{(1 - A_{r1}/A_m)}]^2 \qquad (3-3)$$

$$e_{r2} = e_{r1}[\frac{(1 - (A_{r1}/A_m)^2 + (A_{r2}/A_m))}{(1 - (A_{r1}/A_m)^2 + (A_{r2}/A_m))}]^2 \qquad (3-4)$$

$$h = V * \frac{t}{2} \qquad (3-5)$$

where,

V = velocity of Radar wave, (m/ns)

C = velocity of light in vacuum, 0.3 (m/ns)

e_r = dielectric permittivity of material in question

e_{r1} = dielectric permittivity of surface material

e_{r2} = dielectric permittivity of base material

A_{r1} = Amplitude of reflection from surface material

A_{r2} = Amplitude of reflection from base material

A_m = Amplitude of a metal plate

R = reflection coefficient

t = two way travel time, (ns)

h = thickness of pavement layer, (m)

The dielectric permittivity for the base layer can be calculated using Equation (3-4) suggested by Loizos et al., (2006). The effect of the upper layer is added every time when the dielectric permittivity of the subsequent layers is calculated. The velocity of the electromagnetic pulses should also be computed simultaneously with the dielectric permittivity by using Equation (3-1).

Finally using Equation (3-5) the layer thickness is determined by multiplying the layer velocity with one half of the estimated two way travel time delay that takes place between the reflections at the top and the bottom of a provided layer (Barnes et al., 2012). GPR data collection is performed in accordance with the spatial frequency depending on the transmission frequency and the space range between adjacent waveforms. A 10 cm distance between the waveforms render 10,000 thickness estimates in one kilometer which facilitates a statistically substantial magnitude of thickness variability along a pavement section.

Figure 3-6 GPR Horn antenna attached to the vehicle

The asphalt layer of an old deteriorated pavement with multiple overlays exposing inconsistent thickness, degree of deterioration and accumulation of de-icing salt and moisture may not permit the surface dielectric to evaluate the average velocity adequately along the entire pavement section (Barnes et al., 2012).

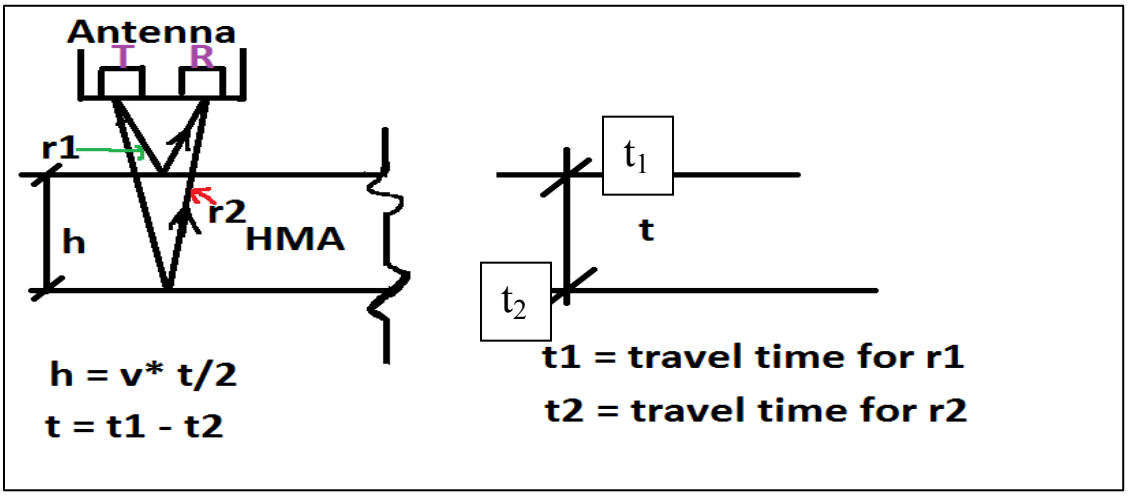

Figure 3-7 Schematic diagram of GPR data collection technique

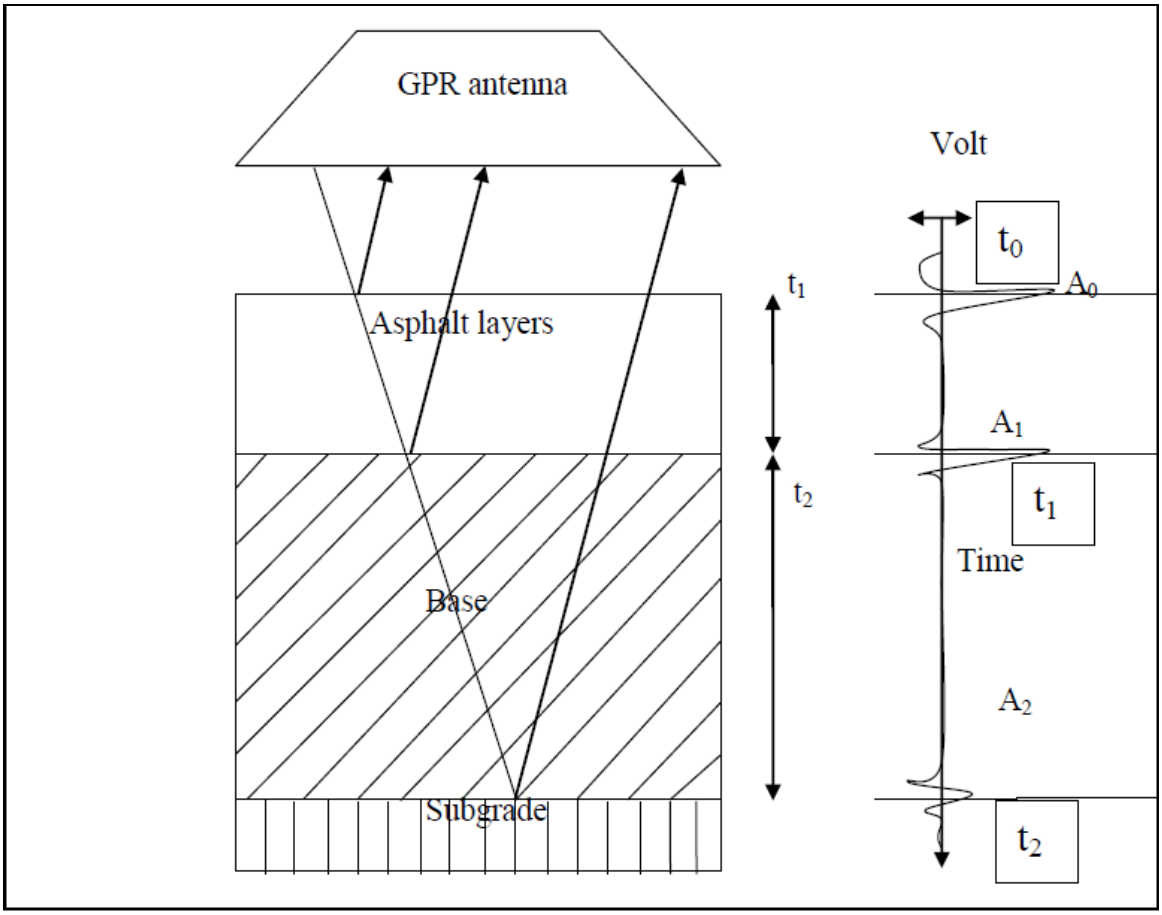

Figure 3-8 GPR concept of electromagnetic pulse reflection (Plati & Loizos, 2012)

Difficulties related to the distinct dielectric material properties that result in a variable average velocity throughout the layer are aggravated with variable lift thickness. Relative dielectric permittivity varies with chloride content and moisture within the pavement. For such cases, calibration of velocity is built upon calculating the average layer velocity, measured from the total thickness values acquired from drilled core specimens and known two way travel time taken between the reflections at the surface and bottom of the heterogeneous asphalt layer (Barnes et al., 2012). The more the cores are taken, the more accuracy would be done on the calibration factor for velocity.

Finally, the GPR analyzed pavement thickness data is supposed to yield accurate results in most cases, though sometimes serious inaccuracy occurs at certain locations where the heterogeneous asphalt layer conflicts electrically from the sampled core locations.

3.3 Comparison of Thickness Measurement by Core Sampling and Ground Penetrating Radar

Table 3-4 is presented to show the comparison in thickness measurement in the both projects done by two different methods, GPR and core sampling. In Route 335, four cores were drilled to measure the average thickness of asphalt in the pavement section. From the core sampling the average asphalt thickness of the pavement was of 95 mm with a standard deviation of 5.8 with a narrow range of coefficient of variation of 6.1%. The minimum asphalt thickness form the core was found to be 90 mm and the maximum asphalt thickness measured was 100 mm. From 47 deflection locations in North Bound and South Bound lane of Route 335, given in Figure 3-2, the thickness data were measured with a GPR which showed the minimum asphalt thickness of the pavement was of 56 mm and the maximum thickness of asphalt was of 182 mm with a wide range of coefficient of variation of 25.56%. From the coefficient of variation of the asphalt thickness measured from two approaches, it was clear that the practical scenario was very different than what was found from the drilled core. It was obvious that the blend ratio would be highly variable for Route 335 materials. Six cores were drilled in Route 790 to measure the average asphalt thickness of the pavement. From the core sampling, the measured asphalt thickness varied from 150 mm to 200 mm with a coefficient of variation of 11.87% while about 65000 data were available when the thickness was measured by GPR in the same pavement section. The GPR controlled thickness of asphalt varied from 91.6 mm to 287.4 mm with a coefficient of variation of 14.77%. The GPR gave better estimation of the asphalt thickness than the drilled core. From the asphalt thickness measured from GPR, the pulverization depth of Route 790 was controlled by diving pavement into several sub-sections to obtain a specific blend ratio.

Table 3-4 GPR vs Core sampling to measure variability in asphalt concrete thickness

Pavement Section	Method of Measuring Pavement Thickness	n	Asphalt Concrete Thickness (mm)				
			Mean	Standard Deviation	Coefficient of Variation (%)	Min.	Max.
Rte 335	Core Sampling	4	95.0	5.8	6.10	90.0	100.0
	GPR	47*	102.1	26.1	25.56	56.0	182.0
Rte 790	Core Sampling	6	175.2	20.8	11.87	150.0	200.0
	GPR	~65k	156.4	23.1	14.77	91.6	287.4

* Rte 335 stats computed from GPR at deflection stations.

During the rehabilitation of Route 335, the retroactive process was adopted for pulverization control to establish a 0.67 RAP/total depth ratio according to the Job Mix Formula (JMF) to fit the detailed gradation limit set by NBDOT.

The pulverization depth in the FDR sample collection locations were selected according to the nominal 0.746 RAP / total depth ratio established in the JMF though the GPR measured asphalt concrete thickness altered. FDR samples were collected after the initial pulverization in six distinct locations. The blend ratios of the materials collected from the both projects are enlisted in Table 3-5.

Table 3-5 Blend ratio for different locations of Route 335 and Route 790

Route 335		Route 790	
Station	Blend Ratio	Station	Blend Ratio
7+725	0.90	1+769	0.74
7+790	0.80	2+185	0.74
7+075	0.57	2+550	0.75
7+750	0.50	3+128	0.76
7+772	0.43	3+446	0.76
7+703	0.31	4+040	0.76
Mean	0.59		0.75
Standard Deviation	0.22		0.01
Coefficient of Variation (%)	37%		1.3%

The acquired FDR aggregate samples, with almost uniform blend ratios using the proactive control method, were anticipated to accommodate improved consistency in the quality compared to the samples with variable blend ratio derived from the retroactive control method along Route 335.

3.4 Test Procedures for Unstabilized FDR Materials

The experimental program combined all the tests generally used to assess the materials in pavement engineering with the elementary material properties provided by the advanced testing procedures discussed in previous chapter.

The quality and consistency of the unstabilized, as-obtained materials from six different locations of both projects were assessed by the following tests according to ASTM and AASHTO standards:

- Gradation for grain size distribution
- Laboratory compaction for moisture-density relationship
- Theoretical Maximum Density (TMD) to obtain zero air void in materials
- California Bearing Ratio (CBR) of materials
- Direct shear strength for granular materials
- Resilient modulus for granular materials

All the materials were dried in the oven at 40ºC to a constant mass prior to all the aforementioned tests. The purpose of drying materials at 40ºC was to take out the moisture without melting the asphalt cement. Several samples were dried at 60 ºC, 55 ºC and 50ºC also to a constant mass, but it was observed that the asphalt cement started to melt within the first one hour. The fine particles were adhered to the asphalt cement and the tray which afterwards affected the gradation severely. The shape of the aggregates also changed at a high temperature. After trying at several temperatures, it was found that at 40 ºC the moistures were gone from the aggregates without melting the asphalt content.

Results of the tests were utilized to evaluate the quality and consistency of as-obtained materials from the Route 335 and Route 790 projects. The gradation, laboratory compaction test, theoretical maximum density test, and CBR test were done in AMEC Earth and Environment laboratory. Direct shear test and resilient modulus test for granular materials were done in the Dalhousie University Civil Engineering Construction Materials Laboratory.

3.4.1 Gradation for Grain Size Distribution

Gradation is one of the fundamental physical properties of materials that is used to arrange particles according to size ranges. The quantitative mass of particles in each size range can be determined by sieving a sample through a series of successively smaller mesh screens according to ASTM D6913 – 04. Different size distributions of the material mix influence a variety of other attributes such as stiffness, strength, density, and moisture susceptibility. The FDR materials depend on inter-particulate contact to transfer loads as a result, maximizing the density in the FDR is important. A tightly compacted FDR shows low air void content. It has high load transfer ability and it reduces stresses exerted on the subgrade. Sieve analysis is conducted during initial testing at the time of the mix design phase to ensure adequate gradation will be provided.

ASTM standard (ASTM D6913 – 04) was used to obtain the grain size distribution for both Route 335 and Route 790 materials. The washed sieve procedure was adopted. The procedure for the test is listed below:

- Oven dried materials were washed to separate adhered fines from coarser sized particles
- After washing, the materials were again dried to a constant mass at 40ºC
- Later the materials were placed in a standard set of sieves and were shaken for 13 minutes in a mechanical sieve shaker
- Materials from different sieves were then separated and weighed
- Percentage by mass passing through each sieve size was recorded to the nearest 0.1 g
- The grain size distribution was then plotted in a semi-logarithmic scale (ordinate: cumulative percent passing in normal scale, and abscissa: sieve opening in logarithmic scale)

Observations: This test was repeated three times and provided consistent results. The temperature during drying was controlled carefully so that excessive heat could not melt

the asphalt coated materials and break apart and encapsulate fines. If this happened, then the gradation would not represent the actual materials.

Figure 3-9 Set of sieves in a mechanical sieve shaker

3.4.2 Laboratory Compaction for Moisture-Density Relationship

The optimum moisture during the mixing, and maximum dry density of the mix can be determined from laboratory compaction using standard Proctor effort according to ASTM D698 at the FDR mix design stage. According to NSTIR (2012) during construction, more than 83% of the maximum theoretical density should be achieved in the field. Optimization of density and moisture content is necessary as insufficient compaction can lead to some problems like excessive permanent deformation in the base layer.

Compaction increases the density of the FDR materials. If adequate compaction is not attained in the field, the inter-granular contact of FDR materials will be low. The load on the base materials will cause the FDR materials to slip, which will eventually cause rutting. Variation of density in a pavement section can lead to variability in the performance of the pavement. Pavement materials from all the locations should have consistent maximum dry density to ensure desired performance. Field compaction to values that approach optimum density results will perform best in a stabilized base layer.

Even though the modified Proctor test is advised for expanded asphalt mix designs by Iowa Department of Transportation (Lee et al., 2003), Ministry of Transportation Ontario (MTO, 2011) and North Dakota Department of Transportation (2011), it can be difficult to achieve compaction in the field when based on the modified Proctor. As too much energy is induced in modified proctor, sometimes it may not be achieved in field. The standard proctor is a common practice in industry such as AMEC and Industrial Cold Milling. The standard Proctor was used in this research because it provides reliable values. The procedure for the test is listed below:

- The dried materials were passed through the 4.75 mm sieve
- Different amounts of water by mass were thoroughly mixed with the FDR materials to prepare several samples with various water contents
- A 4 inch Proctor mold of (101.6 ± 0.4-mm) average inside diameter, (116.4 ± 0.5 mm) of height, and (943.0 ± 14 cm^3) of volume was assembled with a base plate and an extension collar
- The sample mixed with water was placed in three equal layers with 25 compactions in each layer with a manual rammer
- The rammer was dropped freely from 12 inch (305 mm) height producing a compactive effort of 12 400 ft-lbf/ft^3 (600 kN-m/m^3).
- After compacting three layers, the collar was taken out and the sample was leveled with a straightedge
- The weight of the sample was measured and subtracted from the previously known weight of mold and base plate

- After measuring the mass, the sample was dried in oven at 40ºC to a constant mass to measure the molding moisture content after the test
- The moist density of the material was calculated using the Equation (3-6) according to the ASTM D698

$$\rho_m = K * \frac{M_t - M_{md}}{V_c} \qquad (3-6)$$

where,

ρ_m = moist density of compacted specimen (compaction point), g/cm^3

M_t = mass of moist soil in mold and mold, nearest g

M_{md} = mass of compaction mold, nearest g

V_c = volume of compaction mold, cm^3

K = conversion constant, depending on density units and volume units, (1 for g/cm^3 and volume in cm^3)

- The dry density was calculated after determining the molding water content using the Equation (3-7) provided by the ASTM standard

$$\rho_d = \frac{\rho_m}{1 + \frac{\omega}{100}} \qquad (3-7)$$

where,

ρ_m = moist density of compacted specimen (compaction point), g/cm^3

ρ_d = dry density of specimen at compaction point, g/cm^3 (later converted to kg/m^3)

ω = molding water content of compaction point, nearest 0.1 %

- The compaction curve was then plotted in a normal graph with molding water content in abscissa and dry density in ordinate

Observations: The values of optimum moisture and maximum dry density of FDR samples obtained from the laboratory compaction test were further used in other tests such as CBR, direct shear test, and resilient modulus. It took several days to test 6 different samples from each location of both the projects.

Figure 3-10 Samples after Proctor compaction (picture adopted from TEST-LLC, 2013)

3.4.3 Theoretical Maximum Density to Obtain Zero Air void in Materials

Theoretical Maximum Density (TMD) is a test to measure the density of materials without air voids between the particles. During construction, zero air voids in field is unattainable. TMD is used to assess the amount of air voids contained in the actual compacted mix. The TMD test was performed according to ASTM D2041/D2041M – 11 standards.

The procedure is summarized as follows:

- The dried sample was weighed and placed in a vacuum vessel
- Water of 25ºC was added to completely submerge the particles
- The lid of the vessel was carefully tightened and the vessel was placed in a machine to reduce the residual pressure inside the vessel as shown in Figure 2-11
- To reduce the residual pressure to 4 kPa, the vacuum was gradually applied to the vessel
- Then the vessel was kept at rest for 15 minutes
- The vacuum was gradually released after the vacuum period
- The vessel was filled with water and the lid was placed on the vessel to measure the total mass of vessel, lid, water, and sample mix in the air to determine the volume of the sample
- The temperature was also measured
- From the mass of the sample, the maximum specific gravity was measured using the following Equation (3-8) as mentioned in ASTM standard:

$$G_{mm} = \frac{A}{A + D_l - E_l} \qquad (3-8)$$

where,

G_{mm} = maximum specific gravity
A = mass of dry sample in air, g
D_l = mass of lid and vessel filled with water at 25ºC, g
E_l = mass of lid, vessel, sample and water at 25ºC, g

- After measuring the maximum specific gravity, the mass of the sample was taken at saturated surface dry condition to measure the specific gravity at saturated surface dry condition using the following Equation (3-9):

$$G_{mb} = \frac{B}{B + D_l - E_l} \qquad (3-9)$$

where,

G_{mb} = bulk specific gravity (at saturated surface dry condition)

B = mass of sample at saturated surface dry condition, g

D_l = mass of lid and vessel filled with water at 25ºC, g

E_l = mass of lid, vessel, sample and water at 25ºC, g

- For measuring the absorption of the materials the sample was dried in the oven at 40ºC to a constant mass. The absorption of the material was measured using the following Equation (3-10):

$$\%\ water\ absorption\ = \frac{B - A}{A} \qquad (3-10)$$

where,

A = mass of dry sample in air, g

B = mass of sample at saturated surface dry condition

- For measuring the air void contents of the materials Equation (3-11) was used.

$$\%\ air\ void\ contents = \frac{G_{mm} * \gamma_w - \rho_d}{G_{mm} * \gamma_w} * 100 \qquad (3-11)$$

where,

G_{mm} = maximum specific gravity

γ_w = unit weight of water,1000 (kg/m^3)

ρ_d = optimum density, (kg/m^3)

Observations: The theoretical maximum density of materials from both the projects was measured by following the above procedure.

Figure 3-11 Test procedure for Theoretical Maximum Density (Pavement Interactive, 2011)

3.4.4 California Bearing Ratio of Materials

California Bearing Ratio (CBR) test is an empirical test used to evaluate the relative strength of a material compared to that of standard well graded crushed rock that resists penetration by a steel piston. As it is a quick method, the CBR test is sometimes chosen in lieu of resilient modulus testing for estimating the relative stiffness of materials by correlation. The CBR was done in soaked and dry conditions. The CBR is articulated as the ratio of the unit load on the piston required to penetrate 0.1 in. (2.5 mm) and 0.2 in (5 mm) of the test soil to that of the standard material of well-graded crusted stone.

The CBR was determined according to ASTM D1883-07. A brief procedure for the test is listed below:

- Materials were dried at 40ºC to a constant mass for both soaked and dry CBR
- Water by percent of the materials was added to meet the optimum moisture level (optimum moisture level was found through standard Proctor for moisture-density relationship)
- Compaction was done using the standard effort with 6 inch mold and 56 blows per layer for three layers
- For the dry CBR, the test was done immediately, and for the soaked CBR, the sample was immersed in water for 96 hours
- Calibration was done prior to the test to confirm the machine would apply the loads at the exact displacement rate
- The load rate of 0.05 in. (1.27 mm)/min was maintained within ±20% over the range of loads developed during penetration
- A filter paper is recommended to be used so that the fines particles remain within the mold during compaction at optimum moisture content.
- During the compaction plastic instead of filter paper was used so that the materials would not stick to the mold, and during the soaked CBR, some holes were created in the plastic so that the materials could be soaked with water
- For the soaked CBR, the compacted sample with the mold and spacer disk attached with a gauge was soaked in water for 96 hours
- The gauge was attached to see how much the materials swelled after 96 hours
- The load was applied at same rate in the both top and bottom side of the samples in both soaked and unsoaked CBR
- The stress was calculated after determining the load from the dial gauge
- After the test, samples from the top and bottom sides were collected from the mold to measure the moisture content at the end of the test
- Stress versus penetration was plotted in a normal graph

Observations: From the plot of stress versus penetration for the CBR samples, it was observed that the penetration measured at 0.1 in (2.5 mm) and 0.2 in (5.0 mm) for both soaked and unsoaked samples showed very little variation in most of the cases. In some cases, there was huge variation in soaked and dry CBR, as the filter paper was used and samples were stuck to the paper and lost during the test. After that, the plastic was put on the disk instead of filter paper and no materials stuck to the plastic. Therefore, the materials showed more reliable results.

Figure 3-12 CBR testing Machine (image adopted from Geodata.info, 2010)

3.4.5 Direct Shear Strength for Granular Materials

Direct shear testing in pavement materials is rarely conducted in pavement engineering practice. Two important parameters of pavement materials, such as shear strength and friction angle can be measured by using this test. These two parameters are evaluated from material classification. The strength and level of cohesiveness in materials can be measured from direct shear testing. This test was used to compare the strength of materials from different locations in this project.

ASTM D3080 standard was used for the direct shear testing. A 12" x 12" shear box was used in this test. A short summary of the procedure has been listed below:

- The materials were dried at 40ºC to a constant mass
- The shear box was assembled in the load frame
- All the samples were tested at optimum moisture content determined from the moisture-density relationship
- The samples were compacted as close as possible to the maximum dry densities
- A wooden mallet was used to compact the samples
- The mass of the materials and the volume of the shear box was measured
- Materials were compacted in three layers
- After each layer compaction with the wooden mallet, the volume of the materials is measured and the compaction continues until the sample had reached close to the maximum density
- Shear strength was measured in three different normal stresses at 50.2 kPa, 98.2 kPa and 150 kPa
- The horizontal and vertical displacements were measured every one minute until the sample failed under shear loading

Observations: The shear failure in the samples was assumed when the upper portion of the shear box slid over a significant part of the lower portion. The cohesion and the angle of internal friction were measured from the plot of maximum shear stress to the applied normal stress. For each applied normal stress, the shear stress to the horizontal

displacement was also plotted for samples from six different locations for direct comparison for both projects. It was a laborious and time consuming test.

Figure 3-13 Compacted sample for direct shear testing

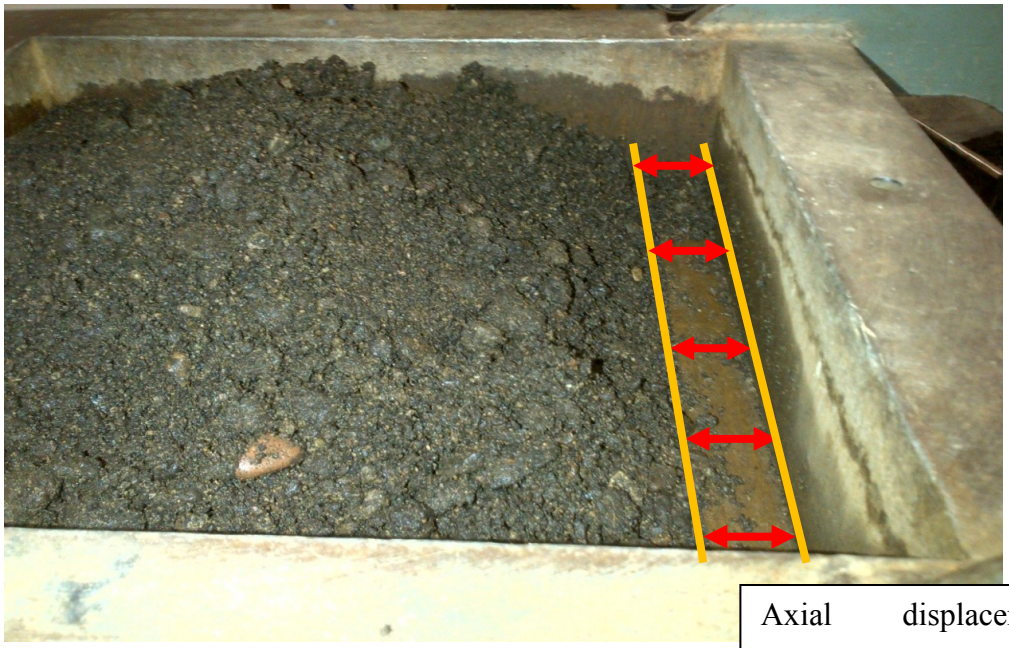

3-14 Sample after the shear failure took place

3.4.6 Resilient Modulus for Granular Materials

The performance and capacity of pavement materials to resist load can be determined by the resilient modulus of those materials. Greater resilient modulus of materials indicates the ability of materials to resist higher load at a given deformation. Though this test is important it is not frequently exercised on granular materials of pavement. The test is extremely strenuous and time consuming. Specialized equipment is necessary to perform this test in the field. A common practice for estimating resilient modulus in pavement design is to correlate it with the CBR of materials. The test was done on the materials of both the projects to compare the stiffness. The easy though less reliable correlation of CBR and resilient modulus was not used in this research. For watching the effect of water in the resilient modulus of FDR aggregate materials, 18 samples were prepared at three different moisture levels, such as at optimum moisture, 1.5 % drier than the optimum moisture and 1.5 % wetter than the moisture content.

To characterize the quality of unbound granular materials, the resilient modulus was also considered as a strong and reliable tool along with the preliminary testing such as grain size distribution and laboratory compaction. AASHTO T307 standard was the standard that was adhered to during the granular resilient modulus testing. The Instron 8501 loading frame was used for the test.

A short description of the procedure for the resilient modulus testing is listed below:

- All the materials were dried at 40ºC to a constant mass
- The samples were prepared at optimum moisture content and divided into six equal amounts
- The six lifts of samples were kept in plastic bags so the moisture content would remain the same
- A base plate with O-rings, split steel mold, extension collar and a cylindrical rubber membrane was set up
- The air between the rubber membrane and the split mold was taken out using a motor

- Filter paper was used on the top of the base plate so that the materials would not get stick to the metal
- Once the rubber membrane was stuck to the mold with no air in between, the six lifts of samples were put inside the mold layer by layer and compacted with an electric rotary hammer of 750 Watts with 1800 blows per minute, each time a new layer was added
- A metal spatula was used to scarify the top layer after compacting each layer
- After a firm compaction the split mold was taken out and the compacted sample was embedded in a rubber membrane on a steel plate
- An enclosure was placed over the sample to create a triaxial chamber
- The whole triaxial chamber was then placed on the Instron 8501 loading machine
- Two Linear Variable Differential Transducers (LVDT) were fixed on the top of the triaxial chamber to measure the axial deformation. These transducers were located equidistant from the piston rod and were placed on hard, fixed surfaces which were perpendicular to the LVDT axis. For 152 mm diameter specimen, the range of LVDT should be ±6 mm. Both LVDT s should meet the following specifications: (a) Linearity, ±0.25 percent of full scale, (b) Repeatability, ±1 percent of full scale and (c) Minimum Sensitivity, 2 mv/v (AC) or 5 mv/v (DC)
- A positive contact between the vertical LVDTs and the surface on which the tips of the transducers rest should always be maintained during the test procedure. In addition, the two LVDTs should be wired so that each transducer could be read and reviewed independently and the results averaged for calculation purpose
- Suitable signal excitation, conditioning and recording equipments were necessary for simultaneous recording of axial load and deformations. The signal should be clean and free of noise. The LVDTs were wired separately so each LVDT signal could be monitored independently. A minimum of 200 data points from each LVDT should be recorded per load cycle
- The air gauge was set up to supply the required amount of air pressure inside the chamber
- After the set up was completed the test was started by conditioning the materials
- The test sequences according to AASHTO T307 were followed for each sample

- Conditioning was done on the samples prior to the test by applying a 500 repetitions of load equivalent to a maximum axial stress of 27.6 kPa and corresponding cyclic stress of 24.8 kPa using a haversine shaped load pulse with duration 0.1 sec and resting period 0.9 sec.
- During the preconditioning phase, the two vertical deformation curves were viewed to ensure the acceptable vertical deformation ratios were being measured. The vertical deformation ratio, R_v can be defined as, $R_v = Y_{max} / Y_{min}$ where Y_{max} equals the larger of the two vertical deformations. Effort was given to achieve R_v values of 1.10 or less.
- The acceptable value for R_v is 1.30. Test was discontinued when R_v was higher than 1.30 which meant that there was alignment difficulties in vertical deformation
- The conditioning was terminated when vertical permanent strain reached 5% during conditioning

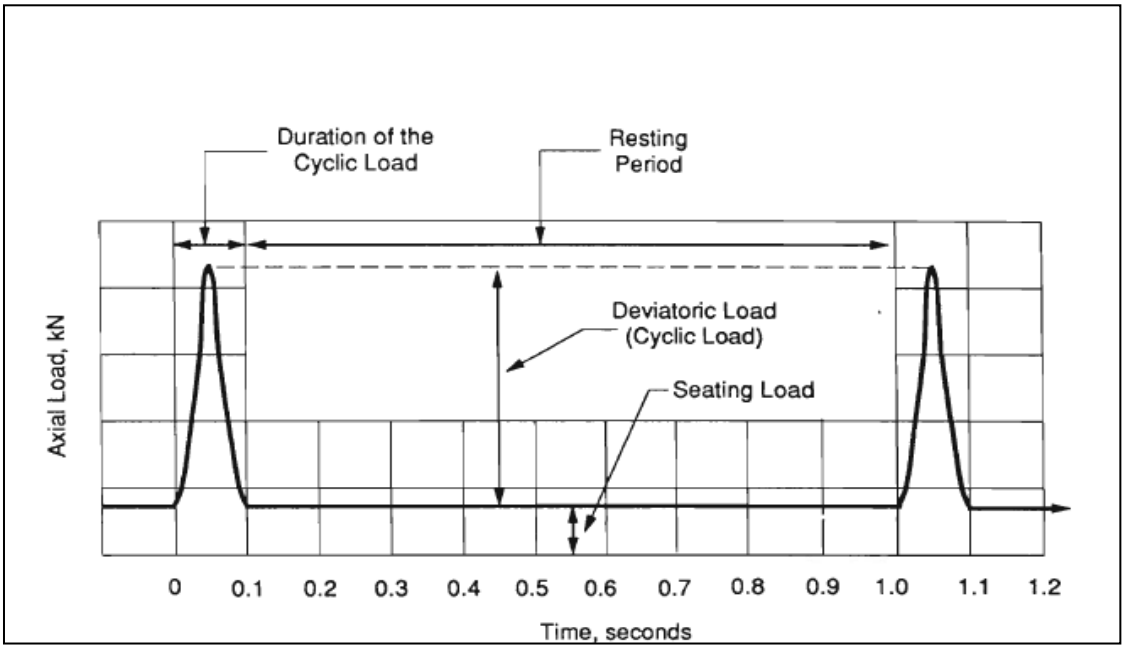

Figure 3-15 Load rate and waveforms of resilient modulus (Nazarian et al., 1996)

- For each sequence 100 cycles of load were applied. Duration of each cycle was 1 sec. The data were acquired at 1000Hz. For 1 cycle there were 1000 data points. The average recovered deformation for each LVDT was recorded for past five cycles
- The testing was terminated when the sequences were complete or if anytime the permanent strain of the sample exceeded 5 percent and the results were recorded.
- The time, load, and strain were measured for each cycle in each sequence for all six samples
- To determine the instantaneous deformation values, it is recommended to perform regression in three portions of the deformation curve:

    1. Linear regression in the straight portion of the unloading path.
    2. Regression in the curved portion that connects the unloading path and the recovery portion to yield the following hyperbolic Equation (3-12):

$$Y = a + \frac{b}{X} \qquad (3-12)$$

where,

Y = deformation value,

X = time, and

a, b = regression constants

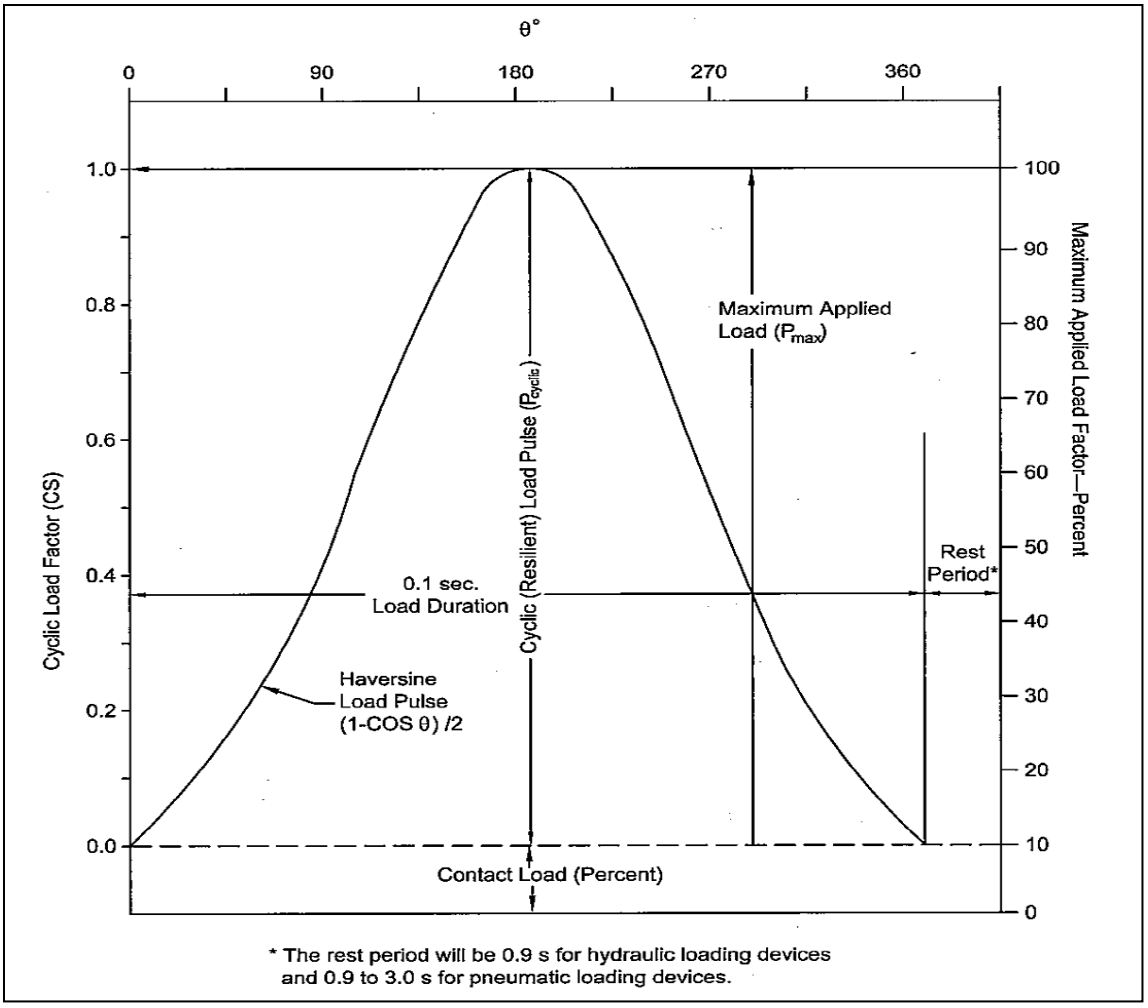

Figure 3-16 Definition of Resilient Modulus Terms Cyclic Axial Load (Resilient Vertical load P_{cyclic}) – Repetitive Load Applied to a Test Specimen (AASHTO, 2007)

3. Regression in the recovery portion between 40% and 90% (recommended range) of the rest period to yield a hyperbolic equation. A tangent should be drawn to this hyperbola at the point corresponding to 55% (recommended point) of the rest period. Two linear equations, one from the unloading path and other from the tangent of the hyperbola in the recovery period, shall be solved to determine the intersection. Then the point on the hyperbolic curve corresponding to the time coordinate of the intersection (for convenience, say point A) is selected to determine the

instantaneous deformation by subtracting the deformation at the point A from the peak deformation.

- Resilient Modulus (M_R) is defined as S_{cyclic} /ε_r where, ε_r is the resilient (recovered) axial strain due to S_{cyclic}
- The chamber confining pressure for the testing sequences were recorded. Only one entry was needed for past five load cycles
- The nominal axial cyclic stress for the testing sequence was documented. Only one entry needed for the past five load cycles. The entry exactly corresponded to the nominal axial cyclic stress required for the subgrade materials in AASHTO T307-99
- The actual applied load and stresses were recorded for each of the past five load cycles. The recoverable axial deformation of the sample for each LVDT independently for each of the past five load cycles were recorded
- The average of the response from the two LVDTs was measured. This value was used to calculate the axial strain of the material. The axial strain for each of the past five load cycles were calculated to determine the axial deformation
- A MATLAB program was written to take out the noise from the data collected and plot a smooth log-log graph (ordinate: resilient modulus in logarithmic scale, and abscissa: stress invariant in logarithmic scale)
- The resilient modulus and stress invariant were calculated using the Equation (2-7), and Equation (2-9)
- The regression constants k_1 and k_2 were determined from the graph

Observations: During the compaction care was taken so that the sample would not be tilted. The rubber membrane was placed inside the mold very carefully so that it would not get pinched within the mold and ripped by the sharp edge of the electric hammer. If the membrane was ripped, a new set up would be required and the test would need to be started from the beginning. Precautions were needed for the triaxial chamber as well. The supply of air had to be regulated carefully. During the test the sequences needed to be stopped when there was not adequate air pressure inside the chamber. The LVDTs were

placed very carefully so that the excessive load would not smash them. The test had to be halted when the LVDTs were not placed correctly and the test had to be restarted.

All the figures related to resilient modulus test are provided in Figure 3-17 to Figure 3-21.

Figure 3-17 Base plate, rubber membrane, O-rings, split mold, and extension collar set up

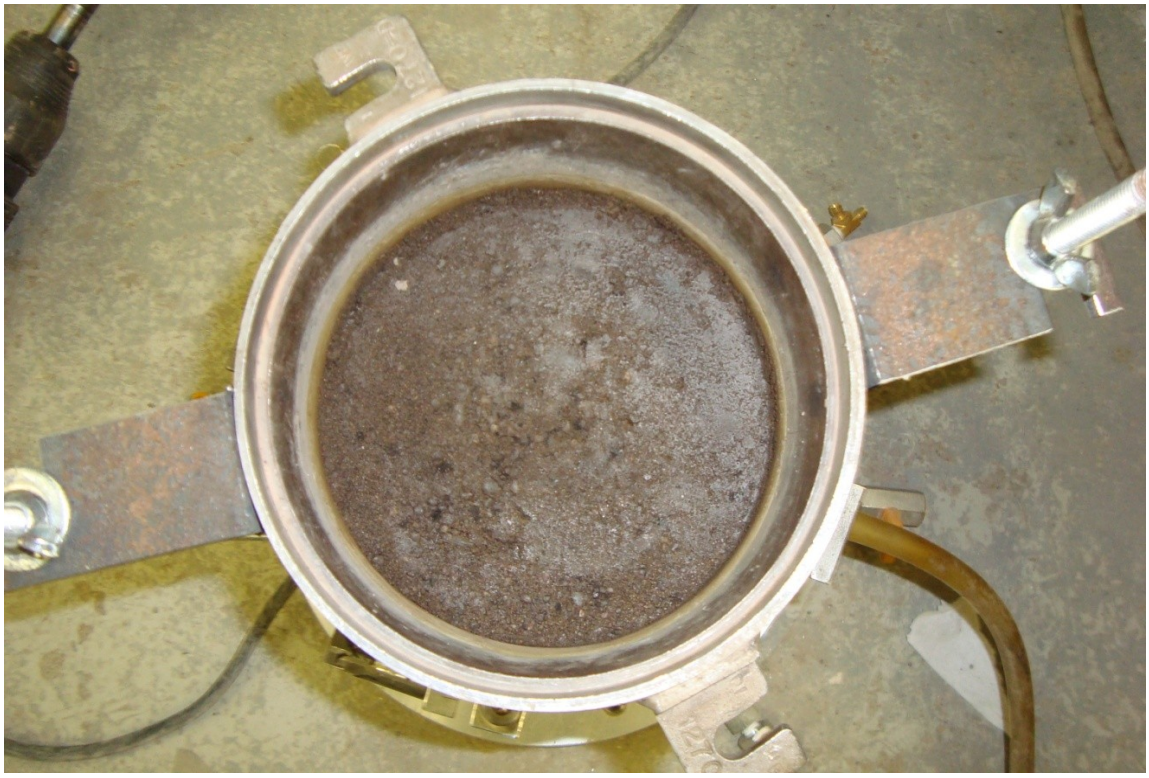

Figure 3-18 Sample face after compaction by electric hammer

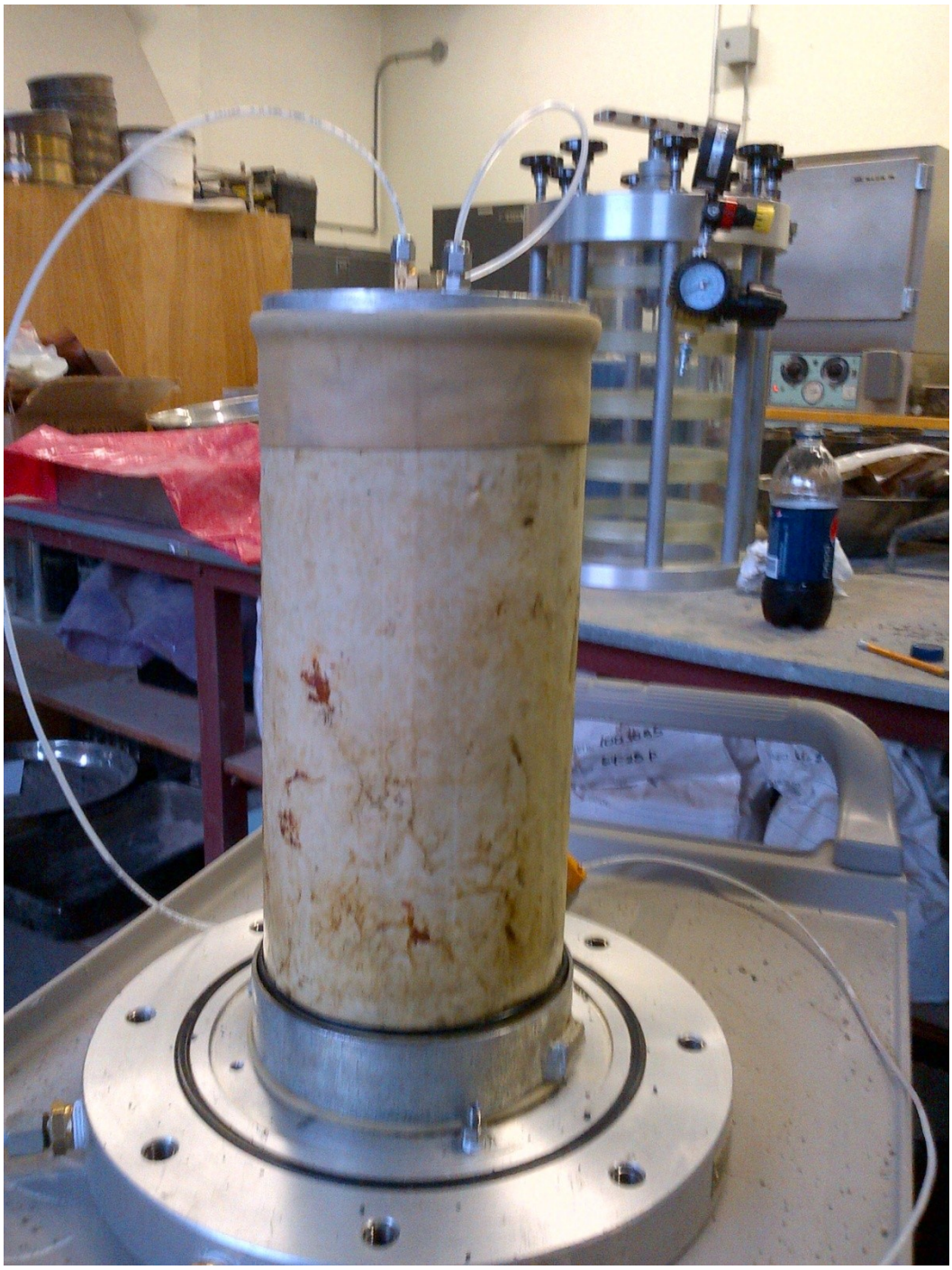

Figure 3-19 Sample after compaction without split steel mold

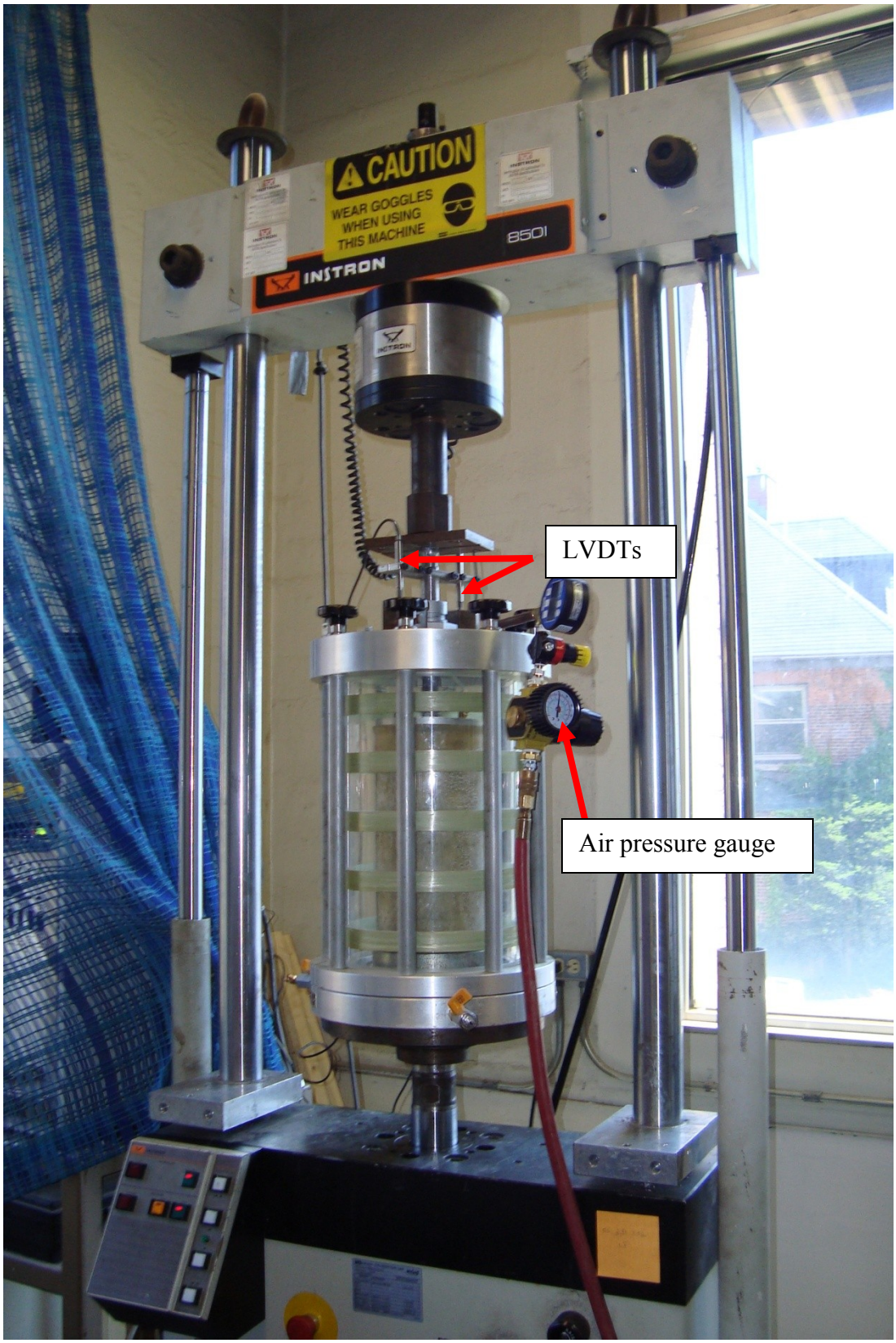

Figure 3-20 A complete set up of triaxial chamber with air pressure gauge and LVDTs

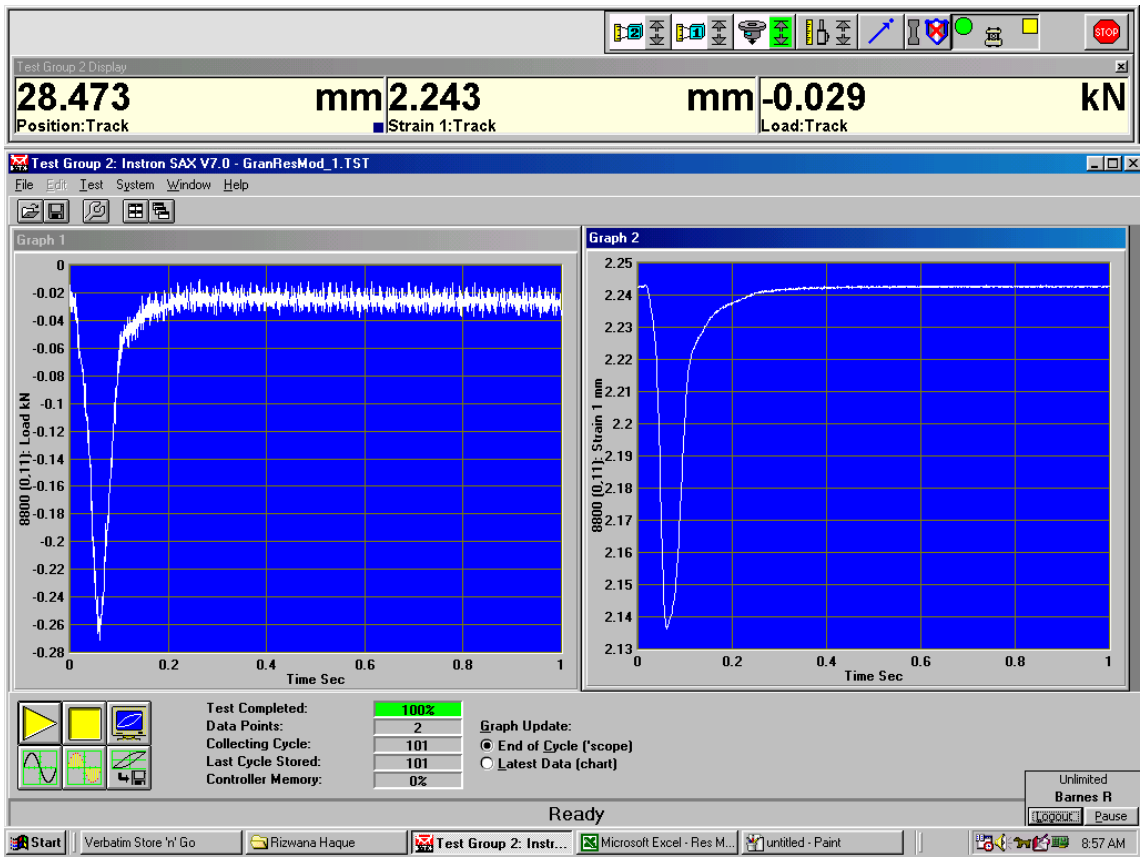

Figure 3-21 Screen shot of applied load and strain in resilient modulus test

CHAPTER 4: TEST RESULTS AND DISCUSSION

4.1 Introduction

The purpose of this chapter is to present a summary and discussion of the experimental results. All the test results of the unbound granular materials are presented in conjunction with a discussion.

The first stage of the project included obtaining the samples from six locations along Route 335 that were produced using a retroactive depth control method. Different combinations of asphalt concrete thickness and pulverization depths were observed throughout the road section. Inconsistency arose in blend ratio as the depth of pulverization was adjusted frequently to meet the average thickness of the test pit. Tests were performed to evaluate the effect of the variable thickness blend ratio on the consistency of material properties.

On the contrary, in the Route 790 project, sample locations were selected where the blend ratios should have been constant according to the GPR survey. The pulverization depth used in each subsections varied according to asphalt concrete thickness so that consistency could be maintained in the thickness blend ratio. All the samples from both the projects were tested to demonstrate the advantage of using GPR instead of a conventional retroactive method of pulverization. Consistent blend ratio and consistent material properties can be achieved through GPR controlled appropriate pulverization depth.

4.2 Test Results for Unbound Granular Materials

In Route 335, the as-built blend ratio varied as the pulverization depth of the recycling machine had to be adjusted as the pavement varied from a thin asphalt layer to a thick asphalt layer. The thickness of the asphalt concrete varied between 40 mm to 180 mm over a 200 m section that was studied. In Route 335 the coefficient of variation of blend

ratio was 37%. In Route 790, samples were obtained from the locations which exhibited a blend ratio almost identical to 0.75 in the GPR survey and the coefficient of variation of blend ratio was 1.3% only.

4.2.1 Grain Size Distribution of Unbound Granular Materials

Sieve analyses on the FDR material samples were carried out after the first pulverization stage from both projects to assess the consistency in grain size distribution of the different samples versus the gradation specified in the job mix formula. A comparison between the two pavement sections showed that consistency of the materials could be obtained by controlling the blend ratio.

The first question arises here, does the wide range of blend ratio have an effect on the material properties?

A graphical representation of the results from the six locations of the Route 335 and Route 790 projects, along with the blended job mix formula supplied by the consultant before the projects, are displayed in Figure 4-1 and Figure 4-2 respectively.

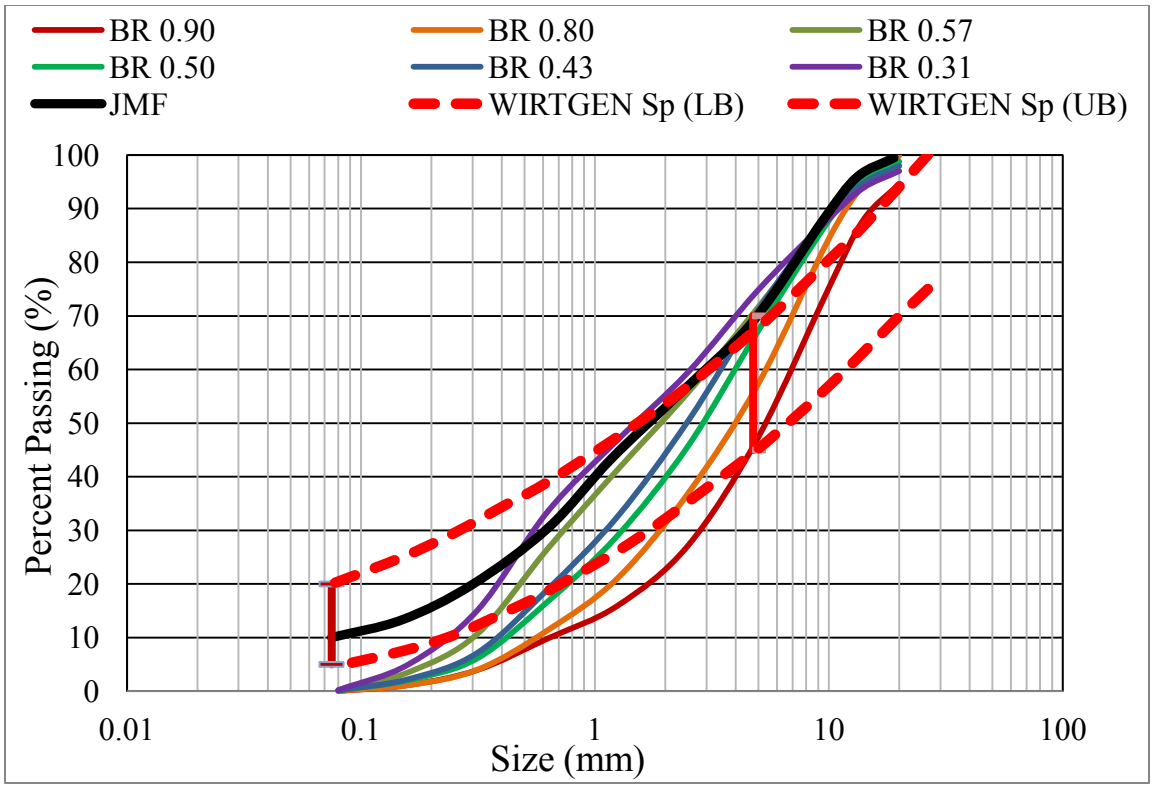

Figure 4-1 Route 335 FDR aggregate gradation and blended job mix formula with Wirtgen Specification

*BR is the acronym for Blend Ratio.

Most of the incidents have shown that unbound dust generation in gradation after the first pulverization is approximately one percent which is completely based on the ratio of the total asphalt thickness to the full pulverization depth. The possibility of presence of dust in the blended material will be higher with larger proportions of granular materials in the full pulverization depth.

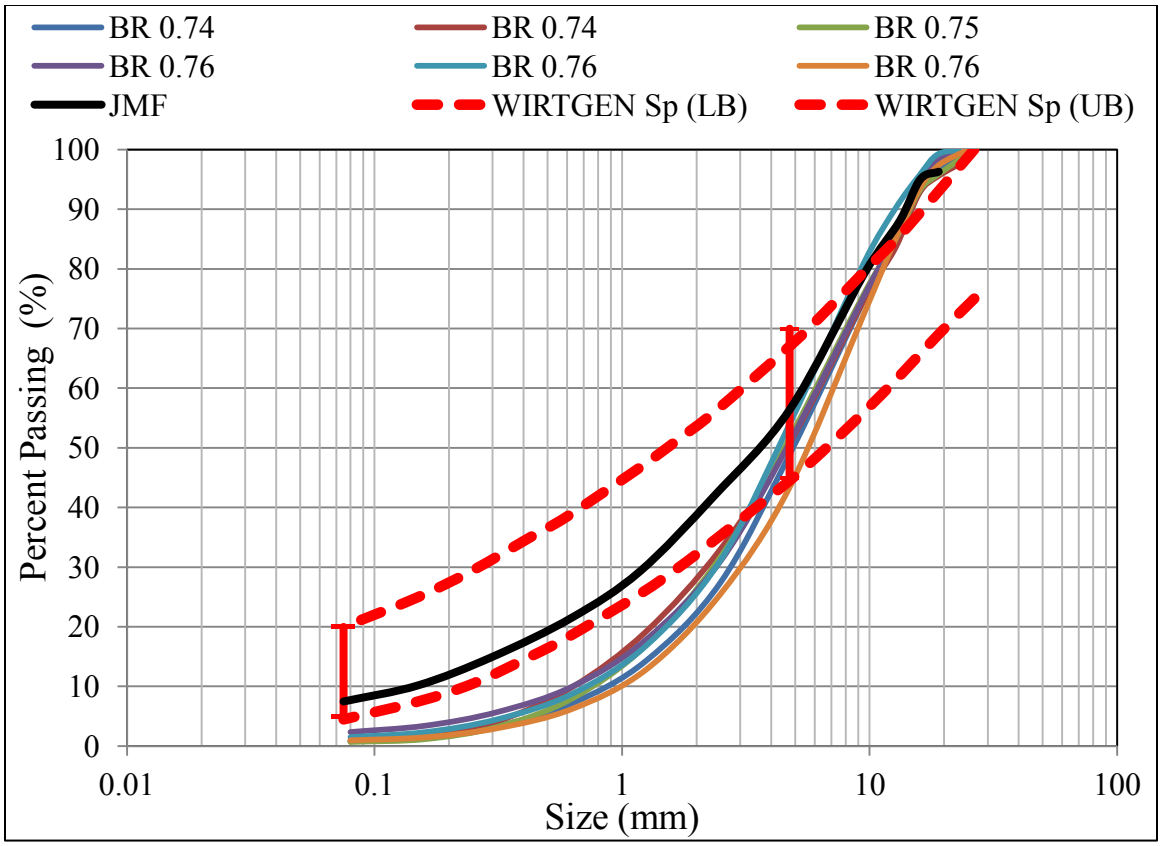

Figure 4-2 Route 790 FDR aggregate gradation and blended job mix formula with Wirtgen Specification

From Figure 4-1 it can be seen that the gradation was highly inconsistent but the aggregates obtained from the Route 335 section almost entirely satisfied the specification limits established by the NBDOT and recommended by the Wirtgen Group (2010). The intermediate particle sizes between 0.600 to 5 mm generally fell between the specified limits, but the gradation exhibited an excessive amount of coarse particles and inadequate fines. As a result, it was difficult to obtain the desired particle packing according to the optimal 0.45-power grading curve.

Route 790 materials in Figure 4-2 display a good consistency between the samples, but a large difference from the designed JMF size distribution. The samples exhibit excessive coarse materials above 9.5 mm size which do not satisfy the NBDOT specification and the specification recommended by the Wirtgen Group (2010).

The second question comes as how will the low fine aggregate count affect the physical properties of the FDR aggregate?

The design mix formula for both the projects may have been based on the materials gradation after the asphalt had been extracted, whereas, the tests were done on the as-obtained materials from the field without the extraction of asphalt cement. In as-obtained materials, the fines were bound by the asphalt concrete of existing pavement and acted as conglomerate particles. As a result, inadequate fines were available to fill the voids in a new layer. An example of Route 790 material is given in Figure 4-3 to show the difference between the gradations of as-obtained materials and the gradations after the asphalt cement extraction. The inadequate fines would not allow proper dispersion of foamed asphalt particles, which would result in a poor adhesion of the recycled particles. The inadequate fines would result in a weak interlock between the particles which causes them to slide over one another when the normal stress is applied.

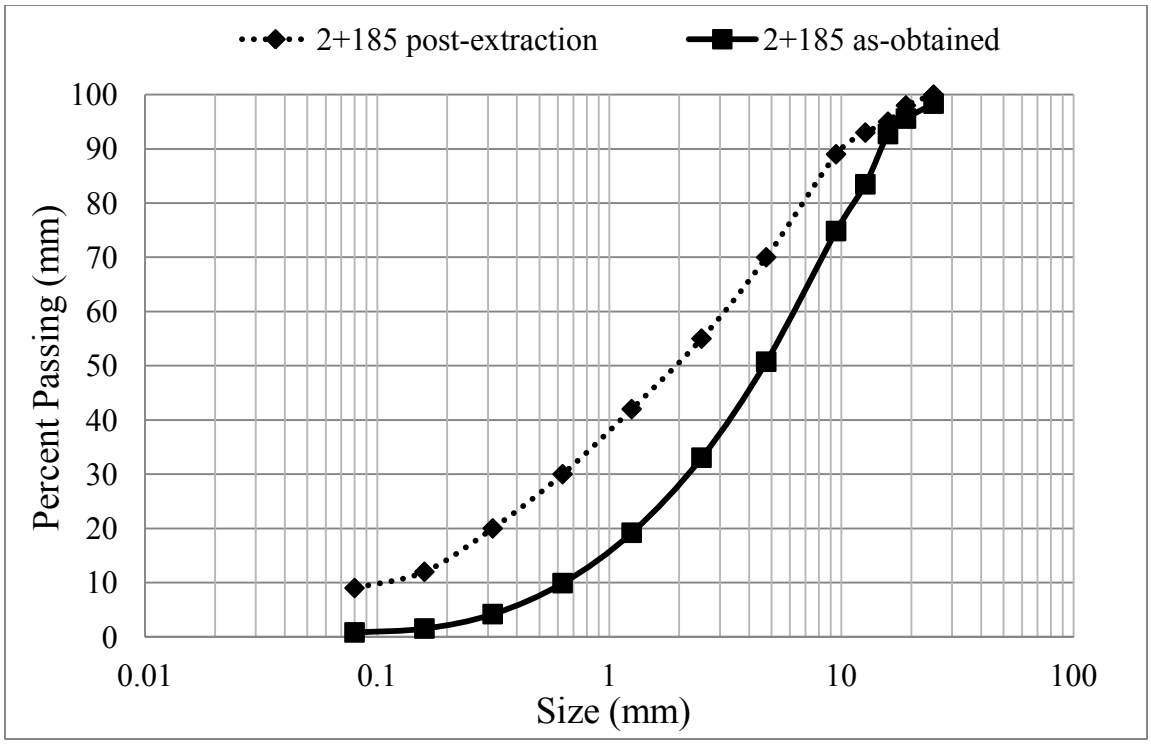

Figure 4-3 Grain size distribution of post extracted materials and as-obtained materials from Route 790 project (Salah, 2013)

Figure 4-3 shows that the materials after post extraction contain a significant amount of fines which were bound with asphalt cement in the as-obtained materials. These fines cannot be liberated as FDR is a cold method and sufficient heat is not generated during the pulverization process, which may not have taken into consideration during the mix design process.

The ideal gradation should aim to obtain an optimum particle packing according to the 0.45-power curve. A corrective aggregate could be used to reach the approximate shape of the ideal gradation curve which is expected to provide a stronger, denser, aggregate structure which will eventually improve the strength of the stabilized base.

The fineness modulus of the materials from both projects is given in Table 4-1. The following table notes that the higher the blend ratio the more the fineness modulus, which

means that a higher blend ratio corresponds to coarser particles. A higher blend ratio means a higher amount of hot mix asphalt concrete content.

Table 4-1 Fineness Modulus for materials from both the projects of Route 335 and Route 790

Route 335			Route 790		
Station	Blend Ratio	Fineness Modulus	Station	Blend Ratio	Fineness Modulus
7+725	0.90	7.37	1+769	0.74	5.26
7+790	0.80	6.90	2+185	0.74	5.11
7+075	0.57	6.10	2+550	0.75	5.16
7+750	0.50	6.51	3+128	0.76	5.08
7+772	0.43	6.36	3+446	0.76	5.02
7+703	0.31	5.86	4+040	0.76	5.38
Mean	0.59	6.51		0.75	5.17
Standard Deviation	0.22	0.55		0.01	0.13
Coefficient of Variation (%)	37%	8.5%		1.3%	2.5%

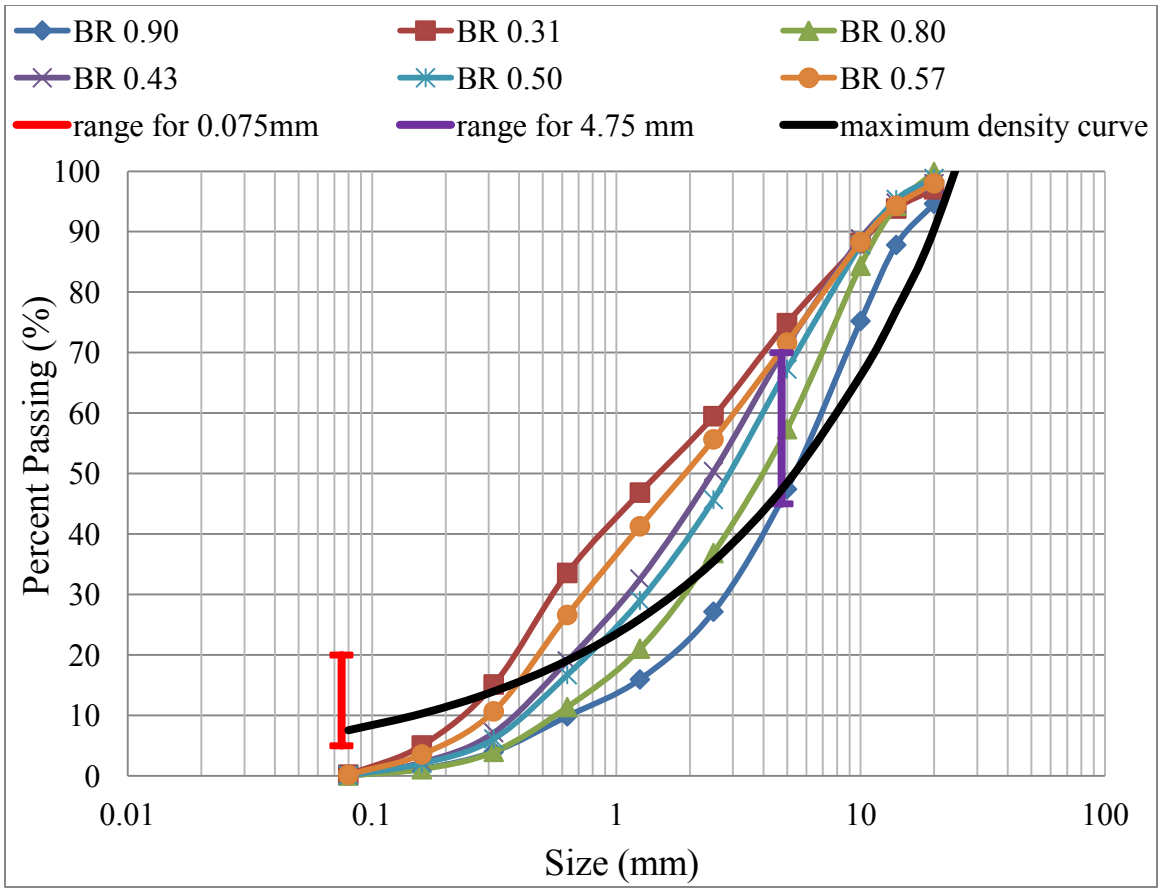

Figure 4-4 Grain size distribution of as-obtained materials from Route 335 project and Maximum Density 0.45 Power Curve

The gradation of the materials from both the projects along with the 0.45 power curve is presented in Figure 4-4 and Figure 4-5. A lack of fines was observed in the materials because of the method used during the mix design stage to estimate the fines' content. Fines were expected to be generated during the second stage of the pulverization process. For Route 335 materials the gradation curve of the aggregates with a blend ratio of 0.9 is closest to the 0.45 power curve, which means that the density of the materials and CBR values should be higher. From Figure 4-4 it can be seen that the materials with a blend ratio of 0.9 exhibit the least amount of fines, which means that the particle packing was not dense and the air void content was 30.84%. As a result, the optimum density was only 1712 kg/m^3 and the CBR value was only 7, which were the lowest among the six

samples. With a CBR value of 7 the materials cannot be used as a base or sub-base material. The gradation curve of the materials with a blend ratio of 0.31 was farthest from the 0.45 power curve, but the amount of fines were higher, which indicates a denser particle packing with an air void content of 22.22%. The result reflected the optimum density and CBR values which are 1955 kg/m^3 and 12 respectively.

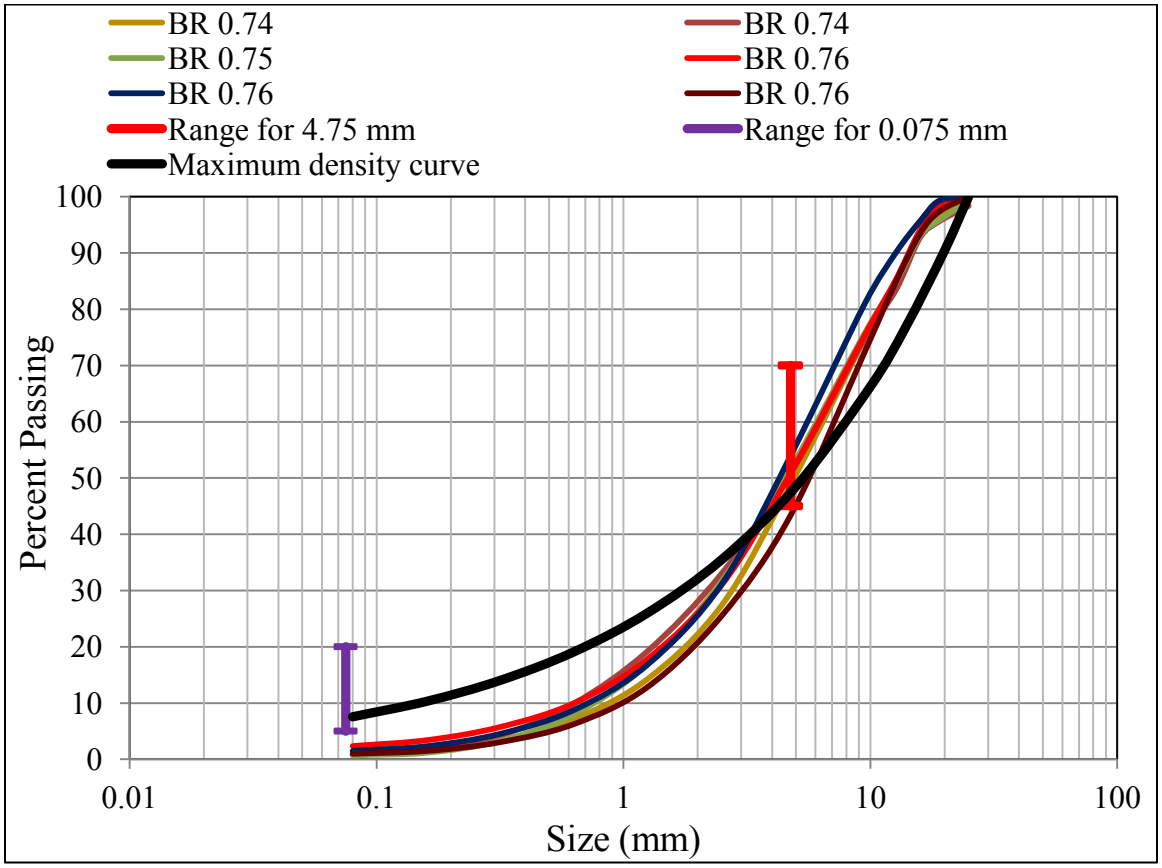

Figure 4-5 Grain size distribution of as-obtained materials from Route 790 project and Maximum Density 0.45 Power Curve

From Figure 4-5 it can be seen that the materials from Route 790 need to add fine particles to obtain the densest particle packing. As the coefficient of variation of gradation was low, the CBR values of samples from six different locations with an almost

identical blend ratio were within the range of 2.9-3.6 with only 15.5% of coefficient of variation.

4.2.2 Moisture-Density Relationship of Unbound Granular Materials

The moisture density relationship was determined by the Standard Proctor method. The test was performed to determine the optimum moisture content at which the maximum density could be achieved in the field. Figure 4-6 shows the relationship between the optimum moisture content and blend ratio for Route 335 materials. The moisture content tends to decrease with increasing blend ratio as less moisture is needed for less fine materials. The optimum moisture content varied from 7.63% to 10.75% with 12% of coefficient of variation. Table 4-2 shows that the materials of the lowest blend ratio needed the highest amount of water and exhibited the highest optimum density. From the gradation curve in Figure 4-1, the lowest blend ratio materials contained a higher amount of fine particles which needed more water for compaction. For the lower blend ratio the fine particles filled the void space; as a result, the materials showed higher density. Figure 4-7 demonstrates that the higher the blend ratio, the lower the density.

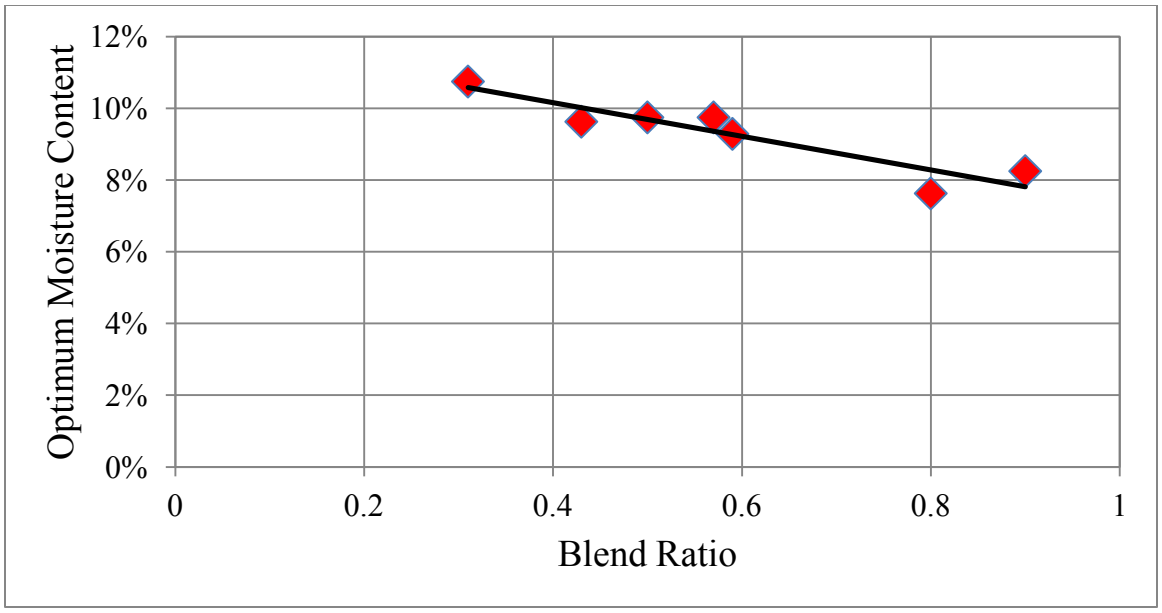

Figure 4-6 Relationship between optimum moisture content and blend ratio for Route 335 materials

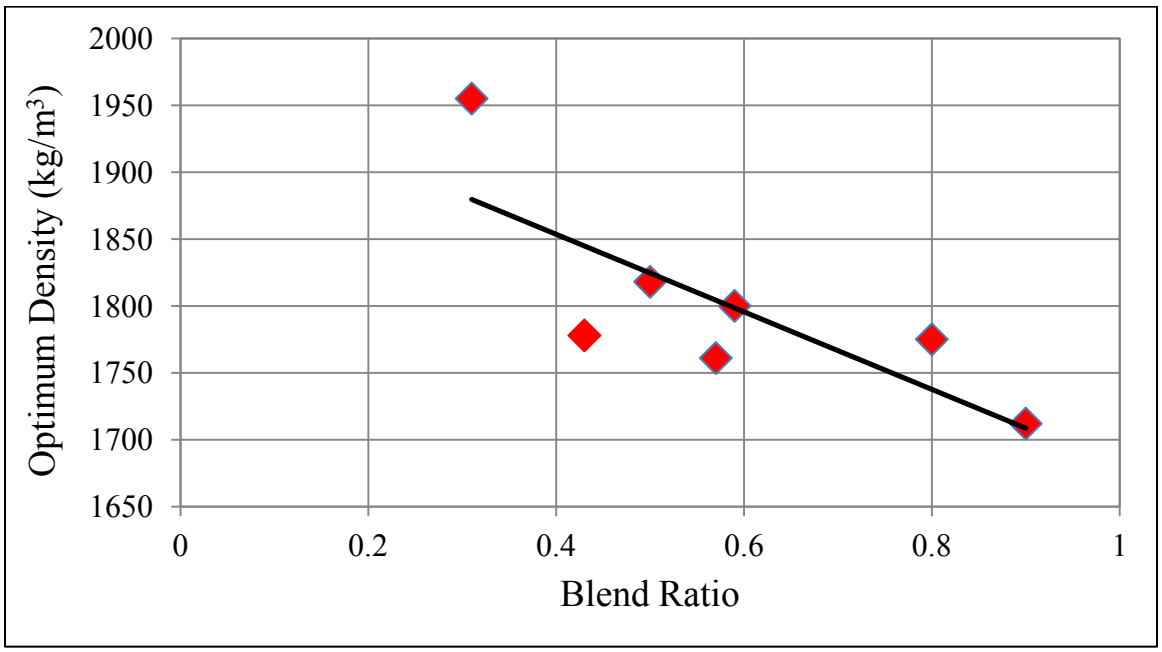

Figure 4-7 Relationship between optimum dry density and blend ratio for Route 335 materials

When the HMA content increased so did the air void contents. The air void contents for materials from both the projects were higher which are shown in Table 4-2 and Table 4-3. The aggregates from both the projects acted as conglomerated particles since the fines were not liberated during pulverization, therefore, the air void content in as-obtained materials rose.

Table 4-2 Optimum Moisture Content and Optimum Density for Route 335 materials

Station	Blend Ratio	Optimum Moisture Content	Optimum Density (kg/m^3)	Air void Content (%)
7+725	0.90	8.25%	1712	30.84
7+790	0.80	7.63%	1775	29.3
7+075	0.57	9.75%	1761	30.46
7+750	0.50	9.75%	1818	27.03
7+772	0.43	9.63%	1778	29.24
7+703	0.31	10.75%	1955	22.22
Mean	0.59	9.29%	1800	28.12
Standard Deviation	0.22	1.14%	83.3	3.21
Coefficient of Variation (%)	37%	12%	4.6%	11%

As the sample locations were selected where the blend ratio should have been constant according to the GPR survey, the variability in the blend ratio is not observed in the sampled Route 790 materials. The materials showed consistency in gradation, moisture content and optimum dry density. The optimum moisture content varied from 4.58% to 6.7%. The optimum density varied from 1760 kg/m^3 to 1859 kg/m^3. The coefficient of variation for optimum density of the Route 790 materials is half that of the route 335 materials. The asphalt content in the materials of Route 790 was almost the same for each location which is reflected in the maximum specific gravity and air void contents in the materials. The co efficient of variation in the air void contents was very low for the Route 790 materials comparing to those of Route 335.

Table 4-3 Optimum Moisture Content and Optimum Density for Route 790 materials

Station	Blend Ratio	Optimum Moisture Content	Optimum Density (kg/m^3)	Air void Content (%)
1+769	0.74	5.59%	1760	28.60
2+185	0.74	5.85%	1796	28.27
2+550	0.75	5.30%	1802	28.18
3+128	0.76	4.58%	1859	25.79
3+446	0.76	6.70%	1818	26.87
4+040	0.76	5.37%	1768	28.91
Mean	0.75	5.57%	1800	27.77
Standard Deviation	0.01	0.70%	35.9	1.19
Coefficient of Variation (%)	1.3%	12.6%	2%	4.3%

4.2.3 TMD of Unbound Granular Materials

The density of the materials with air void content was measured according to ASTM D 2041/ D2041M - 11. The maximum specific gravity, specific gravity of saturated surface dry condition and specific gravity at oven-dry condition were measured. The data is arranged in Table 4-5 for specimens obtained from Route 335. The maximum specific gravity of materials varied from 2.476 to 2.533 with a coefficient of variation of 0.8%. The saturated surface dry condition was taken when the surface of the aggregates looked dry and water was taken out of the surface. From the coefficient of variation chart, the specific gravity in the saturated surface dry condition showed higher variability. Some errors might have occurred during the judgment of saturated the surface dry condition. The results indicate that the lower blend ratio showed a higher specific gravity.

Table 4-4 Summary of Maximum Relative Theoretical Specific Gravity for materials from projects Route 335 and Route 790

Route 335			Route 790		
Station	Blend Ratio	Maximum Specific Gravity	Station	Blend Ratio	Maximum Specific Gravity
7+725	0.90	2.476	1+769	0.74	2.465
7+790	0.80	2.511	2+185	0.74	2.504
7+075	0.57	2.533	2+550	0.75	2.509
7+750	0.50	2.492	3+128	0.76	2.505
7+772	0.43	2.512	3+446	0.76	2.486
7+703	0.31	2.514	4+040	0.76	2.487
Mean	0.59	2.506		0.75	2.49
Standard Deviation	0.22	0.020		0.01	0.015
Coefficient of Variation (%)	37%	0.8%		1.3%	0.7%

Route 790 materials showed very little variation in maximum relative specific gravity. From Table 4-4, the maximum specific gravity of Route 790 materials varied from 2.465 to 2.509 with a coefficient of variation of 0.7%.

Table 4-5 Summary of Maximum Theoretical Specific Gravity, Specific Gravity at saturated surface dry condition and oven-dry condition for materials from Route 335

Station	Blend Ratio	Maximum Specific Gravity	Specific Gravity in SSD condition	Specific Gravity in oven-dry condition
7+725	0.90	2.476	2.377	2.496
7+790	0.80	2.511	2.461	2.556
7+075	0.57	2.533	2.454	2.537
7+750	0.50	2.492	2.508	2.546
7+772	0.43	2.512	2.487	2.513
7+703	0.31	2.514	2.597	2.594
Mean	0.59	2.506	2.481	2.541
Standard Deviation	0.22	0.020	0.072	0.035
Coefficient of Variation (%)	37%	0.8%	2.9%	1.4%

The materials with a blend ratio of 0.9 have the highest proportion of coarse particles and highest amount of hot mix asphalt concrete content, which can be seen from the gradation curve. These materials show the lowest maximum relative specific gravity. Figure 4-8 shows the increasing trend of air void content with increasing blend ratio. Though the materials with a blend ratio of 0.31 have the highest proportion of fine particles, they show almost same maximum specific gravity as materials with a blend ratio of 0.8 and materials with a blend ratio of 0.43. From Figure 4-1 it can be seen that the particle size

distribution of materials with a blend ratio of 0.57 almost matches the job mix formula which exhibit the highest maximum specific gravity.

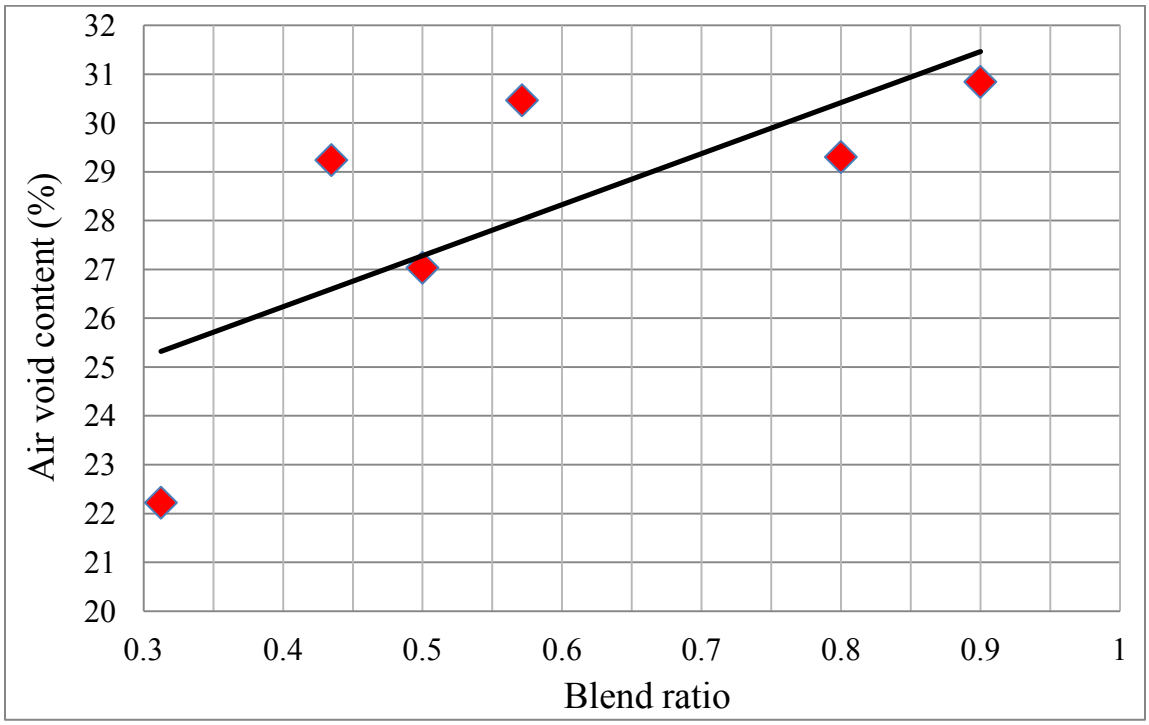

Figure 4-8 Relationship between air void content and blend ratio for Route 335 materials

Typical specific gravity for coarse and fine aggregates and asphalt cement are listed in Table 4-6. The specific gravity of the materials from both the projects renders a satisfactory value. As the materials were asphalt coated, the specific gravity of the materials was not as high as natural aggregates or not as low as asphalt cement. The materials from both projects maintained a range of specific gravity within 2.476-2.533 with a very little variation that is in between the typical specific gravity of natural aggregates and asphalt cement.

Table 4-6 Typical Specific Gravity for aggregates and asphalt cement (InDOT, 2011)

Typical Values for Specific Gravity	
Natural aggregates (both fine and coarse)	2.6
Air cooled blast furnace slag coarse aggregate	2.3
Air cooled blast furnace slag fine aggregate	2.6
Granulated blast furnace slag fine aggregate	2.1
Steel furnace slag, both fine and coarse	3.2
Asphalt cement	1.0

4.2.4 CBR of Unbound Granular Materials

According to Geiger et al. (2007), a high quality base material should exhibit a CBR value in range of 70 to 90, and a sub-base material should exhibit a CBR of around 20 so that the layers are enough stiff to carry higher traffic loads. Flexible pavement design procedures of Texas Department of Transportation specify a minimum CBR for each layer; for example, 80 for the base course, 30 for the second layer (sub-base), and 15 for a third layer (select material). Typical CBR values of different types of base courses according to Wirtgen Manual (2010) are presented in Table 4-7.

Table 4-7 Typical CBR values of different types of base courses (Wirtgen, 2010)

Types of base courses	CBR
Untreated	20-100
Cement Treated	
1. New Graded Crushed Stone	100
2. Coarse Gravel	45-80
3. Sandy silty soil	10-15
4. Graded Crushed Stone	80
5. Natural Gravel	25-45
6. Silty Soil	7-10
Bituminous Treated	
1. Graded Crushed Stone	80
2. Gravel / Soil	15-25
3. Clayey silty soil	3-7

The CBR values of Route 790 indicate that the material is unsuitable for use as a base material without stabilization. The CBR values for Route 790 materials were below 5. The CBR value of Route 790 materials showed less variation than the Route 335 materials.

Poor CBR values were observed in Route 335 materials as well, exhibiting a range between 7 and 18. It is likely that the lack of fines observed for both the Route 790 and Route 335 materials can explain the low test results from the CBR tests. The CBR values of both projects are compared in Table 4-8.

Table 4-8 CBR values of Route 335 and Route 790 materials

Route 335			Route 790		
Station	Blend Ratio	CBR	Station	Blend Ratio	CBR
7+725	0.90	7.0	1+769	0.74	3.6
7+790	0.80	7.0	2+185	0.74	3.2
7+075	0.57	11.0	2+550	0.75	3.2
7+750	0.50	18.0	3+128	0.76	4.2
7+772	0.43	11.0	3+446	0.76	2.8
7+703	0.31	12.0	4+040	0.76	2.9
Mean	0.59	11		0.75	3.32
Standard Deviation	0.22	4.05		0.01	0.52
Coefficient of Variation (%)	37%	37%		1.3%	15.5%

The pressure at each 0.1 in (2.5 mm) penetration up to 0.5 in (12.7 mm) was recorded and its ratio to the bearing value of a standard crushed rock is termed as CBR. The CBR values listed in Table 4-8 for Route 335 and Route 790 are the unsoaked CBR of 2.5 mm (0.1 in) penetration. It might be expected that the addition of corrective aggregate to the as-built FDR aggregate blend could help to approach the 0.45 power Fuller Thompson curve and greatly improve the CBR results. The improved materials then could be used for a better quality unstabilized base. The additional 2% of fines that were generated during stabilization could help to increase the strength of the aggregate structure, but additional corrective aggregate might assure that gradation within the midrange of the specification limits could be provided.

The soaked and unsoaked CBR values were measured for the materials of Route 335. In most of the cases the soaked and unsoaked CBR values varied little, but in some of the cases the unsoaked CBR values were much higher than the soaked CBR values because

some materials were missing in the mold during the test on the soaked sample. For some samples, while the filter paper was taken out before penetration, some soaked materials from top surface stuck to the filter paper. The unsoaked and soaked CBR values for 0.1 in, 0.2 in, 0.3 in, 0.4 in and 0.5 in penetration are listed below in Table 4-9.

Table 4-9 Unsoaked and Soaked CBR values for Route 335 materials

Station	Blend Ratio	Penetration (mm)	Unsoaked CBR	Soaked CBR
7+725	0.90	2.5 (0.1 in)	7	6
		5.0 (0.2 in)	11	10
		7.6 (0.3 in)	13	12
		10.2 (0.4 in)	14	13
		12.7 (0.5 in)	14	13
7+790	0.80	2.5 (0.1 in)	7	7
		5.0 (0.2 in)	13	12
		7.6 (0.3 in)	16	14
		10.2 (0.4 in)	17	15
		12.7 (0.5 in)	18	16
7+075	0.57	2.5 (0.1 in)	11	10
		5.0 (0.2 in)	19	21
		7.6 (0.3 in)	23	24
		10.2 (0.4 in)	25	25
		12.7 (0.5 in)	26	26

Station	Blend Ratio	Penetration (mm)	Unsoaked CBR	Soaked CBR
7+750	0.50	2.5 (0.1 in)	18	8
		5.0 (0.2 in)	25	17
		7.6 (0.3 in)	28	24
		10.2 (0.4 in)	28	26
		12.7 (0.5 in)	29	28
7+772	0.43	2.5 (0.1 in)	11	9
		5.0 (0.2 in)	16	14
		7.6 (0.3 in)	18	18
		10.2 (0.4 in)	19	19
		12.7 (0.5 in)	18	21
7+703	0.31	2.5 (0.1 in)	12	9
		5.0 (0.2 in)	25	18
		7.6 (0.3 in)	33	22
		10.2 (0.4 in)	40	23
		12.7 (0.5 in)	42	24

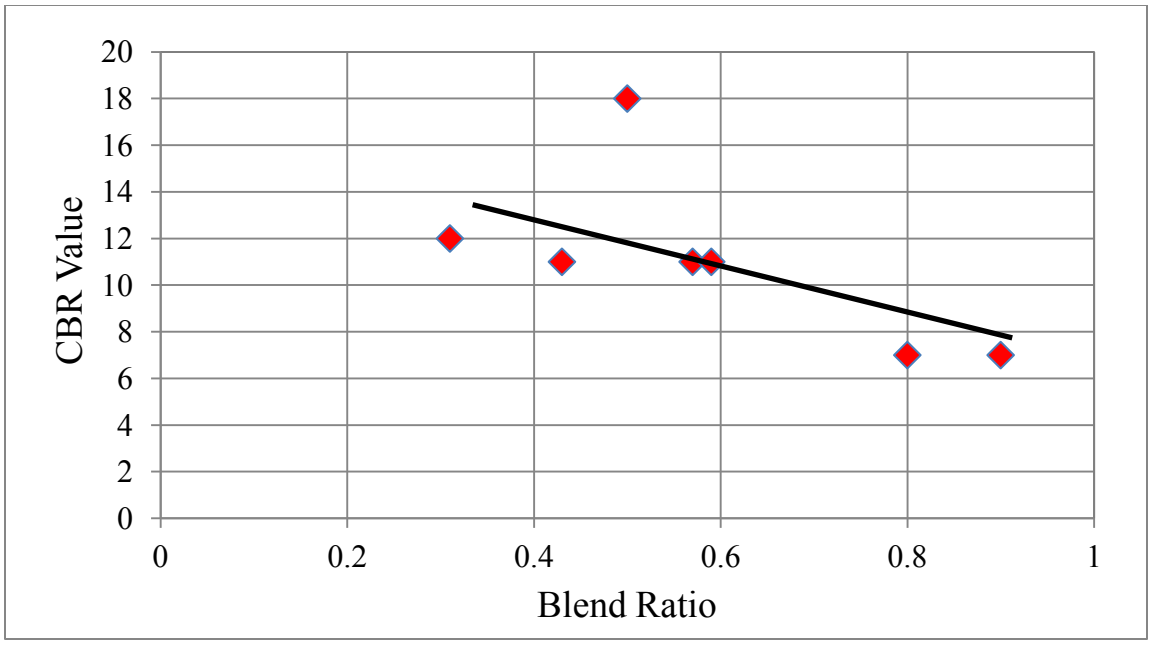

Figure 4-9 Relationship between CBR and blend ratio for Route 335 materials

From Figure 4-9 it can be seen that the CBR value decreases as the RAP content of the materials increases. The CBR values of the materials from Route 335 were comparable to those of silty clay. The CBR value of the materials with a blend ratio of 0.5 showed the highest CBR 18. Route 790 materials with almost the same blend ratio demonstrated almost similar CBR values, which were lower than the typical CBR value of clay materials. The lack of fines might have caused the lower CBR values.

4.2.5 Direct Shear Strength of Unbound Granular Materials

The shearing resistance and angle of internal friction for the aggregate particles were determined by the Direct Shear test using the shear box. Materials from Route 335 showed highest shear resistance when the blend ratio was highest and lowest shear strength when the blend ratio was lowest. Variation in shear resistance was higher for the Route 335 materials than for the Route 790 materials. The cohesion of the materials from both projects is very low. The angle of internal friction of different types of aggregate materials is listed below. All the materials from both the projects showed an almost similar angle of internal friction. It is shown in Table 4-10 that the gravel materials show 40º-60º of angle of internal friction depending on the angularity of the materials. It can be said that the angularity in the materials from both the projects was low as most of the particles from the both the projects were rounded. Results from direct shear test of both projects are presented in Table 4-11 and Table 4-12.

Table 4-10 Different types of materials and their angle of internal frictions (Yoder et al., 1975)

Types of soils	Angle of internal friction
Dry sand	25º-35º
Silts and silty sand	15º-25º
Partially saturated clay	0º-30º
Gravel material with various angularity of the grains	40º-60º
Soft saturated clay	0º

Table 4-11 Direct shear testing results under various normal stress conditions for Route 335 materials

Station	Blend Ratio	$\tau_{max\ (50\ kPa)}$ kPa	$\tau_{max\ (100\ kPa)}$ kPa	$\tau_{max\ (150\ kPa)}$ kPa	ϕ^o	C kPa
7+725	0.90	50.6	97.8	134.0	39.8	11.19
7+790	0.80	47.7	92.0	133.5	40.6	5.73
7+075	0.57	49.5	89.2	136.9	41.2	4.64
7+750	0.50	43.1	88.6	128.3	40.4	1.93
7+772	0.43	47.7	90.9	124.2	37.4	11.54
7+703	0.31	40.3	75.4	114.5	36.4	2.73
Mean	0.59	46.5	89.0	128.56	39.3	6.3
Standard Deviation	0.22	3.98	7.44	8.25	1.93	4.15
Coefficient of Variation (%)	37%	8.6%	8.4%	6.4%	4.9%	66%

Table 4-12 Direct shear testing results under various normal stress conditions for Route 790 materials (Salah, 2013)

Station	Blend Ratio	$\tau_{max\ (50\ kPa)}$ kPa	$\tau_{max\ (100\ kPa)}$ kPa	$\tau_{max\ (150\ kPa)}$ kPa	ϕ^o	C kPa
1+769	0.74	40.2	85.0	126.4	40.7	1.77
2+185	0.74	47.1	85.0	122.9	37.2	9.61
2+550	0.75	41.9	86.2	124.7	39.6	2.06
3+128	0.76	46.5	85.6	125.2	38.2	7.51
3+446	0.76	43.7	82.7	122.4	38.2	4.64
4+040	0.76	45.4	87.3	126.4	39.0	5.85
Mean	0.75	44.1	85.3	124.7	38.8	5.24
Standard Deviation	0.01	2.7	1.5	1.7	1.2	2.8
Coefficient of Variation (%)	1.3%	6.1%	1.8%	1.4%	3.1%	53%

From the coefficient of variation, Route 790 materials showed good consistency in shear resistance. For Route 335 materials variation in shear resistance increased with increasing normal stress. The variation of shear stress for Route 790 materials were less than that of Route 335 materials. As the fine particle counts were very low, the quality of aggregate interlock was poor within the aggregate structure. As a result, when the normal stress was applied on the particles, the aggregates slid over each other causing shear failure.

4.2.6 Resilient Modulus of Unbound Granular Materials

The stiffness of the materials was measured by a dynamic test called the resilient modulus test. Resilient modulus is defined as the ratio of the repeated axial deviator stress to the recoverable strain. The test was conducted to see whether or not the materials could be used as base materials. The haversine load pulse was applied on the materials with 0.1 sec loading period and 0.9 sec rest period. The load and strain were recorded and evaluated using a MATLAB program to determine the stress invariant and resilient modulus. Three different moisture contents (optimum moisture content, 1.5% above and 1.5% below the optimum) were selected to determine the stiffness of the Route 335 materials. Route 790 materials were tested at the optimum moisture content.

The third question from the study is, how does moisture variability affect the resilient modulus?

Most of the materials of Route 335 at various moisture contents reached the 15^{th} sequence of the load as per AASHTO T307-99 specification. The resilient modulus values of materials from Route 335 at the optimum moisture content are listed below. All the materials were tested as subgrade materials as they failed the test under specific loading sequences used for base materials. Tables 4-13, 4-14, 4-15 and 4-16 are presented for the resilient modulus values at different moisture contents.

Table 4-13 Resilient modulus of Route 335 materials at optimum moisture content

Station	7+725	7+790	7+075	7+750	7+772	7+703
Blend Ratio	0.90	0.8	0.57	0.50	0.43	0.31
CBR	7.0	7.0	11.0	18.0	11.0	12.0
Optimum Moisture Content (%)	8.25	7.63	9.75	9.75	9.63	10.75
Sequence						
1	16.012	93.221	44.120	94.440	4.768	56.598
2	15.665	92.992	44.033	94.388	4.590	56.052
3	15.305	92.744	43.909	94.329	4.377	55.442
4	14.865	92.470	43.763	94.268	4.157	54.797
5	14.491	92.181	43.938	94.192	3.928	54.133
6	14.868	92.362	43.803	94.265	3.916	54.733
7	14.456	92.064	43.648	94.197	3.884	54.030
8	14.023	91.735	43.493	94.122	3.687	53.300
9	13.545	91.352	45.621	94.036	3.437	52.442
10	12.998	90.956	44.981	93.938	3.176	51.563
11	12.374	91.213	43.930	94.036		52.390
12	11.713	90.786	44.536	93.940		51.465
13	10.950	90.270	44.569	93.826		50.387
14		89.696	45.192	93.697		49.176
15		89.033		93.543		47.781
Mean	13.944	91.538	44.252	94.080	3.992	52.953
Standard Deviation	1.489	1.225	0.635	0.257	0.497	2.544
Coefficient of Variation (%)	10.7%	1.3%	1.4%	0.3%	12.4%	4.8%

From Table 4-13 it can be seen that the resilient modulus of the materials with a blend ratio of 0.43 is extremely low. The latex membrane might have torn during the compaction as a result, when the load was applied the sample was not completely confined within the membrane. The result can be rejected. The same sample showed higher resilient modulus at 1.5% above and below the optimum moisture contents. The resilient modulus at optimum moisture content should be between the values of those for 1.5% above and below the optimum moisture content. Except for this sample the materials with highest asphalt content showed the lowest resilient modulus value at the optimum moisture content. During the testing of resilient modulus below 1.5% optimum moisture, the sample with a blend ratio of 0.9 failed at conditioning. The sample showed very little stiffness during the test with 1.5% above the optimum moisture content. As a result, it can be said that the materials with the highest asphalt content are very poor in quality and need stabilization to be used as a base material. The higher asphalt content in materials with a blend ratio of 0.9 indicates that the pavement section had undergone too much patching. High amount of HMA made the unbound materials less stiff.

The materials with a blend ratio of 0.8 showed higher stiffness at optimum moisture content than stiffness at 1.5% above the optimum moisture. Table 4-14 shows that the stiffness for the same material at below optimum moisture content is extremely low, which is unusual. Torn latex membrane or inadequate compaction might have occurred during testing. Table 4-15 shows that the materials with a blend ratio of 0.8 show an average resilient modulus of 63 MPa at 1.5% above optimum moisture content. As a result, it can be said that the resilient modulus of the materials below the optimum moisture level is unacceptable and invalid. The materials at optimum moisture content showed the resilient modulus of 93 MPa which is greater than the resilient modulus above the optimum moisture content. From the proctor curve it can be seen that the density at optimum moisture content is 1775 kg/m^3 and density 1.5% above the optimum is 1750 kg/m^3. The density decreases with increasing moisture content so does the stiffness. Thus the resilient modulus at the optimum moisture content is valid.

The materials with a blend ratio of 0.57 showed the valid resilient modulus in 1.5% below and above the optimum moisture contents. The resilient modulus at the optimum

moisture content should be higher than the resilient modulus at 1.5 % below and above the optimum moisture. From the proctor curve for this sample, the density at the dry side of the optimum moisture content was higher than the density at the wet side of the optimum the same trend is followed in the resilient modulus too. The resilient modulus should be highest at optimum moisture content. For this sample the amount of water added at optimum moisture content might be erroneous or the compaction might not be adequate. The resilient modulus at the optimum moisture content is invalid. At moisture content higher than the optimum, the materials started bleeding; as a result, the stiffness was lower.

Approximately 50:50 blend of HMA to granular materials is the best to ensure adequate grinding of HMA. The CBR and resilient modulus results agree to the statement. The CBR value of the materials with a blend ratio of 0.5 is 18. According to the CBR values, this sample shows the highest stiffness among the six. The reflection of the CBR values in terms of the stiffness of materials can be seen at the resilient modulus values as well. The materials with a blend ratio of 0.5 show the highest resilient modulus value at the optimum moisture content among the six samples. The resilient modulus value for the sample below the optimum moisture should be higher than the resilient modulus at 1.5% above the optimum moisture as from the proctor curve it can be seen that the density at 1.5% below the optimum moisture content is higher than that at 1.5% above the OMC. Moreover, excess water makes the materials to flow and less suitable for compaction. Thus the resilient modulus values for the materials from the Station 7+750 that are shown in Table 4-14 are invalid.

The materials with a blend ratio of 0.31 have the lowest amount of asphalt content. From Table 4-8 the CBR value for the materials was 12 which was a little bit higher than the materials with blend ratios of 0.57 and 0.43 (the CBR value for both materials was 11). Table 4-13 shows that the resilient modulus for the materials with a blend ratio of 0.31 was higher than that of the materials with a blend ratio of 0.57 at optimum moisture content. The resilient modulus for this material below the optimum moisture was lower than that at the optimum moisture level. As this material contains a higher amount of fines, the resilient modulus decreased drastically at the moisture level above the

optimum. Even the materials started bleeding during the compaction at the higher moisture level. The resilient modulus for this material at three different moisture contents is shown in Figure 4-10. From the proctor curve (Appendix A: Figure A6) it can be seen that the density at 1.5% below the optimum moisture is 1940 kg/m^3. From the proctor curve it can be seen that the density at 1.5% above the optimum moisture is 1938 kg/m^3. Therefore, the density only varies by 2 kg/m^3 for 3% difference in moisture content. May be the rotary hammer was too strong for the materials at 1.5% above the optimum moisture content and the materials started bleeding during compaction. The materials did not bleed during the compaction by a proctor hammer.

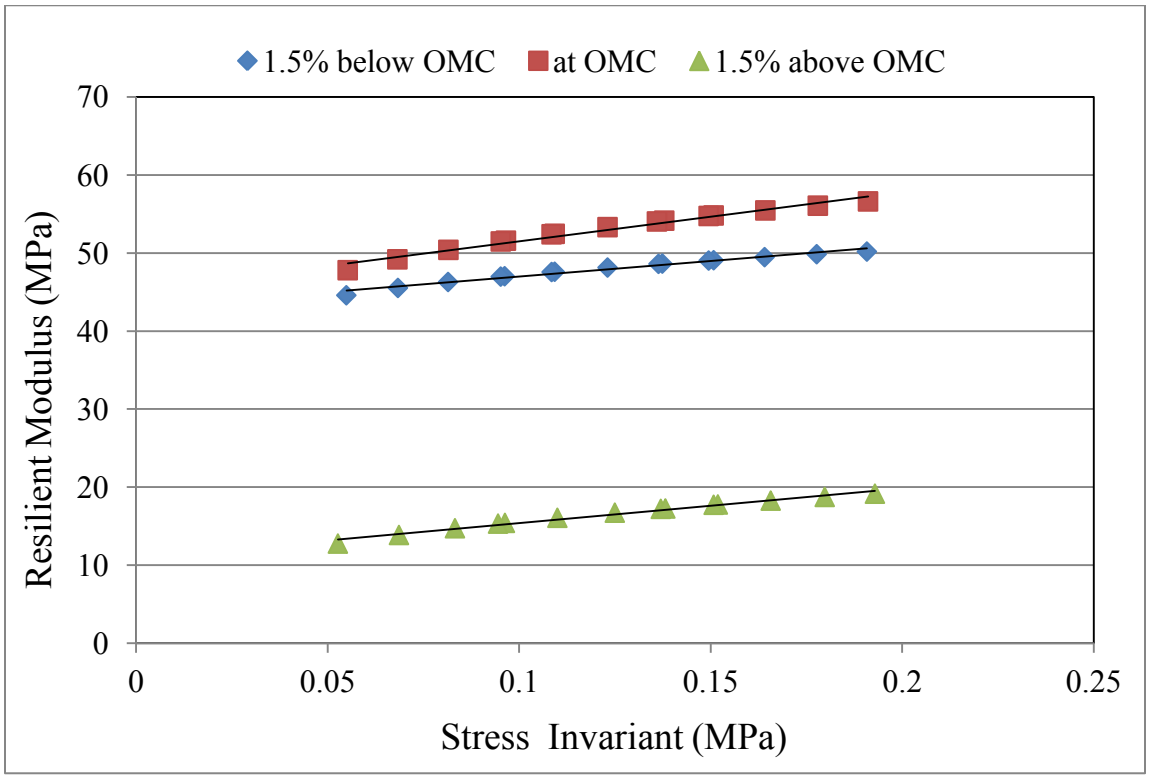

Figure 4-10 Resilient Modulus of materials with a blend ratio of 0.31 at three different moisture contents

Table 4-14 Resilient modulus of Route 335 materials at 1.5% below the optimum moisture content

Station	7+725	7+790	7+075	7+750	7+772	7+703
Blend Ratio	0.90	0.8	0.57	0.50	0.43	0.31
Moisture Content (%)	6.75	6.13	8.25	8.25	8.13	9.25
Sequences						
1		4.991	60.485	46.691	45.863	50.169
2		4.816	59.814	46.146	45.405	49.831
3		4.591	59.059	45.579	44.863	49.456
4			58.282	44.948	44.306	49.060
5			58.288	44.289	43.696	48.628
6			57.449	44.881	44.237	49.020
7			56.488	44.232	43.691	48.594
8			55.472	43.507	43.012	48.123
9			56.973	42.687	42.275	47.582
10			55.526	41.808	41.453	47.010
11			54.422	42.643	41.425	47.549
12			54.088	41.757	41.340	46.963
13			53.042	40.740	40.506	46.272
14			51.586	39.590	39.451	45.508
15			49.227	38.198	38.173	44.570
Mean		4.799	56.013	43.180	42.646	47.889
Standard Deviation		0.2004	3.145	2.441	2.237	1.611
Coefficient of Variation (%)		4.2%	5.6%	5.7%	5.2%	3.4%

Table 4-15 Resilient modulus of Route 335 materials at 1.5% above the optimum moisture content

Station	7+725	7+790	7+075	7+750	7+772	7+703
Blend Ratio	0.90	0.8	0.57	0.50	0.43	0.31
Moisture Content (%)	9.75	9.13	11.25	11.25	11.13	12.25
Sequences						
1	12.033	65.919	38.310	62.441	42.680	19.144
2	11.871	65.457	37.749	62.131	42.060	18.727
3	11.638	64.943	37.170	61.787	41.381	18.254
4	11.379	64.397	36.581	61.410	40.674	17.763
5		63.814	35.961	61.028	39.939	17.723
6		64.355	36.631	61.367	40.579	17.198
7		63.773	35.966	60.984	39.819	17.245
8		63.123	35.226	60.533	38.979	16.711
9		62.395	34.410	60.029	38.070	16.056
10		61.595	33.593	59.500	37.127	15.401
11		62.361	34.546	59.994		14.715
12		61.543	33.644	59.441		15.310
13		60.624	32.614	58.788		13.851
14		59.576	31.447	58.069		12.751
15		58.289	30.123	57.210		
Mean	11.730	62.811	34.931	60.314	40.131	16.489
Standard Deviation	0.285	2.192	2.341	1.510	1.732	1.887
Coefficient of Variation (%)	2.4%	3.5%	6.7%	2.5%	4.3%	11.4%

Table 4-15 shows that the materials with a blend ratio of 0.8 exhibit the highest resilient modulus value at 1.5% above the optimum moisture level. The materials with blend ratios of 0.8, 0.57 and 0.5 did not fail after fifteen sequences of load at 1.5% above the optimum moisture level. Like the CBR values, the stiffness of the materials from Route 335 was higher than that of the Route 790 materials.

Figure 4-11 and Figure 4-12 are presented below to show the relationship of stiffness coefficient k_1 and k_2 with blend ratio at optimum moisture content.

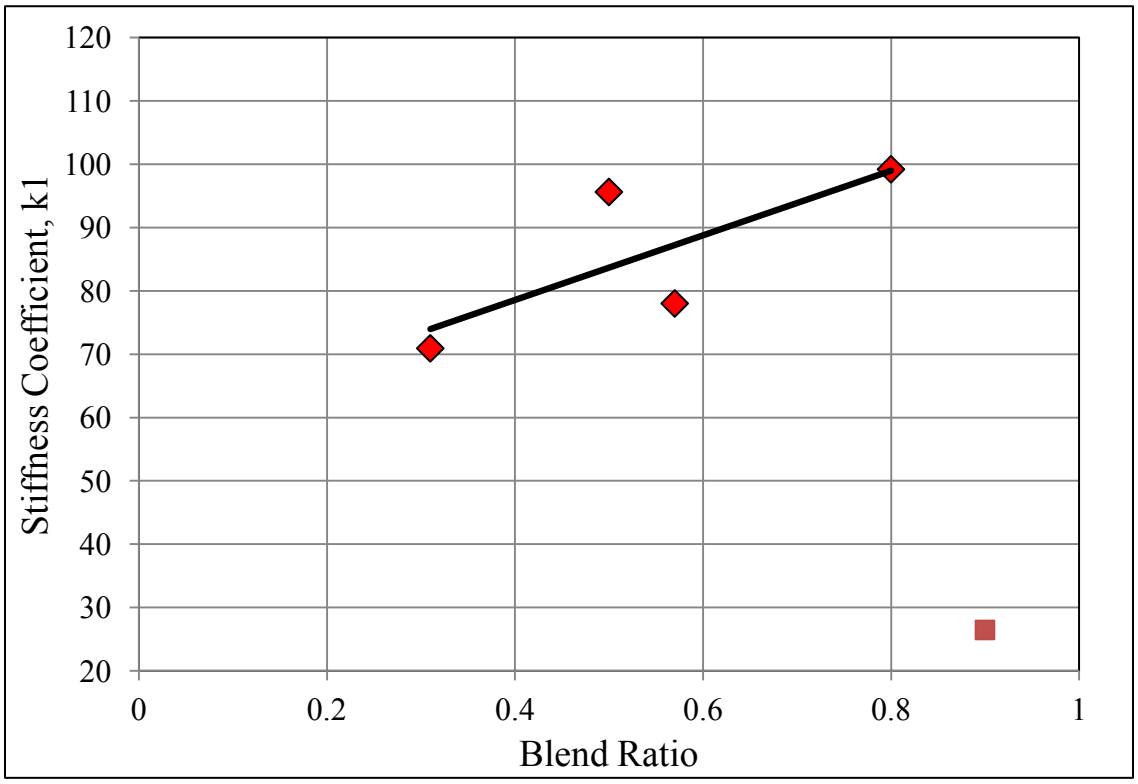

Figure 4-11 Relationship between stiffness coefficient, k_1 to blend ratio at optimum moisture content

From Figure 4-11, it can be seen that at optimum moisture content the materials with blend ratios of 0.5 and 0.8 showed higher values in k_1 which reflected in the resilient modulus. The value of k_1 tends to increase with increasing blend ratio. The resilient

modulus at the optimum moisture content for those materials was higher than the rest. From Figure 4-12 below, it can be seen that the stiffness coefficient, k_2 was lower for the materials with blend ratios of 0.5 and 0.8. The value of k_2 tends to decrease with increasing blend ratio. From the relationship given in Equation (2-10),

$$M_R = k_1\theta^{k_2}$$

The highest value of k_1 for the materials with a blend ratio of 0.5 showed the lowest value in k_2 and the materials showed highest resilient modulus.

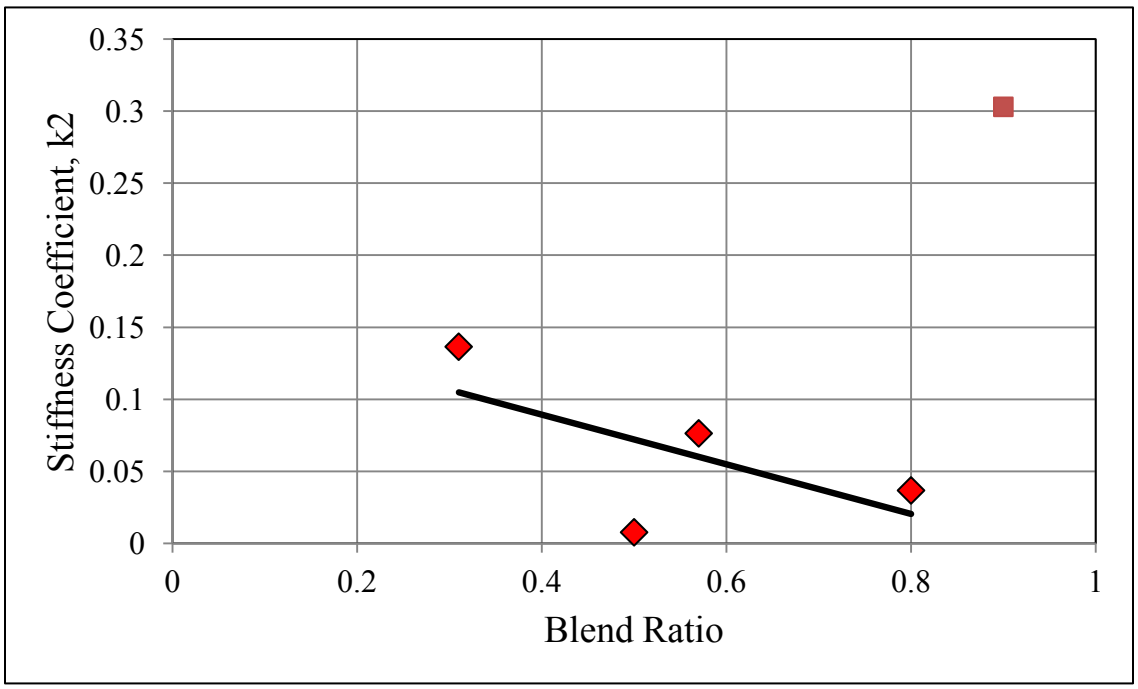

Figure 4-12 Relationship between stiffness coefficient, k_2 to blend ratio at optimum moisture content

The resilient modulus for the materials from Route 790 is presented in Table 4-16. All the samples were tested at the optimum moisture content. Most of the materials failed at the 4th sequence of the test. The CBR values and stiffness of the materials were very low.

Table 4-16 Resilient modulus of Route 790 materials at optimum moisture content (Salah, 2013)

Station	1+769	2+185	2+550	3+128	3+446	4+040
Blend Ratio	0.74	0.74	0.75	0.76	0.76	0.76
CBR	3.6	3.2	3.2	4.2	2.8	2.9
Optimum Moisture Content (%)	5.59	5.85	5.30	4.58	6.7	5.37
Sequence						
1	51.3	50.1	53.7	45.4	42.8	36.8
2	52.8	57.8	54.2	54.1	50.6	37.0
3		52.4		56.8	50.5	
4				55.2	50.9	
5				50.8	48.7	
6				39.0		
7				44.2		
8				45.8		
9				44.8		
10						
11						
12						
13						
14						
15						
Mean	52.05	53.43	53.95	48.46	48.7	36.9
Standard Deviation	1.061	3.952	0.353	6.018	3.409	0.141
Coefficient of Variation	2.0%	7.4%	0.7%	12.4%	7.0%	0.4%

The materials from both the projects were compared through all the tests mentioned in the previous sections. The coefficient of variation of Route 790 materials was lower than Route 335 materials in each test result. From the test results it can be said that if a consistent blend ratio is maintained, the material properties would be consistent as well.

With the material properties obtained from the previous test, distress analysis was done assuming an old pavement and a new FDR pavement for both projects.

4.3 Distress Analysis in Old Pavement and New FDR Pavement

KENPAVE software was used to analyze a linear-elastic pavement. To calculate the distress on the pavement using the materials from both projects, an 80 KN (18-kip single axle) load representing a standard ESAL was applied over a space considering a tire pressure of 552 kPa (80 psi). The contact radius was taken 10.7442 cm. The software output was taken from mechanistic response of the layers in the pavement with strain at the point of interest. The service life of the pavement was estimated by using these strains. Asphalt Institute and many other agencies have provided some equations to calculate the allowable number of load repetitions for HMA fatigue and rutting model. The Asphalt Institute model is applied here to calculate the allowable number of load repetitions for fatigue and rutting.

In Asphalt Institute design method for fatigue cracking, the allowable number of load repetitions, N_f is related to the tensile strain, ε_t at the bottom of the HMA. The elastic modulus of the HMA is represented as E_1 (Huang, 1993). The equation is as follows:

$$N_f = f_1(\varepsilon_t)^{-f_2} (E_1)^{-f_3} \qquad (4-1)$$

where,

N_f = allowable number of load repetitions to cause fatigue cracking,
ε_t = tensile strain at the bottom of the HMA,
E_1 = elastic modulus of the of the HMA in (psi)
$f_1 = 0.0796$, $f_2 = 3.291$ and $f_3 = 0.854$

Equation (4-1) becomes,

$$N_f = 0.796(\varepsilon_t)^{-3.291} (E_1)^{-0.854}$$

To limit rutting two procedures are used. One of them are limiting vertical compressive strain on the top of the subgrade and the other is to limit the total accumulated permanent deformation on the pavement surface which is based on the permanent deformation properties of each individual layer (Huang, 1993). In the rutting model designed by Asphalt Institute and Shell, the allowable number of load repetitions, N_d is related to the vertical compressive strain, ε_c on the top of the subgrade. The equation for the rutting model is as follows:

$$N_d = f_4(\varepsilon_c)^{-f_5} \qquad (4-2)$$

where,

N_d = allowable number of load repetitions to cause rutting,
ε_c = compressive strain at the top of the subgrade,
According to Asphalt Institute,
$f_4 = 1.365 \times 10^{-9}$, $f_5 = 4.477$ and the rut depth is taken not more than 12.7 mm (0.5 in)

Equation (4-2) becomes,

$$N_d = 1.365\ X\ 10^{-9}(\varepsilon_c)^{-4.477}$$

4.3.1 Comparison of Service Life of Pavements with Different Blend Ratios of Route 335 and Route 790

An old pavement with three layers is considered for the comparison of allowable load repetitions for causing fatigue and rutting. The old pavement consists of HMA, unbound granular layer and subgrade. A new pavement with an added layer of FDR base materials is also taken under consideration for determining the type of distress for failure. Two pavements are shown below.

(a) Old pavement with three layers:

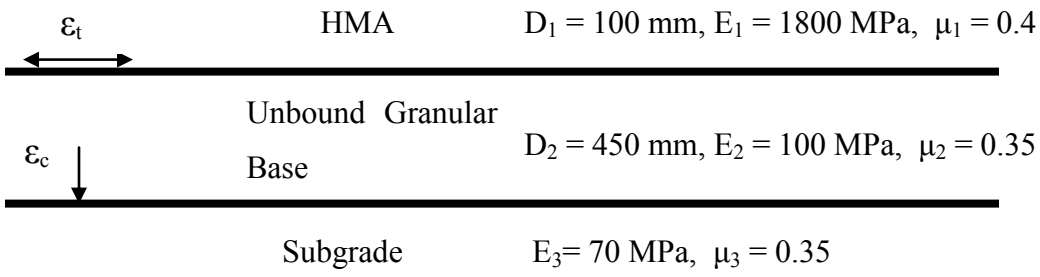

Figure 4-13 A hypothetical old pavement with three layers for Route 335 and Route 790

(b) New FDR pavement with four layers:

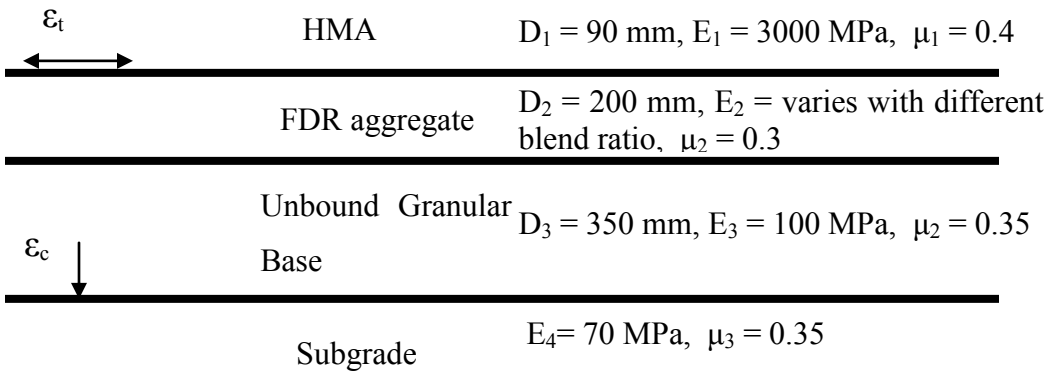

Figure 4-14 A Full Depth Reclaimed new pavement with four layers for Route 335 and Route 790

Table 4-17 Mechanistic analysis results and predicted cycles to fatigue and rutting failure for old and new pavements with Route 335 materials from KENPAVE

	Old Pavement	New FDR Pavement				
Blend Ratio		0.90	0.80	0.57	0.50	0.31
Average Stiffness of FDR (MPa)		14	92	44	94	53
$\varepsilon_{t,\ HMA}$	4.581E-04	6.481E-04	3.87E-04	4.869E-04	3.84E-04	4.63E-04
$\varepsilon_{r,\ HMA}$	1.025E-03	6.07E-04	3.78E-04	4.66E-04	3.75E-04	4.44E-04
$\varepsilon_{v,\ granular\ base}$	2.112E-03	2.70E-03	6.54E-04	1.11E-03	6.41E-04	9.73E-04
$\varepsilon_{c,\ subgrade}$	4.485E-04	3.678E-04	3.551E-04	3.761E-04	3.54E-04	3.77E-04
$N_{f,\ allowable\ HMA}$	**1.836E+6**	**3.788E+05**	**2.067E+06**	**9.709E+05**	**2.12E+06**	**1.145E+06**
$N_{d,\ allowable\ 12.7\ mm\ PD}$	**1.334E+6**	**3.242E+06**	**3.795E+06**	**2.934E+06**	**3.848E+06**	**2.903E+06**
$\delta_{a\ HMA}$	1.1681	1.1523	0.6531	0.7959	0.6486	0.7559
$\delta_{a\ granular\ base}$	0.9024	1.6126	1.0915	1.2473	1.0863	1.2052
$\delta_{a\ subgrade}$	0.4034	0.3509	0.3136	0.3332	0.3128	0.4655
$\delta_{a\ total}$ (mm)	2.4739	3.1158	2.0582	2.3764	2.0477	2.4266

From Table 4-17, it can be seen that the new pavement will fail in fatigue distress while the old pavement will fail by permanent deformation. The allowable load repetitions for fatigue are smaller than the allowable load for rutting.

Table 4-18 Mechanistic analysis results and predicted cycles to fatigue and rutting failure for old and new pavements with Route 790 materials from KENPAVE

	Old Pavement	New FDR Pavement					
Station		1+769	2+185	2+550	3+128	3+446	4+040
Blend Ratio		0.74	0.74	0.75	0.76	0.76	0.76
Average Stiffness of FDR (MPa)		52	53	54	48	49	37
$\varepsilon_{t,\ HMA}$	4.581E-04	4.655E-04	4.619E-04	4.61E-04	4.753E-04	4.746E-04	5.126E-04
$\varepsilon_{r,\ HMA}$	1.025E-03	4.54E-04	4.509E-04	4.497E-04	4.625E-04	4.619E-04	4.949E-04
$\varepsilon_{v,\ granular\ base}$	2.112E-03	9.95E-04	9.758E-04	9.689E-04	1.048E-03	1.044E-03	1.284E-03
$\varepsilon_{c,\ subgrade}$	4.485E-04	3.775E-04	3.768E-04	3.765E-04	3.793E-04	3.792E-04	3.839E-04
$N_{f,\ allowable\ HMA}$	**1.836E+06**	**1.125E+06**	**1.154E+06**	**1.165E+06**	**1.05E+06**	**1.056E+06**	**8.197E+05**
$N_{d,\ allowable\ 12.7\ mm\ PD}$	**1.334E+06**	**2.885E+06**	**2.91E+06**	**2.92E+06**	**2.825E+06**	**2.92E+06**	**2.677E+06**
$\delta_{a\ HMA}$	1.1681	0. 7900	0.7845	0.7825	0.8055	0.8044	0.8695
$\delta_{a\ granular\ base}$	0.9024	1.2728	1.267	1.2648	1.2891	1.2879	1.3551
$\delta_{a\ subgrade}$	0.4034	0.3336	0.3329	0.3327	0.3353	0.3352	0.3415
$\delta_{a\ total}$ (mm)	2.4739	2.3964	2.3844	2.38	2.4299	2.4275	2.5661

From Table 4-17 and Table 4-18, it can be seen that the accumulated permanent deformation is within 12.7 mm, as a result the Asphalt Institute rutting model is

appropriate. In Table 4-18, it is mentioned that the distress in the new pavement will be caused by fatigue while rutting will occur in the old pavement.

The materials from Route 790 were weaker than the materials from Route 335. The highest value of resilient modulus for both projects was 54 MPa and 94 MPa for Route 790 and Route 335 respectively. Hence, for this distress analysis study, the materials with a blend ratio of 0.50 from Route 335 can carry more loads than materials from Route 790 before permanent deformation failure and fatigue.

4.4 Analysis for Service Life and Life Cycle Cost

A hypothetical model was selected with a FDR layer formed by adding the materials from both projects in Figure 4-14. Based on the stiffness found from resilient modulus testing, the distress analysis on that pavement showed that it would fail due to fatigue. The service life of the pavement was determined by assuming that the pavement can carry traffic 50,000 ESAL per year. Equation (4-3) is given to estimate the service life of the pavement.

$$Service\ Life = \frac{N_f}{Allowable\ ESAL\ per\ year} \qquad (4-3)$$

Allowable ESAL per year = 50,000

The estimated service life for the hypothetical new pavement with a FDR layer is presented in Table 4-19.

Table 4-19 Estimated service life for fatigue failure allowing 50,000 ESAL per year

Road Section	Station	Blend Ratio	Load carrying capacity before fatigue failure, N_f	Approximate Service Life (years)
Route 335	7+725	0.90	3.788E+05	8
	7+790	0.80	2.067E+06	40
	7+075	0.57	9.709E+05	20
	7+750	0.50	2.120E+06	40
	7+703	0.31	1.145E+06	23
Mean		0.62		26.2
Standard Deviation		0.236		13.79
Coefficient of variation (%)		39.39%		52.64%
Route 790	1+769	0.74	1.125E+06	23
	2+185	0.74	1.154E+06	23
	2+550	0.75	1.165E+06	23
	3+128	0.76	1.050E+06	21
	3+446	0.76	1.056E+06	21
	4+040	0.76	8.197E+05	17
Mean		0.75		21.3
Standard Deviation		0.01		2.34
Coefficient of variation (%)		1.3%		10.96%

From Table 4-19, it can be seen that the materials from Route 790 rendered a blend ratio very consistent which resulted in the service life. If a FDR road is paved with the materials from Route 790, the average service life would be approximately 21 years with a coefficient of variation of 10.96%. The materials from the project Route 335 showed so much inconsistency that the average service life of FDR pavement built with these materials would be approximately 26.2 years with a coefficient of variation of 52.64%.

The life cycle cost of these pavements was assessed by assuming that the present value cost, inflation rate and discount rate. It was also assumed that the salvage values of all pavements are equal.

For Route 335, the minimum service life of pavement is 8 years and maximum service life is 40 years. To meet the same salvage value, the pavement with minimum service life has to be repaired four times after every five years. It can be assumed that after 4^{th} repair the pavement will serve for another five years and would fail ultimately. A new pavement has to be built after 40 years. Some of the materials from the same road section showed that the service life is 20 years. Therefore, it needs one repair in 20 years to make the pavement good for next 20 years before it fails ultimately. The assessment is shown below diagrammatically in Figure 4-15 and Figure 4-16.

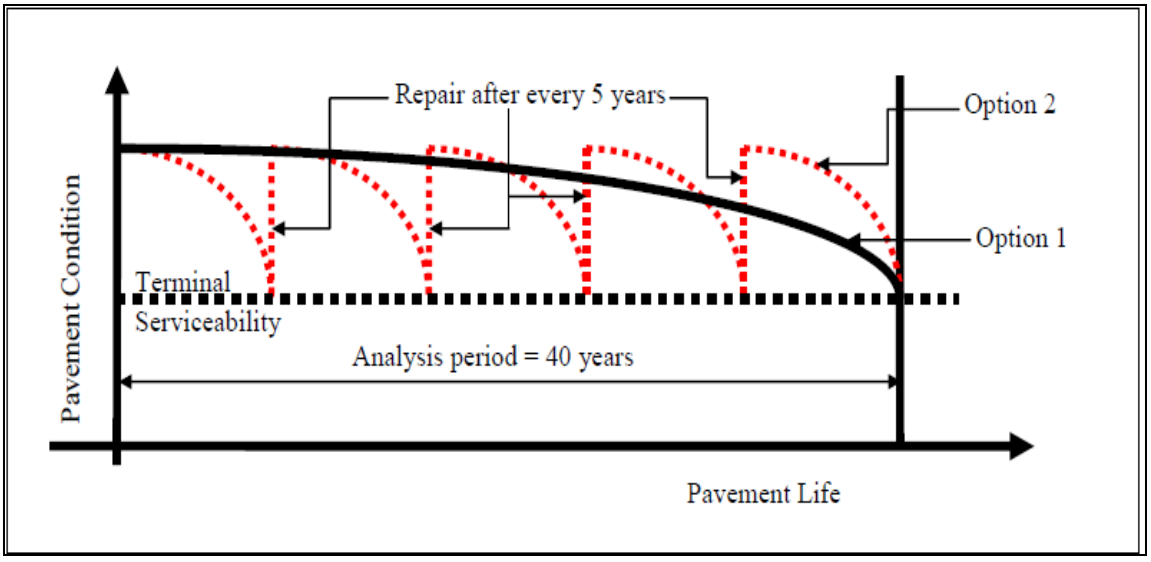

Figure 4-15 Analysis period of a pavement design with first alternative of Route 335 materials

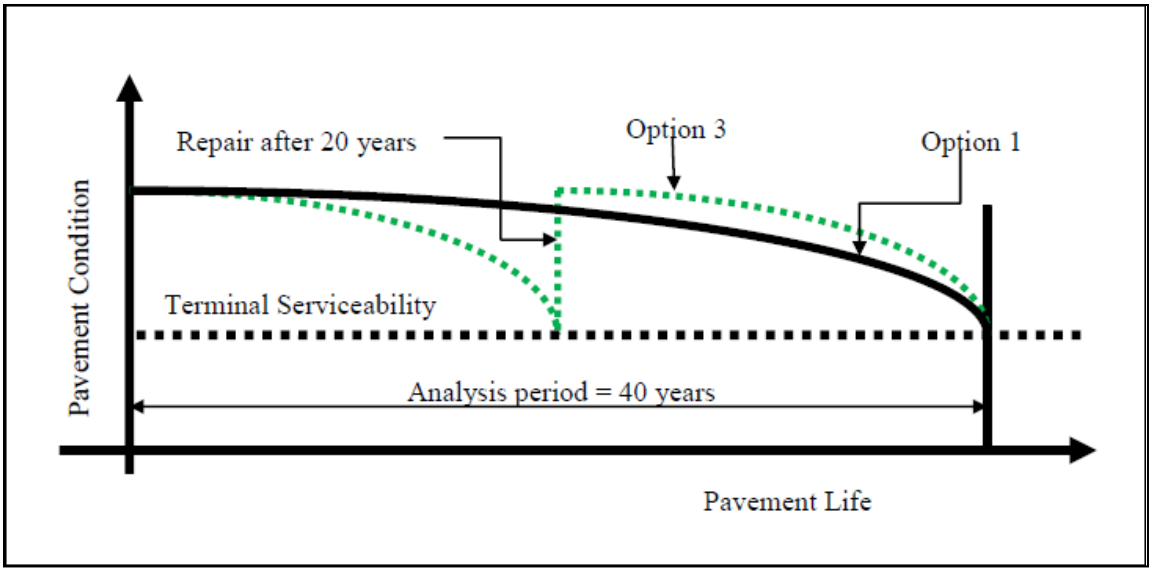

Figure 4-16 Analysis period of a pavement design with second alternative of Route 335 materials

Equation (4-4) is given to estimate the life cycle cost of the pavement.

$$Life\ cycle\ cost = (Present\ value\ cost * (1+i)^n) * (1+r)^{-n} \quad (4-4)$$

where,

i = inflation rate (assumed 2%)
r = discount rate (assumed 4%)
n = number of year after which a maintenance is needed
Present value cost = CAD $350,000/ km (assumed)

Discount rate is the rate at which the amount of money is saved at present for future maintenance. The materials with a blend ratio 0.9 in Route 335 pavement section showed the least stiffness and lowest service life of 8 years. Option 2 from Figure 4-15 is applicable for the pavement built with these materials. In the same road section, option 3 in Figure 4-16 is applicable for the materials with blend ratios of 0.57 and 0.31. It is assumed that the road paved with the materials from Route 335 with a blend ratio of 0.31 would need a repair after 20 years. Using Equation (4-4) the life cycle cost for a FDR road section built with Route 335 materials is shown in Table 4-20. The detail calculation is given in Appendix C.

Table 4-20 Life cycle cost analysis of a FDR pavement with materials from Route 335

Station	Blend Ratio	Option	Life Cycle Cost					Terminal Serviceability	Total cost/km CAD
			Assumed Present Value Cost/km						
7+790	0.80	1	350,000					40 years	350,000
7+750	0.50	1	350,000					40 years	350,000
			Assumed Present Value Cost/km	After 8 years	After 16 years	After 24 years	After 32 years	Terminal Serviceability	
7+725	0.90	2	350,000	299,642	256,530	219,620	188,021	40 years	1,313,813
			Assumed Present Value Cost/km		After 20 years			Terminal Serviceability	
7+075	0.57	3	350,000		237,359			40 years	587,359
7+703	0.31	3	350,000		237,359			40 years	587,359

From Table 4-20 it can be seen that, if a new FDR road is built using the materials from Route 335, the materials with a blend ratio of 0.90 will cost CAD $1.31 million per km for a service life of 40 years. If the materials with blend ratios of 0.80 or 0.50 are taken, the pavement will cost CAD $350,000 per km and last for 40 years without any repair. The materials with blend ratios of 0.57 and 0.31 will cost CAD $587,359 per km to run 40 years with one repair.

From Table 4-19, it can be seen that if a FDR pavement is built using the materials from Route 790, the average service of the pavement would be approximately 21 years. That means the pavement would not need any repair within 21 years before it fails ultimately. If it is assumed that the present value cost for the pavement is CAD $350,000 per km, for the consistent material properties of Route 790, no extra money would be needed to be saved for maintenance, as the pavement would run for whole service life. The service life of the pavement is shown schematically in Figure 4-17.

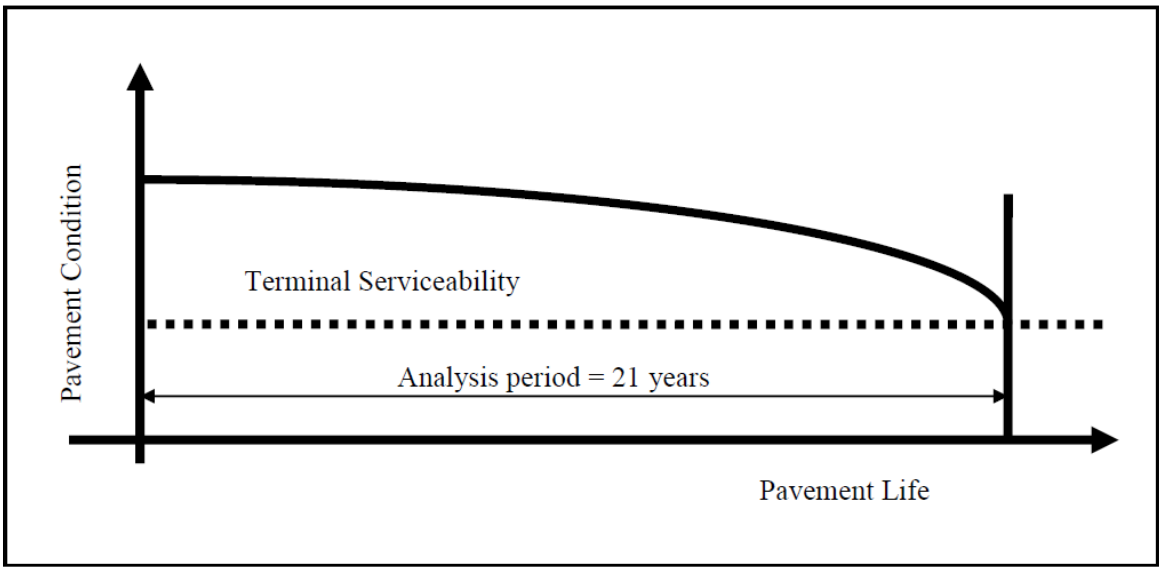

Figure 4-17 Analysis period of a FDR pavement built with Route 790 materials

Though the materials from Route 790 were very poor in quality, the blend ratio was so consistent that the same type of corrective aggregates could be used throughout the section to obtain the same improved material properties. The inconsistencies of blend ratio in Route 335 materials indicate that various amount of corrective aggregates are needed throughout the pavement section to obtain the same material properties. Therefore, GPR survey is needed to maintain a similar blend ratio in materials.

4.5 Summary of Discussion

The advantage of using Ground Penetrating Radar over conventional core and test pits can be explained from the laboratory results obtained from materials of both projects. Though the materials obtained from Route 790 were weak, they showed good consistency. GPR survey showed the thickness of the asphalt material. More data can be obtained in a short span of a pavement by GPR than the test pits. 10,000 scans per kilometer can be obtained from GPR. The pavement was separated in several sub-sections and the sample locations were chosen where the blend ratios were constant. As the materials showed consistency in gradation, maximum dry density, optimum moisture content, maximum theoretical specific gravity, it can be said that the material properties can be controlled by controlling the blend ratio. As the CBR and resilient modulus of six samples from different locations were consistent too, it can be said that the materials had the similar physical and mechanical property. The materials showed similar stiffness. Same type of corrective aggregates and stabilizers can be chosen to improve the material property if the blend ratio of the pavement section is known.

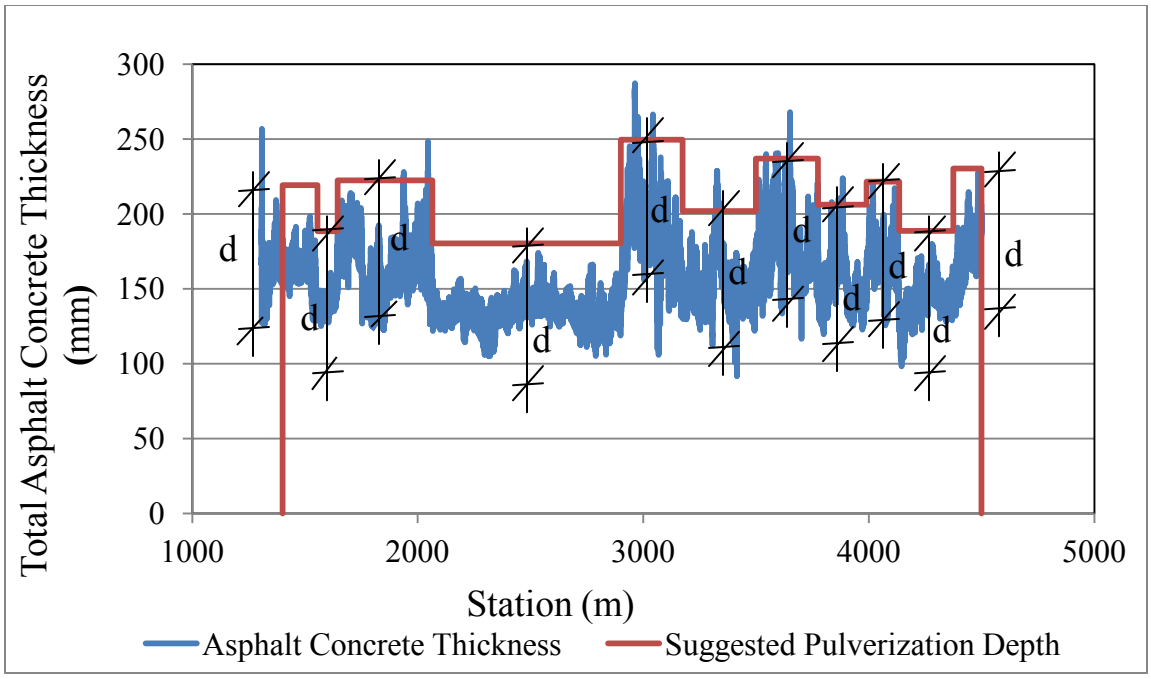

Figure 4-18 Average depth of pulverization for adding stabilizer and corrective aggregate in a pavement, HMA thickness surveyed by GPR

From Figure 4-18, it can be seen that the average depth of pulverization "d" can be maintained in a section to get a consistent blend ratio. Same amount of corrective aggregates and stabilizer can be provided uniformly in this GPR controlled section during construction as the blend ratio is same. In this way, the performance of the pavement will be enhanced. The quality of the additives can be controlled fairly throughout a pavement section.

On the other hand, in core and test pit method, the average depth of HMA of a pavement section is assumed by measuring the asphalt concrete thickness of samples obtained from relatively dispersed cores. To meet the average thickness of the test pit, the pulverization depth had to be adjusted frequently which resulted inconsistency in blend ratio. In Figure 4-19, the average HMA depth is shown along with the HMA thickness at different FWD locations. The orange line indicates the actual situation in site where the inadequate pulverization takes place. The red dotted line in Figure 4-19 suggests the pulverization depth for meeting a constant blend ratio based on the average HMA thickness.

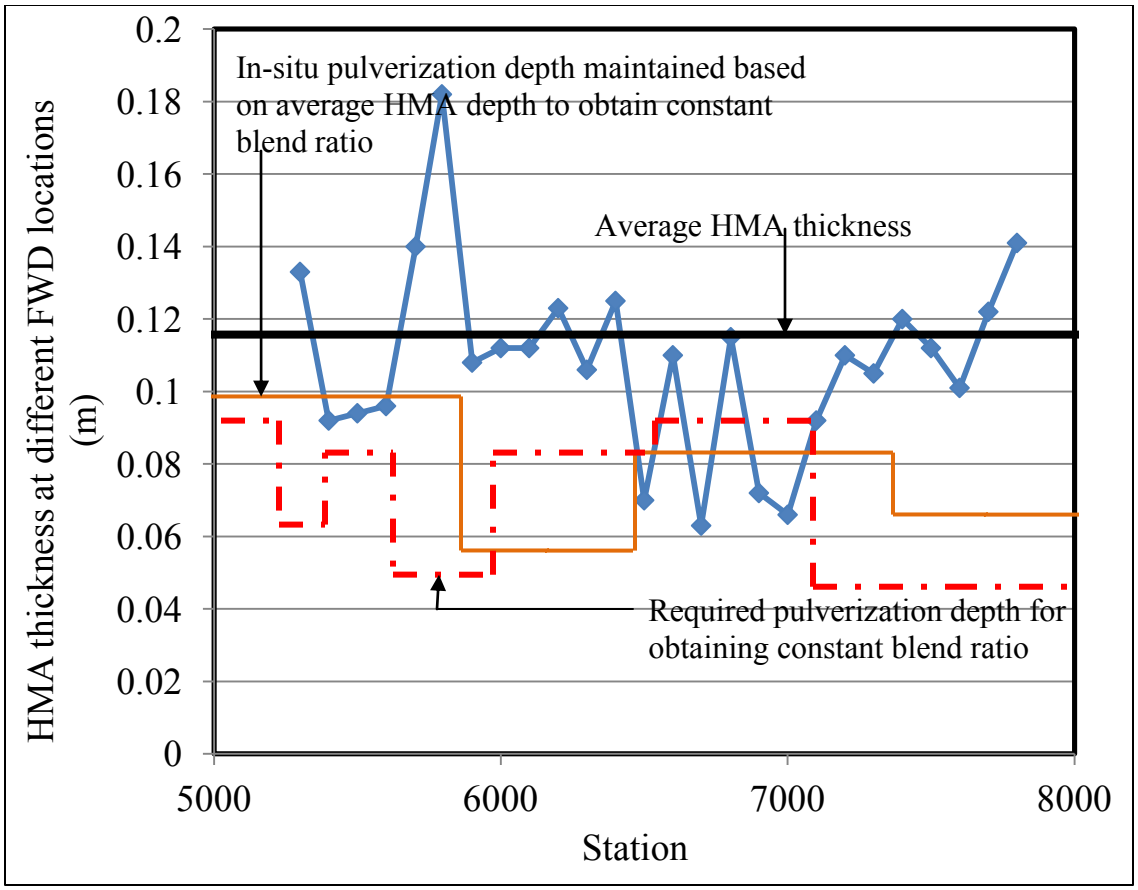

Figure 4-19 Actual in-situ pulverization depth, required pulverization depth for constant blend ratio and average HMA thickness for a typical pavement section

Laboratory test results showed that the material properties such as gradation, optimum moisture, maximum dry density, CBR and resilient modulus were highly inconsistent. Under this circumstance, during construction same amount of stabilizer, corrective aggregate cannot be used throughout the section. Therefore, uniformity in the pavement section cannot be expected. The quality of the additives cannot be controlled fairly throughout a pavement section and pavement will be degraded.

The results provided in this chapter have contributed to an understanding of the properties of FDR materials of variable thickness. The properties of the materials from Route 335 are also discussed here.

The first question was whether or not the wide range of blend ratio has an effect on the material properties.

From Figure 4-4 it can be said that the blend ratio of the materials from Route 335 affected the gradation. The highest blend ratio was 0.9 and the materials lacked in finer particles. Though as per Figure 4-4 the gradation curve of the materials with a blend ratio of 0.9 was closest to the maximum density 0.45 power curve, the materials lacked so much in fine particles that the material properties and air void content were affected. For this material the optimum density was 1712 kg/m^3, lowest among the six samples. The air void content of the materials was 30.84%, highest among the six. The maximum specific gravity of this material was within the acceptable limit. The cohesion of this material was only 11.19 kPa with an angle of internal friction of 39.8º. Thus it can be said that most of the particles were rounded. The CBR of this material was 7, which was very low. The stiffness of the materials was determined by the resilient modulus. From the point of resilient modulus value, the particles were proven to be poor in quality.

The materials with a blend ratio of 0.8 had more fine particles than the materials with a blend ratio of 0.9. The maximum density of the material was 1775 kg/m^3, higher than that of the materials with a blend ratio of 0.9. The air void content was 29.3%. The material was non cohesive with a 40.6º angle of internal friction. Though both the materials with blend ratios of 0.8 and 0.9 had the same CBR value of 7, the materials with a blend ratio of 0.8 showed much higher stiffness than the materials with a blend ratio of 0.9.

The fines' content of the materials with a blend ratio of 0.57 was lower than that of the materials with a blend ratio of 0.31. Though the materials with a blend ratio of 0.57 resulted in higher amount of fines than the materials with blend ratios of 0.8 and 0.9, the air void content was the same as that for the materials with a blend ratio of 0.9. The CBR was higher than that of the previously mentioned materials. This material had a very low amount of cohesion. The angle of internal friction showed that the angularity in the material was also very low. The stiffness of the material was lower than the materials with a blend ratio of 0.8. Without stabilization the material showed the same characteristics as a subgrade material.

The blend ratio of 0.5 means that the material has 50% asphalt content, the density of which was 1818 kg/m^3 higher than those of the blend ratios of 0.9, 0.8 and 0.57 respectively with lower amounts of air voids. The CBR at 2.5 mm (0.1 in) penetration was the highest among the six samples which was also reflected in the stiffness of the materials. The stiffness of the materials with a blend ratio of 0.5 was the highest among the six and the soil was totally non-cohesive with mostly rounded particles.

The gradation curve of the materials with a blend ratio of 0.43 almost matched the gradation curve with a blend ratio of 0.5. The CBR and the stiffness of the materials were similar to those of the materials with a blend ratio of 0.57.

The highest amount of fines' content was observed in the materials with a blend ratio of 0.31 as the asphalt content was very low. For the higher amount of fines, the optimum moisture content and the maximum density of the materials were 10.75% and 1955 kg/m^3 respectively which were the highest among the six. The air void content of the materials with a blend ratio of 0.31 was the lowest with 22.22%. The cohesion between the particles was so low that it could be considered as a non-cohesive soil. The angle of internal friction of these particles was similar to that for dry sand. As the gradation curve of the materials with blend ratios of 0.31 and 0.57 were closer, the CBR of those materials also rendered similar values. The materials with a blend ratio of 0.31 were stiffer than the materials with blend ratio 0.57 at optimum moisture content, though the material with a blend ratio of 0.31 started to flow at higher water content.

On the other hand, the aggregates from Route 790 exhibited almost similar material properties because of the consistent blend ratio. The optimum moisture content, maximum dry density and CBR varied little. Though the CBR of the materials were very low, the range was within 2.8-4.2. The stiffness of the materials, collected from six different locations, were similar.

From the above analysis a conclusion can be drawn that the variability in asphalt thickness resulting in a fluctuating blend ratio has an effect on the material property. Extremely high or low asphalt content such as blend ratios of 0.9 and 0.31 affect the

gradation, maximum density, optimum moisture content, air void content and stiffness of the materials. The materials in which the asphalt content is within an intermediate range (0.43-0.57) show almost the same characteristics. All the tests done on the materials from both projects have proven that the materials are too weak to be used as base materials without proper stabilization. The unstabilized materials could be used in the subgrade of a pavement.

It is clear from the previous sections that, the materials from both projects lacked in fines' content. It is shown in Figure 4-3 that the particles contain a sufficient amount of fines after the asphalt extraction. The JMF was based on post extracted materials whereas the tests were done on the as-obtained conglomerated materials. In the JMF the materials should be treated as conglomerated particles where the fines are stuck to the asphalt content and enough fines are not liberated during the second stage of pulverization.

The second question was how the low fine aggregate count affects the physical properties of FDR aggregate.

From the above analysis it was already said that the low fine aggregate count affected the gradation, optimum moisture content, CBR and optimum density. The inadequate fine aggregate made the aggregate skeleton very weak providing a higher amount of air voids. As a result, the stiffness of the materials was too low. As the materials lacked in fines, the particle interlock was not tight and the materials slid over each other when normal stress was applied. Permanent deformation is likely to occur if the materials with lower stiffness are used without proper stabilization.

The third question how the resilient modulus was affected by moisture variability.

From the result of the resilient modulus of Route 335 materials, it can be said that the materials exhibited low stiffness. Resilient modulus determined at moisture content higher than the optimum was very low. At 1.5% higher than the optimum moisture content the materials started to flow; bleeding started during compaction. Though the

resilient modulus should be the highest at optimum moisture content, some of the materials exhibited higher resilient modulus values at 1.5% below optimum than the optimum moisture content. Materials with blend ratios of 0.31 and 0.57 showed higher stiffness in less moisture than the optimum. The materials with blend ratios of 0.8 and 0.5 showed higher resilient modulus at the optimum moisture content. It is clear that the stiffness tends to decrease with increasing moisture content.

From the analysis of service life of a hypothetical FDR pavement built with Route 335 and Route 790 materials, it was seen that the materials with consistent blend ratio in Route 790 had almost similar service life with a variation of 10.96%. In Route 335, the inconsistent blend ratio caused inconsistent service life of the pavement. The service life of materials in same road section varied between 8-40 years with a variation of 52.64%. The life cycle cost of the pavements built with Route 335 materials were very high compared to Route 790 materials. If the consistent blend ratio can be maintained in the field, the cost of the pavement can be reduced.

CHAPTER 5: CONCLUSIONS

5.1 Conclusion

The purpose of this analysis was to investigate the FDR aggregate properties of variable pavement thickness. The control of blend ratio in the pulverization process is essential. Constructing the JMF gradation relies on matching the HMA to granular blend ratio. The blend ratio is a ratio of thickness of reclaimed asphalt to the thickness of total material pulverized (Salah, 2013). Variation in pavement thickness necessitates the adjustments in pulverization depth for maintaining a persistent blend ratio. Consistency of blend ratio is affected by the method used for determining the pavement layer thickness.

Retroactive control and proactive control methods were used in two expanded asphalt FDR pavement test sections on Route 335 and Route 790 respectively. To evaluate the material properties, several tests were carried out on the unbound materials gathered from both projects.

The samples were collected from two expanded asphalt stabilized FDR projects on Route 335 near Caraquet and Route 790 near Lepreau, New Brunswick. The materials from Route 335 were collected by using the typical retroactive depth control method, which encompassed checking the total in-situ asphalt concrete thickness bordering the pulverized materials, trailing the recycling machine as it moved forward. The new asphalt concrete thickness in front of the recycling machine was predicted by the afore-mentioned asphalt concrete thickness values to establish a suitable pulverization depth aimed at the blend ratio created in the JMF. The average blend ratio was anticipated to be 0.67 which could not be maintained continuously by this procedure.

The proactive method, applied in the Route 790 pavement section, requires a GPR survey to assess the pavement thickness against the distance along the test section. The GPR estimated thickness provided the knowledge of the depth of asphalt concrete layer to set proper pulverization depths for each distinctive location. The Route 790 section was divided into several sub-sections of similar average thickness with equivalent

pulverization depth to satisfy the blend ratio designed in the JMF. On the Route 790 section, an approximate blend ratio of 0.75 was maintained on average by altering the pulverization depth in accordance with the outcome of a GPR survey.

The consistencies of materials from both projects were evaluated by several laboratory tests. The physical and mechanical properties of the materials were appraised by the following tests.

- Grain size distribution by sieve analysis
- Moisture-density relationship by standard Proctor method
- Maximum theoretical density
- CBR
- Direct shear strength
- Granular resilient modulus

A lack of fines, compared to what is specified in NBDOT, was observed for the materials from both projects. A significant difference was noticed between the gradations of materials from both projects compared to what was specified in the job mix formula. The fines' content were significantly overestimated in the job mix formula. Route 335 materials exhibited a considerable amount of fluctuation in blend ratio during construction. The generated FDR aggregates from Route 335 exhibited large discrepancies in the grain size distribution; in the optimum density and optimum moisture content and in the aggregate strength as measured by CBR and resilient modulus.

Generally the gradation results are based on testing done after the extraction of asphalt cement from old specimens, but these do not portray the materials attained during construction. The ideal way is to consider the particles as larger conglomerated particles, adhered together by asphalt cement from the old pavement. The particles behave as conglomerated particles during construction.

Besides the lack of fines, the materials from both projects turned out to be a product of poor quality to be employed as a base material. The density, CBR value and resilient modulus were very low with a higher amount of air void contents. The direct shear test

showed that the particles were cohesion-less and mostly rounded, therefore, the materials slid over one another when normal stresses were applied. All the test results revealed that the unbound granular materials would not execute well as a base material.

Less deviation was noticed for the Route 790 samples that were picked at regions where predicted asphalt thickness and the specified pulverization depth provided an almost similar thickness blend ratio. A significant reduction in material variability implies that the advancement of the GPR controlled proactive method may contribute to intensely persistent material properties which will eventually decrease the variability of the stabilized strength parameters within a given section.

The service life and the cost analysis on a hypothetical FDR pavement, built with Route 335 and Route 790 materials, showed that the consistent material properties give consistent service life. The pavement repair cost can be reduced and controlled if the blend ratio of the materials is controlled.

From the whole research, a conclusion can be drawn that the FDR process can be a legitimate substitute for the conventional restoration methods in impaired pavement. A combination of the construction method, usage of proper stabilizer and a comprehensive inquiry of the characteristics of the pulverized materials are extremely important for the long term efficiency of the pavement. Spatial data in conjunction with the GPR thickness survey will be extremely helpful for controlling the recycling machine pulverization depth. FDR can be recommended as an ideal option for pavement rehabilitation if all these processes are precisely followed.

5.2 Recommendations for Further Studies

From this study of the unbound granular material properties it can be suggested that the mechanical behavior of the materials could be improved by stabilizing with additives. The corrective aggregates can be used to improve the material properties so that the materials could be used as base materials. By adding crusher dust and stabilizing with Portland cement the gradation of the materials will reach to 0.45 maximum density power curve. The properties of the materials would be better compared if the materials are taken from the same pavement section with two different approaches such as GPR method and retroactive method.

Sometimes in situ practice has been to use a direct correlation, $M_R = 1500\ (CBR)$ to obtain resilient modulus from CBR. But if the CBR found from the lab tests of materials from both projects were used to calculate resilient modulus according to the equation mentioned in the parenthesis, it could be shown that resilient modulus calculated from this equation are totally different than the actual resilient modulus of materials found from laboratory tests. Using the actual resilient modulus of materials from the lab tests is highly recommended for the pavement design.

The amount of permanent deformation and rutting properties could be determined from the resilient modulus values of the materials. The consistency in service life of the pavement assessed from Route 790 materials demonstrated that the GPR controlled proactive method is a superior means of regulating the quality of reclaimed materials and thus recommended for obtaining materials with consistent mechanical properties.

The physical properties of the materials from both projects indicated that the consistency in the materials could be attained by regulating the blend ratio of RAP to the granular base materials pulverized efficiently. Instead of manually operating pulverizing machine, a machine controlled pulverization process would perform better by changing the pulverization depth automatically to meet the specified blend ratio in the field.

After the construction of the pavement sections Route 335 and Route 790 by FDR process, a long term observation and assessment of these pavement sections are highly recommended so that the feasibility of the FDR process can be realized.

References

AASHTO T307-99. (2007). “Determining the Resilient Modulus of Soils and Aggregate Materials.” American Association of State Highway and Transportation Officials, Washington DC.

Adu-Osei, A. (2000). “Characterization of Unbound Granular Layers in Flexible Pavements”, Research Report ICAR- 502-3, Research Report Title, “Structural Characteristics of Unbound Aggregate Bases to Meet AASHTO Design Requirement”, Arlington, VA 22201-3062: International Center for Aggregate Research.

Adu-Osei, A., Little, D. N., and Lytton, R. L. (2001). "Structural Characteristics of Unbound Aggregate Bases to Meet AASHTO 2002 Design Requirements: Interim Report." Texas Transportation Institute, The Texas A&M University System, USA.

Alward, C. (2011)."Full Depth Foam Strength Results Summary, 2004-2011", Industrial Cold Milling, Moncton, New Brunswick

American Concrete Pavement Association (ACPA). (2008). "ACPA, Concrete Pvement Technology Series: Unstabilized Granular Sub-bases, TS204.6P." Skokie, Il 60077, USA. Accessed on May 14, 2013 at http://www.pavement.com/Downloads/TS/EB204P/TS204.6P.pdf

American Society for Civil Engineers (ASCE). (2013). “ASCE: Report card for America's infrstructure", Accessed on May 13, 2013 at http://www.infrastructurereportcard.org/a/#p/roads/overview.

American Standard for Testing Materials (ASTM). (2001). "Standards on disc. Section four: Construction, D 2487-92. Soil and rock (I): D 420-D 5779 (CD-ROM)." Vol. 04.08. West Conshohocken, Pa, USA.

Anagnos, J. N., and Kennedy, T. W. (1972). "Practical Method of Conducting Indirect Tensile Test." *Center of Highway Research,* University of Texas, Austin, USA.

Araya, A. A. (2011). "Characterization of Unbound Granular Materials for Pavements." Road and Railway Engineering Section, Faculty of Civil Engineering and Geosciences, Delft University of Technology.

Asphalt Academy. (2009). "A guideline for the design and construction of bitumen emulsion and foamed bitumen stabilized materials." 2nd edition. Pretoria.

Asphalt Academy. (2009). "The Determination of the Maximum Dry Density and Optimum Moisture Content of Materials Using the Vibratory Hammer Compaction." Accessed on June 15, 2013 at http://www.asphaltacademy.co.za/Bitstab/Downloads/Method_8(1)__Determine_MDD_and_OMC_using_Vibr_Hammer_Final-May09.pdf

ASTM D698-07e1. (2007). “Standard Test for Laboratory Compaction Characteristics of Soil Using Standard Effort.” ASTM International, West Conshohocken, PA.

ASTM D1883-07e2. (2007). “Standard Test Method CBR (California Bearing Ratio) of Laboratory Compacted Soils.” ASTM International, West Conshohocken, PA.

ASTM D6913-04. (2009). "Standard Test Methods for Particle Size Distribution(Gradation) of Soils Using Sieve Analysis." Aggregates." ASTM International, West Conshohocken, PA.

ASTM D3080. (2011). "Standard Test Method for Direct Shear Test of Soils Under Consolidated Drained Conditions." ASTM International, West Conshohocken, PA,

ASTM D2041/D2041M-11. (2011). "Standard Test Method for Theoretical Maximum Specific Gravity and Density of Bituminous Paving mixtures." ASTM International, West Conshohocken, PA.

ASTM D6931-12. (2012). "Standard Test Method for Indirect Tensile (IDT) Strength of Bituminous Mixtures." ASTM International, West Conshohocken, PA 19428-2959, USA.

ASTM D3080/D3080 M-11. (2012). "Standard Test Method for Direct Shear Tests of Soils Under Consolidated Drained Conditions." ASTM International, West Conshohocken, PA.

Austroads. (2004). "Pavement Design: A Guide to the Structural Design of Road Pavements." Pavement Design Guide, Sydney, Australia.

Barksdale, R. G. (1971). "Compressive Stress Pulse Times in Flexible Pavements for Use in Dynamic Testing." *Highway Research Record : Journal of Highway Research Board*, (345), pp 32-44.

Barksdale, R. D. (1972). "Laboratory Evaluation of Rutting in Base Coourse Materials." *3rd International Conference on Structural Design of Asphalt Pavements.* London, UK.

Barksdale, R. G. and Itani, S.Y. (1989). "Influence of aggregate shape on base behavior." *Transportation Research Record: Journal of Transportation Research Board, (1227), Washington D. C. pp 173-182.*

Barnes, C. L. (2008). "Evaluating Moisture Damage in Ashphalt Concrete using Surface Waves." *Thesis for Doctor of Philosophy.* Dalhousie University, Halifax, Nova Scotia, Canada.

Barnes, C. L. (2010). "Forrensic investigation of cracking in a Portland cement stabilized full depth recycled pavement", *Transportation Association of Canada Annual Conference,* Halifax, Nova Scotia, September 26-29.

Barnes, C. L., Haque, R., Salah, P. and Alward, C. (2012). "Control of Full Depth Pulverized Aggregate Production using Ground Penetrating Radar." *Transportation Association of Canada Annual Conference*, Fredericton, New Brunswick, October 14-17.

Brown, S. and Chan, F. W. K. (1996). "Reduced rutting in unbound granular pavement layers through improved grading design." *Proceedings of the Institution of Civil Engineers: Transport.* Volume 117- 1, pp 40–49.

Cannon, D. P. (2012). "Full Depth Reclamation with Portland cement." *Twelfth Annual Pennsylvania Concrete Conference: American Concrete Pavement Association.* Pennsylvania, USA. Accessed on May 14, 2013 at http://eztogreen.com/ACPA-PA/Full%20Depth%20Reclamation%20Updates/Full%20Depth%20Reclamation%20Updates.html.

Chem Wiki. (2013). "ChemWiki: The Dynamic Chemistry E-textbook", UC Davis, Accessed on November 23, 2013 at http://chemwiki.ucdavis.edu/Physical_Chemistry/Physical_Properties_of_Matter/Atomic_and_Molecular_Properties/Intermolecular_Forces

Chen, W. F. and Mizuno, E. (1990). "Nonlinear Analysis in Soil Mechanics", *Developments in Geotechnical Engineering*, Vol: 53, Elsvier, New York, NY.

Coduto, D. P. (1999). "Geotechnical Engineering: Principles and Practices." Upper Saddle River, NJ: Prentice-Hall, Inc.

Daniels, D. J. (2004). "Ground Penetrating Radar." *2nd Edition.* Accessed on march 24, 2014 at http://books.google.ca/books?id=16PVfhKasoC&pg=PA73&source=gbs_toc_r&cad=4#v=onepage&q&f=false.

Das, B. M. (2010). "Principles of Geotechnical Engineering." *7th Edition.* Cengage Learning, Stamform, CT 6902, USA.

Diefenderfer, B. K., and Apeagyei, A. K. (2011). "Analysis of Full Depth Reclamation Trial Sections in Virginia." Report on Federally Funded Project, Virginia Department of Transportation: Virginia Center for Transportation Innivation and Research, Charlottesville, VA 22903, USA.

El-Desouky, A., Mostafa, A., Easa, S., and Abd El Halim, A. O. (2008). "Modeling shear properties of airport asphalt mixes using different test methods." In *Pavement Cracking : Mechanisms, Modeling, Detection, Testing and Case Histories*, pp 357-365. Taylor and Francis, London, UK.

Fernandes, J. L., Roque, R., Tia, M., and Casanova, L. (2000). "Uncompacted Void Content of Fine Aggregates as Quality Indicator of Materials Used in Superpave Mixtures." *Transportation Research Record: Journal of Transportation Research Board*, (1723), Washington D. C. pp 37-44.

Fuller, W.B. and, Thompson, S. E. (1907). "The Laws of Proportioning Concrete." *Journal of Transportation Division, American Society of Civil Engineers* Vol: 59.

Geiger, A., Yuan, D., Nazarian, S., and Abdallah I. (2007). "Effects of Pulverization on Properties of Stabilized Bases." Technical Report, Federal Highway Administration & Texas Department of Transportation, El Paso, Texas, USA.

Geiger, A., Garibay, J., Nazarian, S., Abdallah I., and Yuan, D.. (2008). "Impact of Changes in gradation of bases on Performance due to Pulverization." *Advances in Transportation Geotechnics*, pp 719-724. Taylor and Francis, London, UK.

Geodata.info. (2010). "California Bearing Ratio Test" Accessed on August 18, 2013 at http://www.geotechdata.info/geotest/california-bearing-ratio-test.html

Grubba B., and Thomas, T. (2008). "Method of Reconstructing a Bituminous - Surfaced Pavement." United States Patent No.:US 7,455, 476 B2, USA.

Halsted, G.E. (2010). "Design of full-depth reclamation with portland cement (FDR-PC) pavements", *Trasportation Assocition of Canada Annual Conference.* Halifax, NS, September 26 – 29.

Handy, R. L. (2007). "Geotechnical Engineering: Soil and Foundation Principles and Practice." 5th Edition. The McGraw-Hill Companies. Acced on May 30, 2013 at http://accessengineeringlibrary.com/browse/geotechnical-engineering-soil-and-foundation-principles-and-practice-fifth edition/p20012b389970280001#p20012b389970280002

Heukelom, W., and Klomp, A. J. G. (1962). "Dynamic Testing as a Means of Controlling Pavements During and After Construction." *Proceedings, (1st) International Conference on the Structural Design of Asphalt Pavements.* pp 667-685.

Hicks, R. G. and Monismith, C. L. (1971). "Factors Influencing the Resilient Properties of Granular Materials." *Transportation Research Record: Journal of Transportation Research Board*, National Research Council, (345), Washington D. C. pp15-31.

Holt, C., Barnes, C. L., Sullivan, P., and O' Toole, L. (2009). "Full Depth Remediation of Roads Using Portland Cement." *Annual Conference of Transportation Association of Canada.* Vancouver, British Columbia.

Huang, Y. H. (1993). "Pavement Analysis and Design : Chap. 7, Material Characterization." 1st Edition, Prentice Hall, Englewood Cliffs, New Jersey 07632, pp 328-329.

Huang, Y. H. (2004). "Pavement Analysis and Design." 2nd Edition, Prentice Hall Upper Saddle River, Pearson, NJ.

Indiana Department of Transportation, (InDOT). (2009). "Indiana Department of Transportation." Accessed June 20, 2013 at http://www.in.gov/indot/files/209(1).pdf

Indiana Department of Transportation, (InDOT). (2011). "Indiana Department of Transportation." Accessed October 9, 2013 at http://www.in.gov/indot/files/chapter_04.pdf

Jackson, A. (2012). "Full Depth Reclamation: Compaction and Moisture Content." Thesis, University of Arkansas, Fayatteville, Arkansas, USA.

Kearney, E. J. and Huffman, J. E. (1999). “Full Depth Reclamation Process” Transportation Research Record No. 1684, Transportation Research Board, Washington DC. pp. 203-209.

Khosla, N. P. and Harikrishnan, K.I. (2007). "Tensile Strength – A Design and Evaluation Tool For Superpave Mixtures." Report No.: FHWA/NC/2006-24, North Carolina Department of Transportation Research and Analysis Group, Raleigh, North Carolina.

Khoury, N., Brooks, R., Zaman, M. M., and Khoury, C. N. (2009). "Variations of Resilient Modulus of Subgrade Soils with Postcompaction Moisture Contents." *Transportation Research Record: Journal of Transportation Research Board,* (2101), Washington D.C. pp 72 - 81.

Kim, D., and Siddiki, N. Z. (2006). "Simplification of Resilient Modulus Testing for Subgrades." Report No.: FHWA/IN/JTRP-2005/23, Joint Transportation Research Program of Indiana Department of Transportation and Purdue University, West Lafayette, Indiana, USA.

Kuo, C.Y., Fnosr, J.D., Lar, J. S. and Waxc, L. B. (1996). "Three-dimensional Image Analysis of Aggregate Particles from Orthogonal Projections." *Transportation Research Record: Journal of Transportation Research Board,* (1526), Washington D.C. pp 98 - 103.

Lane, B., and Kazmierowski, T. (2012). " Long term performance of full depth reclamation with expanded asphalt on the Trans-Canada highway near Wawa, Ontario." Transportation Association of Canada Annual Conference, Fredericton, New Brunswick, October 14-17.

Lee, H. D. and Kim, Y. J. (1995). "Development of a Mix Design Process For Cold-In-Place Rehabilitation Using Foamed Asphalt", Report on Research Sponsored by Iowa Department of Transporation, Public Policy Center, Accessed on November 24, 2013 at ftp://ftp.mdt.mt.gov/research/LIBRARY/IA_TR474PHASE1.PDF

Lekarp, F., Isaacson, U. and Dawson, A. (2000). "State of the Art. II: Permanent Strain Response of Unbound Aggregates." *Journal of Transportation Engineering* (ASCE) Vol. 126, No. 1, pp 76-83.

Li, Xiang-Tang. (2011). “Sublayer-thickness inversion of asphalt layer from ground penetrating radar data”, *Nondestructive Testing and Evauation* , Taylor & Francis, Guangzhou, China. pp 187-196.

Liang, R. Y. (2008). "Refine AASHTO T283 Resistance of Compacted Bituminous Mixture to Moisture Induced Damage for Superpave." Ohio Department of Transportation Office of Research and Development, pp 10-21. Acced on July 17, 2013 at ftp://ftp.mdt.mt.gov/research/LIBRARY/FHWA-OH-2008-1.PDF

Loizos, A. and Plati, C. (2006). “Ground Penetrating Radar as an enginerring diagnostic tool for foamed asphalt treated pavement layers”, *International Journal of Pavement Engineering, 8(2)*. pp 147-155.

Marquis, B. (2007). “Full depth reclamation with cement along rt. 2A in Reed Plantation”, Accessed on March 9, 2012 at http://www.maine.gov/mdot/tr/documents/pdf/report0506cil.pdf.

Maser, K. R., and Scullion, T. (1992). “Automated Pavement SubsurfaceProfiling Using Radar: Case studies of Four Experimental Field Sites”, Transportation Research Record, No. 1344, Transportation Research Board, Washington DC. pp. 148-154.

Mokwa. R. L., Peebles, C. S., and Robinson, E. (2006). "Strength, Stiffness and Compressibility of RAP/Aggregate Blends." Conference on *Pavement Mechanics and Performance.* American Society of Civil Engineers and GEO Institute, Shanghai, June 6 - 8, pp 247-255.

Molenaar, A.A.A. and Huurman, M. (2006). "Estimation of Resilient and Permanent Deformation Behavior of Granular Bases from Physical Parameters." GeoCongress 2006: Geotechnical Engineering in the Information Technology Age [0-7844-0803-3], American Society of Civil Engineers, Atlanta, Georgia, USA, pp 228-235.

Morian, D.A., Solaimanian, M., Scheetz, B. and Jahangirnejad, S. (2012). "Developing Standards and Specifications for Full Depth Pavement Reclamation." Report No.: FHWA-PA-2012-004-090107, Commonwealth of Pennsylvania Department of Transportation, Harrisburg, PA 17120-0064, USA, pp 2-6.

Muthen, K. M. (1998). "Foamed Asphalt Mixes - Mix Design Procedure."Accessed on March 24, 2014 at http://www.greenmixinc.com/pics/foamasph.pdf

MTO. (2011). "Method of Test for the Determination of Indirect Tensile Strength of Expanded Asphalt Mixes: Test Method LS-297", Ministry of Transportation, Ontario Laboratory Testing Manual, Ontario, pp 1-6. Accessed on November 24, 2013 at http://webcache.googleusercontent.com/search?q=cache:S4AfD1t6HygJ:applications.roadauthority.com/Standards/Home/FileDownload%3FstandardFileId%3D8ed28029-bb70-42b3-a868-676308ea5635+&cd=1&hl=en&ct=clnk&gl=ca

MTO. (2012). " Full Depth Reclamation with Expanded Asphalt Stabilization – Item No. Special Provision No. 331S01." Standard Specifications, Ontario: Ministry of Transportation Ontario, pp 4-10. Accessed on March 1, 2012 at http://www.raqsb.mto.gov.on.ca/techpubs/cdedsp.nsf/7df9b6224fbd62b785257173004de677/c0ed20138338192985257acb0067efdd/$FILE/SSP%20331S01%20-%20Nov%202012.pdf

Nazarian, S., Pezo, R. and Picornell, M. (1996). "Testing methodology for Resilient Modulus for Base materials: Application of Resilient Modulus Tests to Texas base Materials", Texas Department of Transpotation in Corporation with Federal Highway Administration.

NBDOT. (2011). "Standard Specifications, Item: 263, Full Depth Recycling." Standard Specifications, New Brunswick: New Brunswick Department of Transportation, pp 1-8. Accessed on March 1, 2012 at http://www.gnb.ca/0113/publications/2011_Standard_Specs-e.pdf.

NSTIR. (2012). "Full Depth Reclamation With Expanded Asphalt Stabilization (method spec.)" Nova Scotia Transport and Infrastructure Renewal. Accessed on March 4, 2013 at http://www.gov.ns.ca/tran/publications/asphalt/FDR_FoamStabilization_REVMar2012_Method.pdf

NSTIR. (2013). “Highway Construction and Maintenance: A Look Back” , Nova Scotia Transportation and Infrastucture Renewal Accessed on January 4, 2013 at http://www.gov.ns.ca/tran/highways/5yearplan/lookback12_13.asp.

North Dakota Department of Transportation, (2011). "AASHTO T 99 AND T 180 - Moisture-Density Relations of Soils" , Accessed on November 24, 2013 at http://www.dot.nd.gov/manuals/materials/testingmanual/t99180.pdf

Olson, R. E. (1963). "Effective stress theory of soil compaction." Report No.: ASCE, 89(2), J. Soil Mech. and Found. Div., pp 27-45.

Paige-Green, P., Netterberg, F., and Sampson, L. R. (1989). "The carbonation of chemically stabilised road construction materials: Guide to its avoidance." Project Report 89/146/1, South African Roads Board, Pretoria, Department of Transport South Africa.

Pavement Interactive. (2009). "Gradation and Size: Gradation Test." Accessed on June 20, 2013 at http://www.pavementinteractive.org/article/theoretical-maximum-specific-gravity/

Pavement Interactive. (2011). "Theoretical Maximum Specific Gravity." Accessed on August 1, 2013 at http://www.pavementinteractive.org/article/theoretical-maximum-specific-gravity/

Plati, C., Loizos, A. (2012). "Using ground-penetrating radar for assessing the structural needs of asphalt pavements." Nondestructive Testing and Evaluation, 27 (3), pp 273-284

Portland Cement Association (PCA). (2005). Accessed May 14, 2013 at http://www.cement.org/pavements/pv_sc_faq_limits.asp

Portland Cement Association (PCA). (2005). Accessed November 14, 2013 at http://www.cement.org/pavements/pv_sc_faq_comparison.asp

Portland Cement Association (PCA). (2012). “Full Depth Reclamation with Cement”, Accessed on March 10, 2012 at http://www.cement.org/pavements/pv_sc_fdr.asp.

Proctor, R. R. (1933). "Fundamental Principles of Soil Compaction." *Engineering News Record (Aug. 31 and Sept. 7, 21, and 28),* Ed.: ENR [0891-9526], Vol: 111 (9), pp 245.

Raad, L., Minassian, G. H., and Gartin, S. (1992). "Characterization of Saturated granular Bases Under Repeated Loads." *Transportation Research Record: Journal of Transportation Research Board*, (1369), Washington D.C. pp 73-82.

Roberts, F. L., Kandhal, P. S., Brown, E. R., Lee, D-Y., and Kennedy, T. W. (1996). "Hot Mix Asphalt Materials, Mixture Design, and Construction." 2nd edition. National Asphalt Pavement Association Research and Education Foundation, Lanham, Maryland.

Salah, P. J. (2013). "Effective Design and Control of Full Depth Reclaimed Pavements." *Thesis for Master of Applied Science*, Dalhousie University, Halifax, NS.

Saarenketo, T. and Scullion, T. (2000). "Road Evaluation with Ground Penetrating Radar." Accessed on March 20, 2014 at http://d2dtl5nnlpfr0r.cloudfront.net/tti.tamu.edu/documents/1923-2F.pdf

Scott, W. (2010). "Scott's Harangue: A Personal Blog about Construction." Accessed on March 20, 2014 at http://wertel.blogspot.ca/2010/07/cold-colder-really-cold-and.html

Semmelink, C. J. (1991). "The Effect of Material Properties on the Compactability of Some Untreated Road Building Materials." *Dissertation in Department of Civil Engineering*, Faculty of Engineering. University of Pretoria: Pretoria,South Africa.

Srinivasan, G. (2004). "Evaluation of Indirect Tensile Strength to Identify Asphalt Concrete Rutting Potential." *Theiss for Master of Science in Civil Engineering,*University of West Virginia, Morgantown, WV, USA.

Sweere, G. T. H. (1990). "Unbound Granular Base for Roads." *Thesis, Faculty of Civil Engineering and Geosciences*, Delft University of Technology, Delft, The Netherlands.

Sayed, Imran M. (2007). "Full Depth Reclamation with Portland Cement: A Study of Long-Term Performance", Publication SR016, Portland Cement Association, Skokie, Illinois 60077-1083.

Tayfur, S., Ozen, H., and Aksoy, A. (2005). "Investigation of rutting performance of asphalt mixtures containing polymer modifiers." *Construction and Building Materials*, Science Direct: Elsvier, Istanbul, Turkey, Accessed on June 29, 2013 at www.elsevier.com/locate/conbuildmat

TEST-LLC. (2013). "*Timely Engineering Soil Test - LLC.*" Accessed on August 2, 2013 at http://www.test-llc.com/compaction.htm

Texas Department of Transportation (TxDOT). (2005). “Guidelines for modification and stabilization of soils and base for use in pavement structures”, Accesses on March 5, 2012 at ftp://ftp.dot.state.tx.us/pub/txdot-info/cmd/tech/stabilization.pdf.

Texas Department of Transportation (TxDOT). (2010). "Test Procedure for Indirect Tensile Strenth Test ." *TxDOT Designation: Tex-226-F,* Accessed on June 13, 2013 at http://ftp.dot.state.tx.us/pub/txdot-info/cst/TMS/200-F_series/pdfs/bit226.pdf

Thom, N.H. and Brown, S.F. (1987). "The effect of moisture on the structural performance of a crushed-limestone road base." *Transportation Research Record: Journal of Transportation Research Board for National Research Council*, (1121), Washington D.C., pp 50-56.

Thom, N.H., Brown, S.F. (1988). "The Effect of Grading and Density on the Mechanical Properties of a Crushed Dolomite Limestone." *14th ARRB Conference,* pp 94-100.

TPUB. (1994.). "Integrated Publishing." Accessed August 2, 2013 at http://www.tpub.com/inteng/13c.htm

Toll, D. G. (1997). "Pavement Design - Foundation Design." Durham University, Durham, UK. Accessed on July 3, 2013 at http://www.dur.ac.uk/~des0www4/cal/roads/pavdes/pavfound.html

Van Neikerk, A. A.,Van Scheers, J., Muraya, P., and Kisimbi, A. (2000). "The Effect of Compaction on the Mechanical behaviour of Mix Granulate Base Course Materials and on Pavement Performance." *HERON* (Delft University of Technology), Vol: 45, Issue. 3 (2000), pp 197-218.

Wang, H-N., Liu, X-J., and Hao, P-W. (2008). "Evaluating the Shear Resistance of Hot Mix Asphalt by the Direct Shear Test." *Journal of Testing and Evaluation* (ASTM International), Vol: 36, Issue: 6.

Wisconsin Department of Transportation. (1997). "Pavement Recycling Guidelines for State and Local Governments Participant's Reference Book *(Chapter 17. Full Depth Reclamation (Case Histories And QC/QA)).*" Pavement Recycling Guidelines for State and Local Governments: Wisconsin, USA. Accessed on May 13, 2013 at http://www.fhwa.dot.gov/pavement/recycling/98042/17.cfm

Witrgen Group (2002). *Foamed Bitumen - The Innovative Binding Agent for Road Construction,* Wirtgen GmbH, Windhagen, Germany.

Witrgen Group (2010). *Wirtgen Cold Recycling Technology,* Wirtgen GmbH, Windhagen, Germany. Accessed on March 13, 2013 at http://www.wirtgenamerica.com/media/local/1_admin/newsandmeida/download/wirtgen/cold_recyclers_soil_stabilizers/p_manual2010_e.pdf

Yoder, E. J., Witczak, M. W. (1975). "Principles of Pavement Design: Chap. 8, Materials Characterization." 2nd Edition, John Wiley & Sons Inc., New York, USA, pp 250.

APPENDIX A: Test Results for Route 335 materials

A.1 FDR Gradation Analysis

Table A-1 Gradation analysis for Route 335 pulverized materials

Location	**7+725**	**7+790**	**7+075**	**7+750**	**7+772**	**7+703**	**Mean**	**Standard Deviation**
RAP/Total Depth	0.9	0.8	0.57	0.5	0.43	0.31	0.59	0.22
Size (mm)	% Passing							
50	100	100	100	100	100	100	100	0.00
20	94.63	99.88	98.00	98.82	97.95	97.02	97.71	1.79
14	87.81	94.31	94.29	95.34	94.73	93.83	93.39	2.78
10	75.23	84.37	88.28	87.80	88.83	88.12	85.44	5.25
5	47.43	57.36	71.66	67.27	71.14	74.88	64.96	10.51
2.5	27.16	36.87	55.66	45.70	50.36	59.49	45.87	12.11
1.25	15.97	21.05	41.29	29.01	32.57	46.86	31.12	11.74
0.63	9.87	11.39	26.62	16.74	19.04	33.58	19.54	9.11
0.315	4.00	4.00	10.7	6.13	7.16	15.13	7.85	4.3
0.16	1.18	1.12	3.56	2.06	2.25	5.04	2.54	1.51
0.075	0.053	0.073	0.21	0.13	0.14	0.22	0.14	0.07
Fineness Modulus	7.37	6.90	6.10	6.51	6.36	5.86	6.51	0.55

A.2 Moisture-Density Relationship: Sta 7+725

Mass of the mold + plate: 4183.2 gm

Mold: Diameter: 101.6 mm
Height: 116.4 mm
Volume: 9.437E-04 m^3

Sample No.	1	2	3	4	5
Date Tested	09/08/11	10/08/11	10/08/11	11/08/11	11/08/11
Mass of Sample (g)	2100.0	2100.3	2100.3	2100.4	2100.3
% Water added	7.0%	8.0%	9.0%	10.0%	11.0%
Mass of water added (g)	147.9	168.1	189.1	210.1	231
Compacted					
Mass of sample+ mold+ plate (g)	5958.4	6022.6	6048.8	6021.7	6019.1
Mass of wet sample (for moisture content) (g)	2200.9	2239.7	2246.2	2246.5	2229.7
Tare (g)	437.8	304.8	576	395	439
Mass of dry sample (g)	2062.4	2079.6	2070.6	2069.4	2057.3
Actual Moisture content	6.72%	7.7%	8.5%	8.56%	8.38
Moist Density (kg/m^3)	1890	1956	1980	1960	1953
Dry Density (kg/m^3)	1769	1816	1829	1801	1802

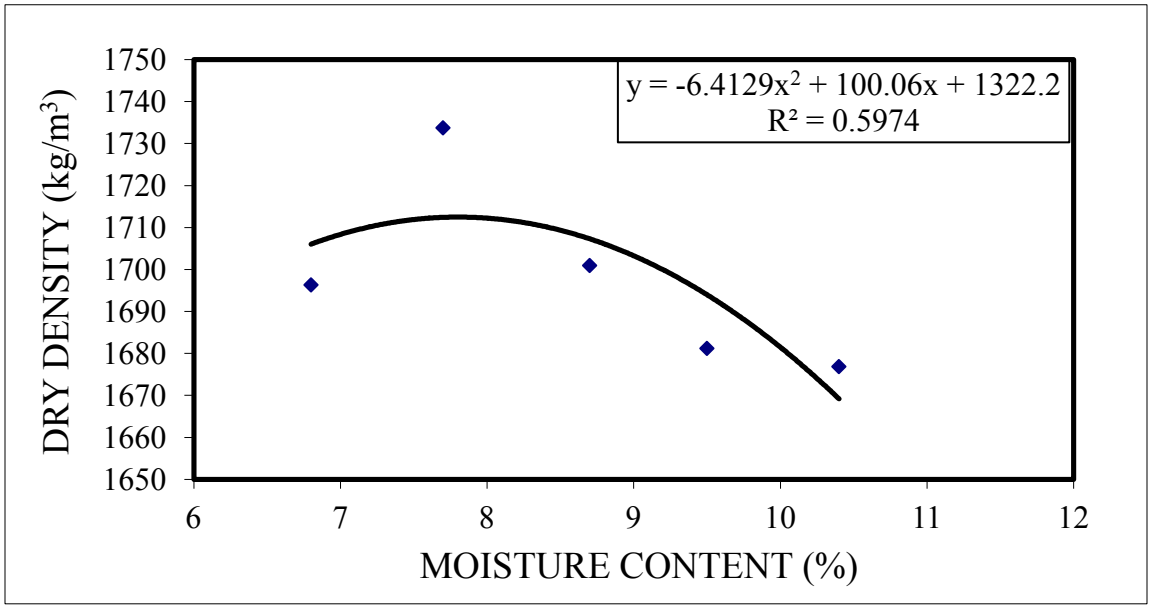

Figure A-1 – Sta 7+725 Moisture Density Relationship

Optimum Density: 1712 kg/m^3. Optimum Moisture Content: 8.25%

A.3 Moisture-Density Relationship: Sta 7+790

Mass of the mold + plate: 4183.2 gm

Mold: Diameter: 101.6 mm
Height: 116.4 mm
Volume: 9.437E-04 m^3

Sample No.	1	2	3	4	5
Date Tested	17/08/11	17/08/11	18/08/11	18/08/11	19/08/11
Mass of Sample (g)	2100.1	2100.4	2100.3	2100.0	2100.2
% Water added	7.0%	8.0%	9.0%	10.0%	11.0%
Mass of water added (g)	147.3	168.5	189.8	211.1	231.4
Compacted					
Mass of sample+ mold+ plate (g)	5963.3	5968.8	5981.7	5914.7	5895.1
Mass of wet sample (for moisture content) (g)	2233.8	2251.8	2250.1	2272.2	2294.5
Tare (g)	394.8	304.6	646.3	433	303
Mass of dry sample (g)	2089.7	2087.4	2069.8	2070.6	2075.8
Actual Moisture content	6.9%	7.9%	8.71%	9.74%	10.54%
Moist Density (kg/m^3)	1894	1900	1913.8	1840	1820
Dry Density (kg/m^3)	1772	1760	1760	1680	1650

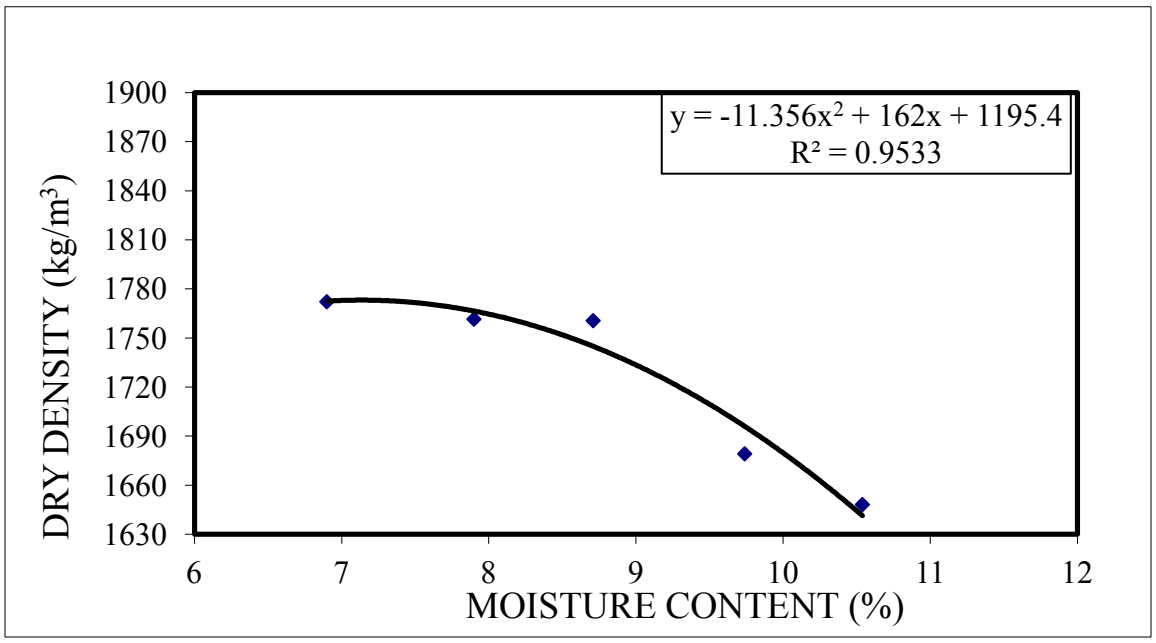

Figure A-2 – Sta 7+790 Moisture Density Relationship

Optimum Density: 1775 kg/m^3. Optimum Moisture Content: 7.63%

A.4 Moisture-Density Relationship: Sta 7+075

Mass of the mold + plate: 4182.7 gm

Mold: Diameter: 101.6 mm
Height: 116.4 mm
Volume: 9.437E-04 m^3

Sample No.	1	2	3	4	5
Date Tested	18/08/11	18/08/11	19/08/11	19/08/11	20/08/11
Mass of Sample (g)	2100.1	2100.1	2100.0	2100.3	2100.2
% Water added	7.0%	8.0%	9.0%	10.0%	11.0%
Mass of water added (g)	147.1	170.7	189.1	210.1	231.2
Compacted					
Mass of sample+ mold+ plate (g)	5933.6	5956.2	5985.7	6004.2	6000.1
Mass of wet sample (for moisture content) (g)	2232.6	2251.9	2275.2	2285	2304.3
Tare (g)	1262.8	1272.3	1256.3	1257.5	1397
Mass of dry sample (g)	2086.8	2086.4	2088.7	2080.5	2084.6
Actual Moisture content	6.986%	7.9%	8.93%	9.83%	10.54%
Moist Density (kg/m^3)	1860	1886	1918	1937.6	1933.5
Dry Density (kg/m^3)	1740	1747.7	1760	1764.2	1750

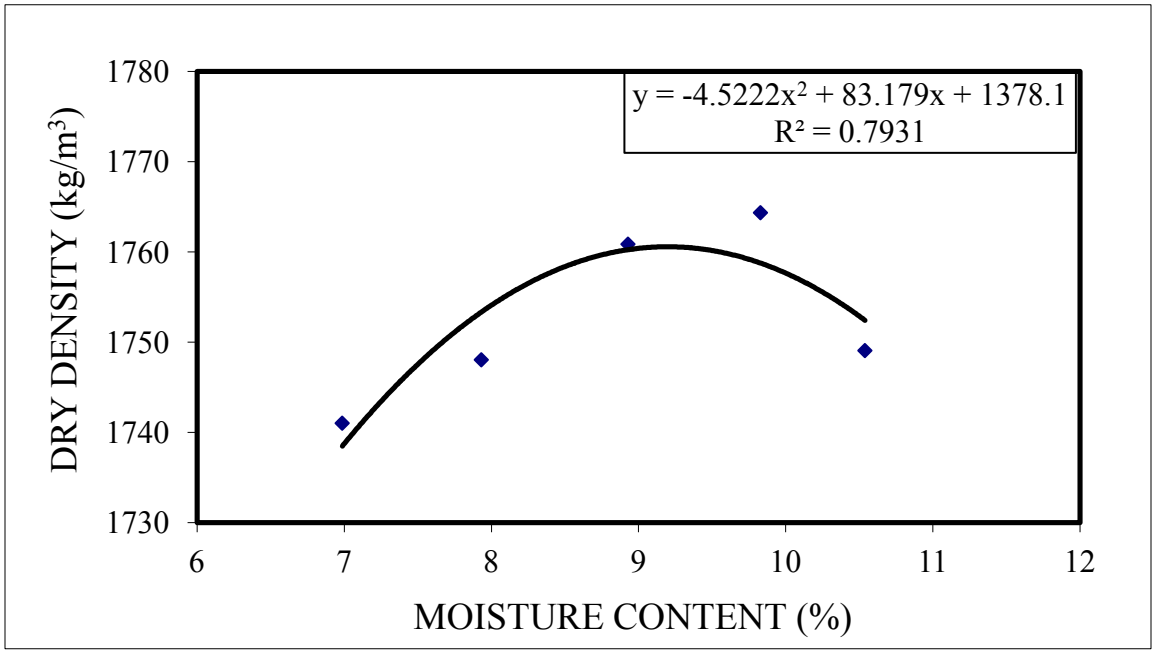

Figure A-3 – Sta 7+075 Moisture Density Relationship

Optimum Density: 1761 kg/m^3. Optimum Moisture Content: 9.75%

A.5 Moisture-Density Relationship: Sta 7+750

Mass of the mold + plate: 4182.7 gm

Mold: Diameter: 101.6 mm
Height: 116.4 mm
Volume: 9.437E-04 m^3

Sample No.	1	2	3	4	5
Date Tested	17/08/11	17/08/11	18/08/11	18/08/11	19/08/11
Mass of Sample (g)	2100.2	2100.0	2100.1	2100.2	2100.1
% Water added	7.0%	8.0%	9.0%	10.0%	11.0%
Mass of water added (g)	147.1	169	189.2	211.1	231.4
Compacted					
Mass of sample+ mold+ plate (g)	5927.9	5983.5	6036	6045.7	6054.3
Mass of wet sample (for moisture content) (g)	2220.7	2228.3	2257.3	2265.8	2298.2
Tare (g)	1262.8	1272.5	1256.2	1257.7	1396.8
Mass of dry sample (g)	2080.2	2070.8	2080.9	2067.4	2077.9
Actual Moisture content	6.75%	7.61%	8.48%	9.83%	10.6%
Moist Density (kg/m^3)	1856	1915	1970	1982	1990
Dry Density (kg/m^3)	1739	1780	1817	1810	1800

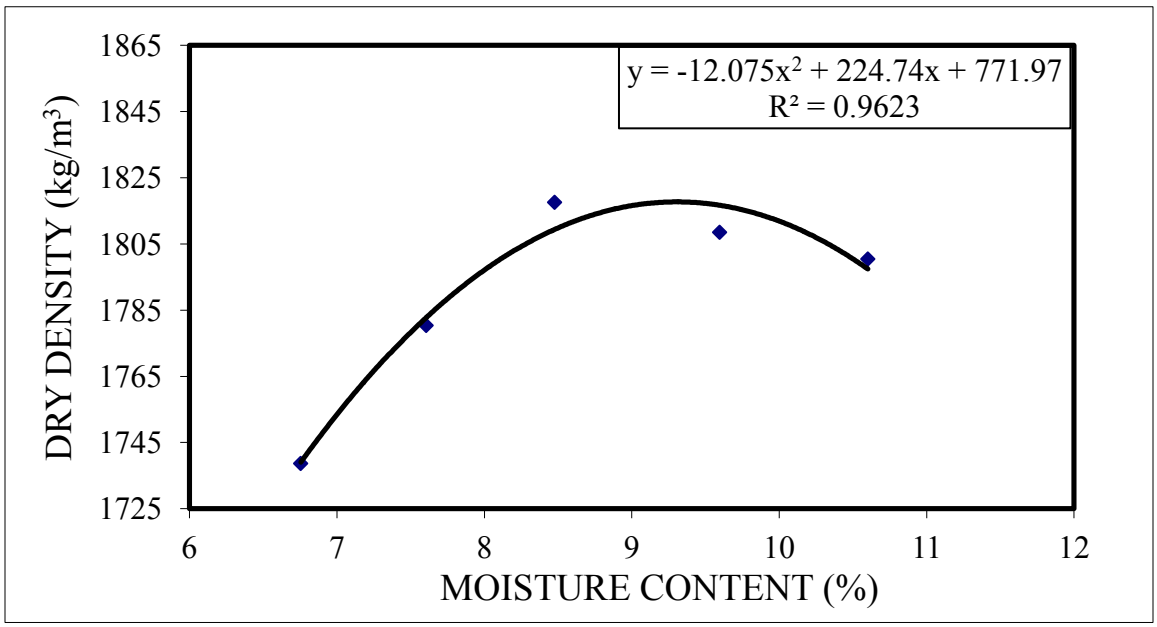

Figure A-4 – Sta 7+750 Moisture Density Relationship

Optimum Density: 1818 kg/m^3. Optimum Moisture Content: 9.75%

A.6 Moisture-Density Relationship: Sta 7+772

Mass of the mold + plate: 4182.7 gm

Mold: Diameter: 101.6 mm
Height: 116.4 mm
Volume: 9.437E-04 m^3

Sample No.	1	2	3	4	5
Date Tested	21/08/11	21/08/11	22/08/11	22/08/11	23/08/11
Mass of Sample (g)	2100.1	2100.3	2100.2	2100.0	2100.3
% Water added	7.0%	8.0%	9.0%	10.0%	11.0%
Mass of water added (g)	147.3	168.3	190	210.2	232.7
Compacted					
Mass of sample+ mold+ plate (g)	5942.5	5964.8	6001.7	6026.7	6008.2
Mass of wet sample (for moisture content) (g)	2204	2241.4	2262.9	2283.6	2274.7
Tare (g)	431.5	437.2	576.3	562.5	438.2
Mass of dry sample (g)	2060	2076.5	2077	2079.7	2053.1
Actual Moisture content	6.99%	7.94%	8.95%	9.8%	10.8%
Moist Density (kg/m^3)	1872	1890	1935	1960	1942
Dry Density (kg/m^3)	1750	1756	1776	1786.54	1752.8

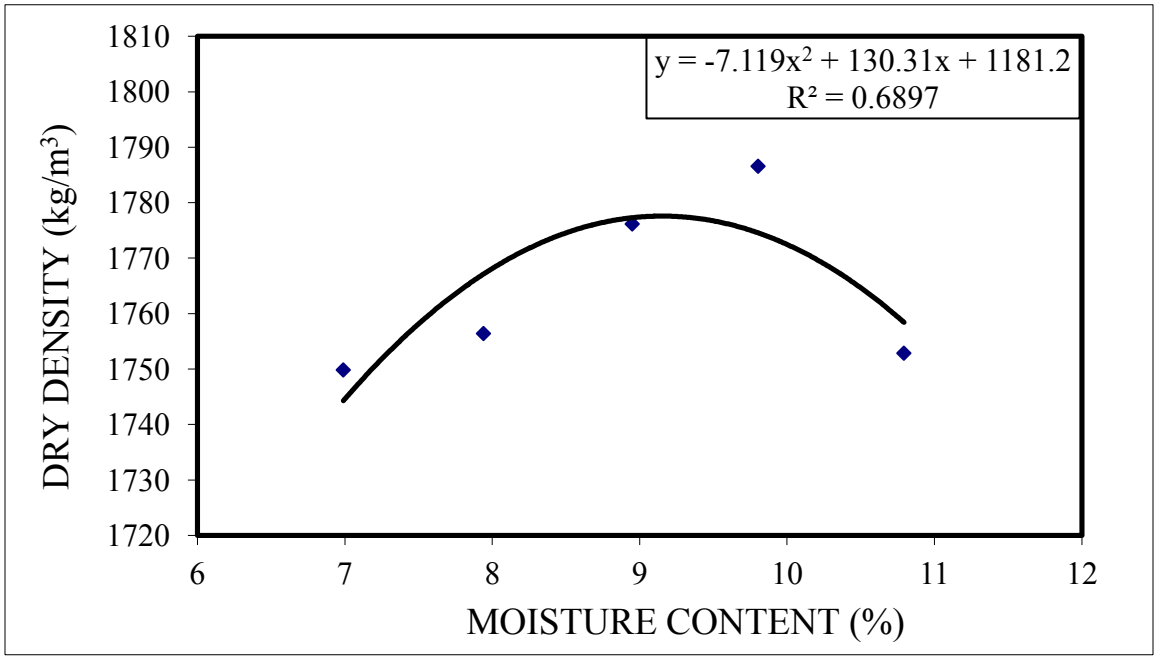

Figure A-5 – Sta 7+772 Moisture Density Relationship

Optimum Density: 1778 kg/m^3. Optimum Moisture Content: 9.63%

A.7 Moisture-Density Relationship: Sta 7+703

Mass of the mold + plate: 4182.7 gm

Mold: Diameter: 101.6 mm
Height: 116.4 mm
Volume: 9.437E-04 m^3

Sample No.	1	2	3	4	5
Date Tested	16/08/11	16/08/11	17/08/11	17/08/11	18/08/11
Mass of Sample (g)	2100.0	2100.1	2100.0	2100.3	2100.1
% Water added	7.0%	8.0%	9.0%	10.0%	11.0%
Mass of water added (g)	147.0	168.2	189	210.0	231.1
Compacted					
Mass of sample+ mold+ plate (g)	6091.6	6136.1	6183.8	6202.2	6216.8
Mass of wet sample (for moisture content) (g)	2239.2	2257.7	2265.6	2275.1	2303.4
Tare (g)	1257.8	1256.3	1272.4	1351.1	1351.1
Mass of dry sample (g)	2089	2087.3	2077.1	2068.3	2080.3
Actual Moisture content	7.19%	8.16%	9.075%	9.99%	10.72%
Moist Density (kg/m^3)	2030	2078	2128	2148	2160
Dry Density (kg/m^3)	1890	1920	1950	1953	1950

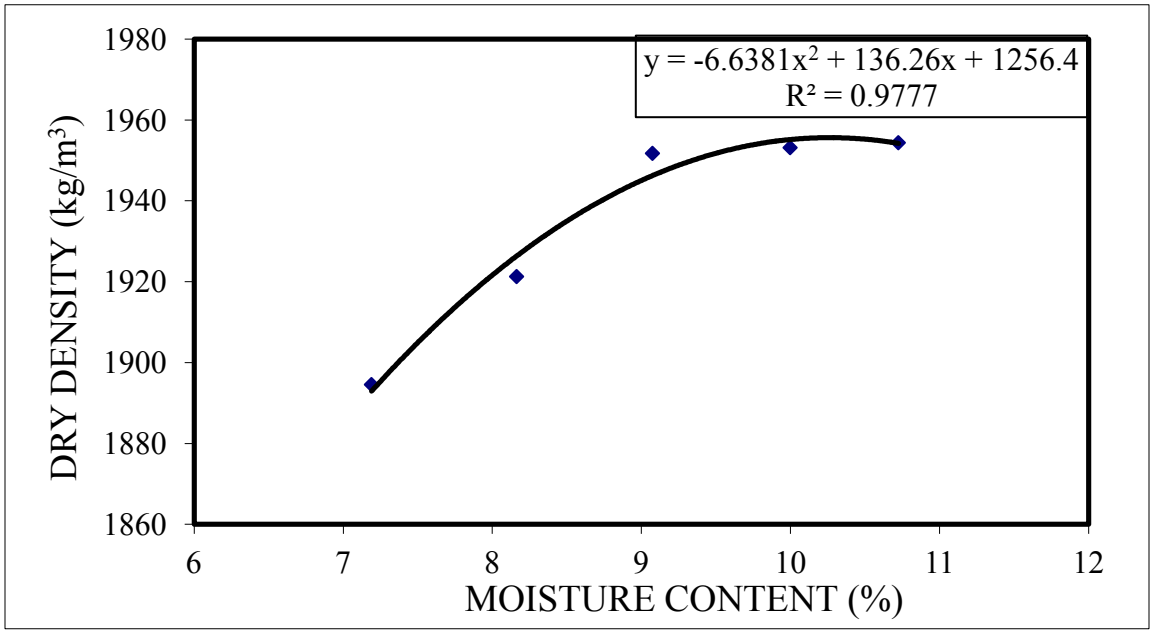

Figure A-6 – Sta 7+703 Moisture Density Relationship

Optimum Density: 1955 kg/m^3. Optimum Moisture Content: 10.75%

A.8 Theoretical Maximum Density Results

ASTM D2041/2041M-11

Weighing Flask determination

Station	7+725	7+790	7+075	7+750	7+772	7+703
Date Tested	02/08/11	25/07/11	25/07/11	04/08/11	29/07/11	29/07/11
Mass of dry sample in air, (g)	1995.4	1996.4	1999.3	1993.5	1989.5	2100.1
Mass of the bowl, (g)	2143	2143	2143.1	2143	2143	2143
Mass of (sample+bowl+water+lid) at 25 ºC, (g)	8564.3	8565.1	8577.3	8569.2	8567.5	8576.4
Mass of (bowl+water+lid) at 25 ºC, (g)	7369.7	7369.7	7369.7	7369.7	7369.7	7369.7
Theoretical Maximum Specific Gravity	2.476	2.511	2.533	2.492	2.512	2.514

A.9 CBR Results: Sta 7+725

Table A-2 – Station 7+725 CBR results

Penetration (in)	Stress (unsoaked) psi	Stress (soaked) psi
0.000	0	0
0.025	1	1
0.050	20	19
0.075	43	39
0.100	67	60
0.125	94	82
0.150	117	104
0.175	142	129
0.200	168	151
0.300	251	229
0.400	321	294
0.500	376	345

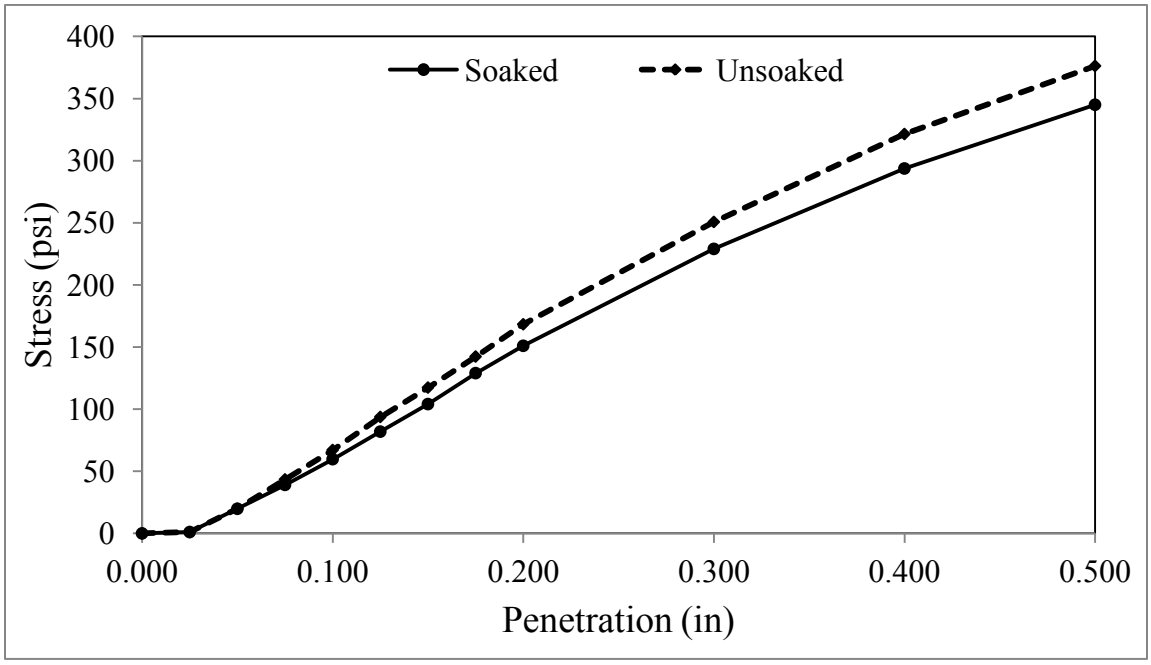

Figure A-7 – Sta 7+725 Stress vs Penetration graph

A.10 CBR Results: Sta 7+790

Table A-3 – Station 7+790 CBR results

Penetration (in)	Stress (unsoaked) psi	Stress (soaked) psi
0.000	0	0
0.025	4	7
0.050	24	27
0.075	46	49
0.100	70	73
0.125	100	101
0.150	128	122
0.175	160	147
0.200	191	173
0.300	298	269
0.400	386	350
0.500	468	425

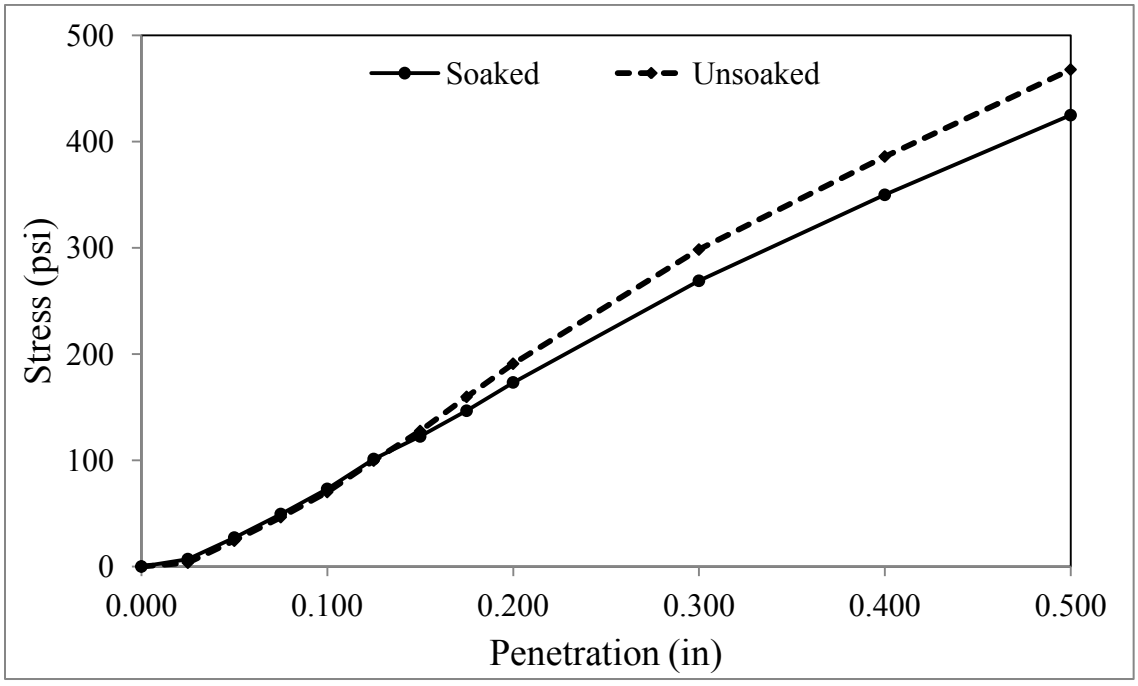

Figure A-8 – Sta 7+790 Stress vs Penetration graph

A.11 CBR Results: Sta 7+075

Table A-4 – Station 7+075 CBR results

Penetration (in)	Stress (unsoaked) psi	Stress (soaked) psi
0.000	0	0
0.025	5	4
0.050	35	33
0.075	72	69
0.100	120	119
0.125	151	168
0.150	193	218
0.175	238	265
0.200	282	311
0.300	439	464
0.400	578	576
0.500	684	668

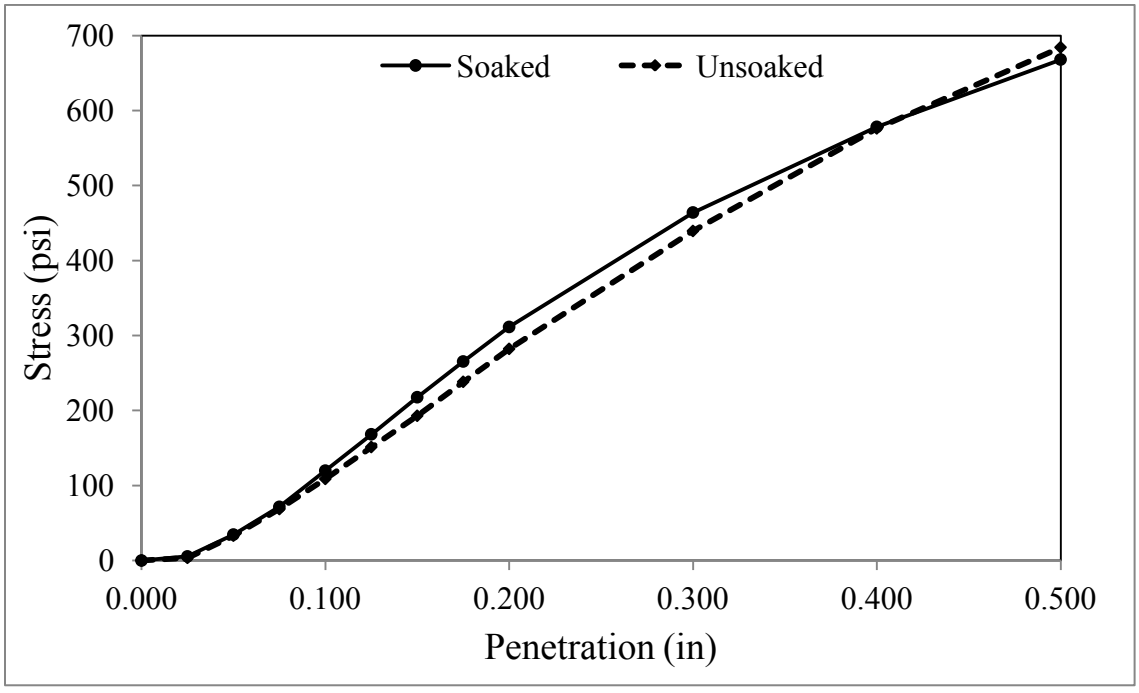

Figure A-9 – Sta 7+075 Stress vs Penetration graph

A.12 CBR Results: Sta 7+750

Table A-5 – Station 7+750 CBR results

Penetration (in)	Stress (unsoaked) psi	Stress (soaked) psi
0.000	0	0
0.025	18	3
0.050	66	20
0.075	119	43
0.100	179	76
0.125	234	118
0.150	288	161
0.175	333	210
0.200	378	262
0.300	535	447
0.400	656	594
0.500	753	719

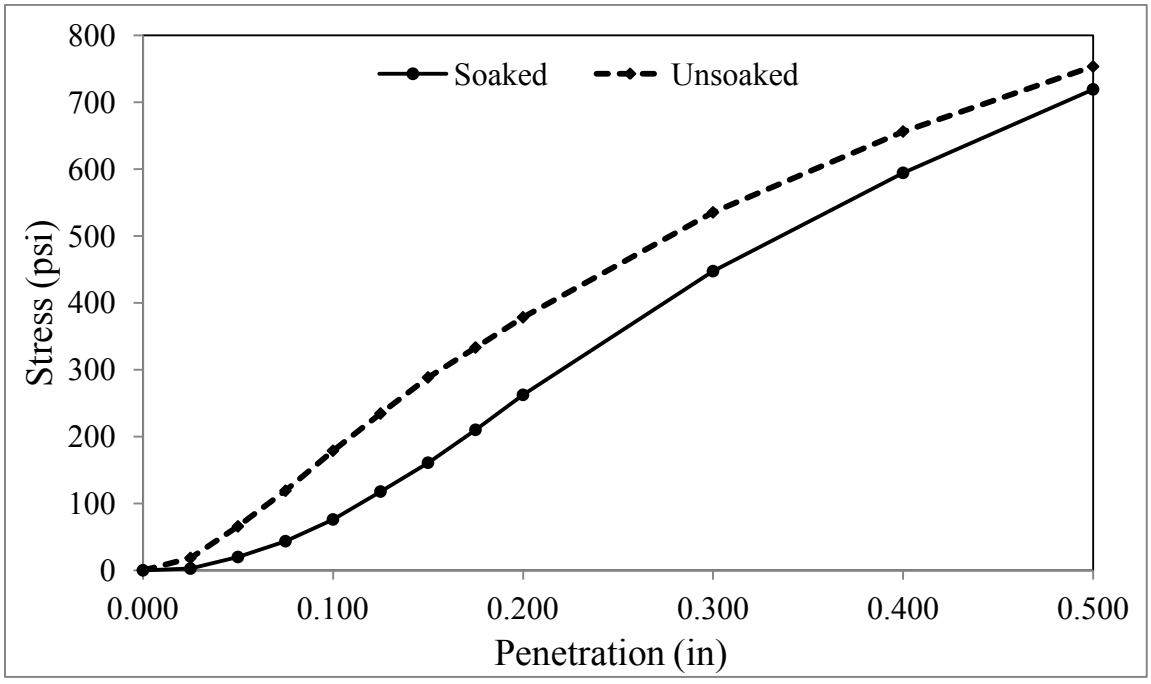

Figure A-10 – Sta 7+750 Stress vs Penetration graph

A.13 CBR Results: Sta 7+772

Table A-6 – Station 7+772 CBR results

Penetration (in)	Stress (unsoaked) psi	Stress (soaked) psi
0.000	0	0
0.025	9	7
0.050	42	30
0.075	79	58
0.100	113	87
0.125	149	118
0.150	182	146
0.175	218	177
0.200	246	209
0.300	344	334
0.400	418	442
0.500	479	537

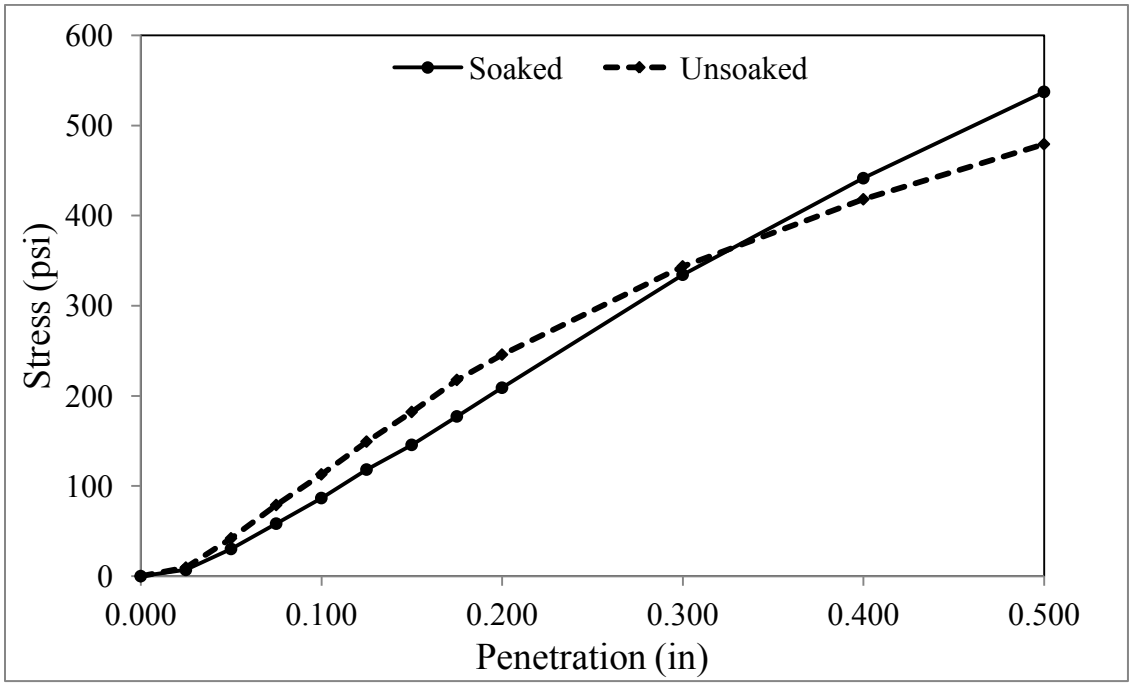

Figure A-11 – Sta 7+772 Stress vs Penetration graph

A.14 CBR Results: Sta 7+703

Table A-7 – Station 7+703 CBR results

Penetration (in)	Stress (unsoaked) psi	Stress (soaked) psi
0.000	0	0
0.025	4	0
0.050	32	24
0.075	73	54
0.100	126	88
0.125	190	130
0.150	256	177
0.175	322	223
0.200	373	264
0.300	619	413
0.400	915	533
0.500	1111	628

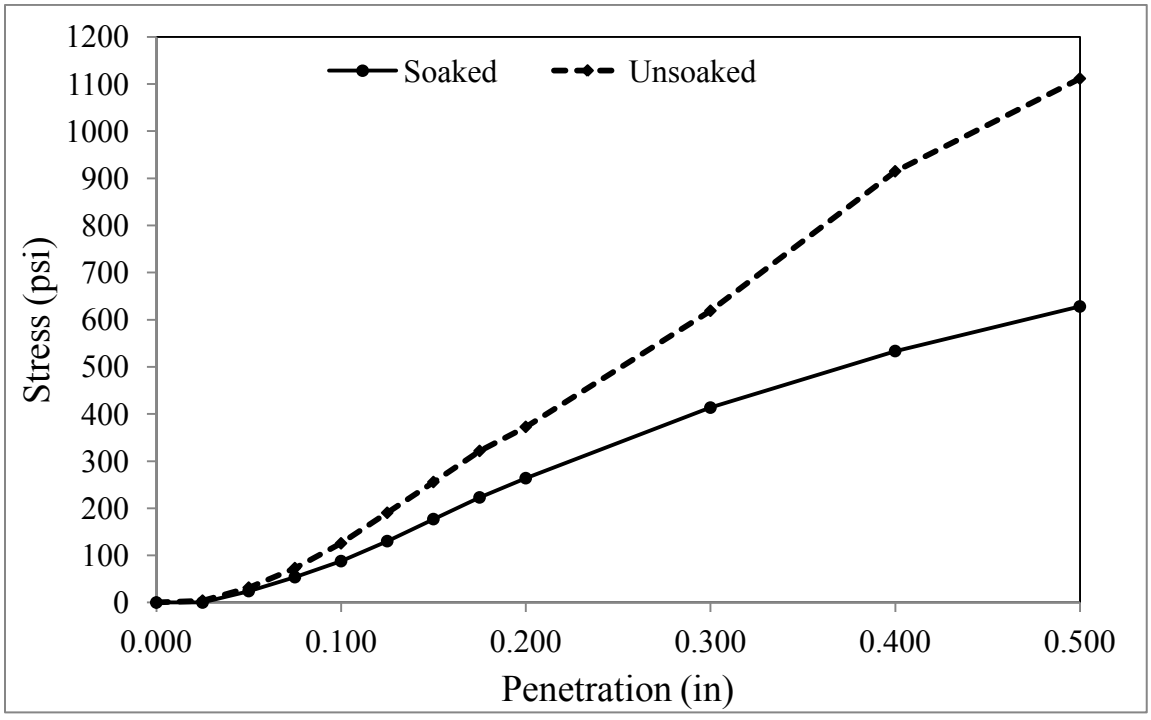

Figure A-12 – Sta 7+703 Stress vs Penetration graph

A.15 Direct Shear Test Results: Sta 7+725

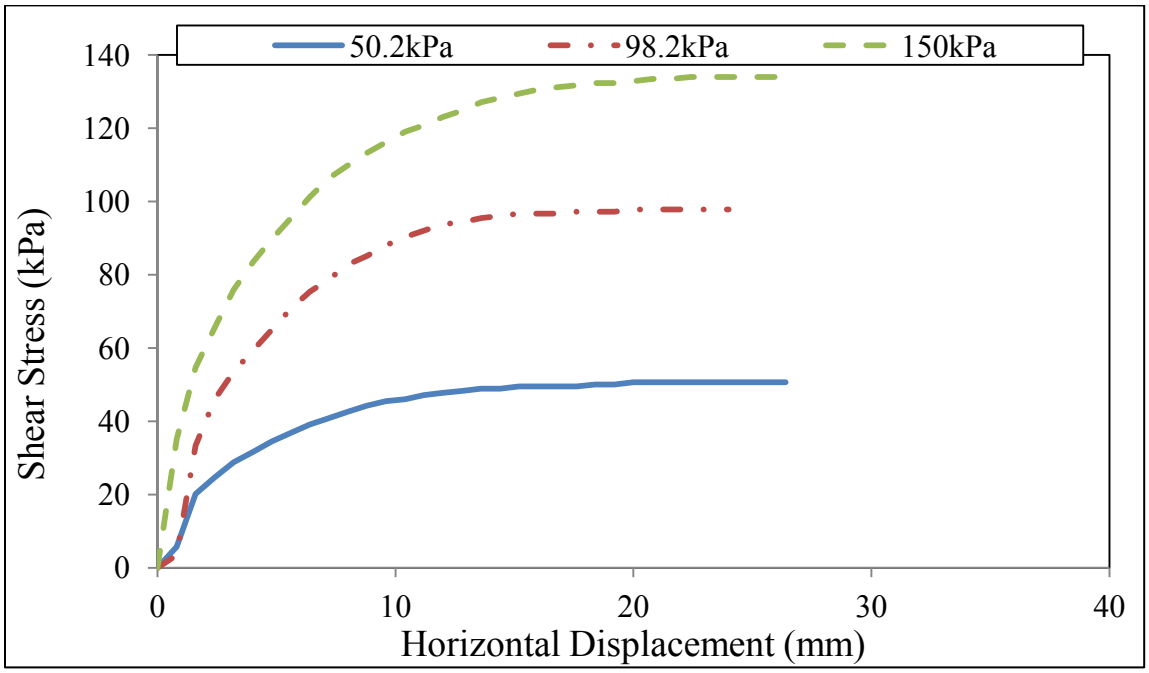

Figure A-13 – Sta 7+725 Shear Stress vs Horizontal Displacement

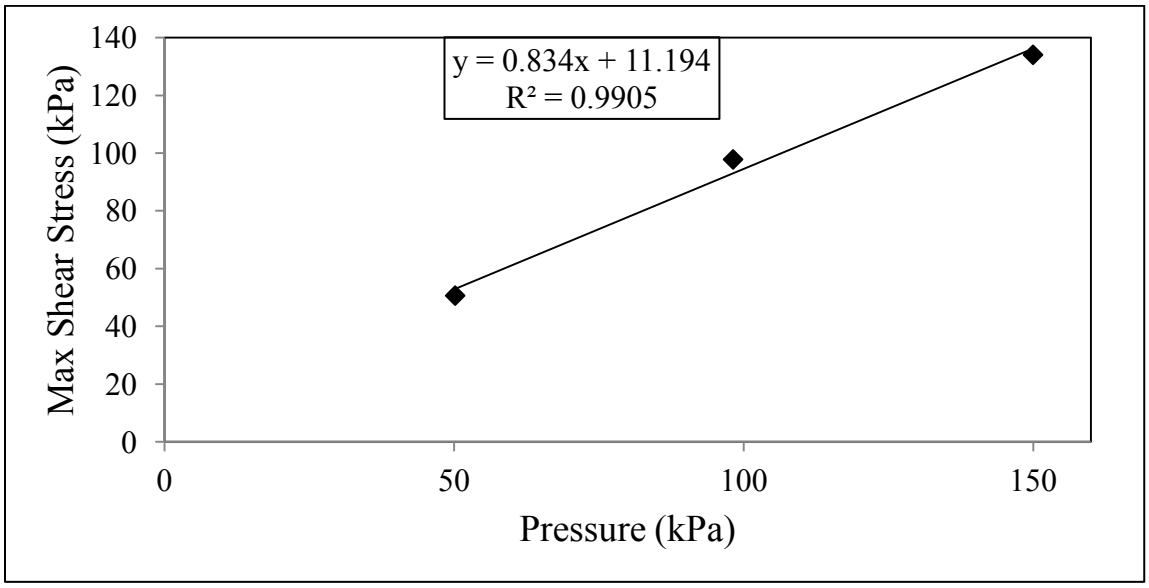

Figure A-14 – Sta 7+725 Maximum Shear Stress vs Confining Pressure

$\phi = \tan^{-1} 0.834 = 39.8^{o}$

C = 11.19 kPa

A.16 Direct Shear Test Results: Sta 7+790

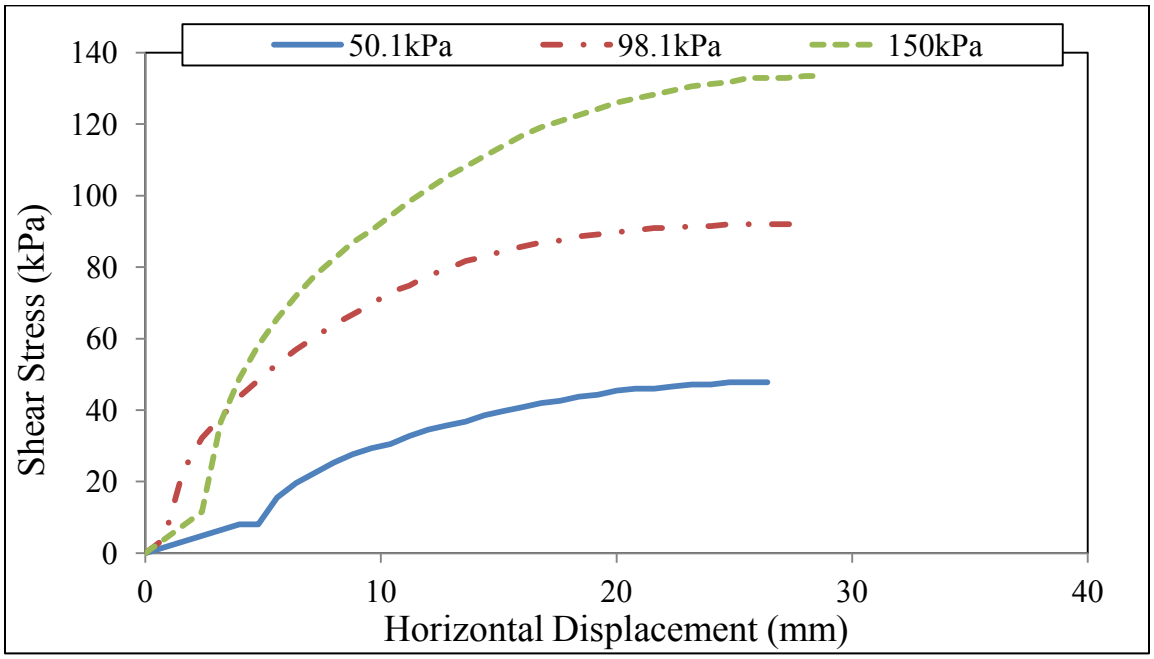

Figure A-15 – Sta 7+790 Shear Stress vs Horizontal Displacement

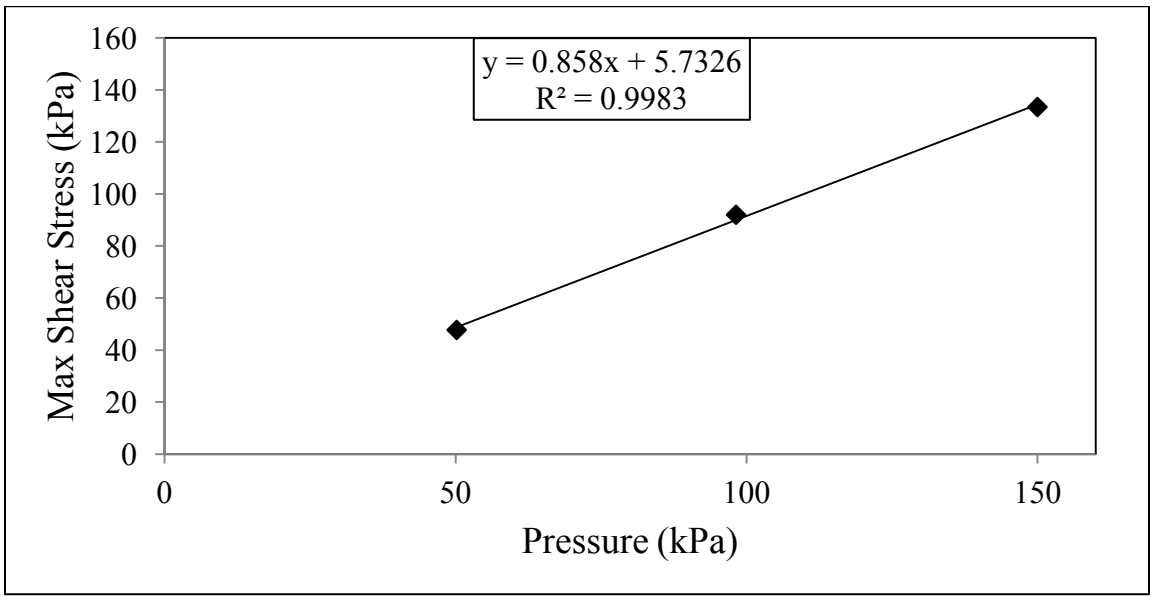

Figure A-16 – Sta 7+790 Maximum Shear Stress vs Confining Pressure

$\phi = \tan^{-1} 0.858 = 40.6^{o}$

C = 5.73 kPa

A.17 Direct Shear Test Results: Sta 7+075

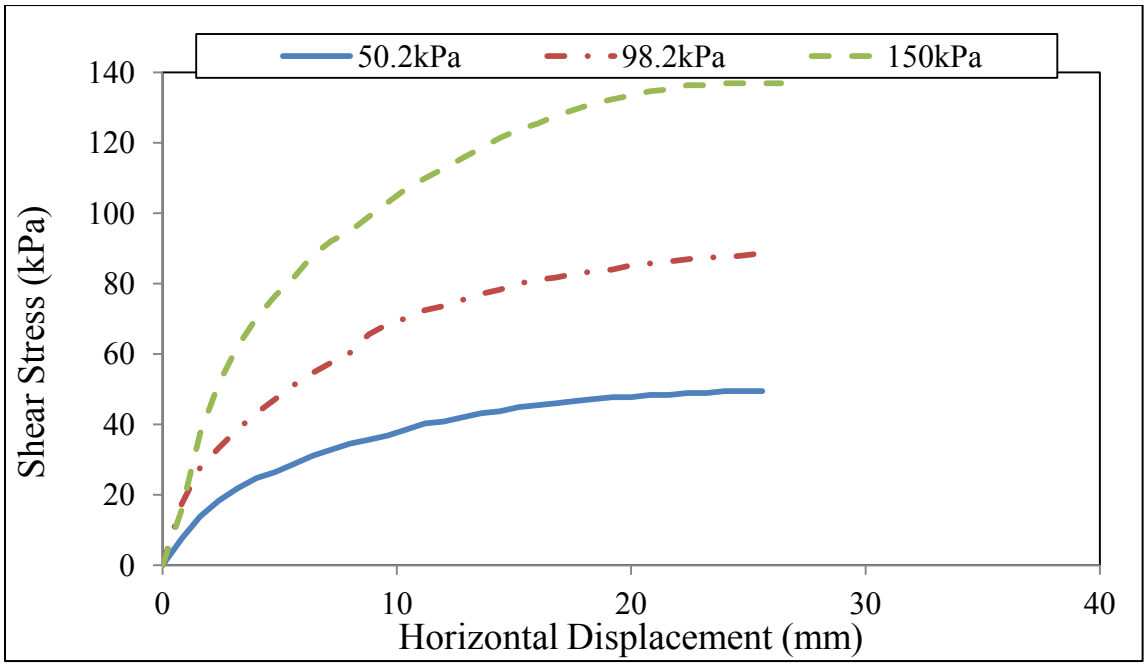

Figure A-17 – Sta 7+075 Shear Stress vs Horizontal Displacement

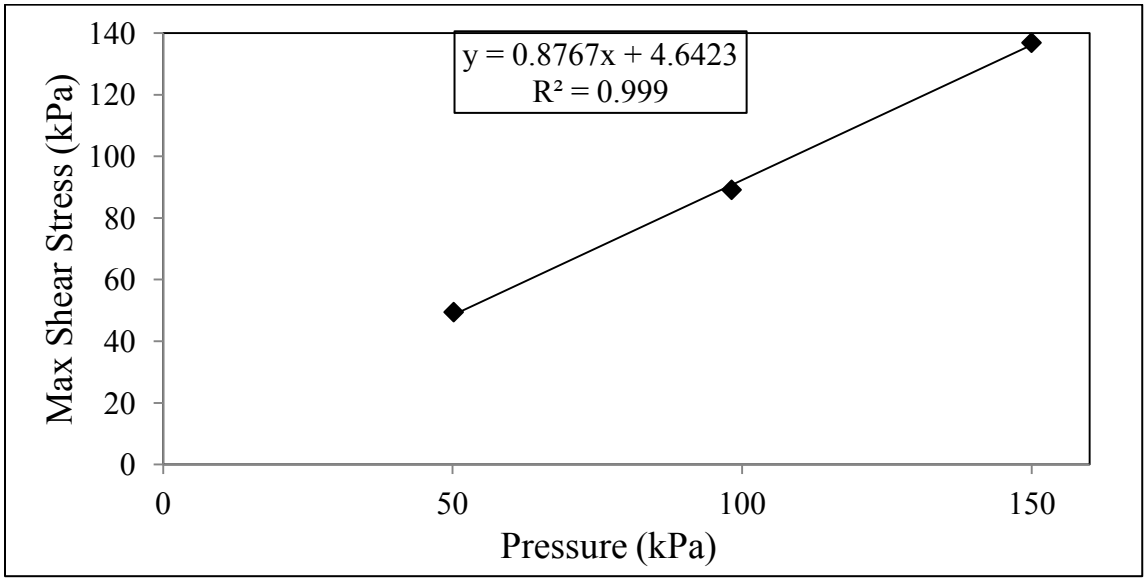

Figure A-18 – Sta 7+075 Maximum Shear Stress vs Confining Pressure

$\phi = \tan^{-1} 0.8767 = 41.2°$

C = 4.64 kPa

A.18 Direct Shear Test Results: Sta 7+750

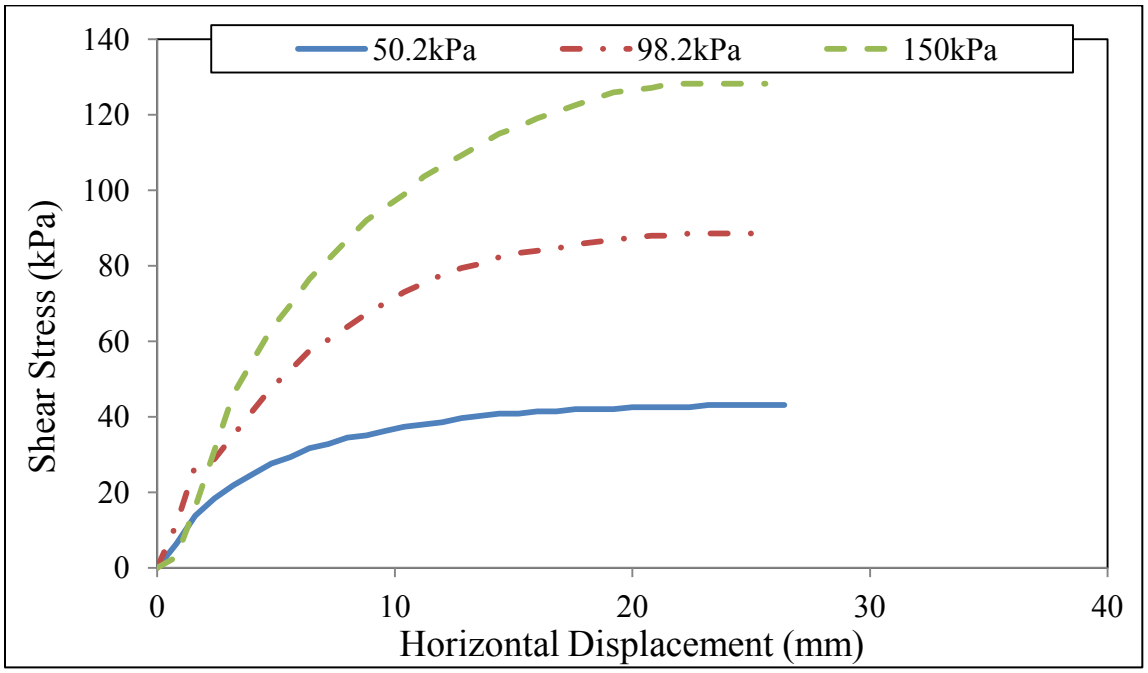

Figure A-19 – Sta 7+750 Shear Stress vs Horizontal Displacement

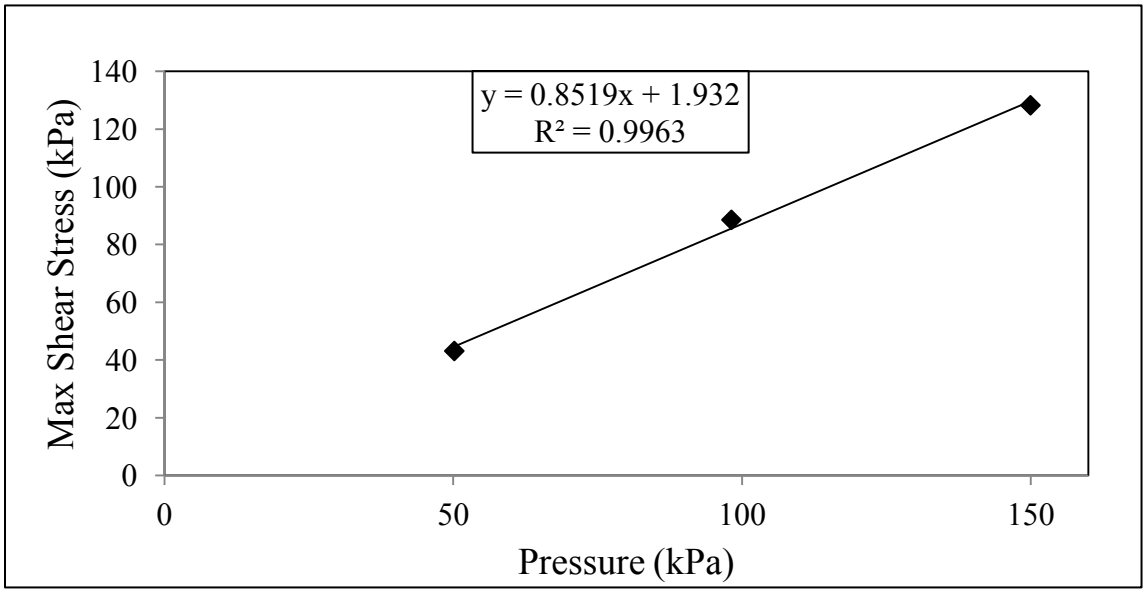

Figure A-20 – Sta 7+750 Maximum Shear Stress vs Confining Pressure

$\phi = \tan^{-1} 0.8519 = 40.4^{o}$

C = 1.93 kPa

A.19 Direct Shear Test Results: Sta 7+772

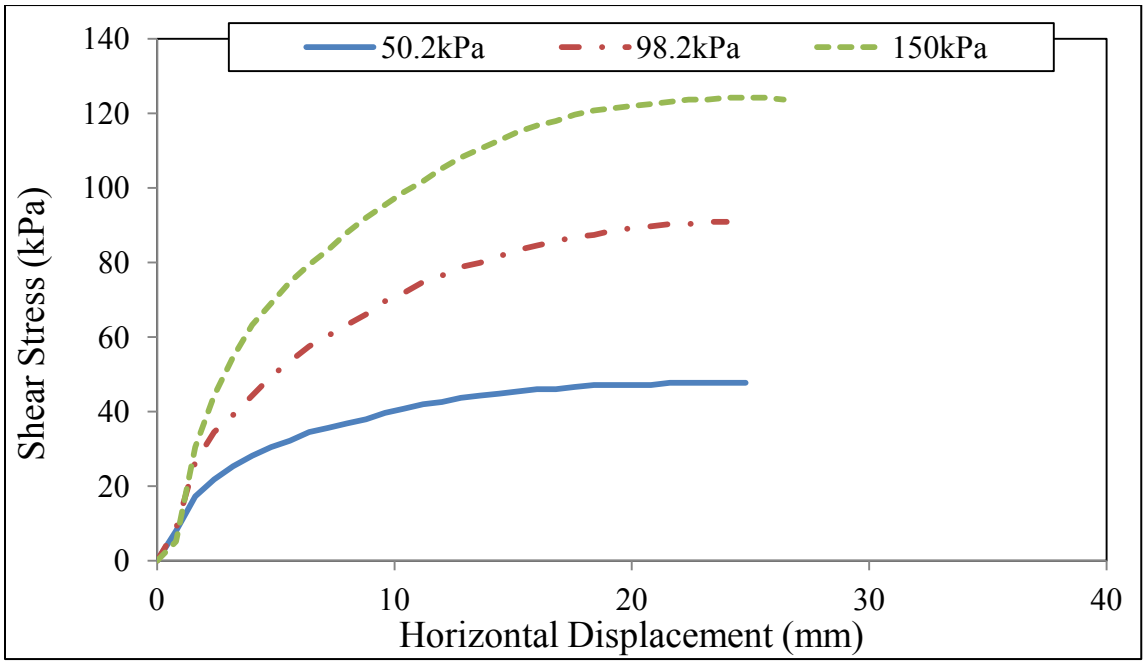

Figure A-21– Sta 7+772 Shear Stress vs Horizontal Displacement

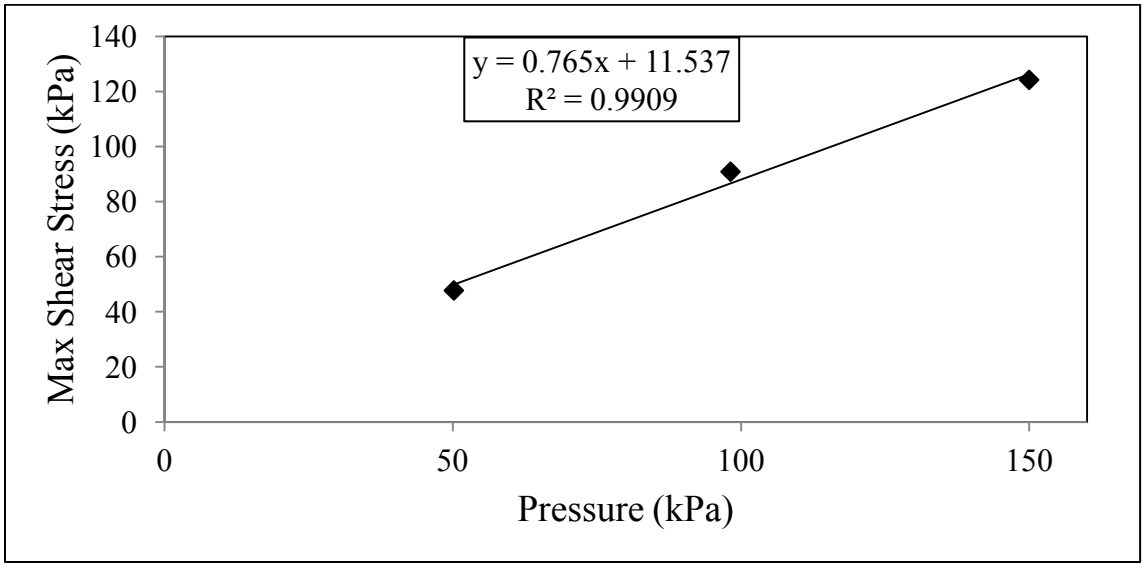

Figure A-22 – Sta 7+772 Maximum Shear Stress vs Confining Pressure

$\phi = \tan^{-1} 0.765 = 37.4^{o}$

C = 11.74 kPa

A.20 Direct Shear Test Results: Sta 7+703

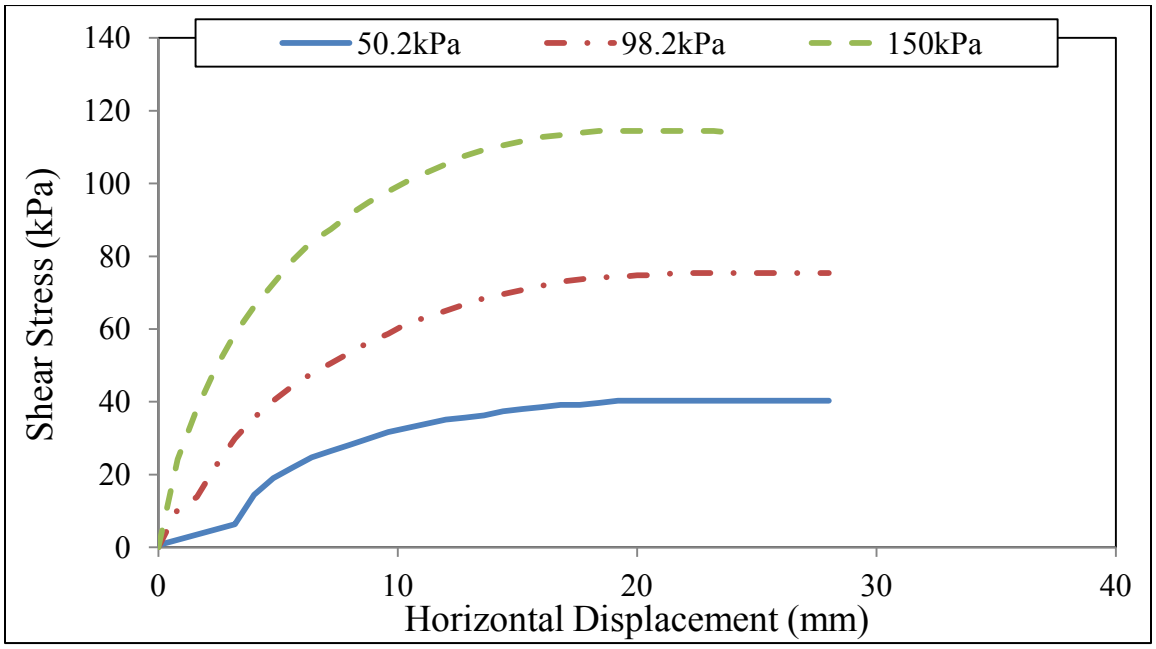

Figure A-23– Sta 7+703 Shear Stress vs Horizontal Displacement

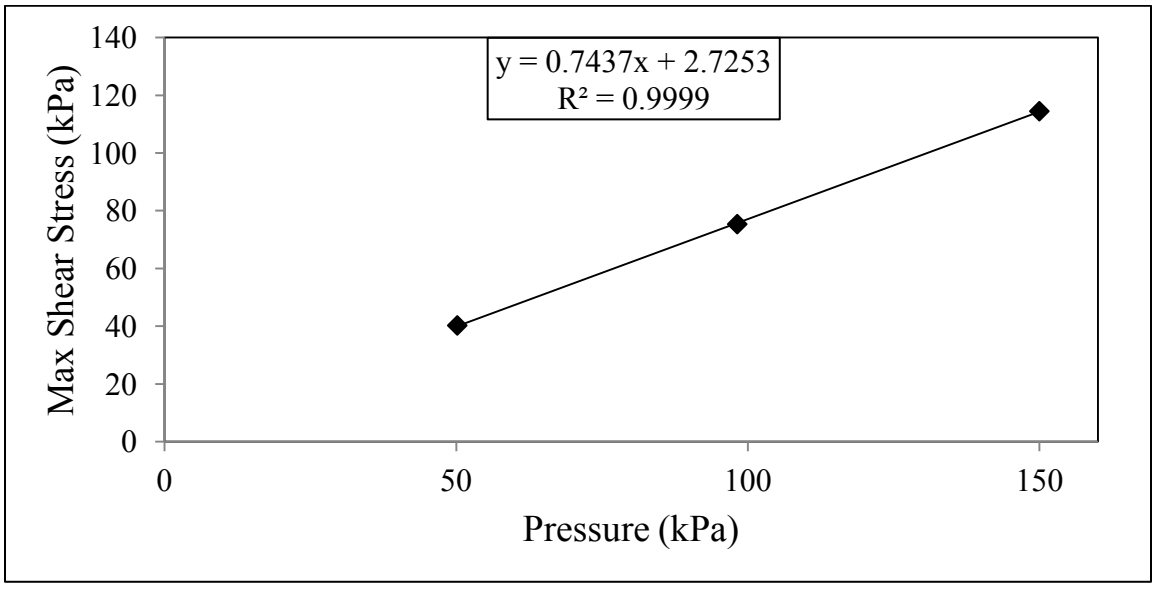

Figure A-24 – Sta 7+703 Maximum Shear Stress vs Confining Pressure

$\phi = \tan^{-1} 0.7437 = 36.4^{o}$

C = 2.73 kPa

A.21 Granular Resilient Modulus Test Result at OMC: Sta 7+725

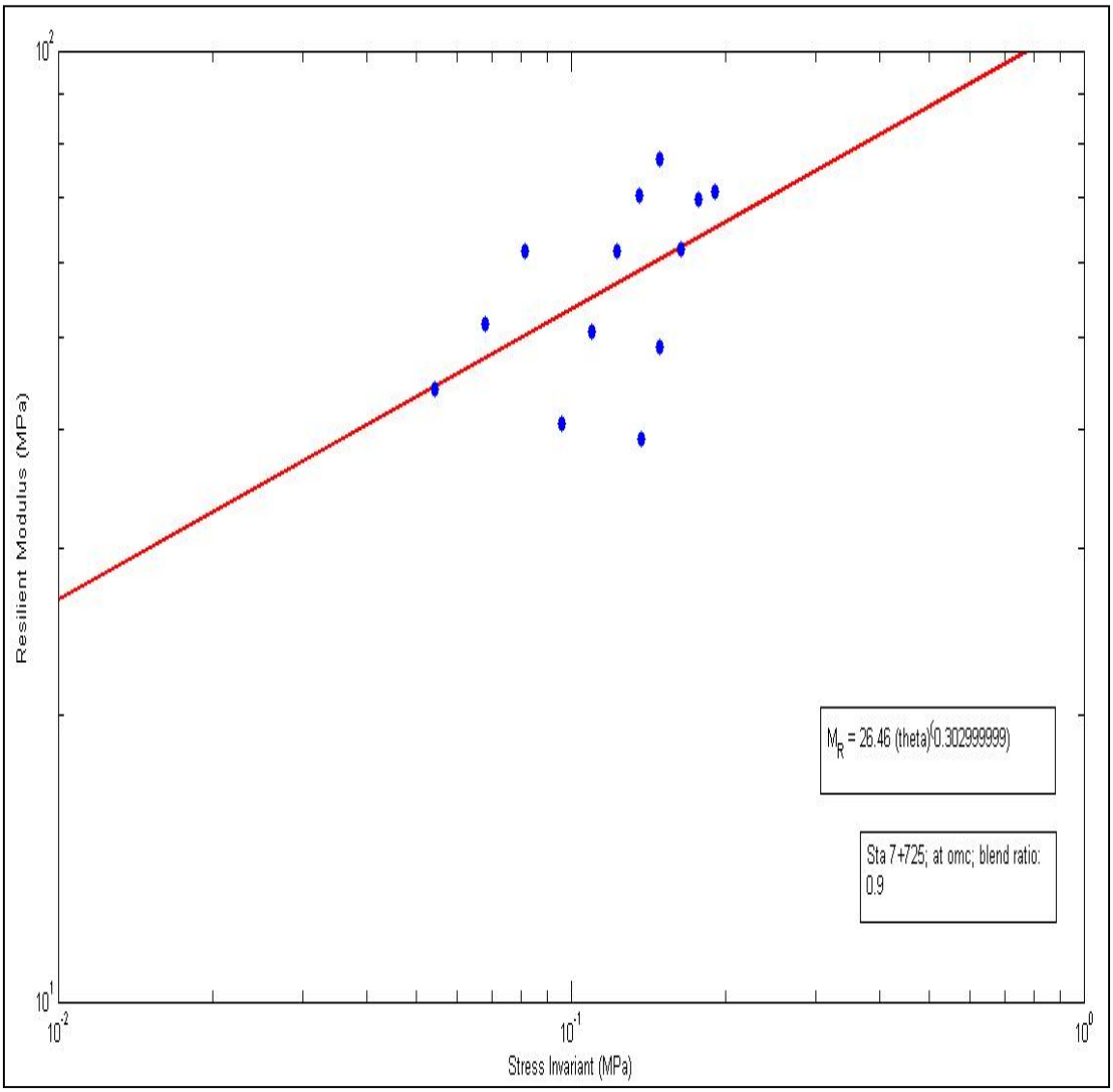

Figure A-25 – Sta 7+725 Resilient Modulus vs Stress Invariant at optimum moisture content

$M_R = 26.46\ \theta^{0.3029}$

$k_1 = 26.46$

$k_2 = 0.3029$

A.22 Granular Resilient Modulus Result at 1.5% above OMC:

Sta 7+725

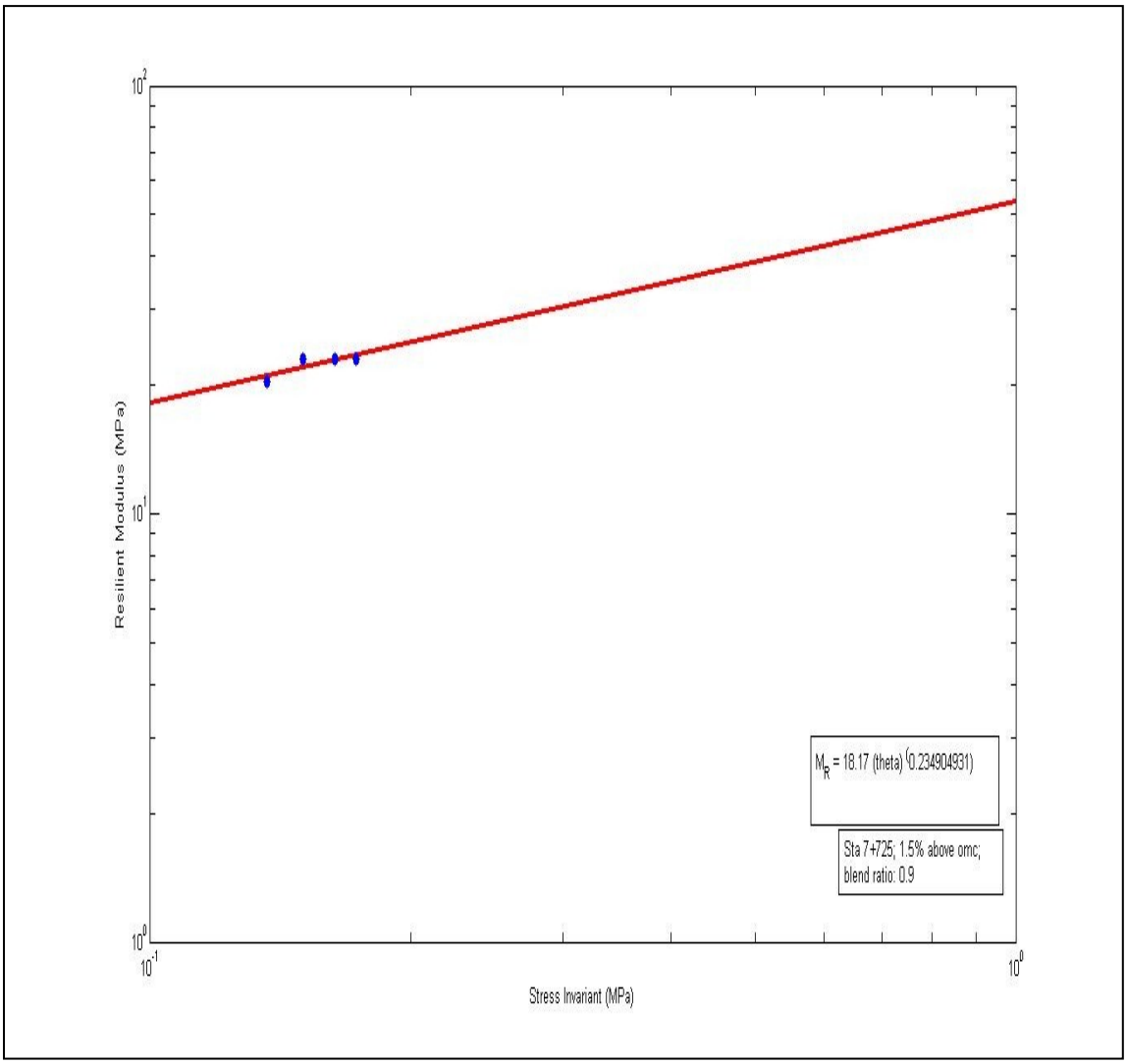

Figure A-26 – Sta 7+725 Resilient Modulus vs Stress Invariant at 1.5% above the optimum moisture content

$M_R = 18.17\ \theta^{0.2349}$

$k_1 = 18.17$

$k_2 = 0.2349$

A.23 Comparison of Granular Resilient Modulus Result at Optimum Moisture Content and 1.5% above OMC: Sta 7+725

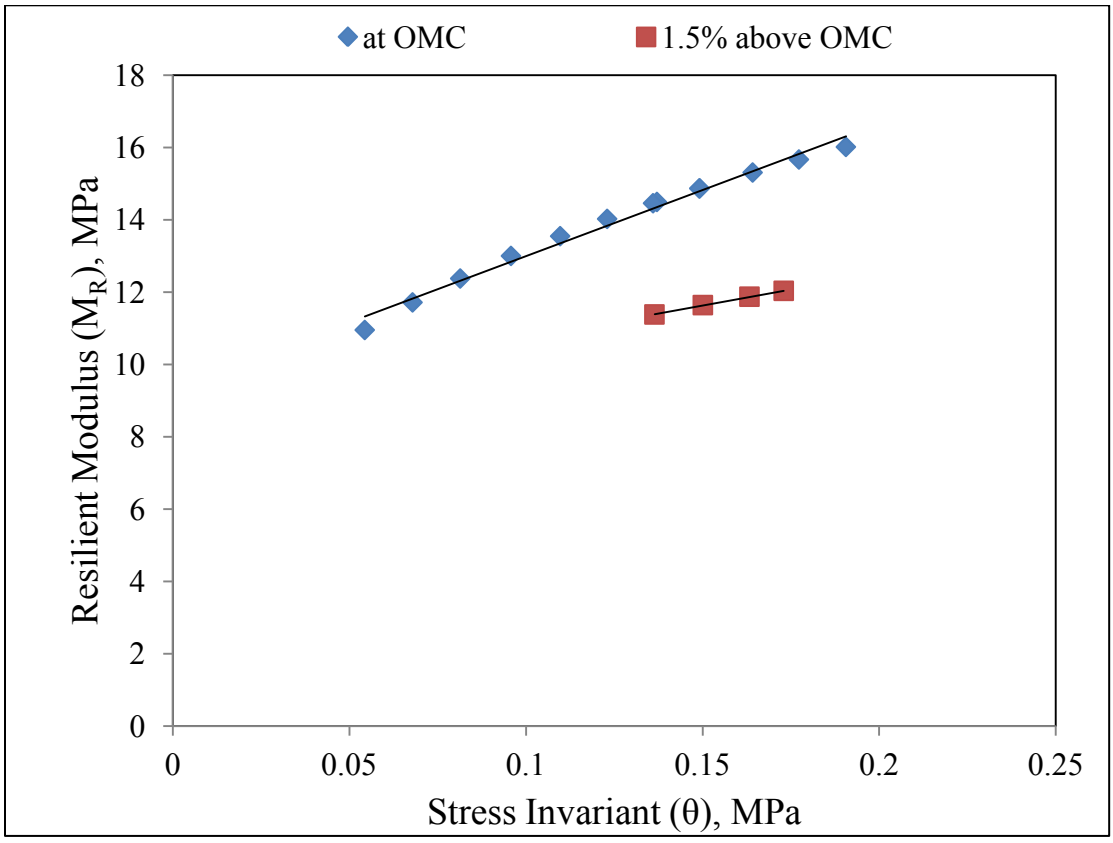

Figure A-27 – Sta 7+725 Resilient Modulus vs Stress Invariant at different moisture levels

A.24 Granular Resilient Modulus Result at 1.5% below OMC:

Sta 7+790

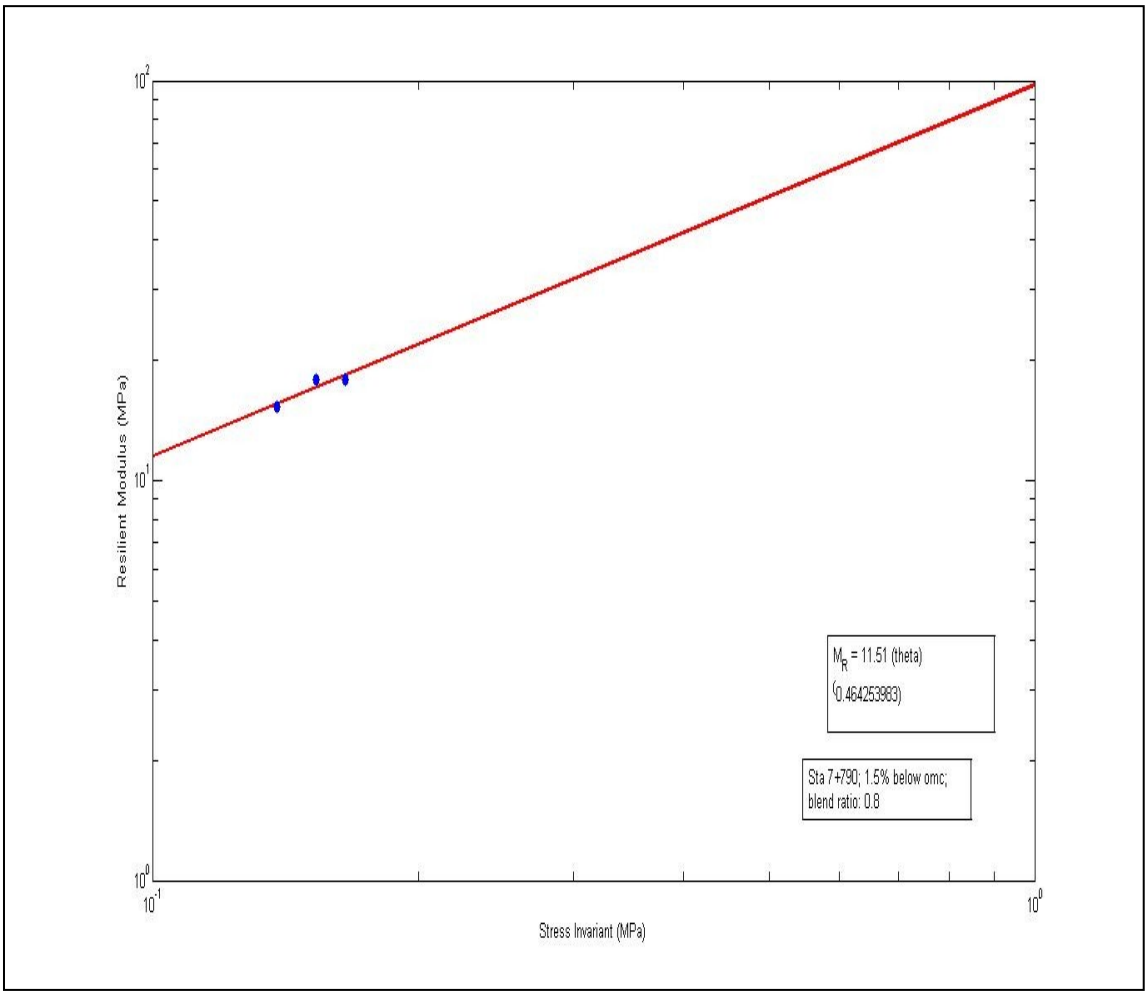

Figure A-28 – Sta 7+790 Resilient Modulus vs Stress Invariant at 1.5% below the optimum moisture content

$M_R = 11.51\ \theta^{0.4643}$

$k_1 = 11.51$

$k_2 = 0.4643$

A.25 Granular Resilient Modulus Result at OMC: Sta 7+790

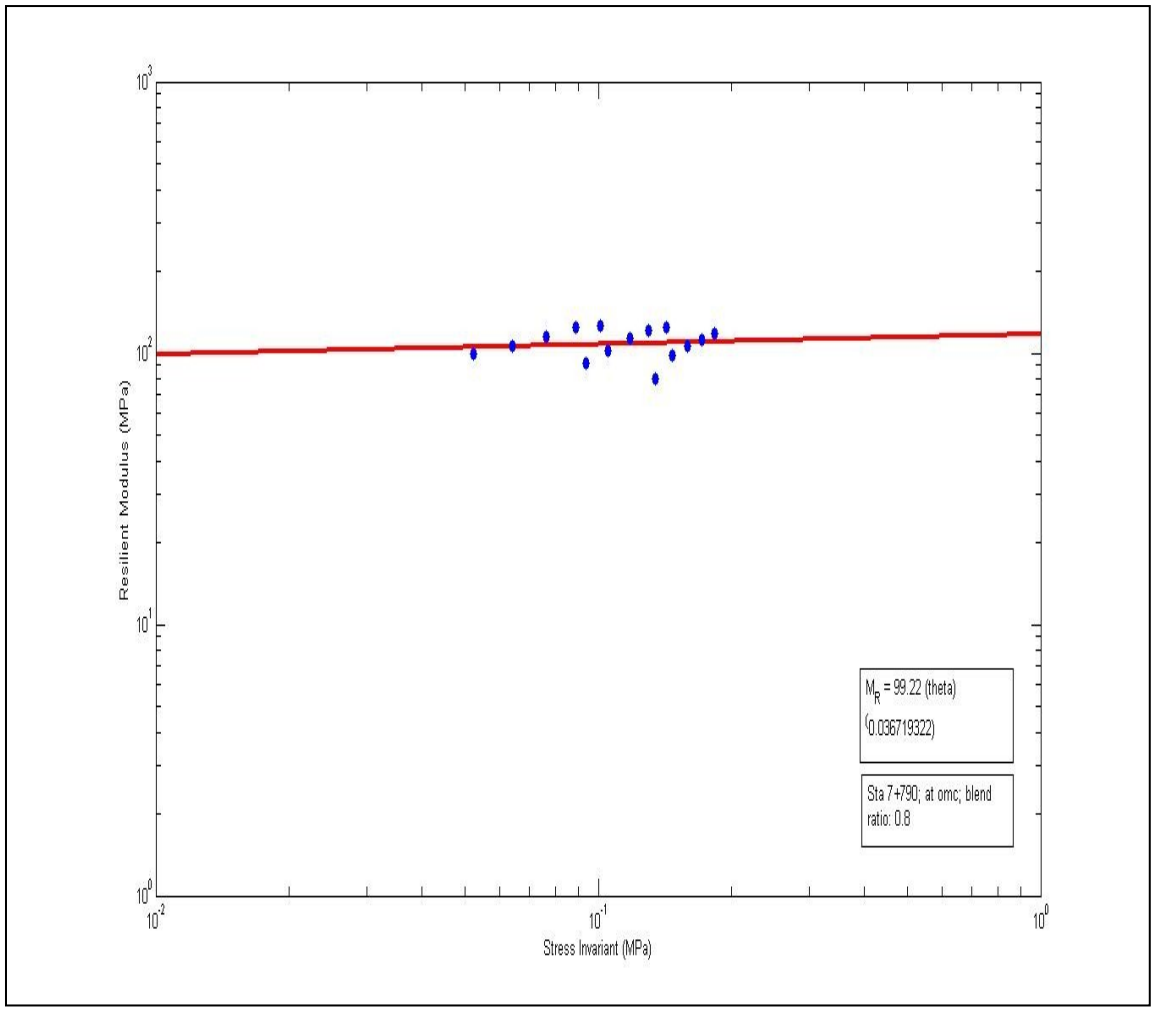

Figure A-29 – Sta 7+790 Resilient Modulus vs Stress Invariant at the optimum moisture content

$M_R = 99.92\ \theta^{0.03672}$

$k_1 = 99.92$

$k_2 = 0.03672$

A.26 Granular Resilient Modulus Result at 1.5% above OMC:

Sta 7+790

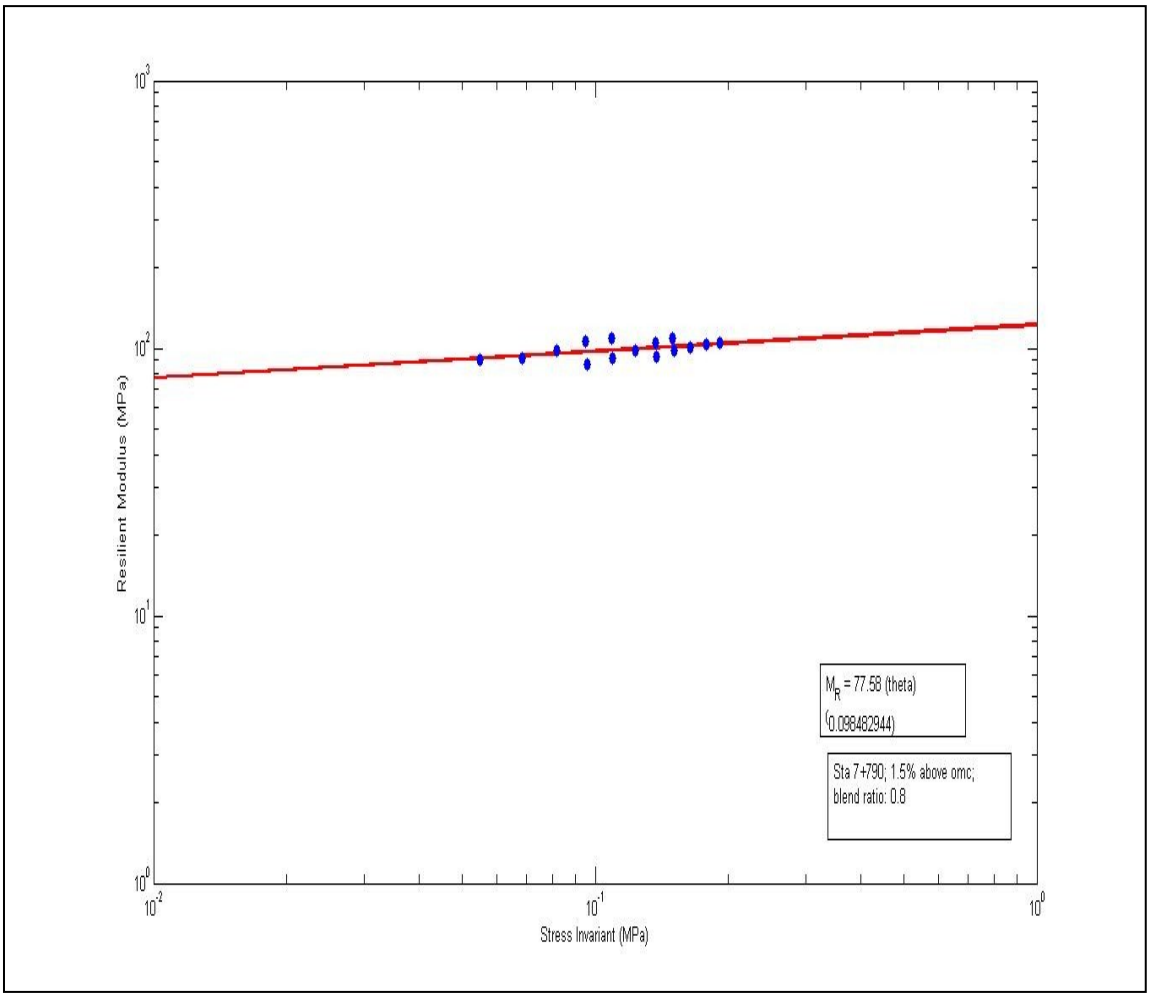

Figure A-30 – Sta 7+790 Resilient Modulus vs Stress Invariant at 1.5% above the optimum moisture content

$M_R = 77.58\ \theta^{0.0985}$

$k_1 = 77.58$

$k_2 = 0.0985$

A.27 Comparison of Granular Resilient Modulus Result at Optimum Moisture Content and 1.5% below and 1.5% above OMC: Sta 7+790

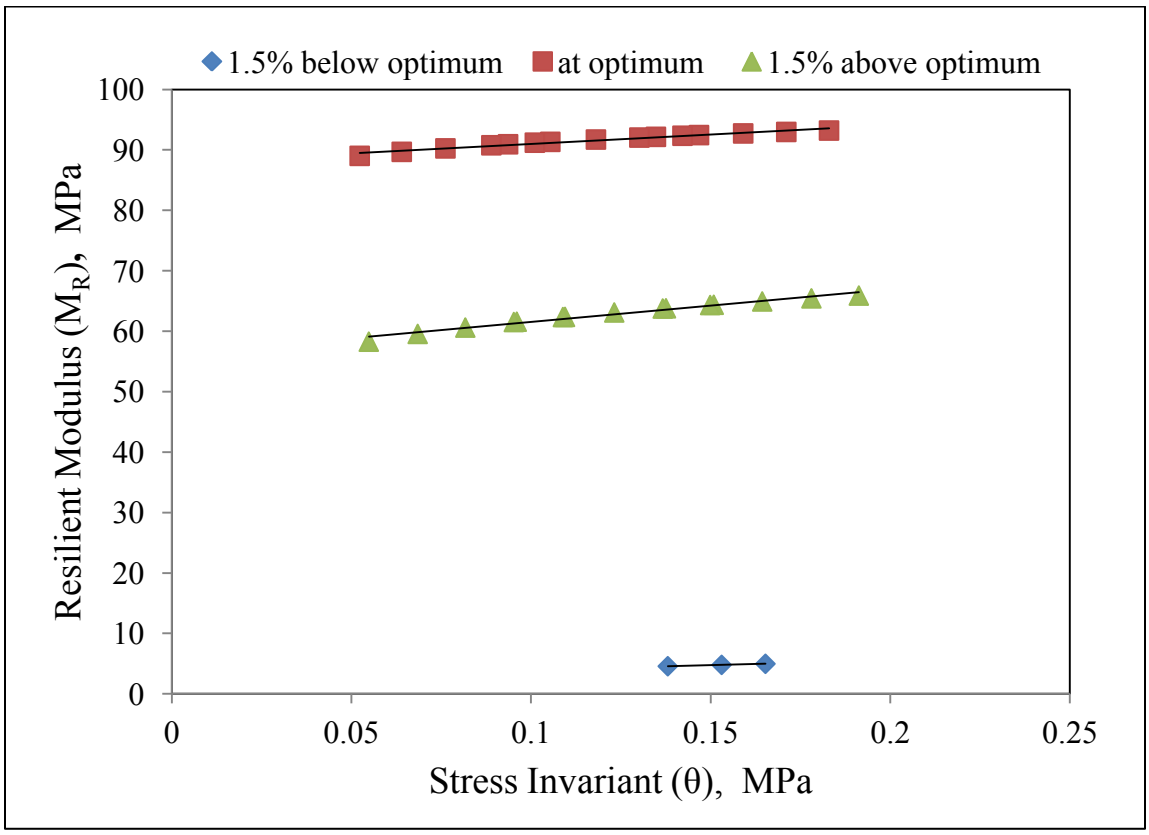

Figure A-31 – Sta 7+790 Resilient Modulus vs Stress Invariant at different moisture levels

A.28 Granular Resilient Modulus Result at 1.5% below OMC:

Sta 7+075

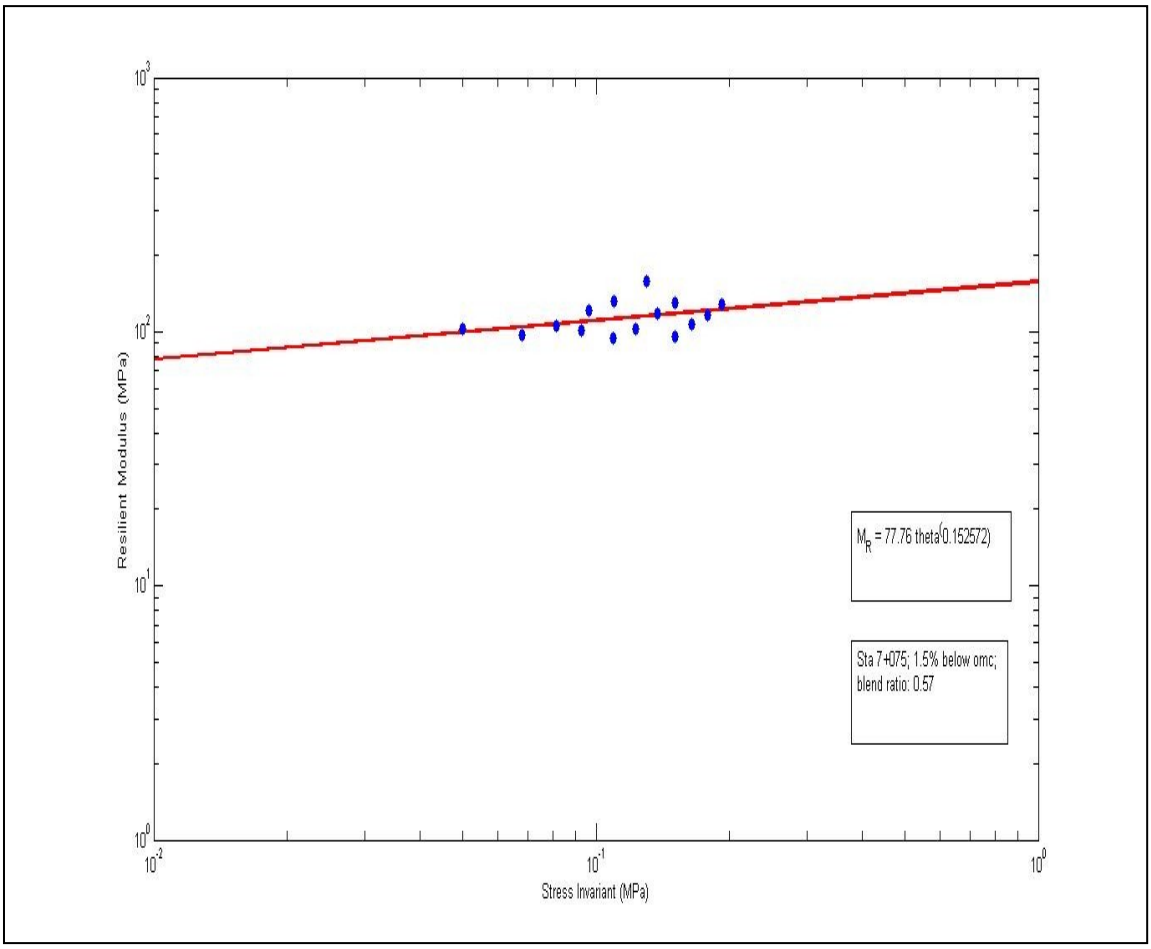

Figure A-32 – Sta 7+075 Resilient Modulus vs Stress Invariant at 1.5% below the optimum moisture content

$M_R = 77.76\ \theta^{0.1526}$

$k_1 = 77.76$

$k_2 = 0.1526$

A.29 Granular Resilient Modulus Result at OMC: Sta 7+075

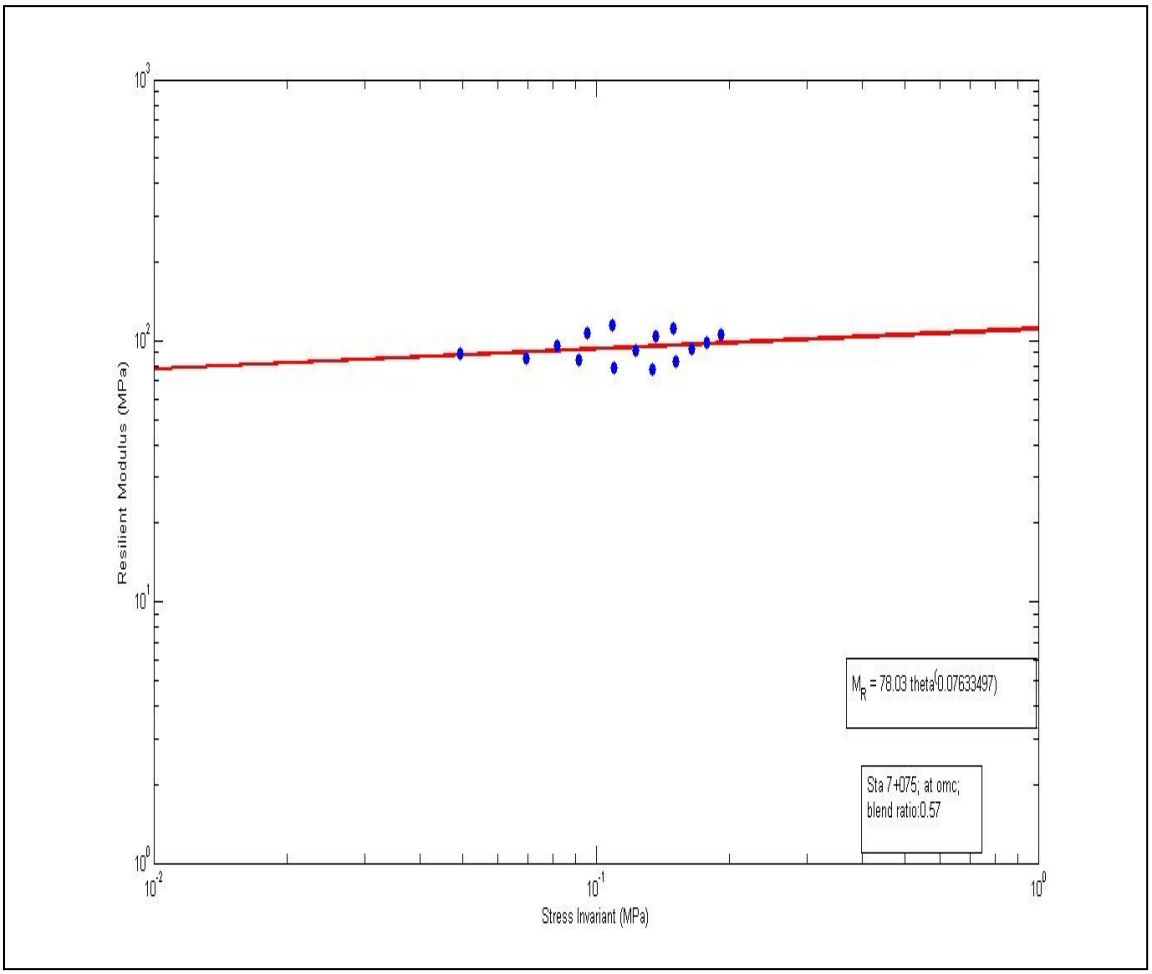

Figure A-33 – Sta 7+075 Resilient Modulus vs Stress Invariant at the optimum moisture content

$M_R = 78.03\ \theta^{0.0763}$

$k_1 = 78.03$

$k_2 = 0.0763$

A.30 Granular Resilient Modulus Result at 1.5% above OMC:

Sta 7+075

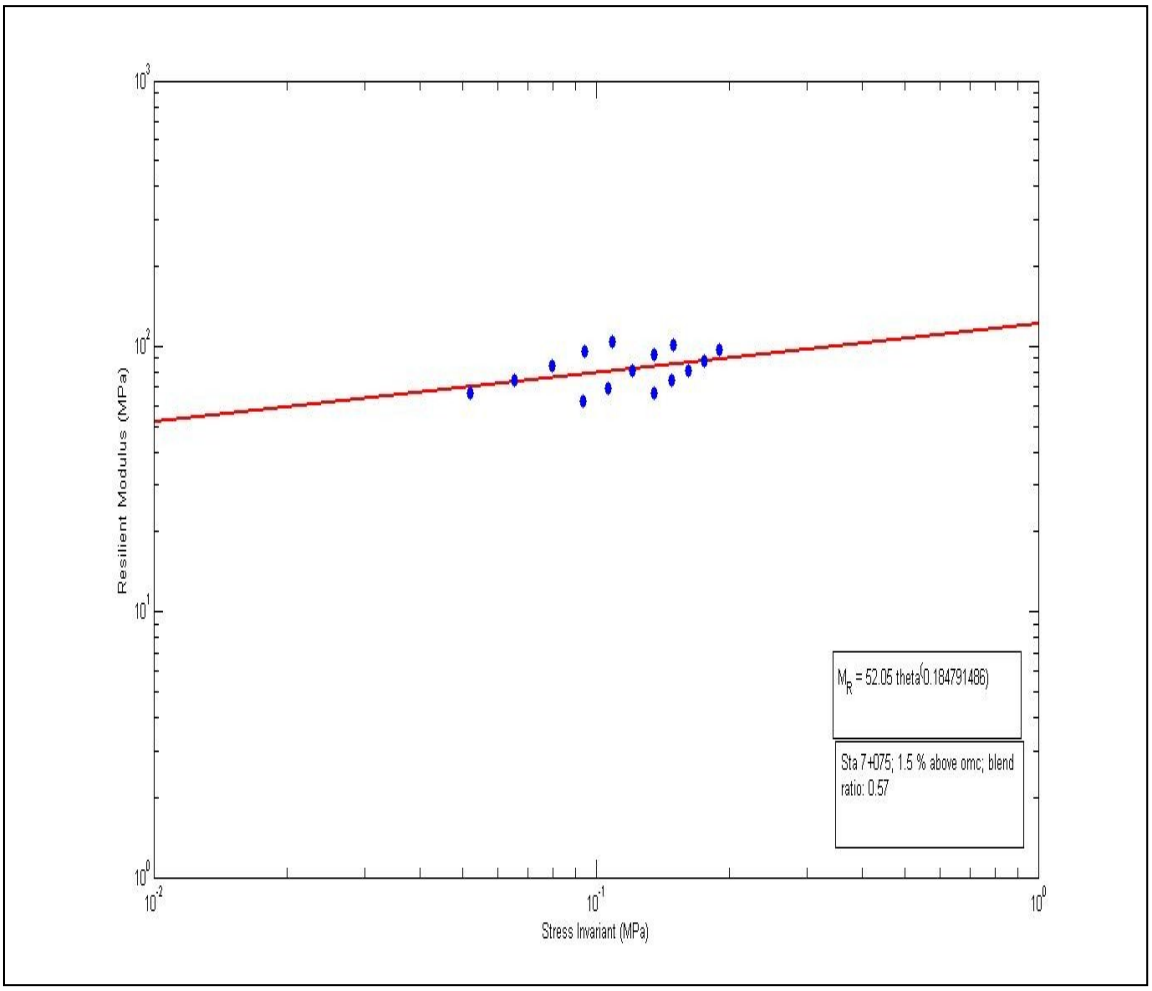

Figure A-34 – Sta 7+075 Resilient Modulus vs Stress Invariant at 1.5% above the optimum moisture content

$M_R = 52.05\ \theta^{0.1848}$

$k_1 = 52.05$

$k_2 = 0.1848$

A.31 Comparison of Granular Resilient Modulus Result at Optimum Moisture Content and 1.5% below and 1.5% above OMC: Sta 7+075

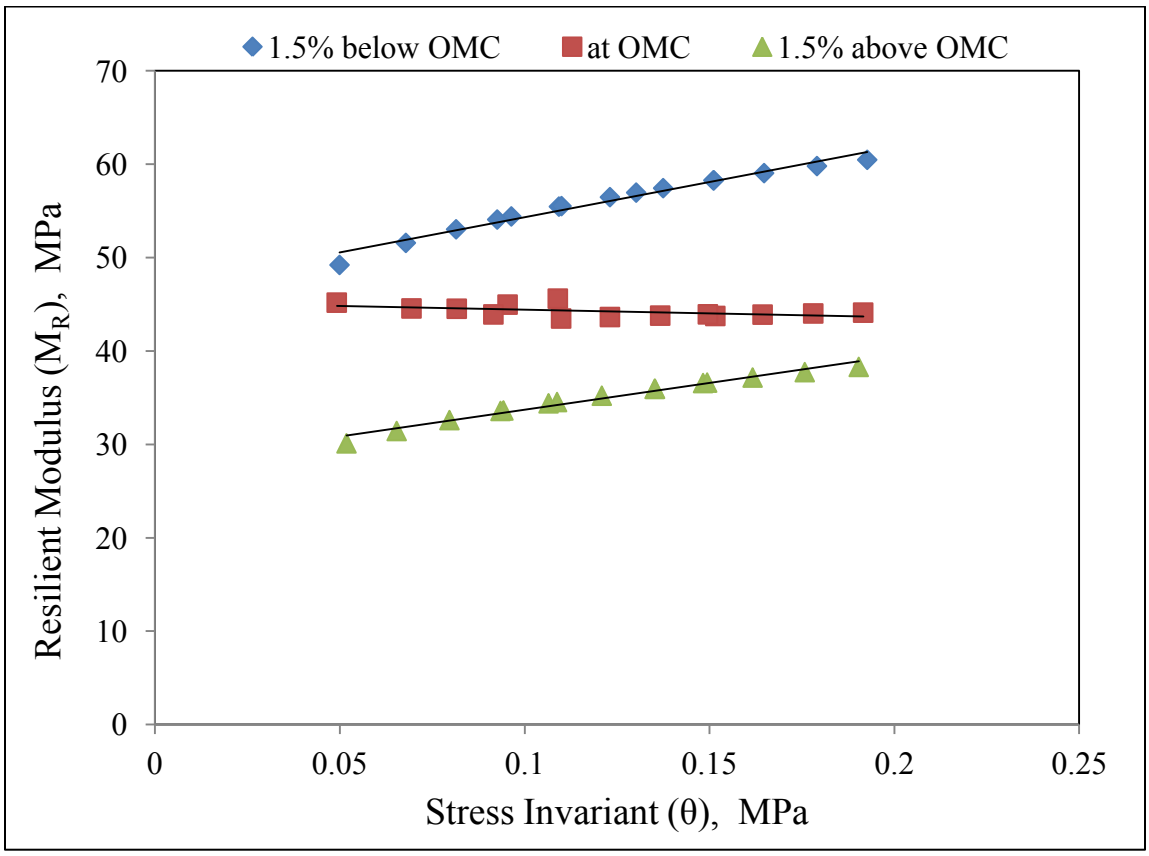

Figure A-35 – Sta 7+075 Resilient Modulus vs Stress Invariant at different moisture levels

A.32 Granular Resilient Modulus Result at 1.5% below OMC:

Sta 7+750

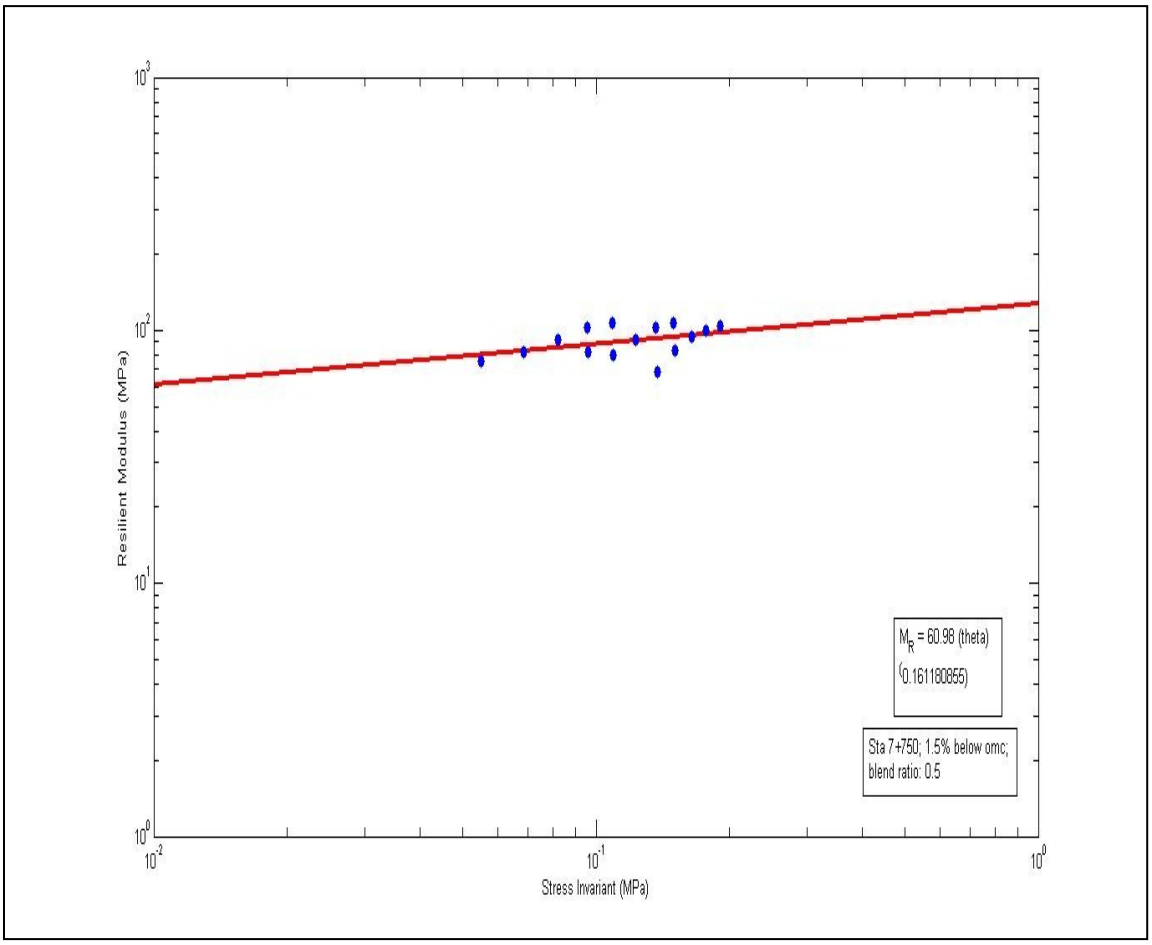

Figure A-36 – Sta 7+750 Resilient Modulus vs Stress Invariant at 1.5% below the optimum moisture content

$M_R = 60.98\ \theta^{0.1612}$

$k_1 = 60.98$

$k_2 = 0.1612$

A.33 Granular Resilient Modulus Result at OMC: Sta 7+750

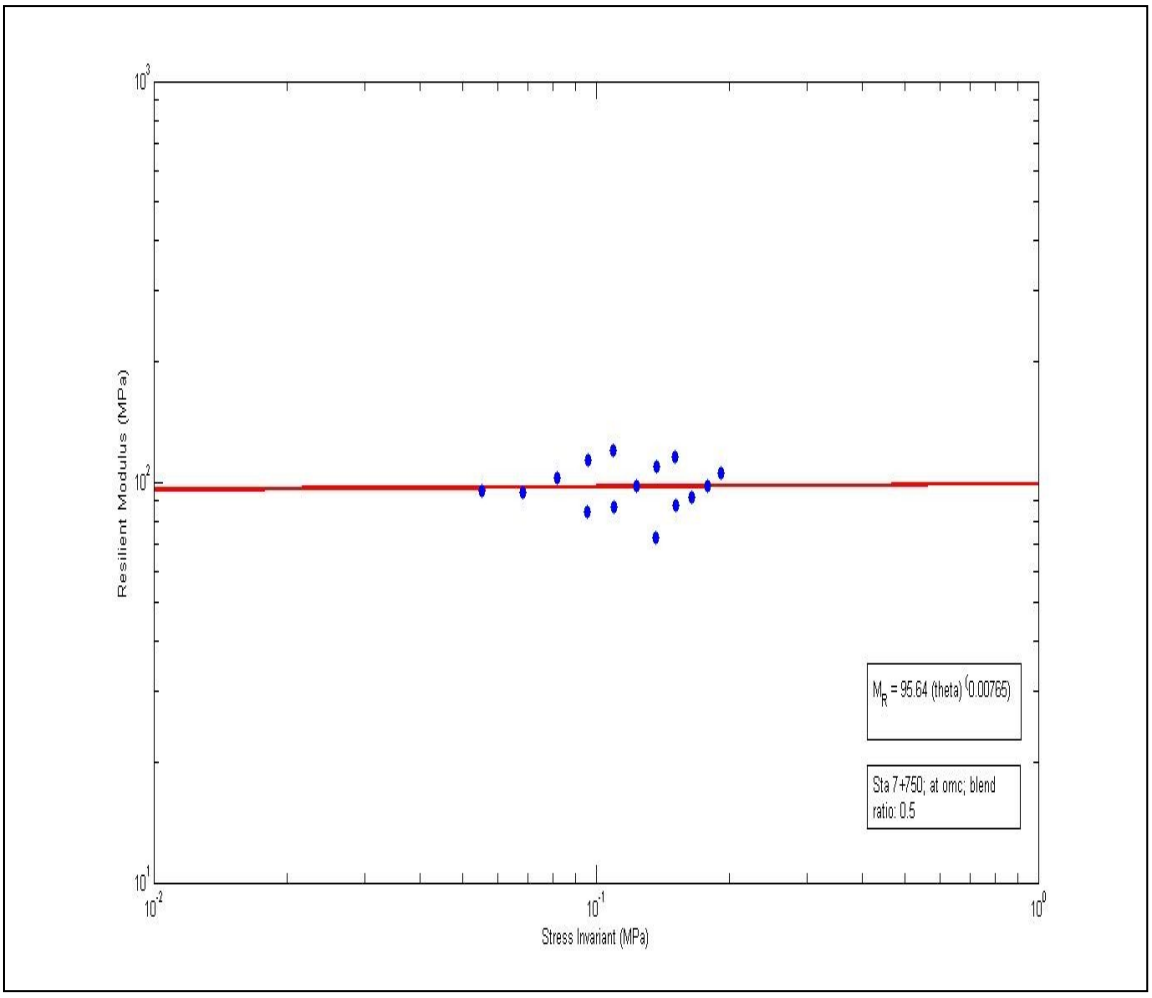

Figure A-37 – Sta 7+750 Resilient Modulus vs Stress Invariant at the optimum moisture content

$M_R = 95.64\ \theta^{0.00765}$

$k_1 = 95.64$

$k_2 = 0.00765$

A.34 Granular Resilient Modulus Result at 1.5% above OMC:

Sta 7+750

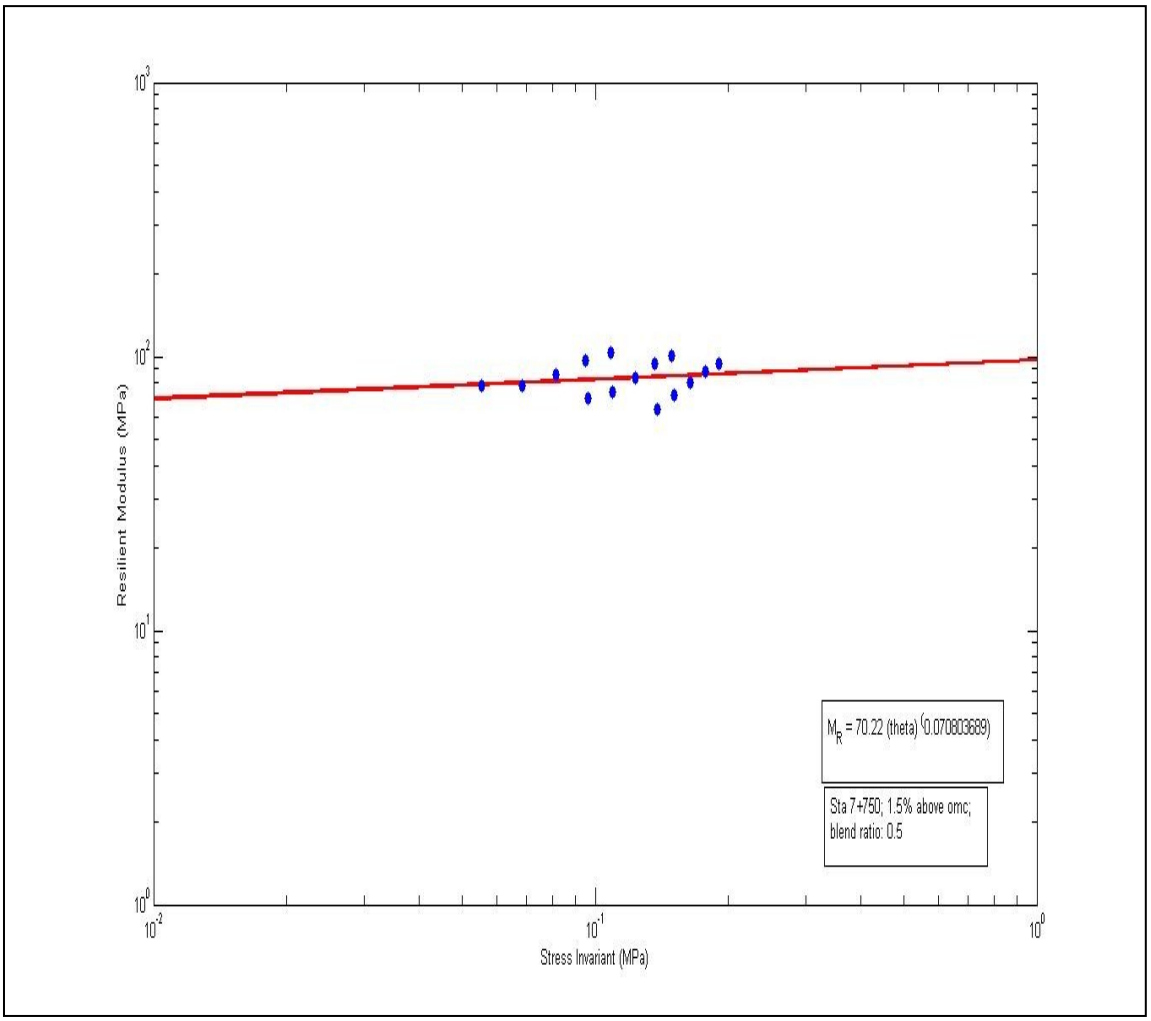

Figure A-38 – Sta 7+750 Resilient Modulus vs Stress Invariant at 1.5% above the optimum moisture content

$M_R = 70.22\ \theta^{0.0708}$

$k_1 = 70.22$

$k_2 = 0.0708$

A.35 Comparison of Granular Resilient Modulus Result at Optimum Moisture Content and 1.5% below and 1.5% above OMC: Sta 7+750

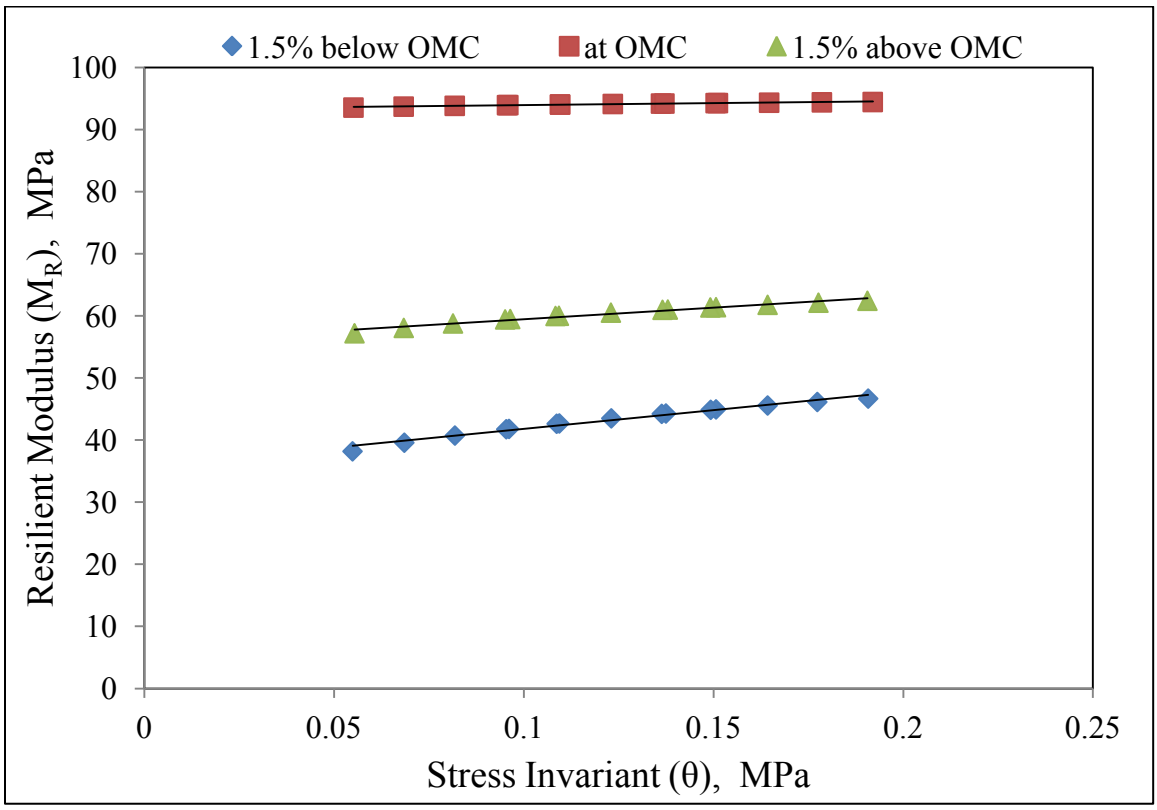

Figure A-39 – Sta 7+750 Resilient Modulus vs Stress Invariant at different moisture levels

A.36 Granular Resilient Modulus Result at 1.5% below OMC:

Sta 7+772

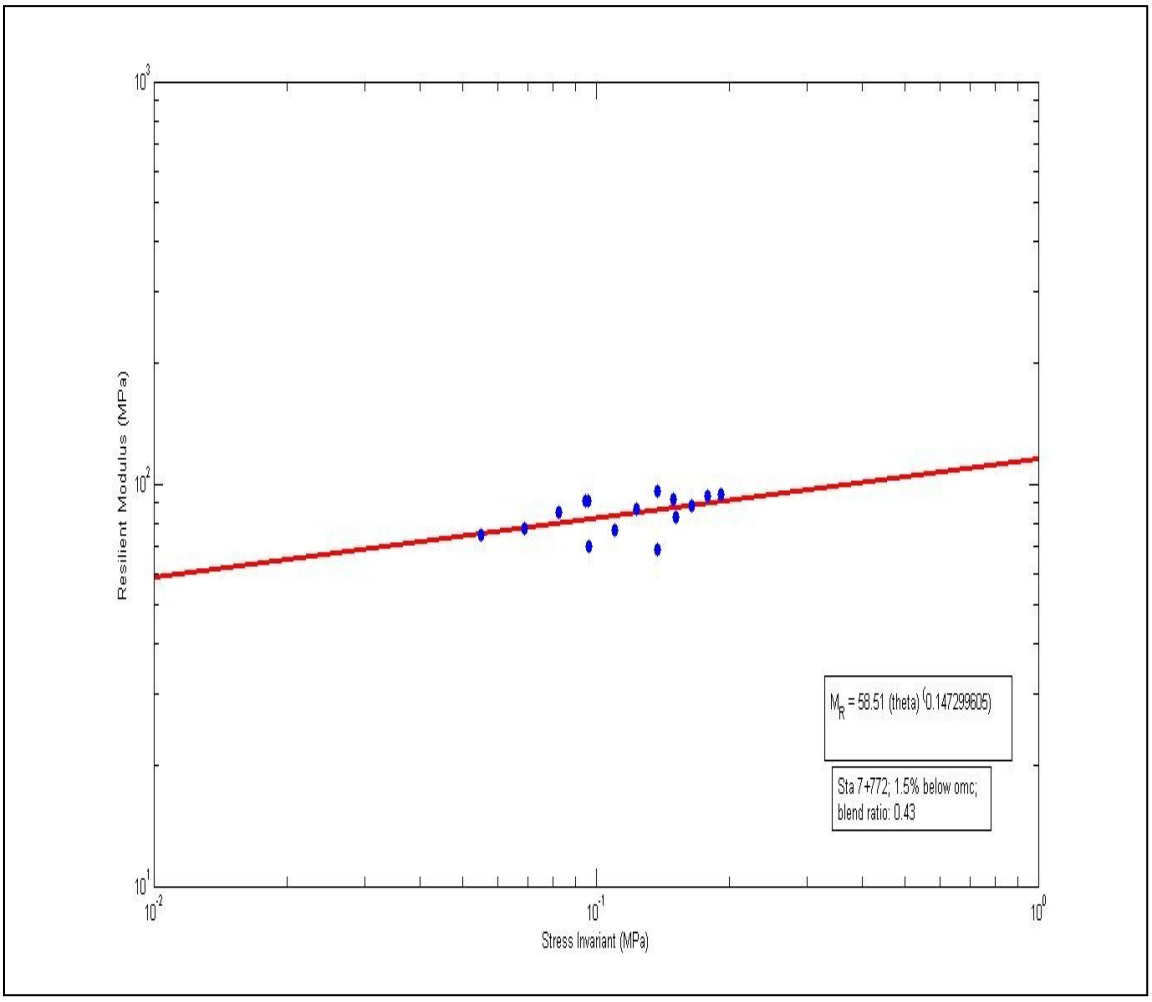

Figure A-40 – Sta 7+772 Resilient Modulus vs Stress Invariant at 1.5% below the optimum moisture content

$M_R = 58.51\ \theta^{0.1473}$

$k_1 = 58.51$

$k_2 = 0.1473$

A.37 Granular Resilient Modulus Result at OMC: Sta 7+772

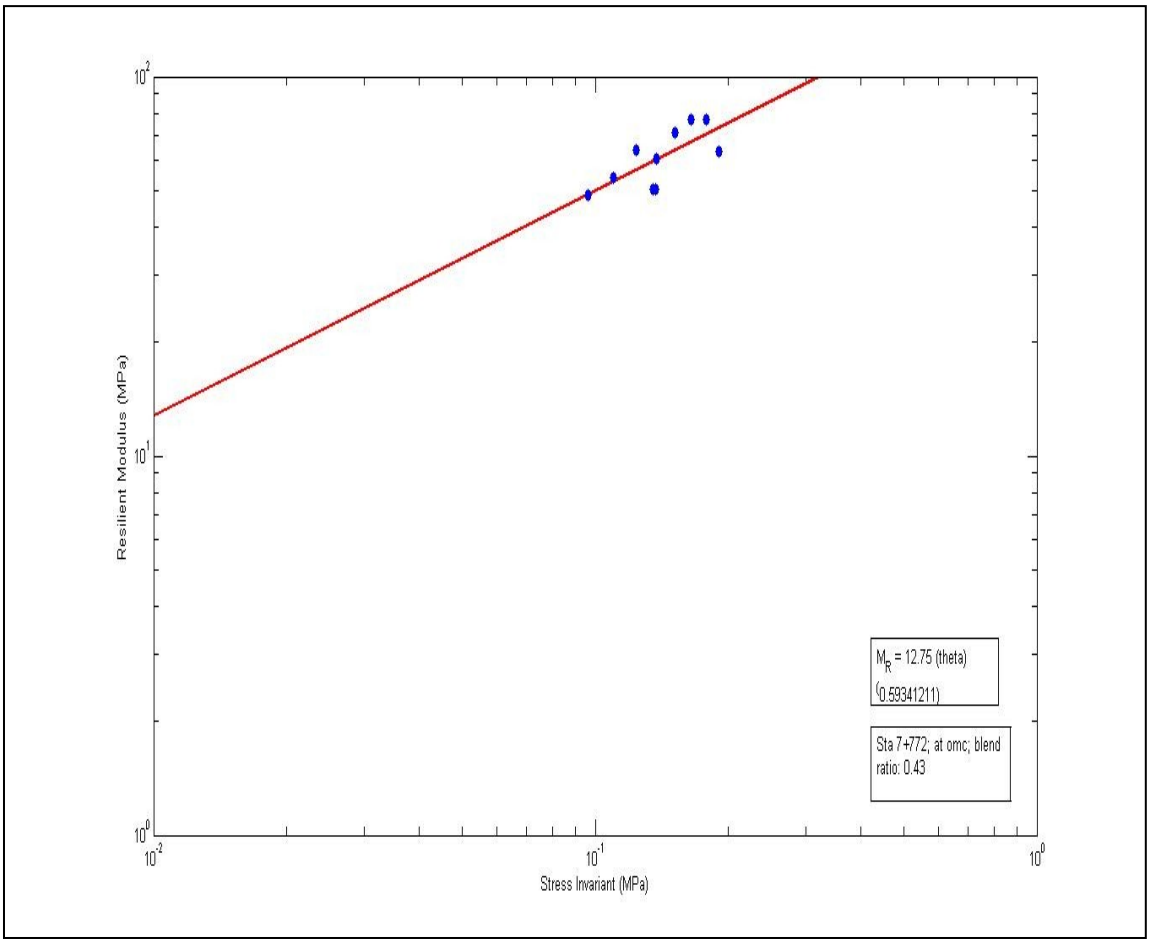

Figure A-41 – Sta 7+772 Resilient Modulus vs Stress Invariant at the optimum moisture content

$M_R = 12.75\ \theta^{0.5934}$

$k_1 = 12.75$

$k_2 = 0.5934$

A.38 Granular Resilient Modulus Result at 1.5% above OMC:

Sta 7+772

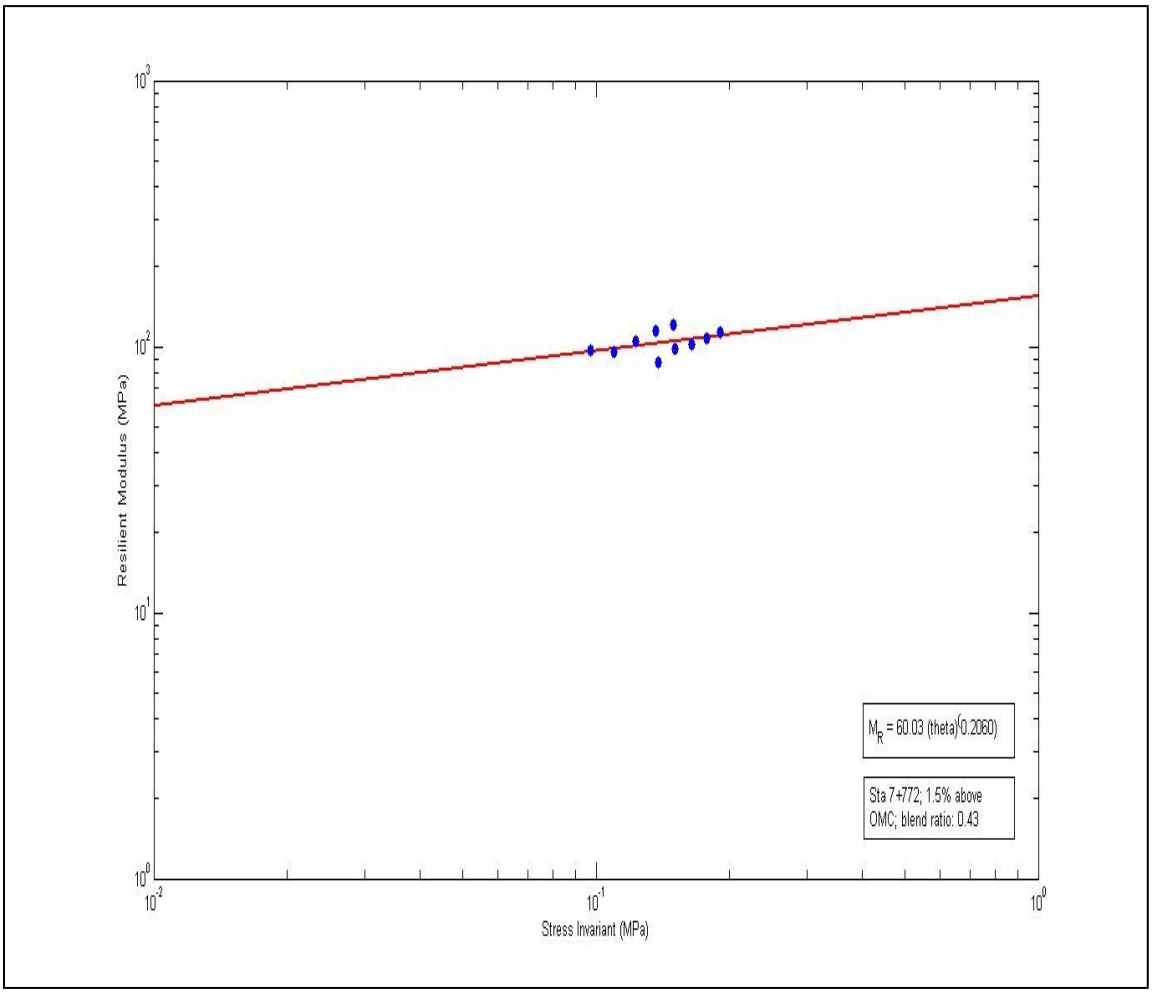

Figure A-42 – Sta 7+772 Resilient Modulus vs Stress Invariant at 1.5% above the optimum moisture content

$M_R = 60.03\ \theta^{0.2060}$

$k_1 = 60.03$

$k_2 = 0.2060$

A.39 Comparison of Granular Resilient Modulus Result at Optimum Moisture Content and 1.5% below and 1.5% above OMC: Sta 7+772

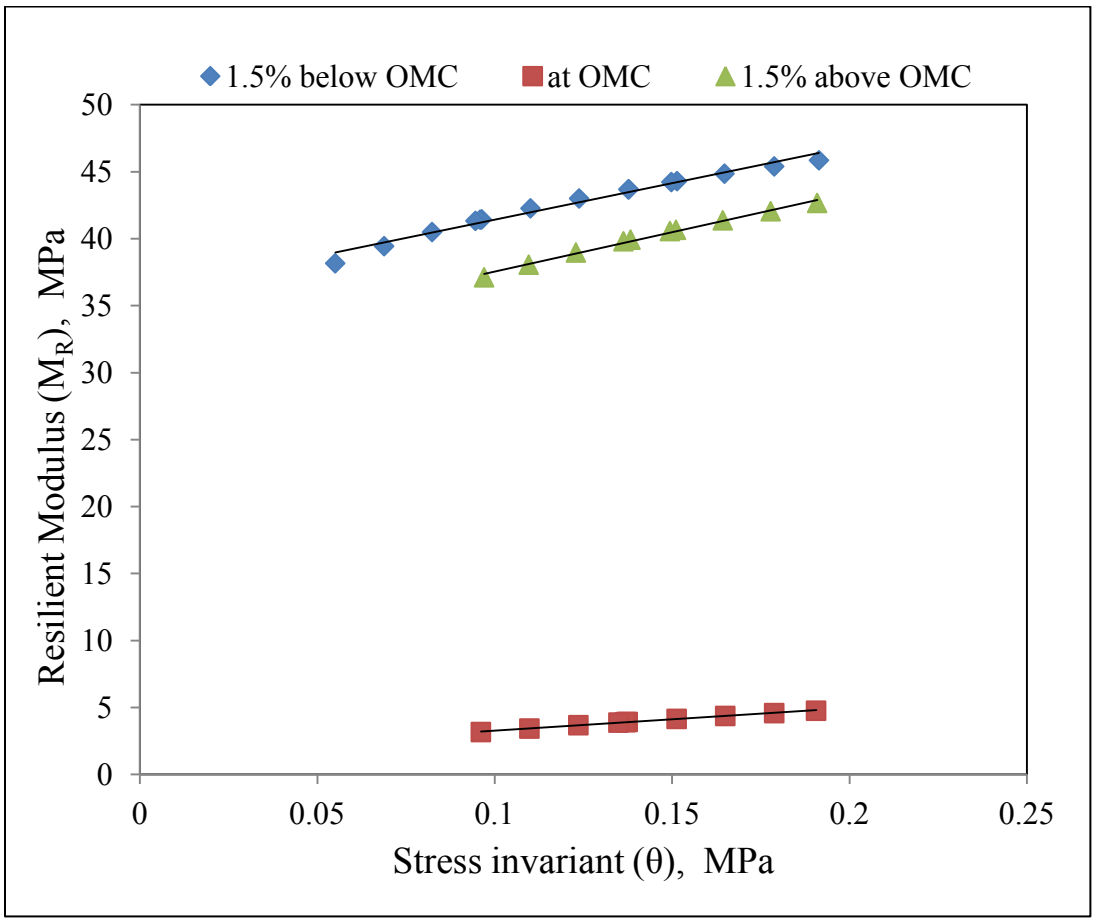

Figure A-43 – Sta 7+772 Resilient Modulus vs Stress Invariant at different moisture levels

A.40 Granular Resilient Modulus Result at 1.5% below OMC:

Sta 7+703

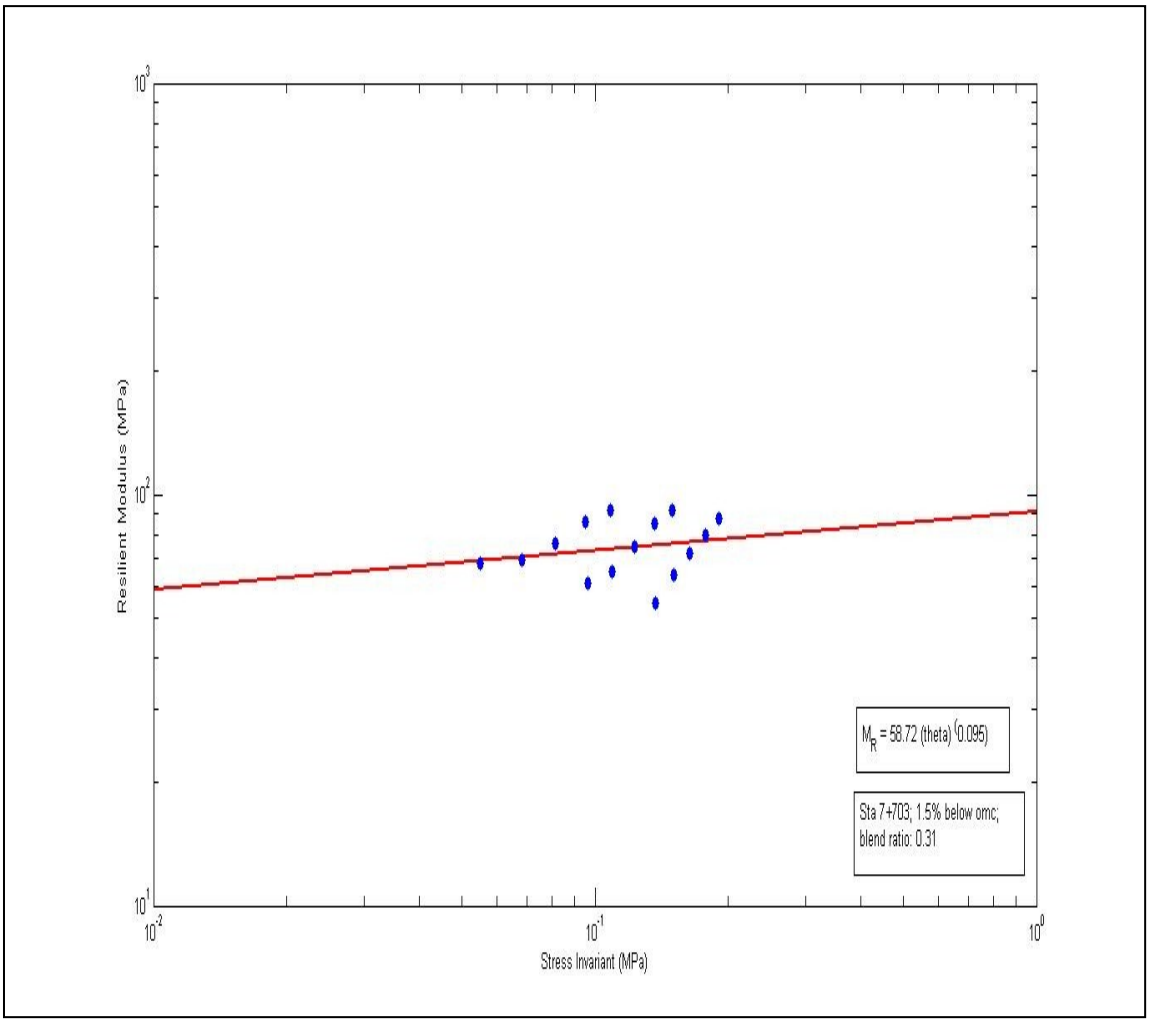

Figure A-44 – Sta 7+703 Resilient Modulus vs Stress Invariant at 1.5% below the optimum moisture content

$M_R = 58.72\ \theta^{0.095}$

$k_1 = 58.72$

$k_2 = 0.095$

A.41 Granular Resilient Modulus Result at OMC: Sta 7+703

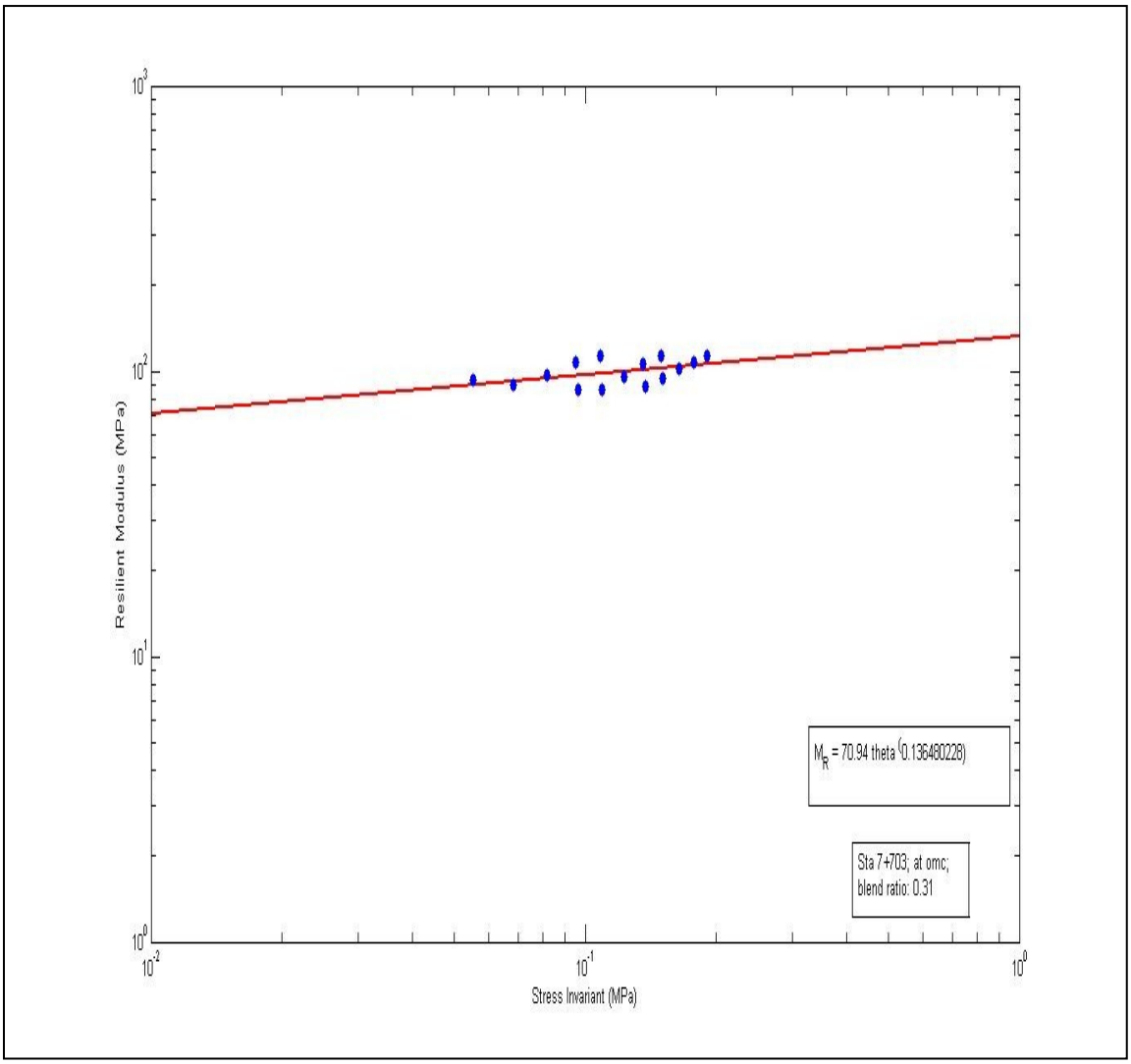

Figure A-45 – Sta 7+703 Resilient Modulus vs Stress Invariant at the optimum moisture content

$M_R = 70.94\ \theta^{0.1365}$

$k_1 = 70.94$

$k_2 = 0.1365$

A.42 Granular Resilient Modulus Result at 1.5% above OMC:

Sta 7+703

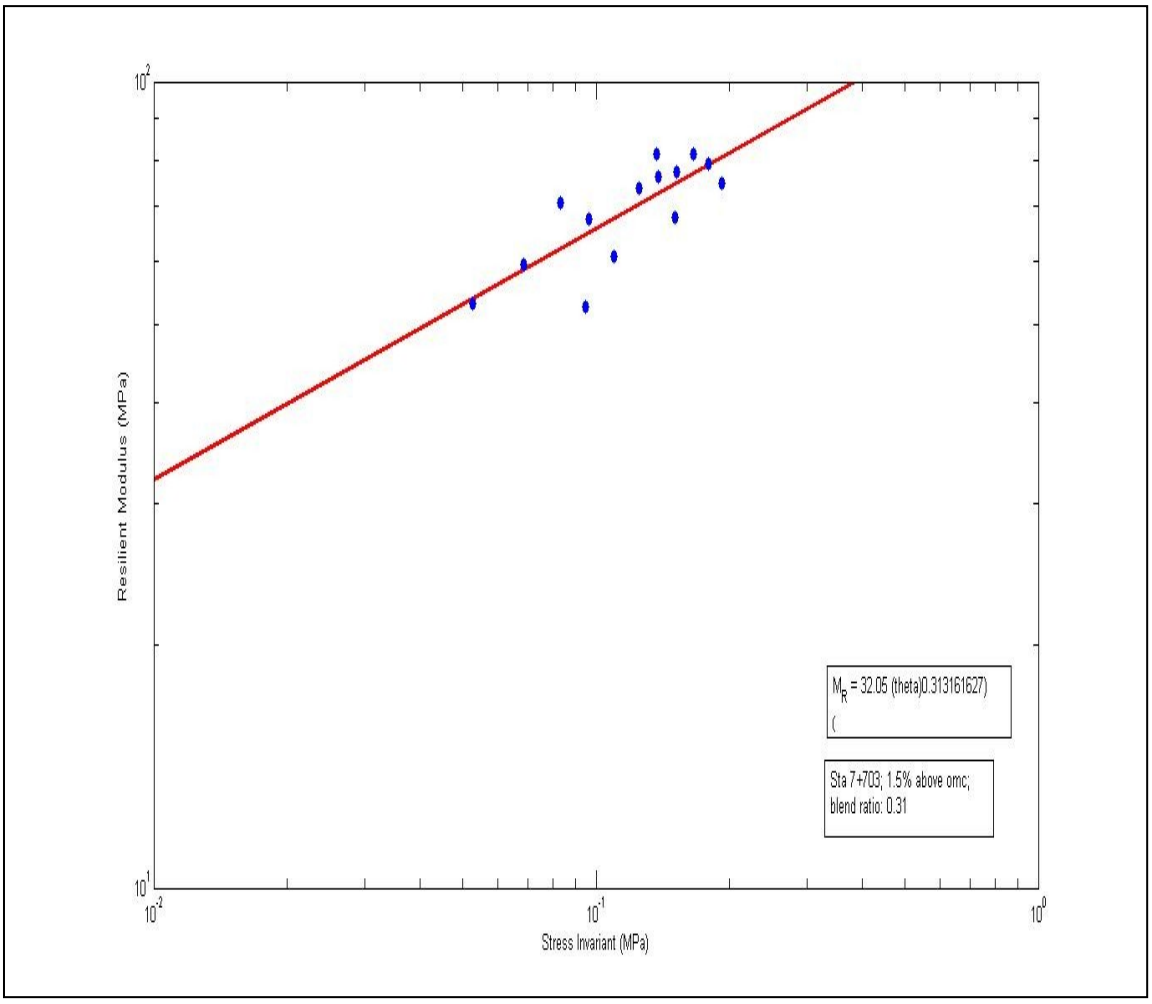

Figure A-46 – Sta 7+703 Resilient Modulus vs Stress Invariant at 1.5% above the optimum moisture content

$M_R = 32.05\ \theta^{0.3132}$

$k_1 = 32.05$

$k_2 = 0.3132$

A.43 Comparison of Granular Resilient Modulus Result at Optimum Moisture Content and 1.5% below and 1.5% above OMC: Sta 7+703

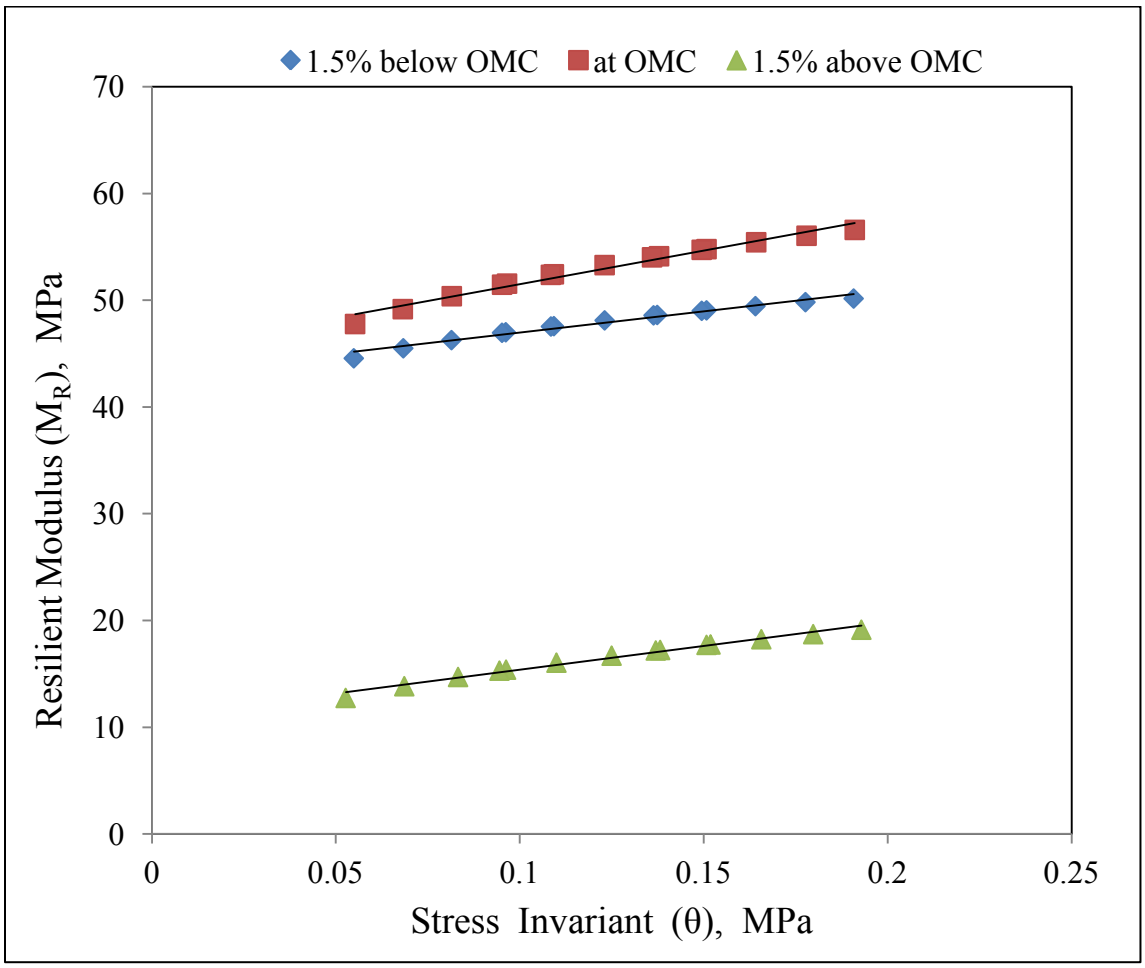

Figure A-47 – Sta 7+703 Resilient Modulus vs Stress Invariant at different moisture levels

APPENDIX B: KENPAVE Results for Distress Model

B.1 Old Pavement of Route 335 and Route 790:

INPUT FILE NAME -C:\KENPAVE\old pavement Rte 335\Old Pavement of Route 335.DAT

TITLE -Old Pavement of Route 335 and Route 790

MATL = 1 FOR LINEAR ELASTIC LAYERED SYSTEM

NDAMA = 0, SO DAMAGE ANALYSIS WILL NOT BE PERFORMED

NUMBER OF PERIODS PER YEAR (NPY) = 1

NUMBER OF LOAD GROUPS (NLG) = 1

TOLERANCE FOR INTEGRATION (DEL) -- = 0.001

NUMBER OF LAYERS (NL)---------- = 3

NUMBER OF Z COORDINATES (NZ)------ = 3

LIMIT OF INTEGRATION CYCLES (ICL)- = 80

COMPUTING CODE (NSTD)---------- = 9

SYSTEM OF UNITS (NUNIT)----------= 1

Length and displacement in cm, stress and modulus in kPa

unit weight in kN/m^3, and temperature in C

THICKNESSES OF LAYERS (TH) ARE : 10 45

POISSON'S RATIOS OF LAYERS (PR) ARE : 0.4 0.35 0.35

VERTICAL COORDINATES OF POINTS (ZC) ARE: 0 10 55

ALL INTERFACES ARE FULLY BONDED

FOR PERIOD NO. 1 LAYER NO. AND MODULUS ARE : 1 1.800E+05 2 1.000E+05 3 7.000E+04

LOAD GROUP NO. 1 HAS 2 CONTACT AREAS

CONTACT RADIUS (CR)---------- = 10.7442

CONTACT PRESSURE (CP)---------- = 552

NO. OF POINTS AT WHICH RESULTS ARE DESIRED (NPT)-- = 3

WHEEL SPACING ALONG X-AXIS (XW)---------- = 0

WHEEL SPACING ALONG Y-AXIS (YW)---------- = 34.29

RESPONSE PT. NO. AND (XPT, YPT) ARE: 1 0.000 0.000 2 0.000 0.000

3 0.000 0.000

PERIOD NO. 1 LOAD GROUP NO. 1

POINT NO.	VERTICAL COORDINATE	VERTICAL DISPLACEMENT (cm)	VERTICAL STRESS (STRAIN)	MAJOR PRINCIPAL STRESS (STRAIN)	MINOR PRINCIPAL STRESS (STRAIN)	INTERMEDIATE PRINCIPAL STRESS (HORIZONTAL PRINCIPAL STRAIN)
1	0.00000	0.11681	552.000	864.695	807.399	855.995
	(STRAIN)		6.620E-04	1.107E-03	6.618E-04	1.039E-03
1	10.00000	0.09024	335.421	335.668	-67.965	-44.336
	(STRAIN)		2.112E-03	4.581E-04	-1.025E-03	-1.025E-03
1	55.00000	0.04034	37.640	38.764	-12.134	-7.943
	(STRAIN)		4.485E-04	4.579E-04	-2.292E-04	-2.292E-04
2	0.00000	0.11681	552.000	864.695	807.399	855.995
	(STRAIN)		6.620E-04	1.107E-03	6.618E-04	1.039E-03
2	10.00000	0.09024	335.421	335.668	-67.965	-44.336
	(STRAIN)		2.112E-03	2.114E-03	-1.025E-03	-1.025E-03
2	55.00000	0.04034	37.640	38.764	-12.134	-7.943
	(STRAIN)		4.427E-04	4.579E-04	-2.292E-04	-2.292E-04
3	0.00000	0.11681	552.000	864.695	807.399	855.995
	(STRAIN)		6.620E-04	1.107E-03	6.618E-04	1.039E-03
3	10.00000	0.09024	335.421	335.668	-67.965	-44.336
	(STRAIN)		2.112E-03	2.114E-03	-1.025E-03	-1.025E-03
3	55.00000	0.04034	37.640	38.764	-12.134	-7.943
	(STRAIN)		4.427E-04	4.579E-04	-2.292E-04	-2.292E-04

B.2 New FDR Pavement of Route 335: Blend Ratio 0.90, FDR Stiffness 14 MPa

INPUT FILE NAME -C:\KENPAVE\KENPAVE For correction_Rte335\FDR Pavement of Route 335_Blend Ratio 0.90.DAT

NUMBER OF PROBLEMS TO BE SOLVED = 1

TITLE -FDR Pavement of Route 335_BR-0.9

MATL = 1 FOR LINEAR ELASTIC LAYERED SYSTEM

NDAMA = 0, SO DAMAGE ANALYSIS WILL NOT BE PERFORMED

NUMBER OF PERIODS PER YEAR (NPY) = 1

NUMBER OF LOAD GROUPS (NLG) = 1

TOLERANCE FOR INTEGRATION (DEL) -- = 0.001

NUMBER OF LAYERS (NL)---------- = 4

NUMBER OF Z COORDINATES (NZ)------ = 4

LIMIT OF INTEGRATION CYCLES (ICL)- = 80

COMPUTING CODE (NSTD)---------- = 9

SYSTEM OF UNITS (NUNIT)----------= 1

Length and displacement in cm, stress and modulus in kPa

unit weight in kN/m^3, and temperature in C

THICKNESSES OF LAYERS (TH) ARE : 9 20 35

POISSON'S RATIOS OF LAYERS (PR) ARE : 0.4 0.3 0.35 0.35

VERTICAL COORDINATES OF POINTS (ZC) ARE: 0 9 29 64

ALL INTERFACES ARE FULLY BONDED

FOR PERIOD NO. 1 LAYER NO. AND MODULUS ARE : 1 3.000E+06 2 1.394E+04

3 1.000E+05 4 7.000E+04

LOAD GROUP NO. 1 HAS 2 CONTACT AREAS

CONTACT RADIUS (CR)---------- = 10.7442

CONTACT PRESSURE (CP)---------- = 552

NO. OF POINTS AT WHICH RESULTS ARE DESIRED (NPT)-- = 3

WHEEL SPACING ALONG X-AXIS (XW)---------- = 0

WHEEL SPACING ALONG Y-AXIS (YW)---------- = 34.29

RESPONSE PT. NO. AND (XPT, YPT) ARE: 1 0.000 0.000 2 0.000 0.000

3 0.000 0.000

PERIOD NO. 1 LOAD GROUP NO. 1

POINT NO.	VERTICAL COORDINATE	VERTICAL DISPLACEMENT (cm)	VERTICAL STRESS (STRAIN)	MAJOR PRINCIPAL STRESS (STRAIN)	MINOR PRINCIPAL STRESS (STRAIN)	INTERMEDIATE PRINCIPAL STRESS (HORIZONTAL PRINCIPAL STRAIN)
1	0.00000	0.11523	552.000	2303.840	292.836	2118.749
	(STRAIN)		-4.921E-04	4.464E-04	-4.921E-04	3.600E-04
1	9.00000	0.11493	67.820	67.824	-2690.978	-2239.547
	(STRAIN)		6.800E-04	6.481E-04	-6.074E-04	-6.074E-04
1	29.00000	0.04633	49.969	51.062	19.585	20.402
	(STRAIN)		2.700E-03	2.802E-03	-1.330E-04	-5.682E-05
1	64.00000	0.03509	25.980	26.455	-3.635	-2.454
	(STRAIN)		3.678E-04	2.859E-04	-1.203E-04	-1.203E-04
2	0.00000	0.11523	552.000	2303.840	292.836	2118.749
	(STRAIN)		-4.921E-04	4.464E-04	-4.921E-04	3.600E-04
2	9.00000	0.11493	67.820	67.824	-2690.978	-2239.547
	(STRAIN)		6.800E-04	6.800E-04	-6.074E-04	-6.074E-04
2	29.00000	0.04633	49.969	51.062	19.585	20.402
	(STRAIN)		2.700E-03	2.802E-03	-1.330E-04	-5.682E-05
2	64.00000	0.03509	25.980	26.455	-3.635	-2.454
	(STRAIN)		2.795E-04	2.859E-04	-1.203E-04	-1.203E-04
3	0.00000	0.11523	552.000	2303.840	292.836	2118.749
	(STRAIN)		-4.921E-04	4.464E-04	-4.921E-04	3.600E-04
3	9.00000	0.11493	67.820	67.824	-2690.978	-2239.547
	(STRAIN)		6.800E-04	6.800E-04	-6.074E-04	-6.074E-04
3	29.00000	0.04633	49.969	51.062	19.585	20.402
	(STRAIN)		2.700E-03	2.802E-03	-1.330E-04	-5.682E-05
3	64.00000	0.03509	25.980	26.455	-3.635	-2.454
	(STRAIN)		2.795E-04	2.859E-04	-1.203E-04	-1.203E-04

B.3 New FDR Pavement of Route 335: Blend Ratio 0.80, FDR Stiffness 92 MPa

INPUT FILE NAME -C:\KENPAVE\KENPAVE For correction_Rte335\FDR Pavement of Route 335_Blend Ratio 0.80.DAT

NUMBER OF PROBLEMS TO BE SOLVED = 1

TITLE -FDR Pavement of Route 335_BR-0.8

MATL = 1 FOR LINEAR ELASTIC LAYERED SYSTEM

NDAMA = 0, SO DAMAGE ANALYSIS WILL NOT BE PERFORMED

NUMBER OF PERIODS PER YEAR (NPY) = 1

NUMBER OF LOAD GROUPS (NLG) = 1

TOLERANCE FOR INTEGRATION (DEL) -- = 0.001

NUMBER OF LAYERS (NL)---------- = 4

NUMBER OF Z COORDINATES (NZ)------ = 4

LIMIT OF INTEGRATION CYCLES (ICL)- = 80

COMPUTING CODE (NSTD)---------- = 9

SYSTEM OF UNITS (NUNIT)----------= 1

Length and displacement in cm, stress and modulus in kPa

unit weight in kN/m^3, and temperature in C

THICKNESSES OF LAYERS (TH) ARE : 9 20 35

POISSON'S RATIOS OF LAYERS (PR) ARE : 0.4 0.3 0.35 0.35

VERTICAL COORDINATES OF POINTS (ZC) ARE: 0 9 29 64

ALL INTERFACES ARE FULLY BONDED

FOR PERIOD NO. 1 LAYER NO. AND MODULUS ARE : 1 3.000E+06 2 9.154E+04 3 1.000E+05 4 7.000E+04

LOAD GROUP NO. 1 HAS 2 CONTACT AREAS

CONTACT RADIUS (CR)---------- = 10.7442

CONTACT PRESSURE (CP)---------- = 552

NO. OF POINTS AT WHICH RESULTS ARE DESIRED (NPT)-- = 3

WHEEL SPACING ALONG X-AXIS (XW)---------- = 0

WHEEL SPACING ALONG Y-AXIS (YW)---------- = 34.29

RESPONSE PT. NO. AND (XPT, YPT) ARE: 1 0.000 0.000 2 0.000 0.000

3 0.000 0.000

PERIOD NO. 1 LOAD GROUP NO. 1

POINT NO.	VERTICAL COORDINATE	VERTICAL DISPLACEMENT (cm)	VERTICAL STRESS (STRAIN)	MAJOR PRINCIPAL STRESS (STRAIN)	MINOR PRINCIPAL STRESS (STRAIN)	INTERMEDIATE PRINCIPAL STRESS (HORIZONTAL PRINCIPAL STRAIN)
1	0.00000	0.06531	552.000	1789.400	441.245	1694.962
	(STRAIN)		-3.175E-04	3.116E-04	-3.175E-04	2.676E-04
1	9.00000	0.06394	133.322	133.434	-1622.164	-1355.098
	(STRAIN)		4.414E-04	3.87E-04	-3.778E-04	-3.778E-04
1	29.00000	0.04521	60.866	63.030	-1.292	2.567
	(STRAIN)		6.537E-04	6.844E-04	-2.291E-04	-2.291E-04
1	64.00000	0.03136	23.696	24.239	-7.695	-6.070
	(STRAIN)		3.551E-04	2.906E-04	-1.405E-04	-1.405E-04
2	0.00000	0.06531	552.000	1789.400	441.245	1694.962
	(STRAIN)		-3.175E-04	3.116E-04	-3.175E-04	2.676E-04
2	9.00000	0.06394	133.322	133.434	-1622.164	-1355.098
	(STRAIN)		4.414E-04	4.414E-04	-3.778E-04	-3.778E-04
2	29.00000	0.04521	60.866	63.030	-1.292	2.567
	(STRAIN)		6.537E-04	6.844E-04	-2.291E-04	-2.291E-04
2	64.00000	0.03136	23.696	24.239	-7.695	-6.070
	(STRAIN)		2.832E-04	2.906E-04	-1.405E-04	-1.405E-04
3	0.00000	0.06531	552.000	1789.400	441.245	1694.962
	(STRAIN)		-3.175E-04	3.116E-04	-3.175E-04	2.676E-04
3	9.00000	0.06394	133.322	133.434	-1622.164	-1355.098
	(STRAIN)		4.414E-04	4.414E-04	-3.778E-04	-3.778E-04
3	29.00000	0.04521	60.866	63.030	-1.292	2.567
	(STRAIN)		6.537E-04	6.844E-04	-2.291E-04	-2.291E-04
3	64.00000	0.03136	23.696	24.239	-7.695	-6.070
	(STRAIN)		2.832E-04	2.906E-04	-1.405E-04	-1.405E-04

B.4 New FDR Pavement of Route 335: Blend Ratio 0.57, FDR Stiffness 44 MPa

INPUT FILE NAME -C:\KENPAVE\KENPAVE For correction_Rte335\FDR Pavement of Route 335_Blend Ratio 0.57.DAT

NUMBER OF PROBLEMS TO BE SOLVED = 1

TITLE -FDR Pavement of Route 335_BR-0.57

MATL = 1 FOR LINEAR ELASTIC LAYERED SYSTEM

NDAMA = 0, SO DAMAGE ANALYSIS WILL NOT BE PERFORMED

NUMBER OF PERIODS PER YEAR (NPY) = 1

NUMBER OF LOAD GROUPS (NLG) = 1

TOLERANCE FOR INTEGRATION (DEL) -- = 0.001

NUMBER OF LAYERS (NL)---------- = 4

NUMBER OF Z COORDINATES (NZ)------ = 4

LIMIT OF INTEGRATION CYCLES (ICL)- = 80

COMPUTING CODE (NSTD)---------- = 9

SYSTEM OF UNITS (NUNIT)----------= 1

Length and displacement in cm, stress and modulus in kPa

unit weight in kN/m^3, and temperature in C

THICKNESSES OF LAYERS (TH) ARE : 9 20 35

POISSON'S RATIOS OF LAYERS (PR) ARE : 0.4 0.3 0.35 0.35

VERTICAL COORDINATES OF POINTS (ZC) ARE: 0 9 29 64

ALL INTERFACES ARE FULLY BONDED

FOR PERIOD NO. 1 LAYER NO. AND MODULUS ARE : 1 3.000E+06 2 4.425E+04 3 1.000E+05 4 7.000E+04

LOAD GROUP NO. 1 HAS 2 CONTACT AREAS

CONTACT RADIUS (CR)---------- = 10.7442

CONTACT PRESSURE (CP)---------- = 552

NO. OF POINTS AT WHICH RESULTS ARE DESIRED (NPT)-- = 3

WHEEL SPACING ALONG X-AXIS (XW)---------- = 0

WHEEL SPACING ALONG Y-AXIS (YW)---------- = 34.29

RESPONSE PT. NO. AND (XPT, YPT) ARE: 1 0.000 0.000 2 0.000 0.000

3 0.000 0.000

PERIOD NO. 1 LOAD GROUP NO. 1

POINT NO.	VERTICAL COORDINATE	VERTICAL DISPLACEMENT (cm)	VERTICAL STRESS (STRAIN)	MAJOR PRINCIPAL STRESS (STRAIN)	MINOR PRINCIPAL STRESS (STRAIN)	INTERMEDIATE PRINCIPAL STRESS (HORIZONTAL PRINCIPAL STRAIN)
1	0.00000	0.07959	552.000	2103.341	441.245	1978.444
	(STRAIN)		-3.972E-04	3.785E-04	-3.972E-04	3.202E-04
1	9.00000	0.07790	102.846	102.882	-2031.035	-1686.277
	(STRAIN)		5.299E-04	4.869E-04	-4.659E-04	-4.659E-04
1	29.00000	0.04683	59.572	61.680	16.053	16.068
	(STRAIN)		1.114E-03	1.176E-03	-1.643E-04	-1.642E-04
1	64.00000	0.03332	25.685	26.251	-6.700	-5.118
	(STRAIN)		3.761E-04	3.039E-04	-1.410E-04	-1.410E-04
2	0.00000	0.07959	552.000	2103.341	441.245	1978.444
	(STRAIN)		-3.972E-04	3.785E-04	-3.972E-04	3.202E-04
2	9.00000	0.07790	102.846	102.882	-2031.035	-1686.277
	(STRAIN)		5.299E-04	5.299E-04	-4.659E-04	-4.659E-04
2	29.00000	0.04683	59.572	61.680	16.053	16.068
	(STRAIN)		1.114E-03	1.176E-03	-1.643E-04	-1.642E-04
2	64.00000	0.03332	25.685	26.251	-6.700	-5.118
	(STRAIN)		2.962E-04	3.039E-04	-1.410E-04	-1.410E-04
3	0.00000	0.07959	552.000	2103.341	441.245	1978.444
	(STRAIN)		-3.972E-04	3.785E-04	-3.972E-04	3.202E-04
3	9.00000	0.07790	102.846	102.882	-2031.035	-1686.277
	(STRAIN)		5.299E-04	5.299E-04	-4.659E-04	-4.659E-04
3	29.00000	0.04683	59.572	61.680	16.053	16.068
	(STRAIN)		1.114E-03	1.176E-03	-1.643E-04	-1.642E-04
3	64.00000	0.03332	25.685	26.251	-6.700	-5.118
	(STRAIN)		2.962E-04	3.039E-04	-1.410E-04	-1.410E-04

B.5 New FDR Pavement of Route 335: Blend Ratio 0.50, FDR Stiffness 94 MPa

INPUT FILE NAME -C:\KENPAVE\KENPAVE For correction_Rte335\FDR Pavement of Route 335_Blend Ratio 0.50.DAT

NUMBER OF PROBLEMS TO BE SOLVED = 1

TITLE -FDR Pavement of Route 335_Blend ratio - 0.50

MATL = 1 FOR LINEAR ELASTIC LAYERED SYSTEM

NDAMA = 0, SO DAMAGE ANALYSIS WILL NOT BE PERFORMED

NUMBER OF PERIODS PER YEAR (NPY) = 1

NUMBER OF LOAD GROUPS (NLG) = 1

TOLERANCE FOR INTEGRATION (DEL) -- = 0.001

NUMBER OF LAYERS (NL)---------- = 4

NUMBER OF Z COORDINATES (NZ)------ = 4

LIMIT OF INTEGRATION CYCLES (ICL)- = 80

COMPUTING CODE (NSTD)---------- = 9

SYSTEM OF UNITS (NUNIT)----------= 1

Length and displacement in cm, stress and modulus in kPa

unit weight in kN/m^3, and temperature in C

THICKNESSES OF LAYERS (TH) ARE : 9 20 35

POISSON'S RATIOS OF LAYERS (PR) ARE : 0.4 0.3 0.35 0.35

VERTICAL COORDINATES OF POINTS (ZC) ARE: 0 9 29 64

ALL INTERFACES ARE FULLY BONDED

FOR PERIOD NO. 1 LAYER NO. AND MODULUS ARE : 1 3.000E+06 2 9.408E+04 3 1.000E+05 4 7.000E+04

LOAD GROUP NO. 1 HAS 2 CONTACT AREAS

CONTACT RADIUS (CR)---------- = 10.7442

CONTACT PRESSURE (CP)---------- = 552

NO. OF POINTS AT WHICH RESULTS ARE DESIRED (NPT)-- = 3

WHEEL SPACING ALONG X-AXIS (XW)---------- = 0

WHEEL SPACING ALONG Y-AXIS (YW)---------- = 34.29

RESPONSE PT. NO. AND (XPT, YPT) ARE: 1 0.000 0.000 2 0.000 0.000

3 0.000 0.000

PERIOD NO. 1 LOAD GROUP NO. 1

POINT NO.	VERTICAL COORDINATE	VERTICAL DISPLACEMENT (cm)	VERTICAL STRESS (STRAIN)	MAJOR PRINCIPAL STRESS (STRAIN)	MINOR PRINCIPAL STRESS (STRAIN)	INTERMEDIATE PRINCIPAL STRESS (HORIZONTAL PRINCIPAL STRAIN)
1	0.00000	0.06486	552.000	1778.020	441.245	1684.581
	(STRAIN)		-3.146E-04	3.092E-04	-3.146E-04	2.656E-04
1	9.00000	0.06351	134.642	134.758	-1606.507	-1342.475
	(STRAIN)		4.381E-04	3.84E-04	-3.745E-04	-3.745E-04
1	29.00000	0.04512	60.822	62.972	-2.302	1.787
	(STRAIN)		6.413E-04	6.710E-04	-2.310E-04	-2.310E-04
1	64.00000	0.03128	23.605	24.146	-7.712	-6.089
	(STRAIN)		3.54E-04	2.898E-04	-1.403E-04	-1.403E-04
2	0.00000	0.06486	552.000	1778.020	441.245	1684.581
	(STRAIN)		-3.146E-04	3.092E-04	-3.146E-04	2.656E-04
2	9.00000	0.06351	134.642	134.758	-1606.507	-1342.475
	(STRAIN)		4.381E-04	4.381E-04	-3.745E-04	-3.745E-04
2	29.00000	0.04512	60.822	62.972	-2.302	1.787
	(STRAIN)		6.413E-04	6.710E-04	-2.310E-04	-2.310E-04
2	64.00000	0.03128	23.605	24.146	-7.712	-6.089
	(STRAIN)		2.825E-04	2.898E-04	-1.403E-04	-1.403E-04
3	0.00000	0.06486	552.000	1778.020	441.245	1684.581
	(STRAIN)		-3.146E-04	3.092E-04	-3.146E-04	2.656E-04
3	9.00000	0.06351	134.642	134.758	-1606.507	-1342.475
	(STRAIN)		4.381E-04	4.381E-04	-3.745E-04	-3.745E-04
3	29.00000	0.04512	60.822	62.972	-2.302	1.787
	(STRAIN)		6.413E-04	6.710E-04	-2.310E-04	-2.310E-04
3	64.00000	0.03128	23.605	24.146	-7.712	-6.089
	(STRAIN)		2.825E-04	2.898E-04	-1.403E-04	-1.403E-04

B.6 New FDR Pavement of Route 335: Blend Ratio 0.31, FDR Stiffness 53 MPa

INPUT FILE NAME -C:\KENPAVE\KENPAVE For correction_Rte335\FDR Pavement of Route 335_Blend Ratio 0.31.DAT

NUMBER OF PROBLEMS TO BE SOLVED = 1

TITLE -FDR Pavement of Route 335_BR-0.31

MATL = 1 FOR LINEAR ELASTIC LAYERED SYSTEM

NDAMA = 0, SO DAMAGE ANALYSIS WILL NOT BE PERFORMED

NUMBER OF PERIODS PER YEAR (NPY) = 1

NUMBER OF LOAD GROUPS (NLG) = 1

TOLERANCE FOR INTEGRATION (DEL) -- = 0.001

NUMBER OF LAYERS (NL)---------- = 4

NUMBER OF Z COORDINATES (NZ)------ = 4

LIMIT OF INTEGRATION CYCLES (ICL)- = 80

COMPUTING CODE (NSTD)---------- = 9

SYSTEM OF UNITS (NUNIT)----------= 1

Length and displacement in cm, stress and modulus in kPa

unit weight in kN/m^3, and temperature in C

THICKNESSES OF LAYERS (TH) ARE : 9 20 35

POISSON'S RATIOS OF LAYERS (PR) ARE : 0.4 0.3 0.35 0.35

VERTICAL COORDINATES OF POINTS (ZC) ARE: 0 9 29 64

ALL INTERFACES ARE FULLY BONDED

FOR PERIOD NO. 1 LAYER NO. AND MODULUS ARE : 1 3.000E+06 2 5.295E+04 3 1.000E+05 4 7.000E+04

LOAD GROUP NO. 1 HAS 2 CONTACT AREAS

CONTACT RADIUS (CR)---------- = 10.7442

CONTACT PRESSURE (CP)---------- = 552

NO. OF POINTS AT WHICH RESULTS ARE DESIRED (NPT)-- = 3

WHEEL SPACING ALONG X-AXIS (XW)---------- = 0

WHEEL SPACING ALONG Y-AXIS (YW)---------- = 34.29

RESPONSE PT. NO. AND (XPT, YPT) ARE: 1 0.000 0.000 2 0.000 0.000

3 0.000 0.000

PERIOD NO. 1 LOAD GROUP NO. 1

POINT NO.	VERTICAL COORDINATE	VERTICAL DISPLACEMENT (cm)	VERTICAL STRESS (STRAIN)	MAJOR PRINCIPAL STRESS (STRAIN)	MINOR PRINCIPAL STRESS (STRAIN)	INTERMEDIATE PRINCIPAL STRESS (HORIZONTAL PRINCIPAL STRAIN)
1	0.00000	0.07559	552.000	2023.414	441.245	1906.704
	(STRAIN)		-3.769E-04	3.614E-04	-3.769E-04	3.069E-04
1	9.00000	0.07397	109.629	109.677	-1930.724	-1604.540
	(STRAIN)		5.079E-04	4.63E-04	-4.443E-04	-4.443E-04
1	29.00000	0.04655	60.310	62.505	13.265	13.864
	(STRAIN)		9.728E-04	1.027E-03	-1.822E-04	-1.822E-04
1	64.00000	0.03286	25.289	25.855	-7.039	-5.427
	(STRAIN)		3.77E-04	3.022E-04	-1.419E-04	-1.419E-04
2	0.00000	0.07559	552.000	2023.414	441.245	1906.704
	(STRAIN)		-3.769E-04	3.614E-04	-3.769E-04	3.069E-04
2	9.00000	0.07397	109.629	109.677	-1930.724	-1604.540
	(STRAIN)		5.079E-04	5.079E-04	-4.443E-04	-4.443E-04
2	29.00000	0.04655	60.310	62.505	13.265	13.864
	(STRAIN)		9.728E-04	1.027E-03	-1.822E-04	-1.822E-04
2	64.00000	0.03286	25.289	25.855	-7.039	-5.427
	(STRAIN)		2.945E-04	3.022E-04	-1.419E-04	-1.419E-04
3	0.00000	0.07559	552.000	2023.414	441.245	1906.704
	(STRAIN)		-3.769E-04	3.614E-04	-3.769E-04	3.069E-04
3	9.00000	0.07397	109.629	109.677	-1930.724	-1604.540
	(STRAIN)		5.079E-04	5.079E-04	-4.443E-04	-4.443E-04
3	29.00000	0.04655	60.310	62.505	13.265	13.864
	(STRAIN)		9.728E-04	1.027E-03	-1.822E-04	-1.822E-04
3	64.00000	0.03286	25.289	25.855	-7.039	-5.427
	(STRAIN)		2.945E-04	3.022E-04	-1.419E-04	-1.419E-04

B.7 New FDR Pavement of Route 790: Station 1+769: Blend Ratio 0.74, FDR Stiffness 52 MPa

INPUT FILE NAME -C:\KENPAVE\KENPAVE For correction_Rte790\FDR Pavement of Route 790_station- 1+769-blend ratio-0.74.DAT

NUMBER OF PROBLEMS TO BE SOLVED = 1

TITLE -FDR Pavement of Route 790_sta 1+769_BR-0.74

MATL = 1 FOR LINEAR ELASTIC LAYERED SYSTEM

NDAMA = 0, SO DAMAGE ANALYSIS WILL NOT BE PERFORMED

NUMBER OF PERIODS PER YEAR (NPY) = 1

NUMBER OF LOAD GROUPS (NLG) = 1

TOLERANCE FOR INTEGRATION (DEL) -- = 0.001

NUMBER OF LAYERS (NL)---------- = 4

NUMBER OF Z COORDINATES (NZ)------ = 4

LIMIT OF INTEGRATION CYCLES (ICL)- = 80

COMPUTING CODE (NSTD)---------- = 9

SYSTEM OF UNITS (NUNIT)----------= 1

Length and displacement in cm, stress and modulus in kPa

unit weight in kN/m^3, and temperature in C

THICKNESSES OF LAYERS (TH) ARE : 9 20 35

POISSON'S RATIOS OF LAYERS (PR) ARE : 0.4 0.3 0.35 0.35

VERTICAL COORDINATES OF POINTS (ZC) ARE: 0 9 29 64

ALL INTERFACES ARE FULLY BONDED

FOR PERIOD NO. 1 LAYER NO. AND MODULUS ARE : 1 3.000E+06 2 5.205E+04 3 8.000E+04 4 7.000E+04

LOAD GROUP NO. 1 HAS 2 CONTACT AREAS

CONTACT RADIUS (CR)---------- = 10.7442

CONTACT PRESSURE (CP)---------- = 552

NO. OF POINTS AT WHICH RESULTS ARE DESIRED (NPT)-- = 3

WHEEL SPACING ALONG X-AXIS (XW)---------- = 0

WHEEL SPACING ALONG Y-AXIS (YW)---------- = 34.29

RESPONSE PT. NO. AND (XPT, YPT) ARE: 1 0.000 0.000 2 0.000 0.000 3 0.000 0.000

PERIOD NO. 1 LOAD GROUP NO. 1

POINT NO.	VERTICAL COORDINATE	VERTICAL DISPLACEMENT (cm)	VERTICAL STRESS (STRAIN)	MAJOR PRINCIPAL STRESS (STRAIN)	MINOR PRINCIPAL STRESS (STRAIN)	INTERMEDIATE PRINCIPAL STRESS (HORIZONTAL PRINCIPAL STRAIN)
1	0.00000	0.07900	552.000	2068.523	441.245	1946.822
	(STRAIN)		-3.883E-04	3.711E-04	-3.883E-04	3.143E-04
1	9.00000	0.07738	107.266	107.316	-1976.669	-1644.126
	(STRAIN)		5.185E-04	4.655E-04	-4.540E-04	-4.540E-04
1	29.00000	0.04990	58.288	60.204	9.175	10.650
	(STRAIN)		9.945E-04	1.042E-03	-2.321E-04	-2.321E-04
1	64.00000	0.03336	25.705	26.350	-2.776	-1.680
	(STRAIN)		3.775E-04	3.489E-04	-1.426E-04	-1.426E-04
2	0.00000	0.07900	552.000	2068.523	441.245	1946.822
	(STRAIN)		-3.883E-04	3.711E-04	-3.883E-04	3.143E-04
2	9.00000	0.07738	107.266	107.316	-1976.669	-1644.126
	(STRAIN)		5.185E-04	5.185E-04	-4.540E-04	-4.540E-04
2	29.00000	0.04990	58.288	60.204	9.175	10.650
	(STRAIN)		9.945E-04	1.042E-03	-2.321E-04	-2.321E-04
2	64.00000	0.03336	25.705	26.350	-2.776	-1.680
	(STRAIN)		3.380E-04	3.489E-04	-1.426E-04	-1.426E-04
3	0.00000	0.07900	552.000	2068.523	441.245	1946.822
	(STRAIN)		-3.883E-04	3.711E-04	-3.883E-04	3.143E-04
3	9.00000	0.07738	107.266	107.316	-1976.669	-1644.126
	(STRAIN)		5.185E-04	5.185E-04	-4.540E-04	-4.540E-04
3	29.00000	0.04990	58.288	60.204	9.175	10.650
	(STRAIN)		9.945E-04	1.042E-03	-2.321E-04	-2.321E-04
3	64.00000	0.03336	25.705	26.350	-2.776	-1.680
	(STRAIN)		3.380E-04	3.489E-04	-1.426E-04	-1.426E-04

B.8 New FDR Pavement of Route 790: Station 2+185: Blend Ratio 0.74, FDR Stiffness 53 MPa

INPUT FILE NAME -C:\KENPAVE\KENPAVE For correction_Rte790\FDR Pavement of Route 790_station- 2+185-blend ratio-0.74.DAT

NUMBER OF PROBLEMS TO BE SOLVED = 1

TITLE -FDR Pavement of Route 790_sta 2+185_BR-0.74

MATL = 1 FOR LINEAR ELASTIC LAYERED SYSTEM

NDAMA = 0, SO DAMAGE ANALYSIS WILL NOT BE PERFORMED

NUMBER OF PERIODS PER YEAR (NPY) = 1

NUMBER OF LOAD GROUPS (NLG) = 1

TOLERANCE FOR INTEGRATION (DEL) -- = 0.001

NUMBER OF LAYERS (NL)---------- = 4

NUMBER OF Z COORDINATES (NZ)------ = 4

LIMIT OF INTEGRATION CYCLES (ICL)- = 80

COMPUTING CODE (NSTD)---------- = 9

SYSTEM OF UNITS (NUNIT)----------= 1

Length and displacement in cm, stress and modulus in kPa

unit weight in kN/m^3, and temperature in C

THICKNESSES OF LAYERS (TH) ARE : 9 20 35

POISSON'S RATIOS OF LAYERS (PR) ARE : 0.4 0.3 0.35 0.35

VERTICAL COORDINATES OF POINTS (ZC) ARE: 0 9 29 64

ALL INTERFACES ARE FULLY BONDED

FOR PERIOD NO. 1 LAYER NO. AND MODULUS ARE : 1 3.000E+06 2 5.343E+04 3 8.000E+04 4 7.000E+04

LOAD GROUP NO. 1 HAS 2 CONTACT AREAS

CONTACT RADIUS (CR)---------- = 10.7442

CONTACT PRESSURE (CP)---------- = 552

NO. OF POINTS AT WHICH RESULTS ARE DESIRED (NPT)-- = 3

WHEEL SPACING ALONG X-AXIS (XW)---------- = 0

WHEEL SPACING ALONG Y-AXIS (YW)---------- = 34.29

RESPONSE PT. NO. AND (XPT, YPT) ARE: 1 0.000 0.000 2 0.000 0.000 3 0.000 0.000

PERIOD NO. 1 LOAD GROUP NO. 1

POINT NO.	VERTICAL COORDINATE	VERTICAL DISPLACEMENT (cm)	VERTICAL STRESS (STRAIN)	MAJOR PRINCIPAL STRESS (STRAIN)	MINOR PRINCIPAL STRESS (STRAIN)	INTERMEDIATE PRINCIPAL STRESS (HORIZONTAL PRINCIPAL STRAIN)
1	0.00000	0.07845	552.000	2057.204	441.245	1936.637
	(STRAIN)		-3.854E-04	3.687E-04	-3.854E-04	3.124E-04
1	9.00000	0.07684	108.265	108.318	-1962.179	-1632.344
	(STRAIN)		5.154E-04	4.619E-04	-4.509E-04	-4.509E-04
1	29.00000	0.04986	58.349	60.268	8.596	10.198
	(STRAIN)		9.758E-04	1.022E-03	-2.348E-04	-2.348E-04
1	64.00000	0.03329	25.643	26.287	-2.816	-1.718
	(STRAIN)		3.768E-04	3.484E-04	-1.427E-04	-1.427E-04
2	0.00000	0.07845	552.000	2057.204	441.245	1936.637
	(STRAIN)		-3.854E-04	3.687E-04	-3.854E-04	3.124E-04
2	9.00000	0.07684	108.265	108.318	-1962.179	-1632.344
	(STRAIN)		5.154E-04	5.154E-04	-4.509E-04	-4.509E-04
2	29.00000	0.04986	58.349	60.268	8.596	10.198
	(STRAIN)		9.758E-04	1.022E-03	-2.348E-04	-2.348E-04
2	64.00000	0.03329	25.643	26.287	-2.816	-1.718
	(STRAIN)		3.376E-04	3.484E-04	-1.427E-04	-1.427E-04
3	0.00000	0.07845	552.000	2057.204	441.245	1936.637
	(STRAIN)		-3.854E-04	3.687E-04	-3.854E-04	3.124E-04
3	9.00000	0.07684	108.265	108.318	-1962.179	-1632.344
	(STRAIN)		5.154E-04	5.154E-04	-4.509E-04	-4.509E-04
3	29.00000	0.04986	58.349	60.268	8.596	10.198
	(STRAIN)		9.758E-04	1.022E-03	-2.348E-04	-2.348E-04
3	64.00000	0.03329	25.643	26.287	-2.816	-1.718
	(STRAIN)		3.376E-04	3.484E-04	-1.427E-04	-1.427E-04

B.9 New FDR Pavement of Route 790: Station 2+550: Blend Ratio 0.75, FDR Stiffness 54 MPa

INPUT FILE NAME -C:\KENPAVE\KENPAVE For correction_Rte790\FDR Pavement of Route 790_station-2+550-blend ratio-0.75.DAT

NUMBER OF PROBLEMS TO BE SOLVED = 1

TITLE -FDR Pavement of Route 790_Sta 2+550_Blend ratio - 0.75

MATL = 1 FOR LINEAR ELASTIC LAYERED SYSTEM

NDAMA = 0, SO DAMAGE ANALYSIS WILL NOT BE PERFORMED

NUMBER OF PERIODS PER YEAR (NPY) = 1

NUMBER OF LOAD GROUPS (NLG) = 1

TOLERANCE FOR INTEGRATION (DEL) -- = 0.001

NUMBER OF LAYERS (NL)---------- = 4

NUMBER OF Z COORDINATES (NZ)------ = 4

LIMIT OF INTEGRATION CYCLES (ICL)- = 80

COMPUTING CODE (NSTD)---------- = 9

SYSTEM OF UNITS (NUNIT)----------= 1

Length and displacement in cm, stress and modulus in kPa

unit weight in kN/m^3, and temperature in C

THICKNESSES OF LAYERS (TH) ARE : 9 20 35

POISSON'S RATIOS OF LAYERS (PR) ARE : 0.4 0.3 0.35 0.35

VERTICAL COORDINATES OF POINTS (ZC) ARE: 0 9 29 64

ALL INTERFACES ARE FULLY BONDED

FOR PERIOD NO. 1 LAYER NO. AND MODULUS ARE : 1 3.000E+06 2 5.395E+04 3 8.000E+04 4 7.000E+04

LOAD GROUP NO. 1 HAS 2 CONTACT AREAS

CONTACT RADIUS (CR)---------- = 10.7442

CONTACT PRESSURE (CP)---------- = 552

NO. OF POINTS AT WHICH RESULTS ARE DESIRED (NPT)-- = 3

WHEEL SPACING ALONG X-AXIS (XW)---------- = 0

WHEEL SPACING ALONG Y-AXIS (YW)---------- = 34.29

RESPONSE PT. NO. AND (XPT, YPT) ARE: 1 0.000 0.000 2 0.000 0.000 3 0.000 0.000

PERIOD NO. 1 LOAD GROUP NO. 1

POINT NO.	VERTICAL COORDINATE	VERTICAL DISPLACEMENT (cm)	VERTICAL STRESS (STRAIN)	MAJOR PRINCIPAL STRESS (STRAIN)	MINOR PRINCIPAL STRESS (STRAIN)	INTERMEDIATE PRINCIPAL STRESS (HORIZONTAL PRINCIPAL STRAIN)
1	0.00000	0.07825	552.000	2053.017	441.245	1932.879
	(STRAIN)		-3.844E-04	3.678E-04	-3.844E-04	3.117E-04
1	9.00000	0.07664	108.637	108.691	-1956.813	-1627.983
	(STRAIN)		5.142E-04	4.606E-04	-4.497E-04	-4.497E-04
1	29.00000	0.04984	58.370	60.290	8.376	10.026
	(STRAIN)		9.689E-04	1.015E-03	-2.358E-04	-2.358E-04
1	64.00000	0.03327	25.620	26.264	-2.831	-1.732
	(STRAIN)		3.765E-04	3.483E-04	-1.427E-04	-1.427E-04
2	0.00000	0.07825	552.000	2053.017	441.245	1932.879
	(STRAIN)		-3.844E-04	3.678E-04	-3.844E-04	3.117E-04
2	9.00000	0.07664	108.637	108.691	-1956.813	-1627.983
	(STRAIN)		5.142E-04	5.142E-04	-4.497E-04	-4.497E-04
2	29.00000	0.04984	58.370	60.290	8.376	10.026
	(STRAIN)		9.689E-04	1.015E-03	-2.358E-04	-2.358E-04
2	64.00000	0.03327	25.620	26.264	-2.831	-1.732
	(STRAIN)		3.374E-04	3.483E-04	-1.427E-04	-1.427E-04
3	0.00000	0.07825	552.000	2053.017	441.245	1932.879
	(STRAIN)		-3.844E-04	3.678E-04	-3.844E-04	3.117E-04
3	9.00000	0.07664	108.637	108.691	-1956.813	-1627.983
	(STRAIN)		5.142E-04	5.142E-04	-4.497E-04	-4.497E-04
3	29.00000	0.04984	58.370	60.290	8.376	10.026
	(STRAIN)		9.689E-04	1.015E-03	-2.358E-04	-2.358E-04
3	64.00000	0.03327	25.620	26.264	-2.831	-1.732
	(STRAIN)		3.374E-04	3.483E-04	-1.427E-04	-1.427E-04

B.10 New FDR Pavement of Route 790: Station 3+128: Blend Ratio 0.76, FDR Stiffness 48 MPa

INPUT FILE NAME -C:\KENPAVE\KENPAVE For correction_Rte790\FDR Pavement of Route 790_station- 3+128-blend ratio-0.76.DAT

NUMBER OF PROBLEMS TO BE SOLVED = 1

TITLE -FDR Pavement of Route 790_sta 3+128_BR-0.76

MATL = 1 FOR LINEAR ELASTIC LAYERED SYSTEM

NDAMA = 0, SO DAMAGE ANALYSIS WILL NOT BE PERFORMED

NUMBER OF PERIODS PER YEAR (NPY) = 1

NUMBER OF LOAD GROUPS (NLG) = 1

TOLERANCE FOR INTEGRATION (DEL) -- = 0.001

NUMBER OF LAYERS (NL)---------- = 4

NUMBER OF Z COORDINATES (NZ)------ = 4

LIMIT OF INTEGRATION CYCLES (ICL)- = 80

COMPUTING CODE (NSTD)---------- = 9

SYSTEM OF UNITS (NUNIT)----------= 1

Length and displacement in cm, stress and modulus in kPa

unit weight in kN/m^3, and temperature in C

THICKNESSES OF LAYERS (TH) ARE : 9 20 35

POISSON'S RATIOS OF LAYERS (PR) ARE : 0.4 0.3 0.35 0.35

VERTICAL COORDINATES OF POINTS (ZC) ARE: 0 9 29 64

ALL INTERFACES ARE FULLY BONDED

FOR PERIOD NO. 1 LAYER NO. AND MODULUS ARE : 1 3.000E+06 2 4.846E+04 3 8.000E+04 4 7.000E+04

LOAD GROUP NO. 1 HAS 2 CONTACT AREAS

CONTACT RADIUS (CR)---------- = 10.7442

CONTACT PRESSURE (CP)---------- = 552

NO. OF POINTS AT WHICH RESULTS ARE DESIRED (NPT)-- = 3

WHEEL SPACING ALONG X-AXIS (XW)---------- = 0

WHEEL SPACING ALONG Y-AXIS (YW)---------- = 34.29

RESPONSE PT. NO. AND (XPT, YPT) ARE: 1 0.000 0.000 2 0.000 0.000 3 0.000 0.000

PERIOD NO. 1 LOAD GROUP NO. 1

POINT NO.	VERTICAL COORDINATE	VERTICAL DISPLACEMENT (cm)	VERTICAL STRESS (STRAIN)	MAJOR PRINCIPAL STRESS (STRAIN)	MINOR PRINCIPAL STRESS (STRAIN)	INTERMEDIATE PRINCIPAL STRESS (HORIZONTAL PRINCIPAL STRAIN)
1	0.00000	0.08055	552.000	2099.600	441.245	1974.745
	(STRAIN)		-3.962E-04	3.777E-04	-3.962E-04	3.195E-04
1	9.00000	0.07889	104.586	104.631	-2016.179	-1676.297
	(STRAIN)		5.272E-04	4.753E-04	-4.625E-04	-4.625E-04
1	29.00000	0.05002	58.093	59.995	10.652	11.805
	(STRAIN)		1.048E-03	1.099E-03	-2.247E-04	-2.247E-04
1	64.00000	0.03353	25.868	26.513	-2.661	-1.572
	(STRAIN)		3.793E-04	3.499E-04	-1.424E-04	-1.424E-04
2	0.00000	0.08055	552.000	2099.600	441.245	1974.745
	(STRAIN)		-3.962E-04	3.777E-04	-3.962E-04	3.195E-04
2	9.00000	0.07889	104.586	104.631	-2016.179	-1676.297
	(STRAIN)		5.272E-04	5.272E-04	-4.625E-04	-4.625E-04
2	29.00000	0.05002	58.093	59.995	10.652	11.805
	(STRAIN)		1.048E-03	1.099E-03	-2.247E-04	-2.247E-04
2	64.00000	0.03353	25.868	26.513	-2.661	-1.572
	(STRAIN)		3.390E-04	3.499E-04	-1.424E-04	-1.424E-04
3	0.00000	0.08055	552.000	2099.600	441.245	1974.745
	(STRAIN)		-3.962E-04	3.777E-04	-3.962E-04	3.195E-04
3	9.00000	0.07889	104.586	104.631	-2016.179	-1676.297
	(STRAIN)		5.272E-04	5.272E-04	-4.625E-04	-4.625E-04
3	29.00000	0.05002	58.093	59.995	10.652	11.805
	(STRAIN)		1.048E-03	1.099E-03	-2.247E-04	-2.247E-04
3	64.00000	0.03353	25.868	26.513	-2.661	-1.572
	(STRAIN)		3.390E-04	3.499E-04	-1.424E-04	-1.424E-04

B.11 New FDR Pavement of Route 790: Station 3+446: Blend Ratio 0.76, FDR Stiffness 49 MPa

INPUT FILE NAME -C:\KENPAVE\KENPAVE For correction_Rte790\FDR Pavement of Route 790_station- 3+446-blend ratio-0.76.DAT

NUMBER OF PROBLEMS TO BE SOLVED = 1

TITLE -FDR Pavement of Route 790_sta 3+446_BR-0.76

MATL = 1 FOR LINEAR ELASTIC LAYERED SYSTEM

NDAMA = 0, SO DAMAGE ANALYSIS WILL NOT BE PERFORMED

NUMBER OF PERIODS PER YEAR (NPY) = 1

NUMBER OF LOAD GROUPS (NLG) = 1

TOLERANCE FOR INTEGRATION (DEL) -- = 0.001

NUMBER OF LAYERS (NL)---------- = 4

NUMBER OF Z COORDINATES (NZ)------ = 4

LIMIT OF INTEGRATION CYCLES (ICL)- = 80

COMPUTING CODE (NSTD)---------- = 9

SYSTEM OF UNITS (NUNIT)----------= 1

Length and displacement in cm, stress and modulus in kPa

unit weight in kN/m^3, and temperature in C

THICKNESSES OF LAYERS (TH) ARE : 9 20 35

POISSON'S RATIOS OF LAYERS (PR) ARE : 0.4 0.3 0.35 0.35

VERTICAL COORDINATES OF POINTS (ZC) ARE: 0 9 29 64

ALL INTERFACES ARE FULLY BONDED

FOR PERIOD NO. 1 LAYER NO. AND MODULUS ARE : 1 3.000E+06 2 4.870E+04
3 8.000E+04 4 7.000E+04

LOAD GROUP NO. 1 HAS 2 CONTACT AREAS

CONTACT RADIUS (CR)---------- = 10.7442

CONTACT PRESSURE (CP)---------- = 552

NO. OF POINTS AT WHICH RESULTS ARE DESIRED (NPT)-- = 3

WHEEL SPACING ALONG X-AXIS (XW)---------- = 0

WHEEL SPACING ALONG Y-AXIS (YW)---------- = 34.29

RESPONSE PT. NO. AND (XPT, YPT) ARE: 1 0.000 0.000 2 0.000 0.000 3 0.000 0.000

PERIOD NO. 1 LOAD GROUP NO. 1

POINT NO.	VERTICAL COORDINATE	VERTICAL DISPLACEMENT (cm)	VERTICAL STRESS (STRAIN)	MAJOR PRINCIPAL STRESS (STRAIN)	MINOR PRINCIPAL STRESS (STRAIN)	INTERMEDIATE PRINCIPAL STRESS (HORIZONTAL PRINCIPAL STRAIN)
1	0.00000	0.08044	552.000	2097.442	441.245	1972.812
	(STRAIN)		-3.956E-04	3.773E-04	-3.956E-04	3.191E-04
1	9.00000	0.07878	104.769	104.814	-2013.449	-1674.074
	(STRAIN)		5.266E-04	4.746E-04	-4.619E-04	-4.619E-04
1	29.00000	0.05001	58.108	60.011	10.555	11.729
	(STRAIN)		1.044E-03	1.095E-03	-2.252E-04	-2.252E-04
1	64.00000	0.03352	25.857	26.502	-2.669	-1.579
	(STRAIN)		3.792E-04	3.499E-04	-1.424E-04	-1.424E-04
2	0.00000	0.08044	552.000	2097.442	441.245	1972.812
	(STRAIN)		-3.956E-04	3.773E-04	-3.956E-04	3.191E-04
2	9.00000	0.07878	104.769	104.814	-2013.449	-1674.074
	(STRAIN)		5.266E-04	5.266E-04	-4.619E-04	-4.619E-04
2	29.00000	0.05001	58.108	60.011	10.555	11.729
	(STRAIN)		1.044E-03	1.095E-03	-2.252E-04	-2.252E-04
2	64.00000	0.03352	25.857	26.502	-2.669	-1.579
	(STRAIN)		3.390E-04	3.499E-04	-1.424E-04	-1.424E-04
3	0.00000	0.08044	552.000	2097.442	441.245	1972.812
	(STRAIN)		-3.956E-04	3.773E-04	-3.956E-04	3.191E-04
3	9.00000	0.07878	104.769	104.814	-2013.449	-1674.074
	(STRAIN)		5.266E-04	5.266E-04	-4.619E-04	-4.619E-04
3	29.00000	0.05001	58.108	60.011	10.555	11.729
	(STRAIN)		1.044E-03	1.095E-03	-2.252E-04	-2.252E-04
3	64.00000	0.03352	25.857	26.502	-2.669	-1.579
	(STRAIN)		3.390E-04	3.499E-04	-1.424E-04	-1.424E-04

B.12 New FDR Pavement of Route 790: Station 4+040: Blend Ratio 0.76, FDR Stiffness 37 MPa

INPUT FILE NAME -C:\KENPAVE\KENPAVE For correction_Rte790\FDR Pavement of Route 790_station- 4+040-blend ratio-0.76.DAT

NUMBER OF PROBLEMS TO BE SOLVED = 1

TITLE -FDR Pavement of Route 790_sta 4+040_BR-0.76

MATL = 1 FOR LINEAR ELASTIC LAYERED SYSTEM

NDAMA = 0, SO DAMAGE ANALYSIS WILL NOT BE PERFORMED

NUMBER OF PERIODS PER YEAR (NPY) = 1

NUMBER OF LOAD GROUPS (NLG) = 1

TOLERANCE FOR INTEGRATION (DEL) -- = 0.001

NUMBER OF LAYERS (NL)---------- = 4

NUMBER OF Z COORDINATES (NZ)------ = 4

LIMIT OF INTEGRATION CYCLES (ICL)- = 80

COMPUTING CODE (NSTD)---------- = 9

SYSTEM OF UNITS (NUNIT)----------= 1

Length and displacement in cm, stress and modulus in kPa

unit weight in kN/m^3, and temperature in C

THICKNESSES OF LAYERS (TH) ARE : 9 20 35

POISSON'S RATIOS OF LAYERS (PR) ARE : 0.4 0.3 0.35 0.35

VERTICAL COORDINATES OF POINTS (ZC) ARE: 0 9 29 64

ALL INTERFACES ARE FULLY BONDED

FOR PERIOD NO. 1 LAYER NO. AND MODULUS ARE : 1 3.000E+06 2 3.690E+04 3 8.000E+04 4 7.000E+04

LOAD GROUP NO. 1 HAS 2 CONTACT AREAS

CONTACT RADIUS (CR)---------- = 10.7442

CONTACT PRESSURE (CP)---------- = 552

NO. OF POINTS AT WHICH RESULTS ARE DESIRED (NPT)-- = 3

WHEEL SPACING ALONG X-AXIS (XW)---------- = 0

WHEEL SPACING ALONG Y-AXIS (YW)---------- = 34.29

RESPONSE PT. NO. AND (XPT, YPT) ARE: 1 0.000 0.000 2 0.000 0.000 3 0.000 0.000

PERIOD NO. 1 LOAD GROUP NO. 1

POINT NO.	VERTICAL COORDINATE	VERTICAL DISPLACEMENT (cm)	VERTICAL STRESS (STRAIN)	MAJOR PRINCIPAL STRESS (STRAIN)	MINOR PRINCIPAL STRESS (STRAIN)	INTERMEDIATE PRINCIPAL STRESS (HORIZONTAL PRINCIPAL STRAIN)
1	0.00000	0.08695	552.000	2220.411	441.245	2083.048
	(STRAIN)		-4.267E-04	4.036E-04	-4.267E-04	3.395E-04
1	9.00000	0.08519	94.988	95.017	-2166.417	-1799.315
	(STRAIN)		5.604E-04	5.126E-04	-4.949E-04	-4.949E-04
1	29.00000	0.05032	56.979	58.772	15.014	15.237
	(STRAIN)		1.284E-03	1.347E-03	-1.948E-04	-1.948E-04
1	64.00000	0.03415	26.373	27.013	-2.168	-1.117
	(STRAIN)		3.839E-04	3.520E-04	-1.404E-04	-1.404E-04
2	0.00000	0.08695	552.000	2220.411	441.245	2083.048
	(STRAIN)		-4.267E-04	4.036E-04	-4.267E-04	3.395E-04
2	9.00000	0.08519	94.988	95.017	-2166.417	-1799.315
	(STRAIN)		5.604E-04	5.604E-04	-4.949E-04	-4.949E-04
2	29.00000	0.05032	56.979	58.772	15.014	15.237
	(STRAIN)		1.284E-03	1.347E-03	-1.948E-04	-1.948E-04
2	64.00000	0.03415	26.373	27.013	-2.168	-1.117
	(STRAIN)		3.412E-04	3.520E-04	-1.404E-04	-1.404E-04
3	0.00000	0.08695	552.000	2220.411	441.245	2083.048
	(STRAIN)		-4.267E-04	4.036E-04	-4.267E-04	3.395E-04
3	9.00000	0.08519	94.988	95.017	-2166.417	-1799.315
	(STRAIN)		5.604E-04	5.604E-04	-4.949E-04	-4.949E-04
3	29.00000	0.05032	56.979	58.772	15.014	15.237
	(STRAIN)		1.284E-03	1.347E-03	-1.948E-04	-1.948E-04
3	64.00000	0.03415	26.373	27.013	-2.168	-1.117
	(STRAIN)		3.412E-04	3.520E-04	-1.404E-04	-1.404E-04

APPENDIX C: Life Cycle Cost Analysis

The Equation for life cycle cost analysis is

$$Life\ cycle\ cost = (Present\ value\ cost * (1+i)^n) * (1+r)^{-n} \qquad (4-4)$$

where,
i = inflation rate (assumed 2%)
r = discount rate (assumed 4%)
n = number of year after which a maintenance is needed
Present value cost = CAD $350,000/ km (assumed)

For Route 335,

Blend ratio, 0.90

Service life = 8 years

Terminal serviceability = 40 years

The repair would be needed after 8 years, 16 years, 24 years and 32 years. The repair after 32 years would give life for next 8 years that means after 40 years from the beginning, the pavement would fail and a new pavement would be needed to be built.

Per km Repair cost after 8 years,

$$repair\ cost = (350000 * (1+0.02)^8) * (1+0.04)^{-8}$$

$$= 299642.0117$$

Per km Repair cost after 16 years,

$$repair\ cost = (350000 * (1 + 0.02)^{16}) * (1 + 0.04)^{-16}$$

$$= 256529.529$$

Per km Repair cost after 24 years,

$$repair\ cost = (350000 * (1 + 0.02)^{24}) * (1 + 0.04)^{-24}$$

$$= 219620.0689$$

Per km Repair cost after 32 years,

$$repair\ cost = (350000 * (1 + 0.02)^{32}) * (1 + 0.04)^{-32}$$

$$= 188021.1407$$

Total Cost per km = 350000 + 299642.0117 + 256529.529 + 219620.0689 + 188021.1407

= 1313812.75

Life cycle cost of pavement per km with a blend ratio of 0.9 is CAD $1,313,812.75

For Route 335,

Blend ratio, 0.57 and 0.31

Service life = 20 years

Terminal serviceability = 40 years

The repair would be needed after 20 years. The repair after 20 years would give life for next 20 years that means after 40 years from the beginning, the pavement would fail and a new pavement would be needed to be built.

Per km Repair cost after 20 years,

$$repair\ cost = (350000 * (1 + 0.02)^{20}) * (1 + 0.04)^{-20}$$

$$= 237358.448$$

Total Cost per km = 350000 + 237358.448

= 587358.448

Life cycle cost of pavement per km with blend ratios of 0.57 and 0.31 is CAD $587,358.448